UNIVERSITY OF NOTTINGHAM
Institute of Engineering Surveying and Space Geodesy

IMPROVED MODELLING OF HIGH PRECISION WIDE AREA DIFFERENTIAL GPS

Chih Hung Jason Chao
BSc (NCKU, Taiwan), MSc (Nottingham, UK)

Thesis submitted to the University of Nottingham for the degree of Doctor of Philosophy

April 1996

ABSTRACT

Wide Area Differential GPS (WADGPS) aims at overcoming the main drawback of conventional DGPS, namely the limited range over which the differential corrections are valid, due to the rapid decorrelation of the error sources with increasing distance from the reference station to the user. In the WADGPS approach, error sources are generated for users over a large portion of the earth, such as a communication satellite's entire footprint, by separating and modelling the main sources of error in GPS measurements. This has the effect of eliminating the limit imposed on the validity of the corrections by the geographical or atmospheric environment. A main advantage of WADGPS is the fact that far fewer reference stations are needed to cover the same area, compared to conventional DGPS.

Interest in WADGPS has grown during the last few years, the use of WADGPS both for positioning accuracy requirements and the provision of integrity are being explored. Several research establishments have come up with their own WADGPS methodology and algorithms, all sharing a basic principle, namely the requirement that different error sources which affect GPS navigation are dealt with separately, and their spatial and temporal properties are investigated and modelled individually.

Research was carried out to develop an advanced method and the corresponding algorithms, which could provide a high precision WADGPS positioning service. The service would be suitable for single or dual frequency users, and could be introduced with very few reference stations. The two main components of the service are a precise, near real-time orbit determination of the GPS satellites, and an accurate estimation and modelling of ionospheric and tropospheric effects. Results from real data indicate that user position accuracy of the order of 2 m and 3 m (RMS) in plan and height components respectively, were achieved over user-reference distances ranging from 2,000 to 3,500 km.

ACKNOWLEDGEMENTS

The research undertaken for this thesis has been conducted in the Institute of Engineering Surveying and Space Geodesy (IESSG) at the University of Nottingham, with the support of the Director of the IESSG, Professor V Ashkenazi. The author would like to express his deep appreciation to his academic supervisors, Professor V Ashkenazi and Dr T Moore, for their guidance and encouragement throughout this research.

The author would like to express his special thanks to Dr W Y Ochieng, former staff of IESSG, for his invaluable advice and constructive discussions during the research. Thanks are also extended to Dr C J Hill and Dr W Chen for their helpful comments and discussions. The author would also like to give thanks to Dr W Y Ochieng, Dr C J Hill, Dr W Chen and Mr N Penna for proof reading this thesis.

Special thanks go to all the research colleagues, both past and present, within the IESSG, for providing a pleasant environment. Particular thanks are due to Po, CCC, Galera, Debbie and Maria, whose presence has made the research at Nottingham an enjoyable experience.

My utmost gratitude must be given to my parents for their continuous support. Above all, I would like to express my deepest gratitude to my wife, Kathy, who has always stood by me, for the suffering she has endured over all these years. Without her, it would not have been possible to complete this research.

Contents

List of Figures

List of Tables

Chapter 1

Introduction

The development of satellite geodesy, marked by the first launch of the Russian Sputnik satellite in 1957, has advanced the science of geodesy to a new era. By virtue of the increasing accuracy and effectiveness, the technique of satellite geodesy has been used in many other disciplines, such as navigation, geophysics and oceanography. The availability of the US TRANSIT satellites in 1967 have been widely used worldwide both for navigation and surveying. The two main drawbacks of the TRANSIT system, namely the large time gaps between the observation windows and the relatively low navigation accuracy led to the development of the NAVSTAR (NAVigation System with Timing And Ranging) Global Positioning System (GPS).

The GPS provides answers to questions regarding time, position and velocity in a quick, accurate and inexpensive way anywhere on the globe. Research on the use of GPS, with or without integration with other fields, has been successfully carried out for a wide variety of applications. This research project aimed at investigating the processing algorithms for a GPS based navigation system, which would be capable of providing instantaneous, continuous and reliable high precision navigation accuracy over a fairly large area, typically an entire ocean region. The system would provide positioning information, via communication satellites, to users anywhere within the network to achieve highly accurate positioning accuracies in real-time for applications such as the approach and precision landing phases of flight.

GPS is a satellite-based, passive positioning system designed primarily for military use. It was developed and operated by the United States Department of Defense (US DoD), to provide users with high accuracy position, velocity and time information, 24 hours a day, in all weather, anywhere in the world. GPS was designed to provide two positioning services, the Standard Positioning Service (SPS) and the Precise Positioning Service (PPS). SPS provides navigation accuracy of the order of 100 m (2DRMS) horizontally and 156 m (95% probability level) vertically. The PPS is only accessible to the US DoD and other authorised users and provides the full GPS accuracy of 15 m (2DRMS) in plan and 25 m (95% probability level) in height. By employing the relative positioning approach, the use of carrier phase measurement can achieve positioning accuracies of the order of a few centimetres. However, the problems of integer ambiguity resolution and cycle slip detection and repairing restrict the use of the carrier phase observable (Ffoulkes-Jones, 1990).

Responding to the growing demands from military, civil, commercial and scientific users, the US government has adopted a more flexible policy over the future management and use of GPS. The latest US GPS policy released from the White House on March 29, 1996 reveals some important issues (The White House, 1996). The GPS service provided for civilian users is addressed as,

'We will continue to provide the GPS Standard Positioning Service for peaceful civil, commercial and scientific use on a continuous, worldwide basis, free of direct user fees.'

The policy of Selective Availability (SA) (§ 2.6.4), which is a method of deliberately degrading the GPS navigation accuracy, to maintain the difference in accuracy between SPS and PPS is reviewed as,

'It is our intention to discontinue the use of GPS Selective Availability (SA) within a decade .....'

As to the use of GPS, possible international cooperation is promoted as,

'We will cooperate with other governments and international organizations to ensure an appropriate balance between the requirements of international civil, commercial and scientific users and international security interests.'

These policy guidelines could lead to significant changes to the international GPS user community. Cooperation between the US government and the international community, regarding the use of GPS, opens up the possibility for a 'user oriented' policy for future operation and maintenance of GPS. Even though the date of the discontinuation of SA is not yet clear, there is no doubt that the US government understands the need to make higher GPS accuracy available to the civilian community. This will be possible after the US DOD finds other appropriate ways of protecting its military interests. This will allow full point positioning capability of the SPS to be resumed. Reports have indicated that it is possible to achieve an accuracy level of about 20 to 40 m, much better than that originally expected from SPS (Kremer *et al*, 1990). However, since SA is still in place for the foreseeable future (up to ten years from now, April 1996), the design of any high accuracy positioning/navigation system must take into account the effects of SA.

The level of accuracy provided by stand-alone positioning is sufficient for a wide variety of applications, such as the en route and terminal phases of flight, transportation management and leisure purposes. However, for applications such as precision approach and landing phases of flight, this level of accuracy is not acceptable. Another important factor to safety critical applications such as civil aviation is the integrity, which is defined as 'the ability of a system to provide timely warnings to users when the system should not be used for Navigation' (DOT/DOP, 1994). The stand-alone positioning, provided by the code pseudorange observables cannot meet the integrity requirements, in that it is not always possible to identify errors in the measurements (IESSG, 1995).

The need for a higher navigation accuracy as well as integrity has resulted in the development of the technique known as differential positioning. Differential GPS positioning, which is commonly referred to as Differential GPS (DGPS), has been widely applied to improve on the point positioning accuracy. The conventional DGPS concept is based on the assumption that GPS error sources, such as orbital and atmospheric propagation errors, between the reference and user sites are highly correlated. The reference station, being located at a known position, calculates corrections for the effects of the GPS error sources, and bundles them together as a single differential correction to be transmitted to the user. These errors at the user site can be largely eliminated or minimised by applying the differential corrections, resulting in an improved user positioning accuracy (§ 2.7). The DGPS technique has been repeatedly demonstrated to achieve a positioning accuracy of 2 to 5 m over baselines up to 1,000 km (Brown, 1989; Kremer *et al*, 1990; Cannon *et al*, 1992a, b). The drawback of conventional DGPS is that the user needs to be close enough to the reference station to get maximum benefit from the differential corrections. If the user experiences different errors from those at the reference station, the differential corrections do not improve the user navigation position. Reports have suggested that beyond the user-reference station separation of approximate 100 km, the differential correction is not accurate enough to realise the full potential of DGPS (Loomis *et al*, 1991, Kee *et al*, 1991). As a consequence, a large number of reference stations are required to build a conventional DGPS system which will cover a fairly wide area. The Wide Area DGPS (WADGPS) concept is aimed at providing the same level of accuracy as conventional DGPS, but with a less dense network of reference stations.

In the design of a WADGPS system, the main issues that must be addressed include the purpose, accuracy and integrity, and the associated software, hardware and cost. Several organisations are involved in WADGPS research, and different conceptual approaches have been suggested (§ 3.3). The

proposed approaches all share a common basic concept, that the error sources which affect the system are broken down into individual error components and are modelled separately. The differences between the various techniques come from the way in which the different error components are modelled.

The WADGPS concept is being employed in the proposed Global Navigation Satellite System (GNSS), a navigation system designed to meet specified user requirement criteria, in order to provide worldwide sole means navigation system for civil aviation up to category I landing. This concept is being employed in the form of regional systems such as: the European Geostationary Navigation Overlay Service (EGNOS), which is being developed by the Tri-Partite group (Eurocontrol, European Commission and European Space Agency) and scheduled to reach Full Operation Capability (FOC) in the year 2002 (Watt and Storey, 1995); the US Wide Area Augmentation System (WAAS), under the control of the US Federal Aviation Administration (FAA) and planned to reach 'end state' in the year 2001 (Loh *et al*, 1995); and the Japanese Multi-functional Transport SATellite (MTSAT) Satellite-based Augmentation System (MSAS), which is expected to reach initial phase of operation using MTSAT-1 in 2001, and the operation with MTSAT-1 and MASAT-2 is expected to commence in 2005 (Takagi, 1995).

The proposed WADGPS approaches at Nottingham are based on the separation of the error sources into different components. The bundled differential correction in conventional DGPS is broken down into (i) an independent precise ephemeris (not affected by the effect of SA), and transmitted to the user to replace the broadcast ephemeris, (ii) regional optimised atmospheric parameters transmitted to the user to estimate local atmospheric delays and (iii) the remaining errors, assumed to be clock related, transmitted to the user for all satellites in view of the reference network. The pseudorange measurements are the only observable used in the system, since the problems of the integer ambiguities and cycle slips associated with the carrier phase make it unattractive for real time applications.

A key issue in the modelling of the system errors is the type of observable used. The availability of the second frequency plays a very important role in the task of the overall error modelling, as it allows the ionospheric errors to be largely isolated, enabling the other errors to be precisely modelled. However, the implementation of Anti-Spoofing (A-S) (§2.6.4), has meant that the second frequency is only accessible to the US DOD and its authorised users. Since the availability of the L2 frequency is not guaranteed, the design of the WADGPS system should also consider the single frequency scenario.

The WADGPS system proposed by Ashkenazi *et al* (1993), was based on single frequency receivers at both reference and user sites. The use of entirely single frequency receivers was imposed on the research project commissioned by Inmarsat at that time (Ashkenazi *et al*, 1993). The reason for using only single frequency receivers was mainly due to the implementation of A-S which would render the second frequency unavailable for ionospheric delay estimation. However, with the technology advances, some forms of relatively precise second frequency range measurements can be available even under A-S (§2.4). As a result, the 'refined' Nottingham approach was modified to take advantage of dual frequency receivers in the system.

On the other hand, as mentioned above, since the US government only provides the GPS SPS, based on a single frequency, to civilian users, the need for a WADGPS design, based on single frequency receivers has grown significantly over the recent years, especially amongst government agencies and users. Hence research on the design of a single frequency WADGPS system was further investigated, and a new technique, which is capable of providing accurate orbit determination and ionospheric error modelling and hence resulting in high precision user positioning, is proposed.

The scenarios for data processing, error modelling and analysis, and the corresponding software that has been developed for the proposed WADGPS

algorithms, have been assessed by both simulations and with real field data. The simulation studies were essential to assess the sensitivity and capability of the algorithms and the models, as well as to test the correct coding of the software. Simulation data has one major advantage over real field data, in that the errors which affect the system can be defined precisely before the tests. These can then used to study and analyse the system performance. Of course, tests with real data are essential to assess the system's overall performance and to validate the simulation studies. It is the performance with real data that will decide whether the system is feasible or not. Extensive simulation tests were carried out, repeatedly achieving a positioning accuracy of the order of about 1 to 2 m (RMS) in plan and 2 to 3 m (RMS) in the height, with both single and dual frequency methods. Results from real field data showed that a positioning accuracy of better than 2.4 m (RMS) in plan and 2.8 m (RMS) in the height was achieved by both single and dual frequency approaches.

A brief description of the GPS system, the error sources and positioning models with an emphasis on DGPS is given in Chapter 2. The general concept of WADGPS is reviewed in Chapter 3, highlighting some of the different approaches already proposed and the WADGPS single frequency receiver approach proposed at Nottingham. The refined WADGPS methods, which include the dual frequency and the refined single frequency algorithms, are presented in Chapter 4. Chapter 5 describes the software developed for this research project and the difficulties encountered in the software development. Chapter 6 details the simulation studies and presents the results for both the single and dual frequency algorithms. The final system feasibility was assessed by the use of real field data, the results of which are presented and discussed in Chapter 7. Chapter 8 details the conclusions from this research and suggestions are provided for further work.

Chapter 2

The Global Positioning System and Error Sources

2.1 The Basic Concept

The NAVSTAR (NAVigation Satellite with Timing And Ranging) Global Positioning System (GPS) is a satellite-based, passive positioning system developed by the United States Department of Defense (US DoD). It was designed to provide high accuracy, instantaneous and continuous position, velocity, and time information in all weather to users world-wide. Basically, a GPS receiver simultaneously measures the so called 'pseudoranges' (§ 2.5.1) between its antenna and the GPS satellites. With the knowledge of the positions of the satellites, the coordinates of the user antenna can be estimated using these pseudoranges in an appropriate reference frame. GPS has been employed for a wide variety of applications and has been well documented in papers and textbooks, such as *King et al* (*1987*), *Wells et al* (*1987*), *Leick* (*1990*), *Seeber* (*1993*), and *Hofmann-Wellenhof et al* (*1994*).

A broad overview of certain GPS aspects of particular relevance to this research projet is given in this chapter. For full details the reader is referred to the above textbooks. Particular emphasis is given to the characteristics of the error sources of GPS positioning which are of great interest to the error modelling in the WADGPS algorithms.

There are two levels of accuracy provided by GPS, notably the Standard Positioning Service (SPS) and the Precise Positioning Service (PPS). The SPS, affected by the Selective Availability (SA) and Anti Spoofing (A-S), provides an accuracy of around 100 m (2drms) in plan, and 156 m in height, 95% of time. The PPS is only accessible to US DoD and other authorised users. Such users employ a cryptographic key to remove the SA and A-S effects to get the full GPS accuracy of around 16 m in plan, and 23 m in height, at the 95% probability level (DoD/DoT, 1992). SA is a method of deliberately degrading the GPS navigation accuracy and A-S is a method of protecting against hostile imitation of PPS.

SA was activated on March 25, 1990. A-S was exercised intermittently during 1993 and implemented on January 31, 1994. At the time of writing (April 1996), the SA and A-S are still in place. However, the latest GPS policy announced on March 29, 1996 by the US White House (The White House, 1996) has given guidelines as,

'It is our intention to discontinue the use of GPS Selective Availability (SA) within a decade .....'

The actual impact of this policy guideline is not clear yet, nevertheless, the effects of SA and A-S are still relevant to this research as they are still present at this moment.

Regarding the status of the system, the GPS Initial Operational Capability (IOC) was declared in December 1994, with a constellation of 24 GPS satellites (Block I/II/IIA). The GPS Full Operational Capability (FOC) was declared on April 27, 1995, with 24 operational satellites (Block II/IIA) effectively functioning in their assigned orbits and having been successfully tested for operational military functionality.

GPS may be considered as three segments : space, control and user, which are described in Section 2.2, 2.3 and 2.4 respectively. The observables, namely the pseudorange and carrier phase, are described in Section 2.5. The error sources and the positioning model are described in Sections 2.6. and 2.7 respectively. Section 2.8 gives a brief discussion of the system integrity.

2.2 Space Segment

The fully operational space segment consists of 24 satellites evenly spaced in six orbital planes inclined at 55°. The satellites orbit the earth at an altitude of approximately 20,200 km, once every 12 sidereal hours. The basic observable of GPS is the range, derived from the difference between the transmission time of a signal at the satellite and to reception time at the receiver.

Five types of GPS satellites have been designed so far, namely the Block I, Block II, Block IIA, Block IIR and Block IIF satellites. The first series of satellites, Block I satellites, were launched between 1978 and 1985. The last operational Block I satellite (SVN10 or PRN 12), remained in operation until the end of 1995. The constellation of the Block I satellite was slightly different from the later satellites, as the orbits are inclined at 63°, due to an earlier design, compared with the later ones being inclined at 55°. The second type of satellites, the Block II satellites, were first launched in February 1989. From this generation of satellites onwards, the signals have been restricted to US DoD authorised users only, and civilian users have not necessarily had access to the full capabilities all of the time (Hofmann-Wellenhof *et al*, 1994). The Block IIA satellites are capable of mutual communication and some of them can be tracked by laser ranging, the first being launched in November 1990. The Block IIR satellites are designed to have on-board hydrogen masers which are at least one order of magnitude more precise than the current caesium and rubidium clocks equipped on Block II satellites. The Block IIR satellites also have improved facilities for mutual communication, measurements of distance between satellites (crosslink ranges) and on-board ephemeris computation

(Seeber, 1993). The launch of the first Block IIR satellite is scheduled for August 29, 1996, the Block IIF satellites are still under design and are expected to be launched between 2001 and 2010 (Catania, 1995).

The current GPS Block II satellites have two rubidium and two caesium clocks on board with a stability between a few parts of 10^{-13} to 10^{-14} over one day. The hydrogen masers planned for Block IIR's have a stability of 10^{-14} to 10^{-15} over one day (Seeber, 1993). The high performance time standards are the key element to maintain to the system's accuracy, as all signal components are well controlled by these atomic clocks.

GPS satellites transmit at two L-band frequencies L1 (1575.42 MHz) and L2 (1227.6 MHz), both derived from the fundamental frequency of the GPS signal, f_0, of 10.23 MHz. The resulting wavelength of L1 and L2 frequencies are approximately 19 cm and 24 cm respectively. PRN (Pseudo Random Noise) codes are modulated on to the L1 signal to give the Coarse/Acquisition (C/A) codes with a frequency of 1.023 MHz ($f_0/10$) and a period of 1 millisecond. The approximate wavelength of the C/A code is about 300 m. The precise (P) code, with a frequency of 10.23 MHz and a period of 267 days, has a corresponding wavelength of about 30m. The C/A-code is modulated on to the L1 signal only, whilst the P code is modulated on to both the L1 and L2 signals. Under A-S active condition, the P-code is modulated by a relatively simple 50 bps W code which is unknown to unauthorised users. The P+W code is commonly referred to as the Y-code.

Since the P-code is so complicated and difficult to acquire, the navigation message contains the Hand-Over-Word (HOW) to tell the receiver where to search and lock on to the P code. The navigation message also contains the satellite ephemeris, satellite clock correction coefficients, 8 ionospheric Klobuchar parameters, satellite health information and an almanac. The almanac is the approximate ephemeris used for initial acquisition of satellites.

There are various systems used for the identification of satellites. Commonly used are the PRN (pseudo random noise), or SVID (space vehicle identification) numbers. The PRN denotes which of the 37 seven-day segments of the P-code PRN signal is presently used by each particular satellite. The SVN (space vehicle number) or NAVSTAR number, based on the launching sequence, is also sometimes used (Wells *et al* , 1987, Seeber, 1993).

2.3 Control Segment

The control segment consists of the Monitor Stations (MS), the Ground Antennas (GA) and the Master Control Station (MCS). There are five Monitor Stations distributed around the world with well known coordinates: Hawaii, Ascension Island, Colorado Springs, Kwajalein and Diego Garcia. Each MS is equipped with a precise caesium time standard and they continuously track all the satellites in view (Hofmann-Wellenhof *et al*, 1994).

The Master Control Station is located at Colorado Springs, Colorado, which collects tracking data from the MSs for satellite ephemeris and clock correction computation. This information is then transmitted to one of the GAs for uploading to the satellites.

Three Ground Antennas, located at Ascension Island, Diego Garcia and Kwajalein, collect the satellite ephemeris and clock information computed at the MCS and upload this information to the satellites. The uploading was formerly carried out every eight hours (Stein, 1986), but has been reduced to once (or twice) per day (Remondi, 1991).

2.3.1 GPS Reference Time System

GPS measurements are based on the time system. The measured time elapsed from when a signal leaves the satellite to when the receiver receives it, is used to compute the pseudorange. Obviously, a highly stable time system is

required to refer all the timing to the same system. The time system used by GPS is its own particular time scale, GPS time. The GPS time is an atomic time scale which has the same unit (seconds) as the UTC (Coordinated Universal Time). GPS time was coincident with UTC on January 6, 1980. As the GPS time is not corrected by leap seconds, which cause discontinuity in GPS navigation, the difference between GPS and UTC time is increasing. The relationship between UTC and GPS time is available in time bulletins of the USNO (United State Naval Observatory) and the BIPM (International Bureau of Weights and Measures) as well as the GPS satellite message (Seeber, 1993). The GPS time is kept within 100 nano-seconds of UTC, ignoring the leap seconds (Milliken, 1980).

2.3.2 GPS Reference Frame

GPS uses the World Geodetic System WGS-84 (Figure 2.1) as a reference, which provides the basic reference frame for the description of the satellite motion, the modelling of the observables, and the representation and interpretation of results in an Earth-centred and Earth-fixed system (Seeber, 1993). The origin and axes of WGS-84 are adopted from the Conventional Terrestrial System (CTS), which is defined by the former Bureau International de L'Heure (BIH). Note that this service is taken over by the International Earth Rotation Service (IERS) on January 1, 1988.

As shown in Figure 2.1, the origin of the WGS84 is located at the centre of mass of the Earth. The Z-axis is parallel to the direction of the Conventional Terrestrial Pole (CTP). The X-axis is the intersection of the WGS84 reference meridian plane which is parallel to the zero meridian defined by the BIH, and the plane of the CTP's equator. The Y-axis completes the right-handed, earth-fixed orthogonal coordinate system perpendicular to X-axis and Z-axis (DMA, 1987).

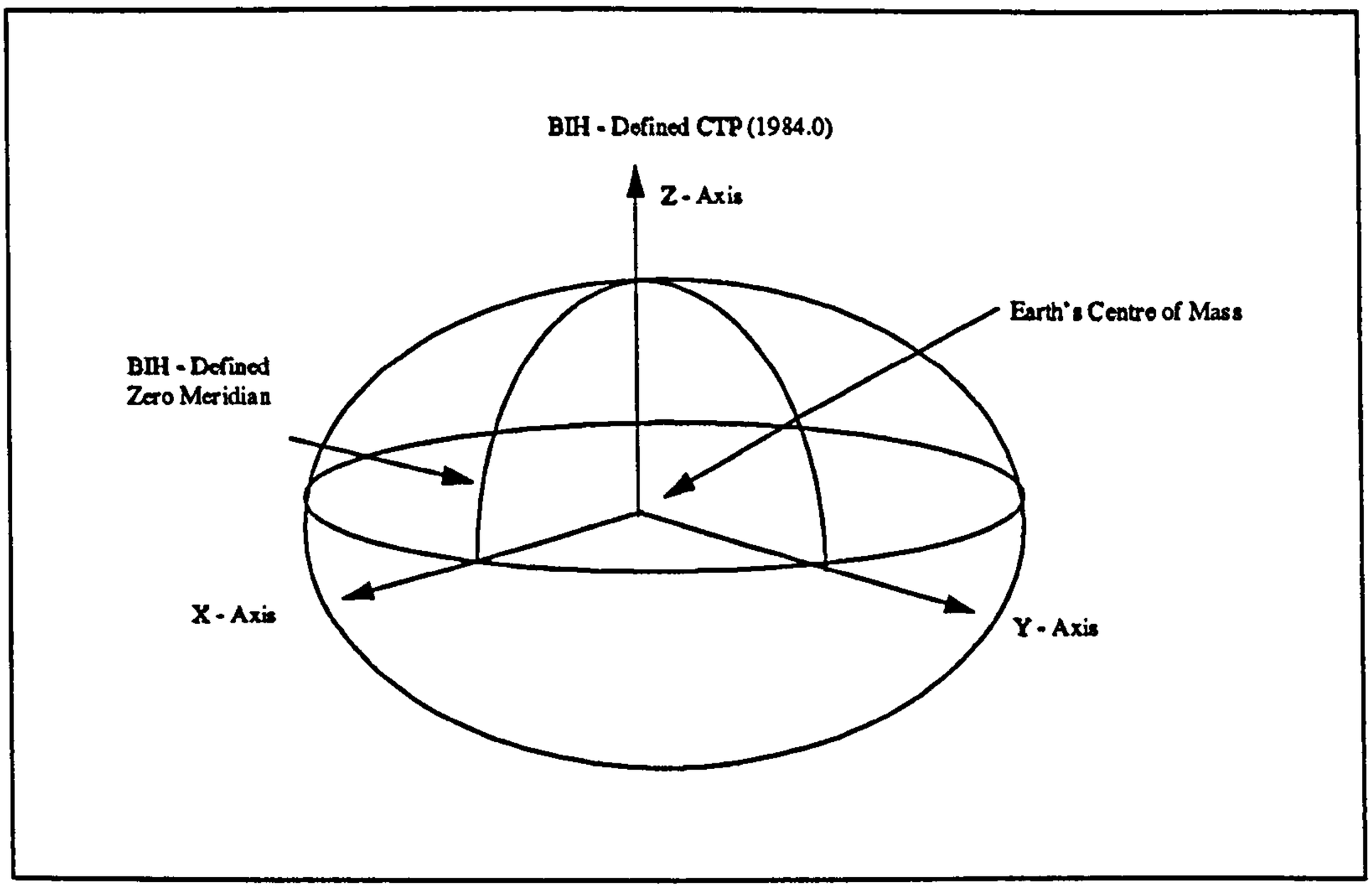

Figure 2.1 WGS-84 Reference Frame

A geocentric equipotential ellipsoid, the Geodetic Reference System 1980 (GRS80), is associated with WGS-84 which provides a best fit to the global geoid. Although the system is defined in such terms, it is difficult to realise such a system as coordinates on the earth. The origin and orientation of the axes of WGS-84 are therefore implicitly defined by a total of 1591 TRANSIT (Doppler) stations around the world determined by the US Defence Mapping Agency (DMA), accurate to 1 to 2 metres. By co-locating TRANSIT and Very Long Baseline Interferometry (VLBI) and Satellite Laser Ranging (SLR) stations, the positions are scaled, rotated and shifted to give WGS-84 (Moore, 1992). For more details of WGS-84 the reader are referred to DMA (1987) and White *et al*, (1989).

2.3.3 IERS Terrestrial Reference Frame (ITRF)

The International Earth Rotation Service (IERS) maintains the most important reference frame, the so-called IERS Terrestrial Reference Frame (ITRF). The IERS, replacing the BIH since January 1, 1988, was jointly established in 1987

by the International Astronomical Union (IAU) and the International Union of Geodesy and Geophysics (IUGG). The ITRF is defined annually by the IERS through a least squares adjustments using coordinates from a global network of stations, which are determined based on precise space techniques, such as VLBI, SLR, LLR (Lunar Laser Ranging) and GPS. Through the analysis of individual data sets obtained by different space techniques and the integration of individual solutions into a unified set of data, the station coordinates and earth orientation parameters can be defined. A velocity field of the motions of the stations has also been included since 1991. The ITRF provides the fundamental definition of the position of the centre of mass of the earth to within 10 cm, and the orientation of the axes to correspondingly high accuracies (Boucher *et al*, 1992, 1993).

The ITRF coordinates of terrestrial stations and their velocity fields are published annually in the IERS annual report or relevant IERS technical notes. The coordinates of the reference stations used in the real data tests in this research are based on ITRF91 (epoch 1992.5), which has a global accuracy of better than 3 cm level (Boucher *et al*, 1992).

2.3.4 Ephemerides

The positions of the satellites have to be known in order to determine the coordinates of the receivers. The GPS satellite positions are provided in three different forms, namely the almanac, the broadcast ephemerides and the precise ephemerides.

- **The Almanac Data**

The almanac data is used for the initial acquisition of satellites or for pre-planning of an observation campaign. The almanac, broadcast via the satellite navigation message, contains less accurate parameters for the orbit representation, satellite clock corrections and other information for all available

satellites. The satellite positions therefore, can be calculated in the WGS-84 coordinate system using the almanac data. With the approximate information of the receiver coordinates, the visibility, azimuth and elevation of the satellites can be calculated as a function of time. The almanac data has an accuracy of some kilometres, and may be valid for several months for planning purposes (Hofmann-Wellenhof *et al*, 1994, Seeber, 1993).

- **The Broadcast Ephemerides**

The broadcast ephemeris is generated by an orbit integration process which involves modelling all the forces acting on the satellites and observations from the five monitor stations. The broadcast ephemeris is predicted using two steps. Firstly, a reference orbit is calculated by a least squares fit based on seven days of observations from the five monitor stations. Secondly, a Kalman Filter is applied with current measurements to estimate an improved satellite orbit for future prediction (Wells *et al*, 1987). The MCS is responsible for the production of the broadcast ephemerides and the subsquent uploading to the satellites.

Basically, the broadcast ephemeris consists of six Keplerian parameters which describe a smooth orbital ellipse at a reference epoch, the satellite clock coefficients and some related perturbation parameters. A fresh set of parameters is broadcast every hour and is valid for about 2 hours before and two hours after the reference epoch (Seeber, 1993). The satellite orbit calculated from broadcast ephemeris could be accurate to 5 m, based on 8 hours update rate (Remondi *et al*, 1989). Under the FOC condition, the broadcast parameters are uploaded once (or twice) a day, the satellite orbit accuracy of 10 m is expected (Hofmann-Wellenhof *et al*, 1994). However, under the implementation of SA, the satellite orbit error could rise to several hundred metres (Loomis *et al*, 1991).

- **Precise Ephemerides**

The precise ephemerides have a much better accuracy than the broadcast ephemerides, as a precise ephemeris is not predicted but calculated based on observations from a global tracking network. The precise ephemerides are provided by several institutions with some 4 to 14 days delay. The precise orbits provided by IGS are estimated to be accurate to 1 to 2 metres, using 3 day arcs. With a 7 to 14 day arcs, the orbit accuracy of the order of 20 cm has been reported by Beutler *et al* (1994).

Traditionally, precise ephemerides were determined by the US Defence Mapping Agency (DMA) based on observations collected at 10 globally distributed stations. Orbits from a global network have a higher accuracy and reliability than those determined from regional networks. Several civilian tracking networks have been set up. The Cooperative International GPS Network (CIGNET) is operated under the coordinating responsibility of the US National Geodetic Survey (NGS). The coordinates of the CIGNET sites refer to the ITRF, while the ephemerides remain in WGS-84. The International GPS Geodynamics Service (IGS) is installed under the auspices of the International Association of Geodesy (IAG) (Muller and Beutler 1992). Both the coordinates of the IGS sites and the ephemerides are referred to the ITRF. The IGS provides precise ephemerides computed from seven analysis centres; namely CODE (Centre of Orbit Determination in Europe, Switzerland), EMR (Energy, Mines, and Resources, Geodetic Survey Division, Canada), ESA (European Space Agency, Germany), NGS (National Geodetic Survey, NOAA, USA), GFZ (GeoForschungsZentrum, Germany), JPL (Jet Propulsion Laboratory, USA), and SIO (Scripps Institute of Oceanography, USA) (Neilan, 1995). The IGS product formats, analysis and reporting have been standardised and the individual orbit solutions are aligned to the current ITRF to be evaluated and combined into the official IGS orbit solutions (Kouba, 1995).

2.4 User Segment

The user segment involves all the civilian and military user equipment that are able to receive the GPS signals and compute the user's position, velocity and time. There are many possible criteria that may be used to classify the receivers, such as the available data type, the user community, or technically through the realisation of the channels. A broad criterion of the available data type is used here to classify receivers as four types : (1) C/A-code pseudorange, (2) C/A-code carrier phase, (3) P-code carrier phase and (4) Y-code carrier phase measuring instruments (Hofmann-Wellenhof *et al*, 1994).

The C/A code pseudorange receivers only measure the pseudorange using the C/A code. This type of receiver is usually a hand-held device, basically aimed for users who do not require high navigation accuracy, typically for leisure purposes. The C/A code carrier phase receiver is capable of measuring code ranges and carrier phases from the L1 carrier. The development of some codeless techniques have enabled the receiver to access the L2 carrier. However, the signal-to-noise ratio (SNR) of the L2 carrier measurements are considerably lower than the C/A-code measurements on L1. This type of receiver is used for all types of precise surveying applications. The P-code receiver is able to measure both the L1 and L2 carriers. The P-code is removed from the carrier by the code correlation technique with the receiver generated code replica. Under A-S active condition, the P-code is replaced by the Y-code. If the code correlation technique is to be applied, the knowledge of the Y-code has to be known. The Y-code receiver, restricted to US DoD authorised users, applies an Auxiliary Output Chip (AOC) in each receiver channel, which allows the decryption of the Y-code into P-code and also the correction of the degradation imposed by SA (Hofmann-Wellenhof *et al*, 1994).

Although, the code correlation technique can not be applied under the implementation of A-S, some other codeless or quasi-codeless techniques can

be employed to provide L2 carrier measurement without the knowledge of the Y-code. Four techniques have been used by receiver manufacturers, namely, signal squaring, cross correlation, code correlation followed by squaring and P-W code tracking. These techniques, along with the traditional code correlation technique, are described briefly as follows.

- **Code Correlation**

With the knowledge of the PRN code, the receiver can generate a reference carrier modulated with a replica of the known PRN code. The incoming satellite signal is then correlated to the receiver generated signal, the signal is shifted with respect to time until optimal match reached. The time shift, ignoring the clock errors, is the time the signal took to travel from the satellite to the receiver. Since the period of the C/A code is one millisecond, it is usually used to lock onto the signal and initialise the tracking loop.

Once the two signals are aligned, the PRN code is removed from the carrier. The navigation message is also decoded, which includes the HOW for the information on which part of the P-code to search for signal correlation. A high-pass filter is then used to remove the navigation message from the carrier, resulting in a Doppler shifted carrier on which a phase measurement can be made. The major drawback of this technique is that the code modulated on to the carrier has to be known. When A-S is activated, this technique is only applicable on L1, or, on L2 for those users who can access the Y-code by the help of AOC.

- **Signal Squaring**

Without the knowledge of the code, the codeless technique may be used to demodulate the signals and hence access the carrier. The *squaring* technique is performed by multiplying the signal itself, resulting in a demodulated carrier with twice the original frequency and half the original wavelength. The

advantage of this technique is that no knowledge of the code is required and, as a result, the L2 carrier can be accessed, irrespective of whether A-S is activated or not. However, the navigation message is lost during the squaring process and therefore an external almanac is required. The resulting carrier, with half of the original wavelength, also increases the difficulty in the solution of the integer ambiguity. Furthermore, the SNR is considerably reduced by 30 dB compared with the code correlation technique (Ashjaee, 1993). This technique was used by many old version receivers, such as the Trimble, Ashtech and Minimac receivers.

- **Cross Correlation**

An alternative codeless technique used when the code is not known and applied by some new receivers, such as the Trimble 4000 SSE and Turbo Rogue, is the *cross correlation* technique. This technique relies on the fact that although the Y-codes are unknown, they are identical on both the L1 and L2 carriers, which can be utilised for cross correlation of the L1 and L2 signal. Due to the ionospheric effects, the Y-code on L2, with a lower frequency than L1, always arrives at the receiver later than the Y-code on L1. The difference in the travel time between the two signals can be obtained by cross correlation of the two signals. The delay is properly adjusted to ensure maximum correlation between the L1 and L2 signals. The time difference is equivalent to the $(Y_2\text{-}Y_1)$ pseudorange. As a result, two observables are generated, namely, the time difference of Y-code on the two carriers and a phase difference from the beat frequency carrier. These two observables are then added to the L1 C/A code pseudorange to derive the L2 code range and phase. This technique generates a full wavelength L2 carrier wave. The SNR is improved by 3 dB over the squaring technique, i.e. 27 dB lower than the code correlation technique (Ashjaee *et al*, 1992).

- **Code Correlating Squaring**

The improved *code correlating squaring* technique is based on the fact that the Y-code is made up of the P-code and the W-code, and that the frequency of the W-code is about 20 times less than the Y-code frequency. Therefore there are always certain portions of the Y-code that are identical to the original P-code (Hofmann-Wellenhof *et al*, 1994). The L2 Y-code signal is correlated with a locally generated replica of the underlying P-code, a low-pass filter is applied by narrowing the bandwidth and subsequently squared to remove the code.

This technique provides the code range and half-wavelength carrier on L2. Due to the narrowed bandwidth, this technique provides a SNR improvement of 13 dB, compared with the direct squaring technique. The SNR degradation of 17 dB is expected compared with the code correlation technique.

- **P-W Tracking**

The latest development of the technique to counter A-S, applied by Ashtech in the ZXII series, is *P-W tracking*. In the signal tracking technique, satellite signals are correlated with locally generated replicas of the P-code and integrated over W-code chip intervals. The L1 and L2 signals are first correlated with a locally generated replica of the P-code separately. This is based on the fact that the Y-code is identical on both L1 and L2 and the W-code has a relative low frequency rate encryption. The bandwidth is then reduced to that of the encrypting W-code, and with enough integration of signal, it is possible to estimate the current value of the W-code for each frequency. This estimated W-code is then fed to the other frequency to remove the encrypting code from the signal (Ashjaee, 1993).

This technique effectively retrieves the same observables as when A-S is not activated. The available observables are code ranges, C/A and Y_1 code on L1,

Y_2 code on L2, and full wavelength L1 and L2 carriers (Ashjaee *et al*, 1992). The SNR is improved by 3 dB compared to code correlating followed by squaring. However, an SNR degradation of 14 dB occurs, compared with the code correlation technique.

2.5 The Observables

There are two fundamental GPS observables : (i) pseudorange, which is primarily used for navigation and (ii) carrier phase, used for high precision positioning applications.

2.5.1 Pseudorange Observable

When the incoming code transmitted from the GPS satellite matches the locally generated replica via a code correlation process, the time difference between the transmitted and received signals, multiplied by the speed of light in a vacuum results in the pseudorange between the satellite and the receiver. As the satellite and receiver clocks are not perfectly synchronised with each other and GPS time (§ 2.3.1), i.e. they operate in different time frame, the resulting distance is termed 'pseudorange', instead of the true range.

The pseudorange is the primary GPS observable usually used for navigation. Two different codes are available for GPS, Coarse/Acquisition (C/A) and Precise (P) code, the wavelengths of which are 300 m and 30 m, respectively. Traditionally, the precision of the pseudorange is derived from 1% of the chip length, which equates to about 3 m and 0.3 m for C/A-code and P-code respectively (Wells *et al*, 1987). Recent developments have demonstrated the ability of achieving a precision of about 0.1% of the chip length (Hofmann-Wellenhof *et al*, 1994).

The basic pseudorange observation equation is given by:

$$\rho = \rho_t + c(dt - dT) + d\rho_{ion} + d\rho_{trop} + \Delta(\rho) \qquad (2.1)$$

where,

ρ	:	observed pseudorange measurement
ρ_t	:	true range
c	:	speed of light in a vacuum
dt	:	the offset of the satellite clock from GPS time
dT	:	the offset of the receiver clock from GPS time
$d\rho_{ion}$	:	ionospheric error
$d\rho_{trop}$	:	tropospheric error
$\Delta(\rho)$	:	pseudorange noise and multipath

The true range is a function of the ground station and the satellite positions. The satellite positions are obtained using the satellite ephemeris. The satellite clock correction parameters are obtained from the broadcast navigation message. If the ionospheric and tropospheric range errors are modelled and assumed to be correct, the only unknowns remaining in equation (2.1) are the receiver clock bias and the coordinates of the ground station. The coordinates of the receiver (X_r, Y_r, Z_r) are contained implicitly in equation (2.1), and may expressed by the relation with the satellite coordinates (X^s, Y^s, Z^s) given as :

$$\rho_t = \sqrt{(X^s - X_r)^2 + (Y^s - Y_r)^2 + (Z^s - Z_r)^2} \qquad (2.2)$$

At least four satellites are required to provide four observations to solve for the four unknowns (three ground station coordinates and one receiver clock bias). The un-modelled errors such as multipath and measurement noise are assumed to be random and are included as a residual term in a least squares solution.

- **Phase Smoothed Pseudorange**

The phase smoothed pseudorange (§ 4.6) is the observable created by the linear combination of the code pseudorange and carrier phase observables. This

technique was first proposed by Hatch (1982), similar algorithms was later proposed by Lachapelle *et al* (1989, 1991). The phase smoothed code is generated by proper weighting between the code pseudorange and carrier phase observables, resulting in an observable which is less noisy than the code pseudorange. However, as the carrier phase is sensitive to cycle slips, it is critical to detect and repair cycle slips to avoid introducing a bias into this observable. The phase smoothed pseudorange is also affected by the problem of code and carrier divergence, the effects of the ionospheric delays on the code and carrier phase are of the same magnitude but of a different sign. The effects may be minimised by the use of the dual frequency ionospherically-free measurements (Hofmann-Wellenhof *et al*, 1994).

2.5.2 Carrier Phase Observable

The carrier phase observable can be obtained by removing the code from the incoming signal. The wavelengths of the carrier frequencies are 19 cm and 24 cm for L1 and L2 respectively. The phase difference of the carriers can be accurately measured to better than 0.01 cycle, which with wavelength of about 20 cm equates to millimetre precision. This makes it possible to obtain very precise positioning using the carrier phase observable. The distance between the satellite and receiver is obtained by measuring the fractional part of the carrier phase, plus the total number of cycles between the satellite and the receiver, which is given as,

$$\lambda\Phi = \rho_t + c(dt - dT) - \lambda d\Phi_{ion} + d\rho_{trop} - \lambda N + \Delta(\Phi) \qquad (2.3)$$

where,

Φ : carrier phase measurement

$d\Phi_{ion}$: ionospheric error on carrier measurements

λ : carrier wavelength

N : integer ambiguity

$\Delta(\Phi)$: carrier phase measurement noise and multipath

The receiver is able to count the change in the number of cycles but not the number of cycles travelled through before the receiver starts to count the cycles, which is referred to as the 'integer ambiguity'. The integer ambiguity remains the same as long as the receiver phase lock loop is maintained. If the signal is lost, resulting in a 'cycle slip', the integer ambiguity needs to be computed again. The cycle slip and integer ambiguity problems have been intensively studied in order to attempt to provide a high accuracy service (Ashkenazi *et al*, 1989c; Walsh, 1993).

2.6 Error Sources

The GPS measurements are subject to errors, notably systematic errors, random errors and gross errors (blunders). Systematic errors have to be removed from the measurements to avoid introducing biases to the results. These errors usually have some physical or mathematical relationship with the measurements and can be modelled as additional terms in the observation equations, or eliminated by appropriate combinations of the observables. Gross errors are those which are obviously outliers in the observation model. The random errors are the discrepancies remaining after the systematic errors and blunders have been detected and removed. For convenience here, the GPS errors are classified into groups by their sources and described accordingly in the following sections.

2.6.1 Satellite Dependent Errors

- **Satellite Orbital Error**

The positions of the satellites are required in order to form the GPS observation equations. The satellite orbit information is provided either in the form of the broadcast ephemeris or precise ephemeris. During GPS data processing, the orbit is usually held fixed so as to solve for the unknown station position, therefore the orbit error propagates directly into the coordinates of

the receiver. This effect may be reduced by differencing techniques. However, as the baseline length increases, the remaining errors experienced at the two different stations will be different, and varying depending on the viewing angle of the satellites. As a result their effect on the positioning accuracy becomes more significant.

A simple but useful rule-of-thumb (equation 2.4) shows the baseline errors as a function of satellite orbital error and the length of the baseline, as given by Wells *et al* (1987),

$$\frac{\Delta r}{\rho} \cong \frac{db}{B} \qquad (2.4)$$

where,

Δr is satellite orbital error,

ρ is the satellite to receiver range, ($\cong$ 20,000 km)

db is baseline error with respect to Δr,

B is the baseline length.

The accuracy of the satellite position given by broadcast ephemeris is no better than 10 m under Full Operational Capability (FOC) (Hofmann-Wellenhof *et al*, 1994). The accuracy of the IGS provided precise ephemeris is estimated at 1 to 2 meters level (Beutler *et al*, 1994).

- **Satellite Clock Error**

GPS satellites carry both rubidium and caesium atomic frequency standards. The clocks are physically left to drift off the GPS time but are kept within one millisecond of UTC. The clock behaviour is carefully monitored and the error is included in the broadcast message in the form of coefficients of a second order polynomial as given in equation (2.5) :

$$dt = a_0 + a_1(t - t_{0C}) + a_2(t - t_{0C})^2 \qquad (2.5)$$

where,

t_{0C} is some reference epoch,

a_0 is the satellite clock time offset

a_1 is the fractional satellite clock frequency offset

a_2 is the fractional satellite clock frequency drift (ageing term)

The size of the satellite clock bias without corrections is of the order of 1 ms, corresponding to 300 km in terms of range. This reduces to about 30 ns (10 m) with corrections (Wells *et al*, 1987).

- **Relativity and Group Delay**

The fundamental frequency of the satellite clock is affected by both the motion of the satellite (special relativity) and the difference of the gravitational field at the satellite and the observing site (general relativity). The effects are compensated by introducing an offset in the fundamental frequency, resulting in an emitted frequency of 10.22999999453 MHz (Spilker, 1980).

The effects of relativity are also relevant for the satellite orbit, the receiver clock and the signal propagation. These effects are compensated for by differencing observations and therefore can be neglected. For details of relativity effects the reader is referred to Zhu *et al* (1988).

Group delay is caused by the processing and passage of the signal through the satellite hardware. The effects are calibrated prior to the launch of the satellite during the ground tests. The corrections are included as part of the satellite clock coefficients. The remaining uncertainty is of the order of 1 metre (Milliken *et al*, 1978).

2.6.2 Receiver Dependent Errors

- **Receiver Clock Offset**

The receivers are generally equipped with quartz crystal clocks. The quality of a quartz crystal clock is not as good as either a rubidium or caesium clock. For this reason, many receivers accept external timing from an atomic standard. The receiver clock offset is usually treated as an extra parameter along with the receiver coordinates to be solved for as part of a least squares solution.

- **Interchannel Biases and Antenna Phase Centre**

Interchannel biases are the offsets that occur between different channels when each channel is dedicated to track a particular satellite in a multi-channel receiver. These biases can be calibrated by tracking the same satellite simultaneously at each channel, therefore an offset is determined with respect to a reference channel. The corrections are accordingly applied to all subsequent measurements.

The geometric antenna centre is not coincident with to the phase centre that the signal measurements are referred to. Depending on the satellite elevation and azimuth, the intensity and frequency of the signal, the offset varies. These variations have to be taken into account, if high accuracy GPS measurements are required. The phase centres are indicated by manufacturers and the variations are kept to an minimum. Some GPS data processing software, such as the Nottingham GAS software (§ 5.2), applies antenna phase centre variation models to model the effects of the variations.

2.6.3 Signal Path Dependent Errors

GPS measurements are subject to errors when the signal passes through the earth's atmosphere which not only bends the ray, but also slows it (Dodson

et al, 1992). The errors are due to two components: (i) the excess path length due to propagation delay and (ii) the excess path length due to bending. The bending effect is usually not significant except at low elevation angles. In most geodetic purposes, these errors can be satisfactorily modelled (Dodson, 1986). Nevertheless, a cut-off angle (typically 15°) is usually specified as a threshold for recording GPS measurements to avoid observations at low elevation angles.

The propagation delay is estimated by the integral of the atmospheric refractive index along the signal path. The atmosphere may be considered as two distinct components, namely the ionosphere and the troposphere, which have different physical characteristics and should be modelled separately.

- **Ionospheric Error**

The GPS electromagnetic signals are affected by the ionised medium when propagating through ionosphere. The ionosphere results in a non-linear dispersion of the signal which is a function of the signal frequency. The relationship between the refractive index, n, in the ionosphere and the frequency is given by Dodson (1986) as,

$$n = 1 \pm \frac{A_1 N_e}{f^2} + \textit{higher order terms} \qquad (2.6)$$

where,

A_1 is a constant (40.3 if using S.I. units),

N_e is the free electron density in the ionosphere (electrons/m^3),

f is the frequency of the signal (Hz).

The $\pm$ sign in equation (2.6) is determined by which observables are considered. The ionosphere delays the GPS code pseudorange, i.e. the observed code range is always too long and hence the positive sign is applied. In contrast, the ionosphere advances the carrier phase, i.e. the observed carrier phase range is always too short and thus the negative sign is applied. The

range errors caused by the ionosphere vary from tens of centimetres to tens of metres depending on the Total Electron Content (TEC) along the signal path through the ionosphere. The TEC is affected by the activity of the sun, which ionises the electrons by emitting ultra-violet and X-ray radiation. As a result, a number of well known periodicities, including the 11 years sun spot cycle, a seasonal cycle and a diurnal cycle are evident in the state of ionosphere. The last maximum in the 11-year sun spot cycle happened in 1990/1991 (Dodson *et al*, 1992). The irregularity over these cycles caused by the magnetic storms makes the prediction of the TEC very difficult.

Since the ionospheric delays are dependent on the signal frequency, the combination of dual frequency observables can be used to estimate the delay (§ 4.2). For single frequency users, the ionospheric delay remains one of the major error sources, which can be corrected by the established ionospheric models. One of the many existing models, the Bent model, can account for up to 80 % of the ionospheric effect but is extremely complex and involves a lot of computations (Llewellyn and Bent, 1973). The Klobuchar model is a simple ionospheric model which is basically a cosine wave expressed as a function of local time and geomagnetic latitude with a daily peak at 14:00 hour local time, and a constant value at night (Klobuchar, 1977, 1982). The Klobuchar model can accommodate about 50 % of the total effect which is a compromise between accuracy and the computational complexity.

The use of a standard ionospheric model for single frequency receiver users in a fairly large network, such as the size of a Wide Area DGPS (WADGPS) network, is not enough. The localised effects in the network have to be taken into account to improve the accuracy of the estimation of the corresponding delays. In the Nottingham WADGPS algorithms, the locally best fitted ionospheric correction model is generated based on the ionospheric delays estimated by various methods at the reference stations (§ 4.2, 4.7.2).

- **Tropospheric Error**

The troposphere is not a dispersive medium at radio frequencies, hence the use of the combination of dual frequency measurements to estimate the propagation delays that works for the ionosphere cannot be applied for the troposphere. The tropospheric delay, T_r^s, is estimated by the integral of the refractive index, n, along the tropospheric signal path, s, which can be given as,

$$T_r^s = 10^{-6} \int_a^b N ds \tag{2.7}$$

where,

$N = (n\text{-}1) \times 10^6$, the refractivity

a and b define the limits of the troposphere boundary

Smith and Weintraubcan (1953) provide a model for the tropospheric refractivity, dependent on the pressure (P), temperature (T) and partial water vapour pressure (e), given as,

$$N = 77.6\frac{P}{T} + 3.73 \times 10^5 \frac{e}{T^2} \tag{2.8}$$

where,

P	is the total atmosphere pressure (mbars)
T	is the absolute temperature (Kelvin)
e	is the partial water vapour pressure (mbars)

The refractivity, N, can be considered as two terms as shown in equation (2.8). The first term is the dry part and the second term is the wet part. The dry component is responsible for about 90 % of the total zenith range error and may be reasonably modelled using surface meteorological data. The wet component contributes only about 10 % of the delay but is very complex and not easily modelled as accurately as the dry component. This is because the wet component is sensitive to the water vapour pressure along the signal path

and the measurements at the antenna site are not able to represent the variations. The range error caused by tropospheric delays vary from about 2 m at the zenith to up to about 20 m at 10° above horizon (Wells *et al*, 1987; Shardlow, 1994).

There are several techniques available for measuring the water vapour pressure along the signal path, such as a Water Vapour Radiometer (WVR), details of which are given by Shardlow (1994). However, the use of WVRs is not practical for WADGPS because of the expense and inconvenience. In terms of WADGPS accuracy potential, the modelling of the dry part of the tropospheric delay together with the GPS measurements in a least squares adjustment process, should provide the required accuracy. The refractivity is sensitive to the physical parameters in equation (2.8), the variations of the parameters to cause 1 ppm change in the refractivity are listed in Table 2.1 (Shardlow, 1994).

Table 2.1 Sensitivity of Parameters to Refractivity (after Shardlow, 1994)

Parameter	**Sensitivity**
Pressure (P)	4 mbars
Temperature (T)	1 Kelvin
Partial water Vapour Pressure (e)	0.2 mbars

From Table 2.1, it is clear that the surface meteorological (SM) measurements have to be validated carefully to avoid any bias being introduced by the poorly-calibrated equipment or carelessness. Reports detailed by Shardlow (1994) indicate that in some cases, using the same tropospheric estimation procedure, the use of SM data produces poorer results than standard atmospheric data due to the problem of using often biased SM measurements (Shardlow, 1994).

The Magnet model (§ 4.3.1), implemented by Texas Instruments, is an empirical model which does not require any meteorological data (Curley, 1988). The model assumes that the tropospheric delay is a function of the atmospheric pressure which is based on the Julian Day (JD), station latitude

and height. Consequently, the wet part of the delay is neglected in the model. However, if the wet part of tropospheric delay is estimated with the GPS measurements in a least squares adjustment, in many cases, the model performs comparably well with respect to the other SM models (Shardlow, 1994).

2.6.4 Selective Availability and Anti-Spoofing

Selective Availability (SA) and Anti-Spoofing (A-S) are two methods of denying the full use of the GPS system by civilian users. Though the latest US GPS policy guidelines (§ 2.1) make it clear that SA is going to be turned off within a decade however, at the time of writing (March 1996), SA and A-S are still in place. Since these methods for the denial of accuracy are still enforced, and when they may be removed is still not clear, the SA and A-S are described and discussed as follow.

- **Selective Availability**

SA is a method of denying the unauthorised user real-time access to the full GPS navigation accuracy as provided by the Precise Positioning Service (PPS). The navigation accuracy under SA is degraded to 100 m in plan, 156 m for height and 0.3 m/s in velocity at the 95% confidence level. SA was formally implemented on the Block II satellites on March 25, 1990. Two ways of SA are implemented, namely *epsilon* and *dither*. *Epsilon* is the alteration (degradation) of the navigation message (ephemeris), while *dither* is the manipulation of the satellite clock.

The *epsilon* part of the SA results in the orbit position being erroneous, but can be largely reduced by differencing techniques. However, for WADGPS, the satellite orbital error remains one of the major error sources, which degrades the real-time user navigation accuracy and must be modelled properly (§ 4.4). The variation of the radial orbit error, with SA activated, has been observed up to the level of several hundred metres (Hofmann-Wellenhof *et al*, 1994). The

dither part of the SA affects the system by introducing varying errors into the fundamental frequency of the satellite clocks. The effect of the SA *dither* error is position independent, i.e. all users experience the same errors and hence this error can be totally cancelled out by the differential corrections (§ 4.5), as long as the measurements are observed simultaneously.

- **Anti Spoofing**

Anti Spoofing (A-S) is a method of protecting against hostile imitation of the PPS signal. When A-S is activated, the P-code is modified to the Y-code which consists of P and W codes. Therefore the civilian users are denied access to the P-code. Only the US DoD and other authorised users are in a position to employ a cryptographic key to remove SA and A-S. A-S was tested when the satellites were first launched, and it has been activated since January 31, 1994.

2.6.5 Cycle Slip and Multipath

The cycle slip is caused by the loss of phase lock loop which generates a discontinuity in the accumulation of the integer number of cycles. The cycle slips can be caused by obstructions of the satellite signal, low SNR due to atmospheric disruptions, multipath, high receiver dynamics and low satellite elevation, and receiver software failure (Hein, 1990). The cycle slip is unlikely to affect the measurement of the fractional part of the phase, only a jump in the count of the integer number of the cycles is experienced. However, the cycle slips have to be detected and repaired to avoid introducing any bias in the measurements. Various techniques for cycle slip detection and repair have been proposed (Ffoulkes-Jones 1990).

The multipath effect is caused by the satellite signal which arrives at the receiver via more than one path, and is mainly due to reflecting surfaces near the receivers. The other minor effects are caused by reflections at the satellite

itself during signal transmission. As a result, multipath effect causes the measured range to be erroneous. While both code and carrier measurements are affected by multipath, the effect on code is two orders of magnitude larger than carrier phase observations (Seeber, 1993).

There is no general model to correct the effects of multipath as the effects are dependent on the station environment. Although, some repetitive patterns can be found in many cases from day to day static observations, when the same environment exists, this approach is not practical for real-time applications. Therefore possible measures to minimise multipath effects are carefully chosen reference sites, carefully designed antennas and some accessories such as ground planes and choke rings. The effects of multipath are also responsible for many cycle slips and are one of the major problems when code and carrier phase combination techniques are used for ionospheric delay estimation (§ 4.6).

2.7 Positioning Model

GPS data processing can be classified into two categories, namely post-mission and real-time processing. The advantages and drawbacks of the two processes are listed in Table 2.2.

Table 2.2 Comparison of Real-time and Post-mission Data Processing

	Real-time	**Post-mission**
Advantages	• result available in the field • little data storage required	• more accurate • blunder detection easier • analysis of residuals possible • no real-time data link
Drawbacks	• less accurate • data often not stored • blunder detection difficult • real-time data link needed	• result not available in the field • data storage problem

(after Lachapelle, 1991)

The real-time processing is usually used in navigation applications which require instantaneous results. The requirement of real-time positioning restricts the batch least squares or smoothing techniques to be applied in the process. In either real-time or post-mission processing, the processing techniques may still involve different positioning modes, namely the absolute point positioning and the relative point positioning.

- **Absolute Point Positioning**

The basic observation equation of the absolute (stand-alone) point positioning is given in equation (2.1). The pseudorange observables are commonly used in the absolute point positioning mode which involves only one receiver. In order to solve for the three coordinate unknowns and one receiver clock bias, at least four measurements are required. If more than four measurements are available, a least squares adjustment is carried out to obtain an improved position.

The positioning accuracy (σ_x) is a function of measurement accuracy (σ_0) and satellite geometry, in the form of Dilution Of Precision (DOP), expressed as,

$$\sigma_x = \text{DOP} * \sigma_0 \qquad (2.9)$$

where,

σ_x = positioning accuracy

σ_0 = measurement accuracy

DOP = dilution of precision (geometry)

The measurement accuracy, represented by the User Equivalent Range Error (UERE), depends on the propagation error, satellite bias (ephemeris and clock error, including SA), receiver clock error and hardware noise. The DOP is used as an indicator of the strength of satellite geometry which changes according to the satellite configuration. As the satellites travel along the orbits,

the DOP value changes with respect to time and location. DOP is a function of the *a posteri* variance-covariance matrix of the solution, which can be defined by the covariances of the three position (x,y,z) and one receiver clock (t) components in the form:

$$\begin{vmatrix} \sigma^2_{xx} & \sigma_{xy} & \sigma_{xz} & \sigma_{xt} \\ \sigma_{yx} & \sigma^2_{yy} & \sigma_{yz} & \sigma_{yt} \\ \sigma_{zx} & \sigma^2_{zy} & \sigma^2_{zz} & \sigma_{zt} \\ \sigma_{tx} & \sigma_{ty} & \sigma_{tz} & \sigma^2_{tt} \end{vmatrix} \tag{2.10}$$

Various DOP values are then obtained by the combinations of the variances (diagonal elements) as,

$HDOP = (\sigma^2_{xx} + \sigma^2_{yy})^{1/2}$, Horizontal DOP, 2 dimension

$VDOP = (\sigma^2_{zz})^{1/2}$, Vertical DOP, 1 dimension

$PDOP = (\sigma^2_{xx} + \sigma^2_{yy} + \sigma^2_{zz})^{1/2}$, Position DOP, 3 dimension

$TDOP = (\sigma^2_{tt})^{1/2}$, Time DOP, 1 dimension

$GDOP = (\sigma^2_{xx}+\sigma^2_{yy}+\sigma^2_{zz}+\sigma^2_{tt})^{1/2}$, Geometric DOP, 4 dimension

From equation (2.9), it is clear that the smaller the DOP factor, the better the position accuracy. A poor satellite geometry results in a large DOP factor which occurs when the satellites in view are bundled together. When satellites are spread evenly across the sky, good geometry is expected. The ideal geometry would be so that one satellite is overhead and three others are spread evenly 120° apart in azimuth just above the horizon.

- **Relative Positioning**

Relative positioning basically involves the determination of coordinate differences. The technique creates the possibility that the errors which are

common to both stations can be removed. There are many combinations of the relative positioning observables, the most commonly used are the single and double differences. The combinations could involve differencing across two receivers, across two satellites and across receivers and satellites.

The across receiver single difference technique is the basic idea of conventional differential GPS which involves two receivers observing the same satellite. The satellite clock error is eliminated by the differencing process. By applying the same principle, the across satellite single difference eliminates the receiver clock error. The double difference technique involves two receivers observing two satellites at the same time which eliminates both the satellite and receiver clock errors. The double difference observable is the most commonly used observables as the satellite and receiver clock errors are eliminated by the differencing process.

The basic mathematical model for conventional DGPS is in the form of an across receiver single difference pseudorange observation. For a pair of stations simultaneously observing the same satellite, the across receiver single difference pseudorange observable can be derived from equation (2.1), by differencing simultaneously two pseudoranges to the satellite, in the form:

$$\Delta(\cdot) = (\cdot)_{\text{receiver 2}} - (\cdot)_{\text{receiver 1}} \tag{2.11}$$

to get,

$$\Delta\rho = \Delta\rho_t + \Delta d\rho + c(\Delta dt) + \Delta d\rho_{ion} + \Delta d\rho_{trop} + \Delta(\rho) \tag{2.12}$$

where,

Δ represents the differences across the two receivers

If real-time processing is employed, an appropriate data link between the monitor and the remote stations is needed. The choice of communication system depends on the distance between the stations, the amount of data to be

transmitted, the reliability and integrity requirements (Lanigan, 1990). The possible applications for conventional DGPS are listed in Table 2.3.

Table 2.3 DGPS Applications

Metre level accuracy	Centimetre level accuracy
• Navigation(positioning & guidance) --- marine --- airborne --- land vehicle • Hydrographic surveying • Agriculture (tractors)	• Setting out • Land surveying • Satellite altimetry • 3D seismic • Remote sensing • Airborne gravity • Gravity vector mapping system • Dredging

(after Lachapelle, 1991)

It is clear that the GPS stand-alone positioning accuracy is not accurate enough for most applications described above, therefore the differential processing, which largely reduce error sources caused by the satellite orbit, ionosphere and troposphere, SA and clock offsets, is necessary to achieve high accuracy positioning.

Apart from the across receiver single difference, another type of single difference, known as the across satellite single difference, can also be derived from equation (2.1). This involves two satellites simultaneously viewed by a receiver, and the mathematical model is given by

$$\delta\rho = \delta\rho_t + \delta d\rho + c(\delta dT) + \delta d\rho_{ion} + \delta d\rho_{trop} + \delta(\rho) \qquad (2.13)$$

where,

δ represents the across satellite single difference

It should be noticed that in equation (2.13), the receiver clock error is eliminated and in equation (2.12) the satellite clock error is eliminated. From equation (2.12) and (2.13), a satellite-receiver double difference can be constructed either by differencing two across satellite single differences or differencing two across receiver single differences. The two results are mathematically identical. The observation equation for double difference pseudorange measurement is given by

$$\Delta\delta\rho = \Delta\delta\rho_t + \Delta\delta d\rho + \Delta\delta d\rho_{ion} + \Delta\delta d\rho_{trop} + \Delta\delta(\rho) \qquad (2.14)$$

where,

$\Delta\delta$ represents the receiver-satellite double difference

The clock error terms in equation (2.14) are eliminated in the double difference processing. As a consequence, the double difference observables, with the additional advantage of minimising common errors such as SA '*dither*' part, and the effects of atmospheric propagation errors, are used for determining high precision satellite orbits (§ 4.4).

2.8 Integrity

Integrity is the issue especially concerning the navigation community when GPS is to be used for navigation purposes. Integrity is defined in the US Federal Radionavigation Plan (FRP) as '*the ability of a system to provide timely warnings to user when the system should not be used for Navigation*' (DOT/DOP, 1994). For civil aviation, the integrity requirements have been investigated by Radio Technical Commission for Aeronautics (RTCA) Special Committee 159 and the Federal Aviation Administration (FAA) for airborne supplemental equipment using GPS (RTCA, 1991, FAA, 1992).

As there are insufficient integrity warnings provided by the GPS control segment when part of the system fails, other solutions have to be applied to meet the integrity demand. In principle, integrity monitoring is to protect users

from navigating with incorrect data. This can be achieved by either the internal or the external methods of integrity monitoring (Brown, 1992, Seeber, 1993).

The Receiver Autonomous Integrity Monitoring (RAIM) is a internal monitoring method, which basically is an internal quality control of the GPS solution. Many types of RAIM algorithms have been proposed (Brown, 1992, Lee, 1994, Parkinson *et al*, 1988 and Sturtz *et al*, 1990) which basically check the consistency of the measurements. A typical integrity monitoring algorithm detects possible satellite failures by using measured data from redundant satellites. This redundancy is used by the algorithm to determine if an error in the measurements could cause an intolerable error in the user navigation accuracy (IESSG, 1995, Michalson *et al*, 1994). Unfortunately, the requirement for redundant satellites (at least 5 satellites in view) with appropriate geometric strength cannot be met by GPS all the time, therefore, external monitoring methods have to be applied if the integrity requirement is critical to the GPS user.

The external monitoring methods generally set up an integrity monitoring network to detect if any large error in the measurements exceeds the specified criteria. The integrity message is then transmitted by the GPS Integrity Channel (GIC) to broadcast warning message to users (Montgomery, 1991) It is aslo possible to merge the integrity monitoring network with the WADGPS, which enables the system to provide the improved integrity as well as higher positioning accuracy. One of the examples is the Wide Area Augmentation System (WAAS), which is being investigated by US FAA. WAAS has been chosen as part of the US navigation system to achieve the required navigation performance and is scheduled to achieve 'end state' up to Category I landing at year 2001 (Loh *et al*, 1995).

Chapter 3

Wide Area Differential GPS : Review

The levels of accuracy achievable by the Global Positioning System can be classified into two categories according to the main observables, namely the code pseudorange and carrier phase. The pseudorange observable is capable of providing the stand-alone point positioning accuracy of the order of 15 to 25 m, if the military Precise Positioning Service (PPS) is available, or 100 m employing the civilian Standard Positioning Service (SPS). The carrier phase observable can provide centimetric positioning accuracy, if the problems of the determination of integer ambiguities and cycle slips can be overcome. Due to the lack of precise algorithms for the determination of integer ambiguity and the detection and repair of cycle slips in real-time, this observable is not very attractive for real time navigation.

The SPS accuracy is sufficient for many applications, such as the en route (2.8 nm, 95%) and terminal (1.7 nm, 95%) phases of flight. However, this level of accuracy is not sufficient for applications such as the precision approach phase of flight. The need for higher navigation accuracy using the robust pseudorange observable resulted in the development of the technique known as differential positioning. This method has been used for many years to improve on the stand-alone accuracy and is commonly referred to as Differential GPS (DGPS). It has been repeatedly demonstrated that DGPS can achieve 2 to 5 metre position accuracy (Blanchard, 1990; Kremer *et al* , 1990; Cannon *et al*, 1992a, b).

The conventional DGPS technique (also known as Local Area DGPS, LADGPS) is based on the assumption that the error sources between the reference and user site are highly correlated. This is true for those error sources which are independent of the user's position such as clock related errors (satellite and receiver clock errors, including SA 'dither'). However, error sources such as those due to atmospheric propagation offsets, ephemeris and SA 'epsilon' are dependent on the user's position and suffer from spatial decorrelation as the separation between the user and reference station increases. Since the baseline lengths over which LADGPS differential corrections are applicable are fairly short, the data link employed is usually a terrestrial based radio broadcast system. Therefore, in a situation where the area of applicability of the differential corrections is to be extended, the use of such a data link system becomes a serious limitation.

In order to extend the area of applicability of the differential corrections, several concepts have been developed including the multi-reference station DGPS, often referred to as Network DGPS (NDGPS). NDGPS does not involve the separation and modelling of the individual error sources in the system. The algorithm applied for the NDGPS is to generate a weighted sum of the DGPS differential corrections from multiple reference stations. With

this approach, not only the accuracy but also the integrity is improved compared with single reference station DGPS.

The Wide Area DGPS (WADGPS) system was developed so to provide differential corrections applicable over a wide area, such as a communication satellite's entire footprint, without loss of accuracy. The limitation of the coverage of the data links is removed by the availability of the geostationary communication satellites. Therefore geostationary satellites, such as Inmarsat, are used as data communication systems to provide the ability of transmitting differential corrections over a wide area, typically an entire ocean region. If the position dependent errors can be separately modelled and applied to the user in a way which breaks the position dependence, the user navigation accuracy limitation due to the user-reference station separation in the case of LADGPS, can be largely removed. As a consequence, the WADGPS technique provides a consistent user navigation accuracy over a wide area with a less dense reference network than an equivalent conventional DGPS system.

In this chapter, the principles and various algorithms currently available for WADGPS are discussed. In order to highlight the need for WADGPS, the conventional DGPS and the Network DGPS are briefly reviewed in the following sections.

3.1 Conventional DGPS

3.1.1 System Configuration

The conventional DGPS technique assumes that the error sources experienced at both the reference and user sites are highly correlated and hence can be largely eliminated by the 'differencing' technique. The system requires at least one station of known coordinates (referred to as the reference station), to be occupied with a GPS receiver. The observed ranges and those computed from

the known satellite and receiver positions are compared resulting in differential range corrections. The differential corrections can be expressed as,

$$d\rho = \rho_{comp} - \rho_{obs} \tag{3.1}$$

where,

ρ_{comp}	is the computed range
ρ_{obs}	is the observed range
$d\rho$	is the differential range correction

The basic principle of DGPS is illustrated in Figure 3.1. All the errors that affect the observed pseudoranges, including the clock related, ephemeris and atmospheric propagation errors, are assumed to be included in the differential range corrections. The differential range corrections are then sent to the user via some form of data link. It is common to use some kind of terrestrial radio system as data links. However, some systems also use communication satellites, such as Inmarsat, as data links for a larger area. If the user also experiences similar errors to the reference station, the errors should be largely cancelled out by applying the differential corrections and the positioning accuracy can be significantly improved.

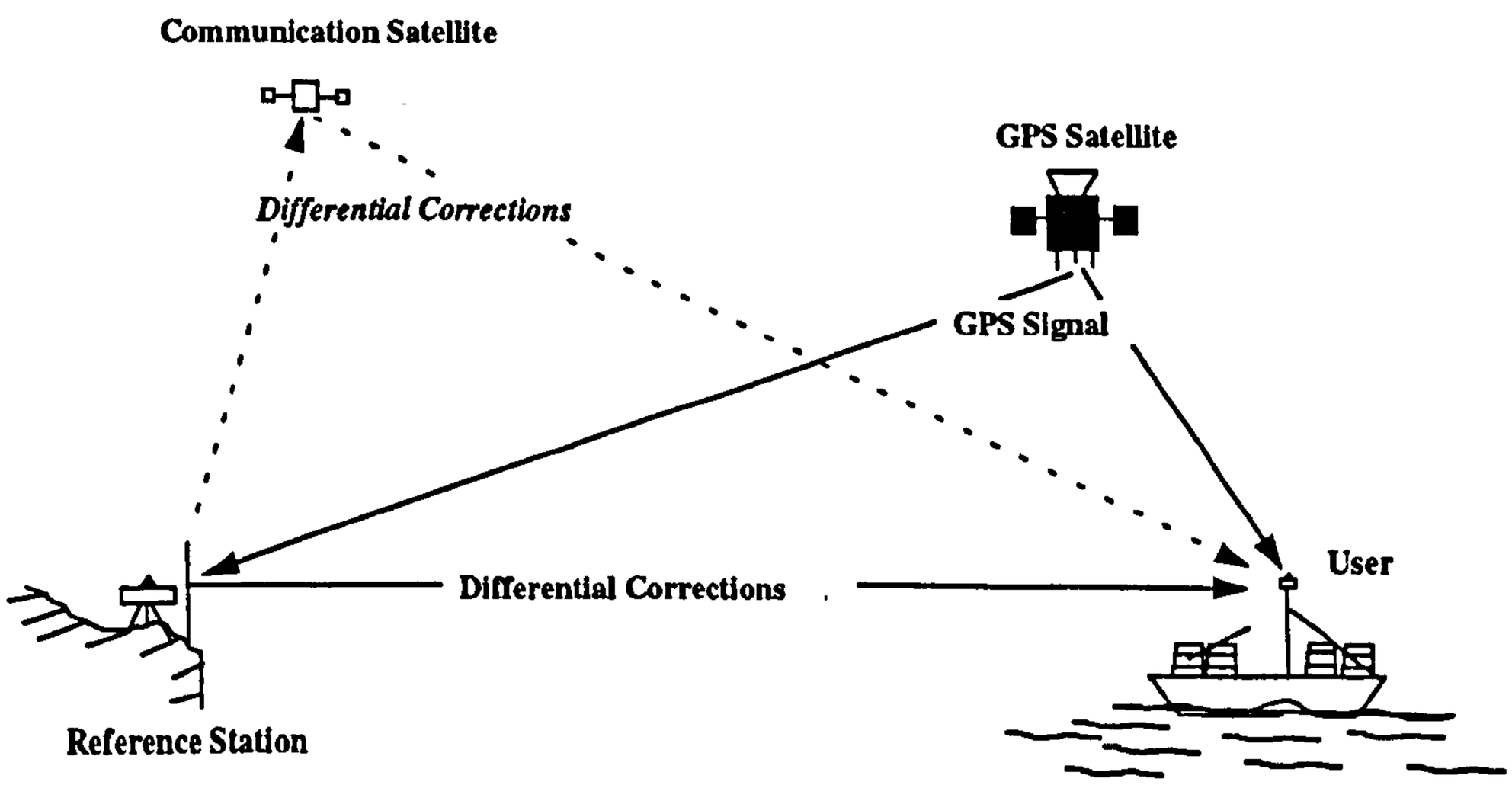

Figure 3.1 Differential GPS Principle

The functional process of conventional DGPS is illustrated in Figure 3.2. The diagram shows the processing procedures at both reference and user sites. At the reference station, the observed ranges are compared with the computed ranges and the differential corrections are generated using the data processor. The corrections are then formatted according to the transmission requirements and modulated on to signals for transmission. The user site receives GPS signals, as well as the differential corrections, which are decoded and formatted to be applied to the user observed ranges. The final improved user position is then obtained and displayed for the user.

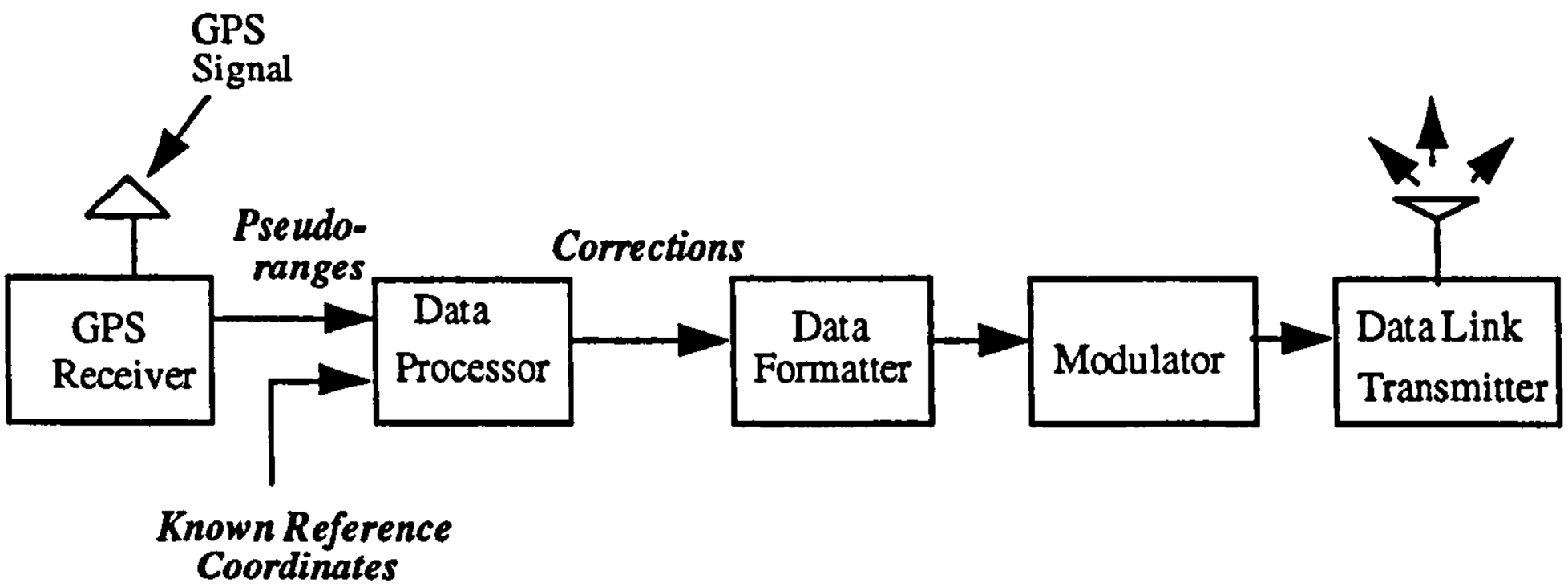

(a) Reference Station

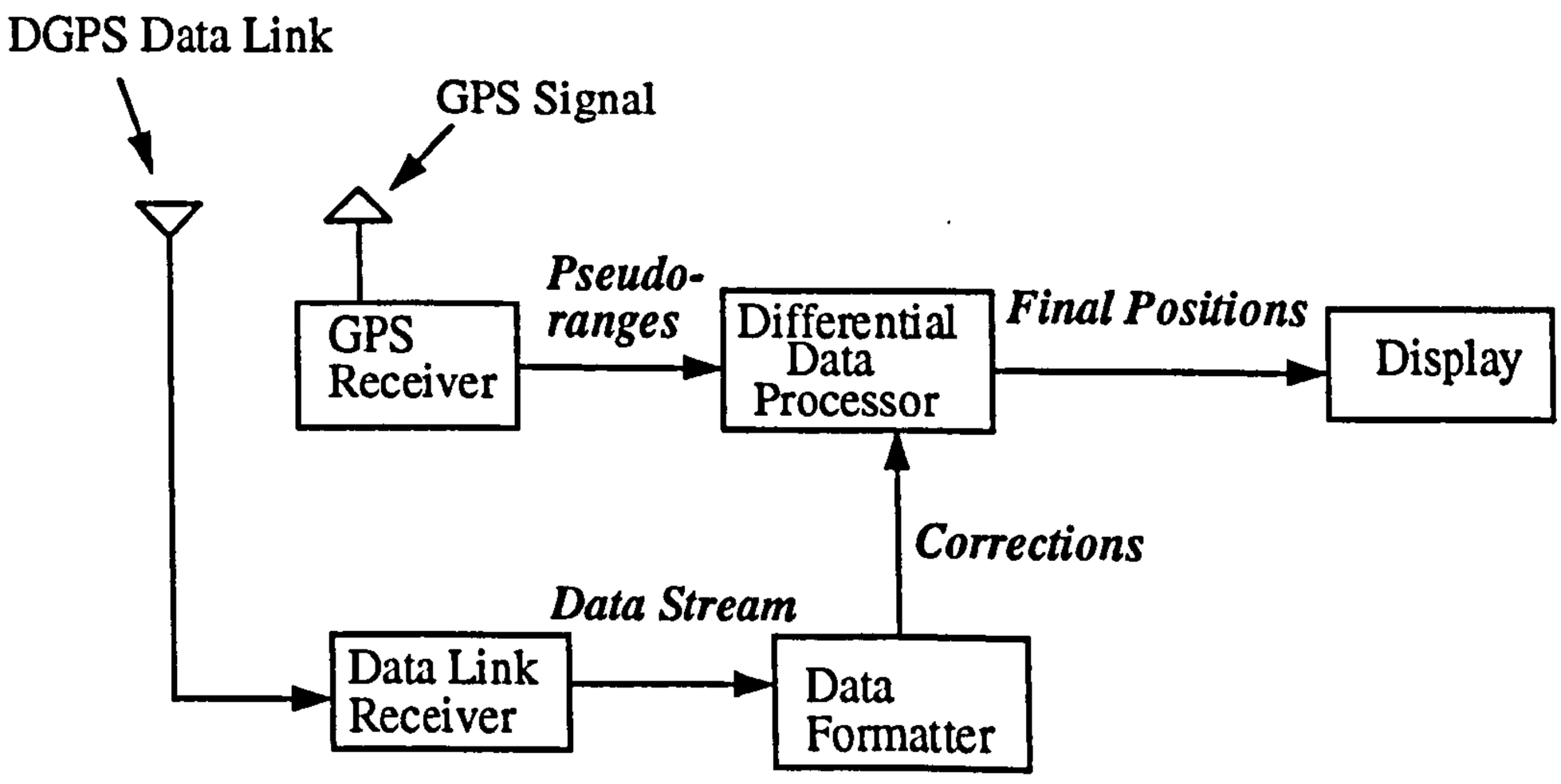

(b) User Station

Figure 3.2 Conventional DGPS Processing Diagram

3.1.2 Correction Algorithm

The algorithm applied at the user to compute the range correction is given by,

$$d\rho\ (t_1) = d\rho\ (t_0) + \partial\ d\rho/\partial t\ (t_1 - t_0) \qquad (3.2)$$

where,

$d\rho\ (t_1)$	is the range correction at epoch t_1
$d\rho\ (t_0)$	is the range correction at epoch t_0
$\partial\ d\rho/\partial t\ (t_1 - t_0)$	is the range correction rate
t_1	is the time of the pseudorange observation at the user site
t_0	is the time the corrections are calculated at the reference site

There are essentially two parts to the computation of the range correction at the user site. The first is the component computed at time t_0 (assuming no delay between the observation, computation and transmission of the correction) and secondly at time t_1 (taking into account the delay caused by the observation, computation and transmission of data from the reference to the user site). Since the corrections are always delayed due to the processing and transmission time, the range correction rate in addition to the range correction are usually used together to predict the instantaneous range corrections to be applied at the user site.

The differential technique reduces the effects of the ephemeris, atmospheric propagation and satellite clock errors. However, due to the rapid variation of the SA 'dither' effect, in addition to the range correction and range correction rate effects, it is also suggested that the range correction acceleration are included, to counter the effect of SA (Loomis, 1989). The phase-smoothed pseudoranges (§4.6) are commonly used as the observable, provided the problems of integer ambiguity and cycle slips are properly handled (Hatch, 1986). Further details about the conventional DGPS processing methods can be found in Cannon (1990a, b), Loomis (1989) and Sharpe (1989).

3.1.3 Data Format and Transmission

The Radio Technical Commission for Maritime Service Special Committee 104 (RTCM SC-104) recommend a standard format for DGPS data transmission. The current version 2.1 of the recommended standards was published in January 1994 (RTCM, 1994). The basic message format remains unchanged from previous version 2.0 (RTCM, 1992). Several message types were added to support real-time kinematic (RTK) applications and some message types previously designed as tentative have been fixed (Langley, 1994). The message types are summarised as follows,

Message Type No.	Current Status	Title
1	Fixed	Differential GPS Corrections
2	Fixed	Delta Differential GPS Corrections
3	Fixed	Reference Station Parameters
4	Retired	Surveying (Carrier Phase)
5	Tentative	Constellation Health
6	Fixed	Null Frame
7	Fixed	Beacon Almanacs
8	Tentative	Pseudolite Almanacs
9	Fixed	High Rate DGPS Corrections
10	Reserved	P-Code Differential Corrections (Reserved)
11	Reserved	C/A-Code L1, L2 Delta Corrections (Reserved)
12	Reserved	Pseudolite Station Parameters
13	Tentative	Ground Transmitter Parameters
14	Reserved	Surveying Auxiliary Message
15	Reserved	Ionosphere (Troposphere) Message
16	Fixed	Special Message
17	Tentative	Ephemeris Almanac
18	Tentative	Uncorrected Carrier Phase Measurements
19	Tentative	Uncorrected Pseudorange Measurements
20	Tentative	RTK Carrier Phase Corrections
21	Tentative	RTK Pseudorange Corrections
22-58	-	Undefined
59	Tentative	Proprietary Message
60-63	Reserved	Multipurpose Usage

The format of the message is given as,

Word 1	Word 2	Message

Word 1 and Word 2 are general message information which are pertinent to any type of message. Each word is designed to be 30 bits as opposed to 32 bits for the convenience of timing calculation. The commonly used messages are briefly described below.

- Message type 1 is the primary message which provides the pseudorange and range rate correction.

- Message type 2 provides the delta differential corrections. This information enables the user to modify the difference in the received corrections when the ephemeris and clock data set at the user site is older than the set used by reference station. This is caused by the change in the satellite navigation data, i.e. the updated broadcast ephemeris. This message is always used to augment a type 1 message.

- Message type 3 contains the reference station parameters which includes the station coordinates, station clock offset and uncertainty, station frequency offset and uncertainty, tropospheric correction, beacon latitude, longitude and range, and station health information.

- Message type 4 provides the information needed for surveying and geodetic users such as the complete instantaneous phase observations and cumulative loss-of-lock count and other related information. This type of message has been retired.

- Message type 5 provides the constellation health which contains the health information for all satellites.

- Message type 6 is a null frame for frame synchronisation.

- Message type 7 provides information for optimum radiobeacon selection for coastal maritime users.

- Message type 8 provides the location, code and health of a number of pseudolites.

- Message type 9 provides higher update rate corrections for those satellites whose range corrections change rapidly.

- Message type 16 provides special messages which may be warnings in case of any detected unusual situations.
- Message types 18-21 are newly introduced in RTCM version 2.1 to support high accuracy real-time kinematic application in surveying and navigation.

(Kalafus, 1992; Langely, 1994))

The selection of the communication system for the data transmission depends on three factors,

(i) the required user navigation accuracy

(ii) the coverage

(iii) the update rate

The kind of message to be transmitted depends on the required user navigation accuracy. When metre level accuracy is required, usually only differential corrections and related information are transmitted to the user. The raw observations at the reference station can also be transmitted to the user in order to perform differential positioning at the user site, depending on the application requirement. The required data transmission rate recommended by RTCM SC-104 is 50 to 100 bps (bits per second) and 1000 to 2000 bps for metre and decimetre level accuracy respectively (Lanigan, 1990). If messages type 1, 2 and 3 are to be transmitted to users, assuming 4 satellites have been tracked at the reference station, it takes about 10 seconds to transmit all of the message at a transmission rate of 50 bits per second.

The range coverage and update rate of a communication system is related to its frequency. The commonly available radio frequency bands are given and briefly described below,

Frequency Band	**Wavelength**	**Identification**	**Range**	**Update rate**
30 - 300 kHz	10 - 1 km	LF	>700 km	<20 sec
300 - 3000 kHz	1000 - 100 m	MF	<500 km	5-10 sec
3 - 30 MHz	100 - 10 m	HF	<200 km	1-5 sec
30 - 300 MHz	10 - 1 m	VHF	<100 km	0.5 - 2 sec
300 - 3000 MHz	100 - 10 cm	UHF	<100 km	0.5 - 2 sec

(Cross *et al*, 1990; Lachapelle, 1991)

- **Low and Medium Frequency Ground Wave System**

The Low Frequency (LF), up to 300 kHz, and Medium Frequency (MF), up to 3,000 kHz, provide the ground wave propagation which is suitable for the DGPS broadcast system. However, these frequencies suffer from the skywave interference and atmospheric noise, which limit the coverage and transmission rate of the data link system. Generally, the LF and upper MF system have the ability to provide data links for metre level navigation over distance greater than 700 km overwater and 100 km overland. However, the coverage of the systems decreases rapidly if the transmission rate is increased (Lanigan *et al*, 1990). The radio beacon system employed by the US Coast Guard (USCG) is one of the examples in this category. The USCG provides a DGPS service for public use in harbour and harbour approach areas of the United States with an accuracy of 10 metres (2drms) or better (USCG, 1996). The DGPS signals are broadcast via USCG marine radiobeacons, with transmission frequencies between 285 and 325 kHz, which will cover the entire US coastal area, Great Lakes, Puerto Rico, most of Alaska and Hawaii, and 20 to 100 km in land

(USCG, 1996, Lanigan, 1990). The Initial Operational Capability (IOC) phase of USCG DGPS has been declared on January 30, 1996 (USCG, 1996).

- **High Frequency Skywave System**

As the surface wave attenuation with distance is faster in this band, the predominant propagation mode of High Frequency (HF) system, with spectrum lies from 3 to 30 MHz, is the skywave. Radio waves in this range are reflected back to Earth by the ionosphere to accomplish the communication purpose. Considerable ranges can be achieved but are not consistent, due to the skywave being directly affected by the activity of the ionosphere. This kind of system has the potential to provide data links for both metre and centimetre level accuracy positioning for overland or overwater coverage. There are many systems available in this category, due to its flexibility over coverage, update rate and costs. For further details, the reader is referred to Barboux (1993) and Lanigan *et al* (1990).

- **Very High Frequency and Ultra High Frequency Systems**

The Very High Frequency (VHF, 30 to 300 MHz) and Ultra High Frequency (UHF, 300 to 3000 MHz) systems provide very stable and predictable signals. These systems allow higher update rates and fairly small aerials can be used. As a consequence, these bands are widely used as communication systems (e.g. cellular phone) but they suffer from shadowing and fading. As a consequence, line-of-sight is needed and the coverage is rather small for these systems (Lanigan *et al*, 1990).

Due to the effects of SA, a higher update rate is required in order to achieve higher user navigation accuracy. The proper choice of the communication system is therefore a compromise between coverage and update rate.

The availability of communication satellites enables the coverage, data rate and integrity to be extended. These kinds of system, such as the Inmarsat communication satellites, are able to provide coverage over an entire ocean region from one satellite, with the ability of high data update rates and high integrity, for the various levels of accuracy required. Therefore, they would be the only choice of data link for WADGPS, and probably technically the best for all the other applications.

3.1.4 Accuracy

The navigation accuracy of conventional DGPS is improved by applying the 'bundled' differential corrections which include corrections for error sources such as those due to satellite ephemeris, satellite clock and atmospheric propagation (troposphere and ionosphere) effects. The navigation accuracy of the order of 2 to 5 metres has repeatedly been demonstrated by various tests in different situations (Blanchard, 1990; Cannon *et al*, 1992a, b). The main drawback of conventional DGPS is that the differential corrections suffer from spatial decorrelation as the user-reference station separation increases, which degrades the navigation accuracy.

3.2 Multi-reference Station DGPS

The multi-reference station DGPS system provides weighted differential corrections to the user, without separating and estimating the individual error components. The system consists of more than one reference station, instead of the single reference station used in conventional DGPS. The user position is obtained by applying multiple sets of differential corrections obtained from the reference stations to the user observed ranges. Not only the user positioning accuracy, but also the integrity, is improved by the introduction of these additional reference stations.

There are basically two types of system which provide multi-reference station DGPS, namely **Networked DGPS** and **Internetting DGPS.**

Networked DGPS sets up a centralised control centre to manage, process and transmit data collected from multiple reference stations. Examples of existing Networked DGPS system include the *Network DGPS* system developed by Trimble Navigation Ltd. (Loomis *et al*, 1991) and the *SeaStar Network DGPS* provided by Wimpol Ltd. (Almond *et al*, 1994).

Internetting DGPS relies on sending multiple sets of differential corrections to the user. The user himself decides the validity of the differential correction data and calculates a weighted least squares position solution for all satellites in view (Johnston, 1994). The Racal *Multi-Fix* system is one of these existing systems.

3.2.1 Networked DGPS

The basic assumption of the Networked DGPS system is the same as in conventional DGPS. The assumption is that the error sources at both reference and user sites are highly correlated within a limited region, and hence can be largely reduced by applying differential corrections. The Networked DGPS has multiple reference stations plus a centralised control centre. The control centre is ideally located at the centroid (geometric centre) of the reference stations. The differential corrections from each of the reference stations are sent to the control centre where error checks and quality control (certification and validation) are performed. A single set of differential corrections is then calculated and transmitted to the user in an RTCM compatible format. The algorithm developed for the Networked DGPS is based on the common-view approach. The basic principle of the common-view network assumes that the user only applies the differential corrections calculated from those satellites visible to all the reference stations in the network.

As has been mentioned above, a unique set of differential corrections needs to be combined from the many differential corrections generated at different reference stations, for eventual transmission to the user. In order to do this, the following issues need to be addressed, (i) the receiver clock error is different for each reference station, (ii) differential corrections are of different sizes, (iii) the reference stations are at different distances from the user and, (iv) the times of computation of the differential corrections are different for each reference station.

Since the receiver clock error forms part of the differential correction, each differential correction contains the effects of a different receiver clock error. Hence it is necessary that the final differential correction for a particular satellite contains the effects of one clock. The solution to this problem is the use of a reference (master) clock, or the use of an implicitly averaged network clock. The averaged network clock is generated by passing the clock errors via common satellites between adjacent stations throughout the network, which makes the external time synchronisation unnecessary (Johnston, 1994).

The control station employs some forms of relative geometric relationship to determine the weight matrix, which is applied to the differential corrections collected from the reference stations in the network. The combined differential correction is derived from individual data sets, which are carefully time tagged to ensure that the composite clock (and hence the differential corrections) is derived appropriately. In order to ensure that the differential corrections are applied correctly, the reference and user station need to use the same broadcast ephemeris, otherwise errors may be introduced.

The combined differential corrections must be based on a 'pseudo-master station', usually the centroid of the reference station network. All the differential corrections at individual reference stations are properly weighted and evaluated by the control station based on the chosen 'pseudo-master

station'. If the control station is not located at the centroid point, the gradient of the corrections within the network is applied, to generate the combined differential corrections at the centroid point. The gradients of the differential correction are also transmitted to the user, to enable the user to calculate a position anywhere in the network.

An important consideration of any differential system is the data capacity required to transmit data between the differential corrections (reference stations to control centre, control centre to user). This is more important when operating under SA condition. Therefore, the substantial demands on communication ability in order to receive multiple differential corrections from several reference stations, should be carefully considered. A high performance data link is required between the centralised control station and the reference stations, to transmit data from multiple reference stations. On the other hand, the user receives only one single differential correction from the control station. This allows a higher update rate to be performed for the differential corrections at the centralised control station, to the user.

3.2.2 Internetting DGPS

Internetting DGPS, as with the Networked DGPS, also employs the use of multiple reference stations, but without a centralised control station. The basic idea behind the system is to allow the user to determine the validity of the differential corrections, and to perform a weighted least squares solution using the differential corrections from the reference stations.

The weight matrix is formed in a similar manner to the Networked DGPS weight matrix. The parameters of the weight matrix vary, depending on different considerations of the system provider. In general, the weight matrix is a function of the relative geometry of the reference and user stations, which includes the correlation distance of the GPS errors and the distance between the reference and user stations (Tang *et al*, 1994). Some other factors, such as

the age of the data and the stability of the individual differential corrections, are also taken into account by the system providers (Johnston, 1994). The user calculates the weight matrix based on his approximate position and then applies the differential corrections to his observations (Loomis *et al*, 1991). However, the requirement of receiving individual differential corrections from all the reference stations in the network puts considerable extra load on the communication system. For example, if there are three reference stations in the network, the user will need three times the communication bandwidth compared with conventional DGPS, to be able to receive all three sets of differential corrections.

3.2.3 Accuracy

The accuracy of the multi-reference station DGPS has been demonstrated by various tests involving differing sizes of networks. It is difficult to compare the performance of each system, due to different data sets and sizes of the networks. However, they all clearly show that the multi-reference station DGPS provides better positioning accuracy than conventional single reference station DGPS (Almond *et al*, 1994; Johnston, 1994; Tang *et al*, 1994). Although the effects of spatial decorrelation are reduced by properly weighting the differential corrections from reference stations, the user positioning accuracy is still degraded as the separation of the user-reference station increases, but only at a slower rate than conventional DGPS (Johnston, 1994, Tang *et al*, 1994).

An overall idea of the size of these types of networks can be obtained from Figure 3.3, which shows the reference network of *SeaStar Network DGPS*, Racal *Network DGPS* and Racal *Multi-Fix* system (Almond *et al*, 1994; Johnston, 1994). Note that the Racal *Network DGPS* shares the same reference stations with the Racal *Multi-Fix* system, except a centralised control station is located at Aberdeen for the Racal *Network DGPS*.

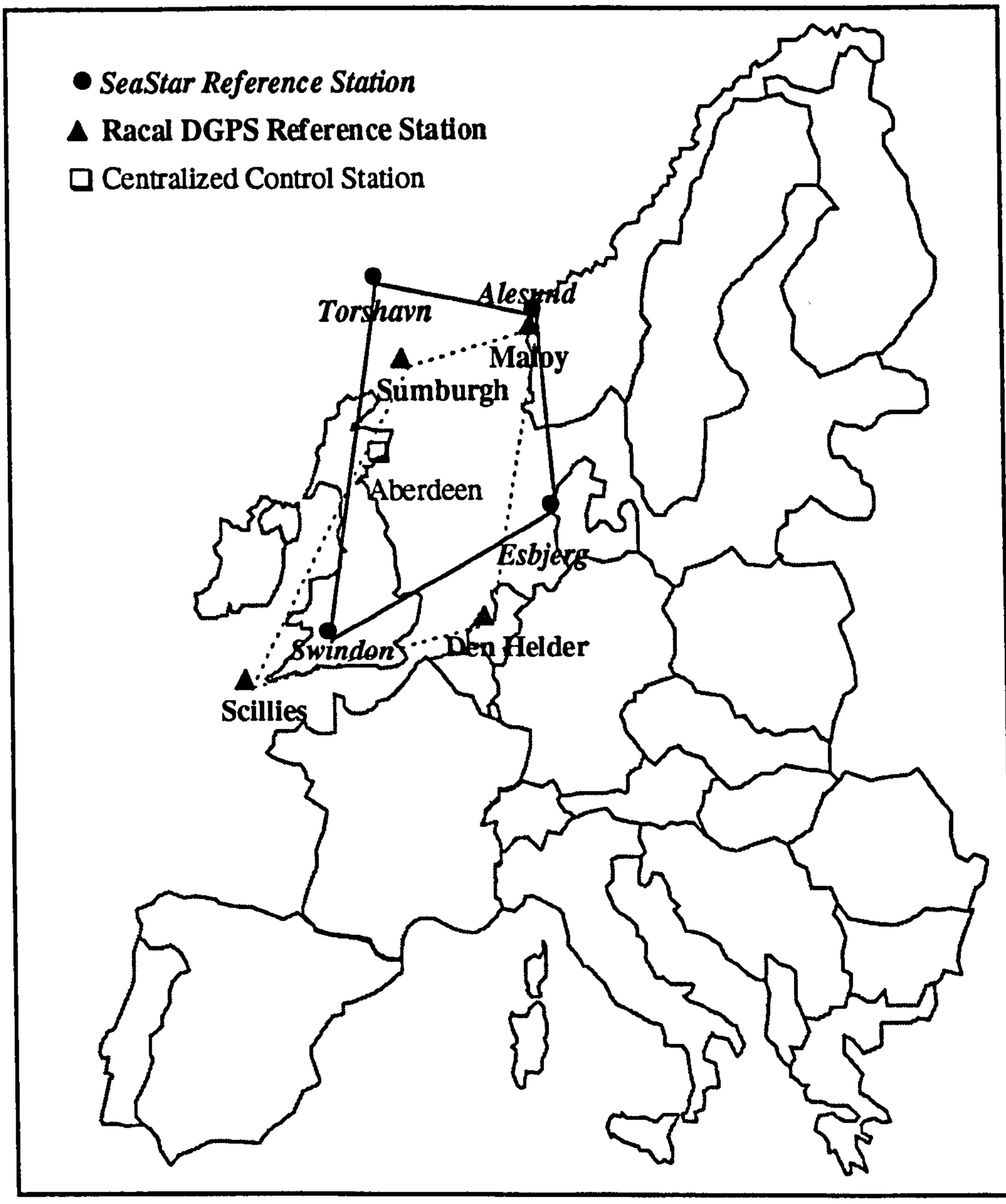

Figure 3.3 Typical DGPS Reference Network

3.3 Wide Area Differential GPS

Wide Area Differential GPS provides consistent accuracy over a wide area, typically a communication satellite's entire coverage, with a less dense distribution of reference stations than conventional DGPS or NDGPS. This is achieved by modelling the error sources separately, in a way that breaks the

spatial correlation in the network. The WADGPS system configuration is illustrated in Figure 3.4. It basically contains one or more control centres, a network of reference stations, communication links and users. The measurements collected at the reference stations are transmitted to the control centres via a data link system which can be either ground or space based. The control centres manage and process the data to generate the differential corrections for eventual uploading to the communication satellites for onward transmission to the user.

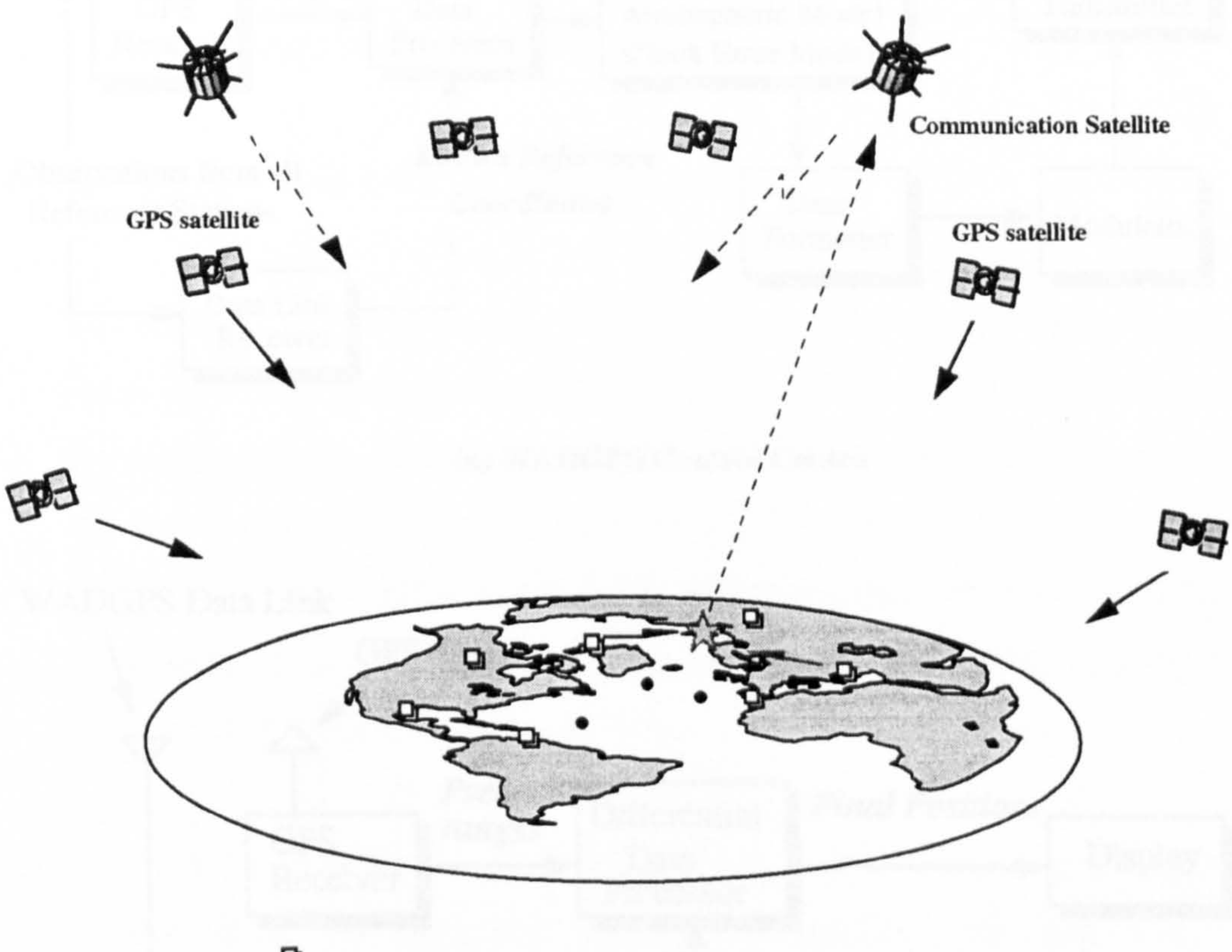

Figure 3.4 WADGPS System Configuration

Although different WADGPS approaches have been proposed, they all share a common basic concept. This is that the error components are separated and modelled individually. The general processes at the control centre and the user stations are shown in Figure 3.5.

As illustrated in Figure 3.5, the control centre receives all the observations collected at the reference stations via data link system. These measurements are then processed to generate error correction models to be formatted and transmitted to the users. The user receives the error correction models and applies them to the observed ranges to obtain the improved position.

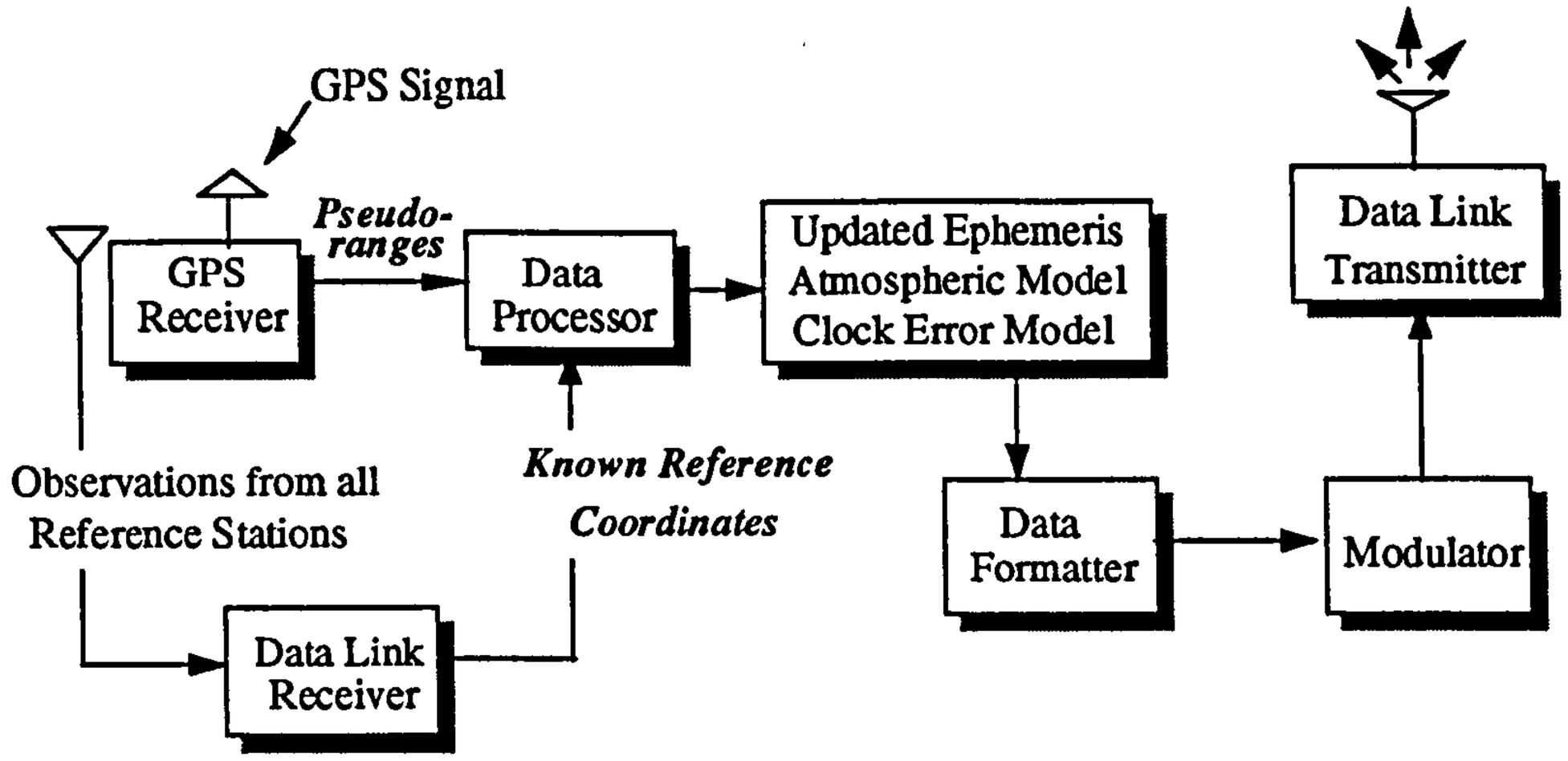

(a) WADGPS Control Centre

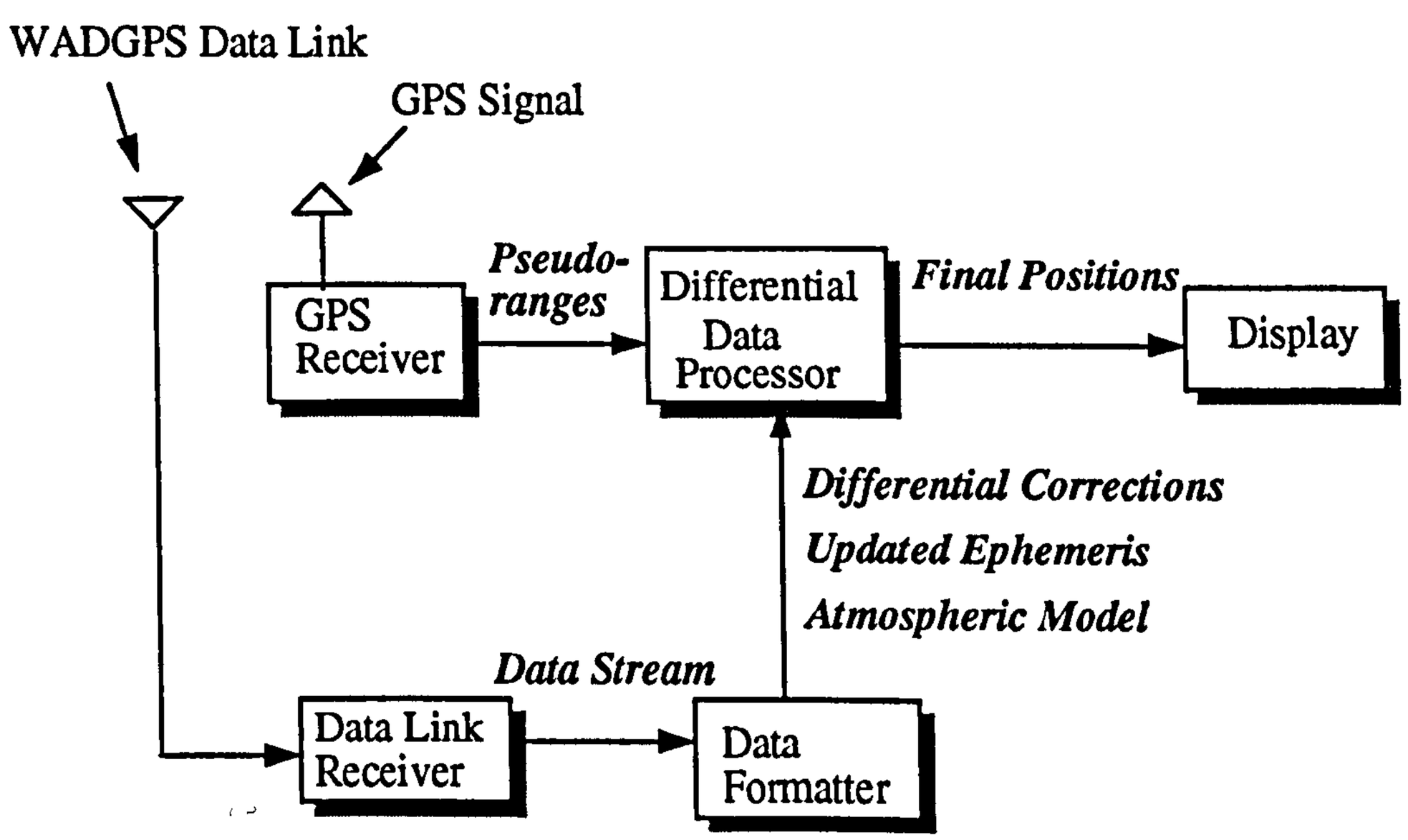

(b) User Station Block Diagram

Figure 3.5 WADGPS Algorithm

The error sources that affect GPS pseudorange measurements can be classified into two categories namely, Position Independent Error Sources (PIES) and Position Dependent Error Sources (PDES)

The PIES have the same effect on all the users regardless of location. These errors do not suffer from spatial decorrelation. The satellite and receiver clock related errors (including SA 'dither') are typical examples. These errors affect all the users in the same manner at the same instance. Hence, the differential corrections eliminate these errors at the user sites.

- Satellite Clock and Selective Availability Error

  The satellite clock error is due to the imperfect nature of the satellite clock offset correction parameters provided by the control segment. This error can be treated as a slow variation of range error which affects all the observers in the same manner, provided the observations were taken at the same time. The satellite clock offset is indistinguishable from the radial component of the satellite orbit errors, and can also be treated as a range error, making it possible to combine these two errors together.

The 'dither' part of the SA error is induced by deliberately manipulating the satellite clock. The errors are injected on the satellite clock coefficient, a_1 term (equation 2.5), with a range rate error variation of up to 25 cm/s (Lachapelle, 1991a). Therefore, the SA 'dither' part can be considered as a rapid variation of the satellite clock behaviour. As a consequence, the SA 'dither' error can be regarded as part of the satellite clock error which has a more rapid fluctuation. Since the satellite clock errors are identical to all observers, regardless of the receiver locations, they can be estimated at the reference site as differential corrections and transmitted to the user, in the same manner as in conventional DGPS. However, due to the fast variation

of the SA error, the differential corrections need to be updated more frequently, to counter the rapid change of the satellite clock errors.

- Receiver Clock Error

The receiver clock errors are due to the non-synchronisation of the receiver clocks with GPS time. In conventional DGPS, the reference station receiver clock error can be regarded as a range error and included in the 'bundled' differential correction. Since the reference station receiver clock error experienced by all observed ranges is identical, provided the observations are taken simultaneously, it can be estimated, together with the user receiver clock error, as a 'composite' clock error. The reference station clock error simply appears to be an additional range error to the user. For WADGPS, the properties of the clock errors are the same as conventional DGPS. However, a network of reference stations generates many sets of receiver clock errors, which have to be combined into an unique set of clock errors for the user to apply.

The PDES have different effects depending on the user location. The atmospheric propagation and satellite ephemeris errors are typical examples.

- Atmospheric Propagation Error

The pseudorange is delayed by both the ionosphere and troposphere, resulting in observed ranges which are always 'too long'. The delays are related to the path through which the signal travels. Hence, these errors are dependent on the receiver location. The DGPS differential corrections are not able to eliminate all the errors caused by the atmospheric propagation effects, though they are generally small and do not decorrelate rapidly. However, recent studies have reported up to 0.5 m differential errors over a 9 km baseline as a result of the ionospheric decorrelation

(Goad, 1990). The effect of this decorrelation is that the area or range validity of conventional DGPS corrections is limited.

- Satellite Ephemeris Error

The effect of the satellite ephemeris error is illustrated in Figure 3.6. The satellite orbit errors experienced at the reference (ε_r) and user (ε_u) sites, are different due to the different viewing angles. The differential satellite orbital error can be written as (ε_r - ε_u). This error will become significant as the distance between the reference and user sites increases. Due to this, the satellite orbital error can not be eliminated totally using the differential corrections and therefore the user position accuracy is degraded.

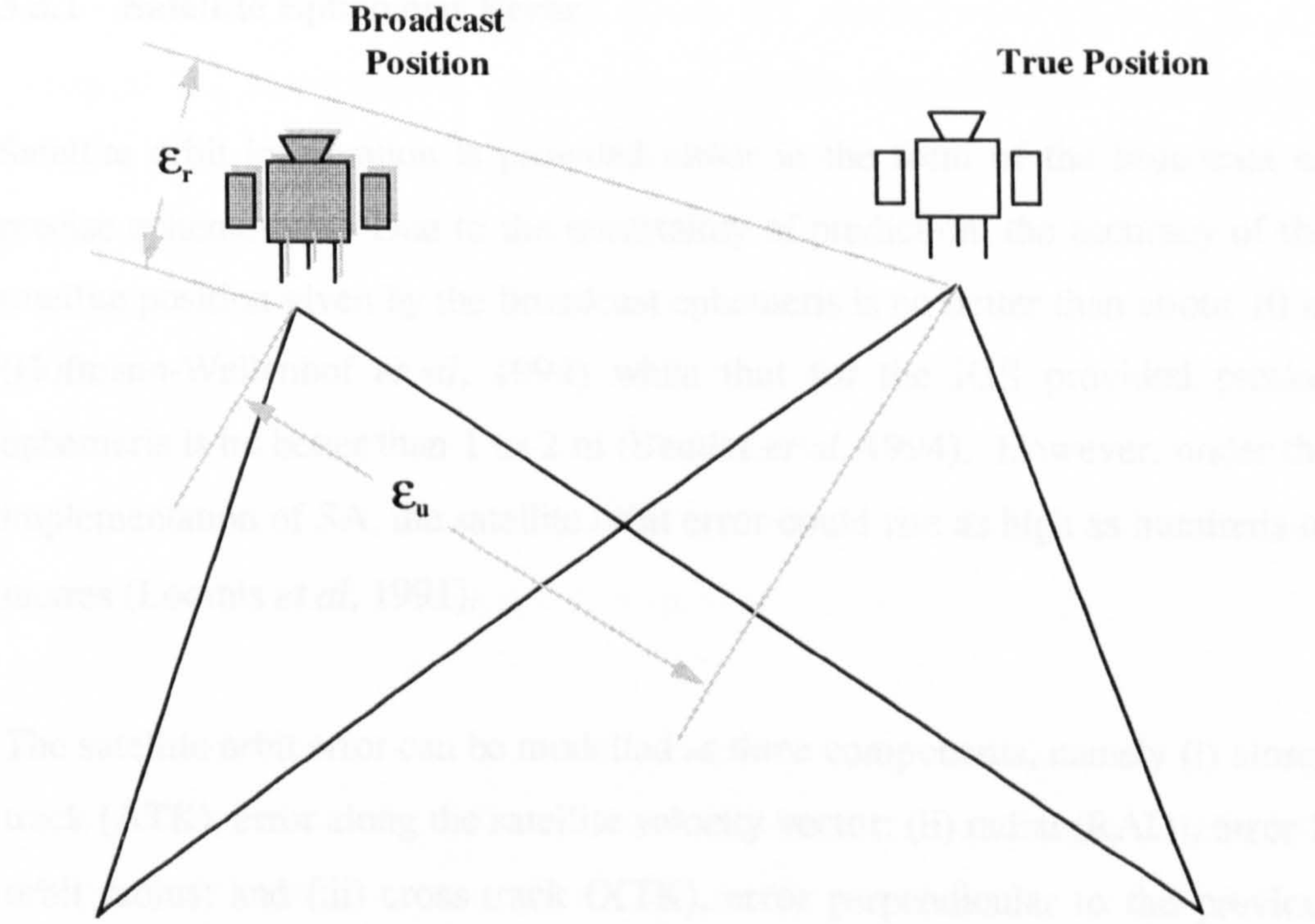

Figure 3.6 Differential Satellite Orbit Error

The basic principle of the Wide Area Differential GPS concept is to break down the error sources that affect satellite navigation and treat them separately, instead of lumping them together, as used in conventional DGPS. This enables the assessment of the spatial and temporal variation of each of the errors, with respect to the user-reference station separation.

Since PIES are common to all sites regardless of location, the errors can be transmitted as differential corrections to the user in the same way as used in conventional DGPS. The PDES must be modelled in such a way that the user can estimate or apply the corrections to the observed pseudorange at his site, by receiving some kind of error correction models from the control centre. The WADGPS concept therefore separates the errors into three components namely, satellite ephemeris, atmospheric (including ionospheric and tropospheric) propagation and clock related errors.

3.3.1 Satellite Ephemeris Error

Satellite orbit information is provided either in the form of the broadcast or precise ephemerides. Due to the uncertainty of prediction, the accuracy of the satellite position given by the broadcast ephemeris is no better than about 10 m (Hofmann-Wellenhof *et al*, 1994) while that for the IGS provided precise ephemeris is no better than 1 to 2 m (Beutler *et al*, 1994). However, under the implementation of SA, the satellite orbit error could rise as high as hundreds of metres (Loomis *et al*, 1991).

The satellite orbit error can be modelled as three components, namely (i) along-track (ATK), error along the satellite velocity vector; (ii) radial (RAD), error in orbit radius; and (iii) cross-track (XTK), error perpendicular to the previous two errors. Since the radial error translates almost directly into the range error, it generates almost identical range errors to users who view the satellite at either the zenith or horizon. Therefore the radial error has little effect on the user position accuracy after the differential correction has been applied and can

be treated almost equivalent to the satellite clock error. However, this does not apply to cross-track and along-track errors. These errors will be significant unless the reference and user stations are close enough to each other (Brown, 1989).

There are three main approaches for the estimation of the satellite orbit errors in WADGPS, namely, the navigation inversion concept, orbit relaxation and full dynamic orbit determination. These approaches are briefly described and compared in the following sections.

- **The Navigation Inversion Concept**

The navigation inversion concept, probably the most conceptually and computationally simple method, involves solving for the satellite coordinates and clock offsets by fixing the receiver coordinates. The receiver position is assumed to be known and hence fixed, the unknowns being the satellite positions and clock offsets (receiver and satellite clock offsets, including SA 'dither'). Thus a network of reference stations have their positions fixed, whilst each satellite position and the satellite clock error are solved for. This approach requires each satellite to be observed by at least four reference stations in order to solve for the four unknowns. In addition, each reference station clock still needs to be estimated precisely, in order to isolate it from the satellite clock related errors, resulting in the need for highly accurate atomic clocks to be installed at the reference stations.

The navigation inversion concept is widely employed in the WADGPS algorithms, with a variety of procedures. In the algorithm proposed by Brown (1989) and Mueller *et al* (1994), the satellite ephemeris errors are computed in three components namely, along track, cross track and radial directions, plus the satellite clock related errors. Since the satellite ephemeris radial errors are almost indistinguishable from the satellite clock related errors, Brown (1989) combines these two errors together for estimation and transmission. This

should not affect the overall WADGPS navigation accuracy, and results in three correction parameters for each satellite being transmitted to the users. Kee *et al* (1991) proposed that the ephemeris errors be computed in the form of geometrical corrections to the geocentric Cartesian coordinates, plus the satellite clock offset (including SA 'dither'), resulting in four correction parameters for each satellite to be transmitted. These ephemeris corrections are then applied to the broadcast ephemeris by the user in order to perform WADGPS positioning.

The drawback of this technique is that considerable extra loads on the data link are introduced, by adding additional correction terms per satellite per epoch. It also requires that the reference and user stations receive the same updated broadcast ephemeris at the same time, to ensure that the corrections are applied to the proper ephemeris.

- **The Orbit Relaxation**

The orbit relaxation is a technique that allows the orbit to change from the broadcast ephemeris, thus moving slightly, resulting in an improved orbit. The GPS satellite orbit, described by the broadcast Keplerian parameters, is assumed not to be perfect within a short period (short-arc). As a consequence, the corrections to the Keplerian parameters are estimated as part of the solution from a regional network, to improve the satellite orbit. The main advantage of this technique is that a maximum of only six extra unknowns are added per period. However, the orbit predicted by the Keplerian parameters is only valid for a short period, as such a prediction would not be reliable if extrapolated beyond the span of the data (Hill, 1989).

This technique has been used by Casewell *et al* (1994) to perform regional orbit improvement over Europe. The problem with using the short-arc orbit relaxation approach for WADGPS is that, as the name implies, it can only be used on a regional basis. A period of observations is needed for the reference

stations to compute the corrections to the six Keplerian parameters to generate improved ephemerides. In order to provide ephemerides to users in the region in real-time and all the time, it is necessary that the reference network stations observe all the satellites before the users do. This is not possible with a regional approach such as the orbit relaxation method. One of the solutions proposed by Casewell *et al* (1994), is to predict the orbit before the satellite is visible to the reference and user stations in the region, by using observations from the neighbourhood region, where the satellites had appeared already. The drawback of this solution is that it requires an additional reference station network installed nearby.

- **The Dynamic Orbit Determination**

The technique applied in the Nottingham WADGPS algorithm is to perform a complete dynamic orbit determination by using data from a fiducial network. The orbit is determined by using the fiducial technique in conjunction with orbit integration. Unlike the use of Keplerian parameters by the GPS broadcast ephemeris, a complete satellite state vector (position and velocity) transmitted by the control segment at regular intervals, is used to replace the broadcast ephemeris. This method is adopted for GLONASS (GLObal NAvigation Satellite System) satellites, where the broadcast ephemeris is given in the form of complete satellite state vectors at regular intervals. The discrete satellite state vectors can be broadcast every 15 minutes or so and the satellite position at the desired epoch can be estimated by the user by performing some form of extrapolation.

The Nottingham approach, even though more sophisticated in concept and computation than the other two approaches, concensequently requires a longer computation time, has advantages compared with the other approaches. The advantages are,

- The ephemeris produced using this technique is free from SA errors. It can be treated as an independent product which provides an alternative to the precise ephemeris available, such as the IGS or JPL precise ephemerides.

- The approach is robust and does not rely on the reference and user sites receiving the same broadcast ephemeris at the same time.

- The approach allows extra state vectors to be computed at epochs in the near future, enabling the user to interpolate a more reliable and accurate satellite position rather than extrapolate.

- The method is not sensitive to epochal satellite-station geometry as cumulative epochs are used in the solution.

Dynamic orbit determination involves the precise modelling of all the forces acting on a satellite. The resulting acceleration is integrated once to give the velocity and twice to give the position of the satellite as a function of time. The initial starting values of the orbit parameters (position and velocity) need not be very accurate as they are improved by the introduction of observations from the fiducial network in a least squares adjustment process. Depending on the accuracy of the starting values, an iterative procedure can be used to further improve the solution.

3.3.2 Atmospheric Propagation Error

The atmospheric propagation error includes two different components, those due to the ionospheric and tropospheric effects, both of them delaying the pseudorange i.e. the observed range is always 'too long'. The ionosphere is a dispersive medium at radio frequencies and therefore the ionospheric delay is a function of the signal frequency and the Total Electron Content (TEC) along the signal path. The TEC is a function of factors such as the local time,

magnetic latitude and the sunspot cycle. This property makes it possible to estimate the ionospheric delay by the use of dual frequency measurements. If both the reference and user sites are equipped with dual frequency receivers, there is no need to either model or transmit the ionospheric delay, since the user can estimate the delay from the measurements. However, if only single frequency receivers are available, the ionospheric delays must be modelled and transmitted to the user.

The tropospheric delay is a function of the atmospheric pressure, temperature and water vapour pressure. Since the troposphere is a non-dispersive medium, dual frequency measurements cannot be used to estimate the delay. As a result, the estimation of the tropospheric delay must rely on one of the existing tropospheric models, which are based on the estimation of the integral of the refractive index along the signal path.

The ionospheric modelling approaches proposed by El-Arini *et al* (1994), Basker *et al* (1994), Brown (1989), Kee, *et al* (1991) and Loomis (1991), are all based on the use of dual frequency observations at the reference stations. In the Brown (1989) approach, the ionospheric data are collected at reference stations and a combination of GPS ionospheric models, i.e. Klobuchar model, and the updated Bent model is proposed to be used. A set of locally fitted eight Klobuchar coefficients are generated for the user to estimate local ionospheric delays. In the Kee *et al* (1991) approach, the broadcast coefficients of the GPS ionospheric model (Klobuchar model) are optimised by a Non-linear Static Estimation (NSE) technique, to generate a set of optimised coefficients using the dual frequency data collected from the reference sites. A grid ionospheric algorithm is proposed by El-Arini *et al* (1994). In this algorithm, the ionospheric delays at the reference stations are estimated using dual frequency GPS receivers and sent to the master station. The master station then collects all the delays, in addition to the elevation and azimuth angles from all the reference stations, and estimates a zenith delay for each node of an imaginary fixed grid (every 10 degrees in latitude and longitude).

Finally, the zenith delays of each node of the grid, as well as the node latitude and longitude, are sent to the user via communication satellites. The user then estimates local ionospheric delays from the received zenith delays of four surrounding nodes.

The troposphere is generally considered to extend from the ground surface to an altitude of about 10 km (Brown, 1989). The tropospheric delays are estimated by the integral of the refractive index along the tropospheric signal path (§ 2.6.3). The dry part of the refractive index is responsible for about 90% of the delays and can be modelled well using the surface meteorological data. The wet component contributes only about 10 % of the delays but is very complex and not easily modelled. This is because the wet component is sensitive to the water vapour pressure along the signal path which is difficult to measure. There are several techniques available for measuring the water vapour pressure along the signal path but they are not practical for use in WADGPS because of the expense and inconvenience. In terms of the WADGPS accuracy potential, the modelling of the dry part of the tropospheric delay should be sufficient to provide the required accuracy.

Various methods for the estimation of the tropospheric delay have been proposed. Kee *et al* (1991) and Casewell *et al* (1994) treat the tropospheric delay as receiver noise in the system. Brown (1989) applies a standard tropospheric model at the reference stations and the delays are then spatially modelled by a three coefficients fit to the surface refractivity measurements. El-Arini *et al* (1994) apply the Air Force Cambridge Research Laboratory (AFCRL) tropospheric model together with weather information at reference stations. The same model but without weather information is applied at the user site. Muller *et al* (1994) estimate the spatially correlated scale factor of the standard tropospheric model from single frequency measurements. The Davis model, together with measured meteorological parameter values, is employed by Loomis *et al* (1991) to remove the tropospheric effect.

The combined effect of the ionospheric and tropospheric delays proposed in one of the Nottingham's single frequency WADGPS algorithms was specially designed for the single frequency receiver environment. This was the strategy for a civilian WADGPS system without the need for dual frequency receivers in consideration of the following two factors,

I. the activation of A-S, denying access to the second frequency measurements necessary for ionospheric delay estimation for unauthorised civilian user
II. the dual frequency receivers being relatively expensive compared with the single frequency receivers.

The treatment of combining the ionospheric and tropospheric delays as a single atmospheric delay was based on the assumption that the wavelengths of the larger scale features of the two are approximately equal and that both produce a pseudorange delay in the same direction, and vary according to the elevation angle of the satellite.

The approach adopted in the Nottingham single frequency WADGPS algorithm for combined atmospheric propagation error modelling, involves the Magnet model in conjunction with the scale factor technique. An extra unknown term, the atmospheric delay scale factor, is introduced as part of the orbit determination in a fiducial network to compensate for any deficiencies in the Magnet model's estimated initial delay.

3.3.3 Clock Related Errors

The approaches proposed by Brown (1989), El-Arini *et al* (1994) and Kee *et al* (1991) apply the inversion of navigation concept to solve for the ephemeris and clock related errors. These approaches rely on the assumption that the main error sources remaining after the atmospheric propagation errors have been modelled and eliminated are the satellite ephemeris and clock (satellite and receiver) related errors, plus stochastic errors. The residual errors are

assumed to be negligible compared with the satellite ephemeris and clock related errors. The offsets of each of the reference station clocks are estimated at the master station as part of a least squares computation, which also estimates the satellite clock related errors (including SA 'dither') and satellite ephemeris errors. In these approaches, the satellite clock errors are transmitted to the user, however, the receiver clock errors are not transmitted to the user in any form. The requirement of at least one highly stable receiver clock at a reference site is essential in these approaches. The reference station clock, to which all the other receiver clock offsets are referred, must be very accurately monitored and the behaviour of the clock must be precisely known, if no extra errors are to be introduced (Basker *et al*, 1994; El-Arini *et al*, 1994). The approach has the advantage of being robust, since the least squares technique is applied throughout the entire computation and no external averaging of the satellite clock errors from the different reference stations is required, producing one satellite clock related error per satellite. Loomis *et al* (1991) estimate the clock related errors through measurement pre-processing. The satellite clock errors are estimated using a least squares filter, after correcting for the effect of the satellite ephemeris errors. Muller *et al* (1994) estimate the satellite clock errors together with the satellite ephemeris errors in a least squares process.

The approach proposed at Nottingham for the estimation of the clock related errors is based on the assumption that, if the ephemeris and atmospheric propagation errors are all well modelled and hence eliminated, the remaining errors are assumed to be clock related errors. This is based on the assumption that the residual errors are very small compared with the 'true' clock related errors (including SA 'dither'), and can be absorbed by the latter without significant differential error.

The satellite clock errors are position independent error sources and are therefore common to all users regardless of location. However, the range errors which contain the receiver clock errors are different for every reference receiver. As many differential corrections as there are reference stations are

generated per satellite. In order to enable the user to receive only one differential correction per satellite, the different differential corrections from the reference sites must be combined somehow. This makes it necessary to refer all of the reference site clocks to a single master clock. In the Nottingham approach, any one of the reference sites' receiver clock can be selected as the master clock. The other reference site clocks are then all referred to it. This generates a unique differential correction per satellite which consists of one receiver clock error and an averaged satellite clock error for each satellite visible within the WADGPS network. Since the reference receiver clock errors can be treated as an extra part of the user's own receiver clock error, the user position accuracy is insensitive to the reference station receiver clock errors. As a result, relatively inexpensive, less accurate clocks can be used as reference clocks without degrading the navigation accuracy. The use of this approach makes it unnecessary to have very accurate clocks at the reference sites as proposed by other approaches.

3.4 Nottingham WADGPS Approach : Prior to This study

The concept and algorithm of the single frequency WADGPS approach at Nottingham prior to this study are described in more detail in this section, therefore preparing ground for the current WADGPS research. The WADGPS algorithm was based on the separation of the GPS error sources into different components by single frequency only receivers. The design of using single frequency only receivers at both reference and user sites, was imposed on the research project commissioned by Inmarsat at that time (Ashkenazi *et al* 1993).

In summary, the bundled differential correction in conventional DGPS is broken down into :

I. an independent ephemeris, not affected by the SA 'epsilon', transmitted to the user to replace the broadcast ephemeris,
II. regional optimised atmospheric parameters transmitted to the user to estimate the local atmospheric delays

III. the remaining errors, assumed to be clock related, transmitted to the user for all the satellites in view within the reference network.

The considerations for the use of single frequency receivers were two fold. Firstly, that the implementation of Anti-Spoofing (A-S) would render the second frequency unavailable for ionospheric delay estimation and, secondly, that dual frequency receivers would be relatively expensive to acquire. However, with the advancement of technology, some forms of relatively precise second frequency measurements can be made even under A-S (§ 2.4). It is also fair to assume that the market for the system would be such that service providers will be willing to employ dual frequency receivers. The single frequency approach is therefore being tuned to cope with the availability of dual frequency receivers (Chapter 4).

On the other hand, as only the GPS Standard Positioning Service (SPS) is provided to civilian users worldwide, the need for WADGPS design based on single frequency receivers has grown significantly over the recent past, especially amongst government agencies and users. (The latest GPS policy signed by the US President on March 29, 1996, confirmed this institutional issue for the near future (The White House, 1996)). Hence research on the design of a single frequency WADGPS system is further investigated, to provide a refined single frequency WADGPS system (§ 4.7).

The following sections summarise the merits and any possible improvement that can be made to the single frequency WADGPS algorithm, which is discussed based on the different error components, namely the satellite ephemeris, atmospheric propagation and clock related errors.

3.4.1 Satellite Orbit Errors

The improved satellite orbit is generated by performing a dynamic orbit determination, using the single frequency double difference pseudorange data

from a reference network to replace the broadcast ephemeris. The double difference pseudorange has the advantage of minimising common errors such as SA 'dither', satellite and receiver clock errors, and errors due to the atmospheric propagation effects. However, as the atmospheric delays are not entirely eliminated by the double differencing, the modelling, estimation and removal of the atmospheric delays are essential for achieving high precision satellite orbits.

The double difference process usually involves the 'base satellite' concept. The base satellite provides the reference to which all the double differences are formed at a certain epoch. If a base satellite is not present then the observations will usually be rejected. Since the orbit determination requires a global network (or, a fairly wide regional network), the conventional baseline processing which requires the same base satellite over the entire network is obviously not possible for WADGPS.

A special technique referred to as the *'Unconnected Double Difference Baseline Approach'* was developed to be used for the determination of satellite orbits (Ochieng, 1993). The unconnected baselines are formed by linking pairs of receivers together, resulting in baselines half the number of stations. This technique enables the double difference pseudorange observable to be used in satellite orbit determination, simplifies the computation of the correlation matrix and allows different base satellites to be chosen for different baselines. However, each pair of baselines is treated as uncorrelated, and some of the observations between them which are available but not applied in the process weaken the final solutions. The computational difficulties imposed by the global network baseline processing is investigated and a technique referred to as the *'Global Independent Double Difference Baseline Approach'* is proposed, to allow all available observations in a global network to be used in the processing (§ 4.4).

As the dual frequency measurements are available irrespective of whether A-S is activated or not, the use of dual frequency ionospherically-free measurements for orbit determination is investigated. The satellite orbit accuracies achievable using simulated and real field data are presented in Chapter 6 and Chapter 7, respectively.

3.4.2. Atmospheric Propagation Errors

The combined atmospheric delays approach enables the errors of atmospheric propagation effects to be estimated under the single frequency environment. The combination of ionospheric and tropospheric delays as a single atmospheric delay, is based on the assumption that the long wavelengths of these two are similar and are of the same sign for the pseudorange observable. This approach also relies on the fact that the delays are related to the elevation angle of the satellite. An initial approximate atmospheric delay is made either empirically or from any atmospheric model. Any difference between the actual delays and the approximation are assumed to be due to a scale error. The estimation of the scale error is performed as part of the orbit determination process, where an extra unknown is added to the orbit determination process to scale the initial value. The estimated atmospheric delays are then fitted into a Klobuchar-like optimiser, to generate the regional best-fitting atmospheric model coefficients for the network. The optimised atmospheric model coefficients are then sent to users at regular intervals in a similar form to the Klobuchar parameters to estimate the local atmospheric delays.

The combination of the ionospheric and tropospheric delays in the approach obviously raises questions as to its validity, since the effects of these two delays are physically different from each other. As a WADGPS based on solely single frequency receivers is still in need, the atmospheric delay modelling using single frequency observables is further investigated. The technique, referred to as the *'Single Frequency Ionospheric Scale Factor Approach'* (§ 4.7.2) is developed and promising test results have been obtained (§ 7.3.3).

In the light of the possibility of employing dual frequency receivers for ionospherically-free measurements, the ionospheric and tropospheric errors are separately estimated and modelled, to further improve the navigation accuracy. The estimation, modelling and transmission of ionospheric and tropospheric errors are discussed in Chapter 4.

3.4.3 Clock Related Errors

The proper modelling and elimination of ephemeris and atmospheric propagation errors result in the remaining errors being assumed to be clock related errors. These include the satellite clock, receiver clock and SA 'dither' errors, and are proposed to be transmitted as differential corrections to the user in a similar manner as in conventional DGPS.

The procedure of forming the differential corrections is virtually the same for all WADGPS algorithms developed at Nottingham. The different differential corrections generated by a network of reference stations are combined to form a unique set of differential corrections. This is done by selecting one of the reference stations to act as a master clock and then having all the clock errors referenced to it, by propagating the clock errors round the network via common-view satellites. The resulting differential corrections, consisting of one reference receiver clock error and an averaged satellite clock error, are transmitted to the user to correct the observed ranges accordingly.

The user performs an independent point positioning computation to solve for the position and its own receiver clock error, uses the corrected pseudoranges. Note that the resulting clock error is not just that of the user's own clock, but the sum of the reference station clock and the user clock errors. However, this is only a conceptual point which has no practical implication and should not affect the user. As a consequence, relatively inexpensive, less accurate clocks can be used as reference clocks without degrading the navigation accuracy.

Chapter 4

The Refined WADGPS : Theory

4.1 Introdcution

In the single frequency combined atmospheric delay approach, the two main components of atmospheric propagation errors, ionospheric and tropospheric errors, are combined as a single parameter in the modelling process. It is well known that the ionospheric and tropospheric have different physical properties and hence the treatment of these error components as one parameter raises the questions on the validity of the modelling process (Ashkenazi *et al*, 1995). Analysis results have shown that, the modelling of the two components should be carried out separately. This chapter is then concentrate on the refinement of the atmospheric propagation errors taking into account the relevant physical properities.

Due to the improvement in receiver technology, dual frequency measurements are available irrespective of whether A-S is operational or not. This makes it possible to estimate the ionospheric delays using the combination of dual frequency measurements. As a consequence, the algorithm designed for use in the single frequency receiver, should be refined in terms of the treatment of atmospheric propagation errors. The scenario of combining the ionospheric and tropospheric propagation errors as a single atmospheric delay, is thus changed to that involving the two components being modelled separately.

In the event that second frequency is rendered completely unavailable to the civilian community, consideration has been given to the development of a refined WADGPS technique capable of modelling the system errors from single frequency measurements. Clearly, the key issue in this scenario is the modelling of the ionospheric delays by the exclusive use of single frequency measurements.

In summary, the research for the refined WADGPS technique involved the improved modelling of the satellite ephemeris, ionospheric and tropospheric errors. The broadcast satellite ephemeris was replaced by an independently generated precise ephemeris, using the full dynamic orbit determination approach. The observables used were the double difference pseudorange code measurements, which involved differencing across two receivers and two satellites. As a result, the majority of the errors are eliminated by the differencing process, giving a more accurate observable. However, as atmospheric delays are not entirely eliminated by double differencing, the modelling, estimation and removal of the atmospheric delays are essential for achieving high precision satellite orbits. Figure 4.1 illustrates the scenario for the refined WADGPS algorithm. The control centre collected measurements from reference stations for the estimation of the satellite ephemeris and atmospheric delay. The refined modelling of the atmospheric delay should result in an improved satellite orbit. The estimated atmospheric delay was then modelled to generated a local best fitting model, and was used to compute the clock related errors. The WADGPS estimated ephemeris, atmospheric error correction model and the clock related errors were then transmitted to the user. The user applies these models to the observed range to achieve an improved position.

The process of estimating and modelling of ionospheric errors by dual frequency observables are described in Sections 4.2. Section 4.3 describe the tropospheric error estimation and modelling. The estimation of the satellite

ephemeris errors is discussed in Section 4.4 and the estimation of the clock related errors is given in Section 4.5. Data pre-processing and validation, the process used to control the quality of the observables, are described in Section 4.6, whilst single frequency WADGPS is described in Section 4.7.

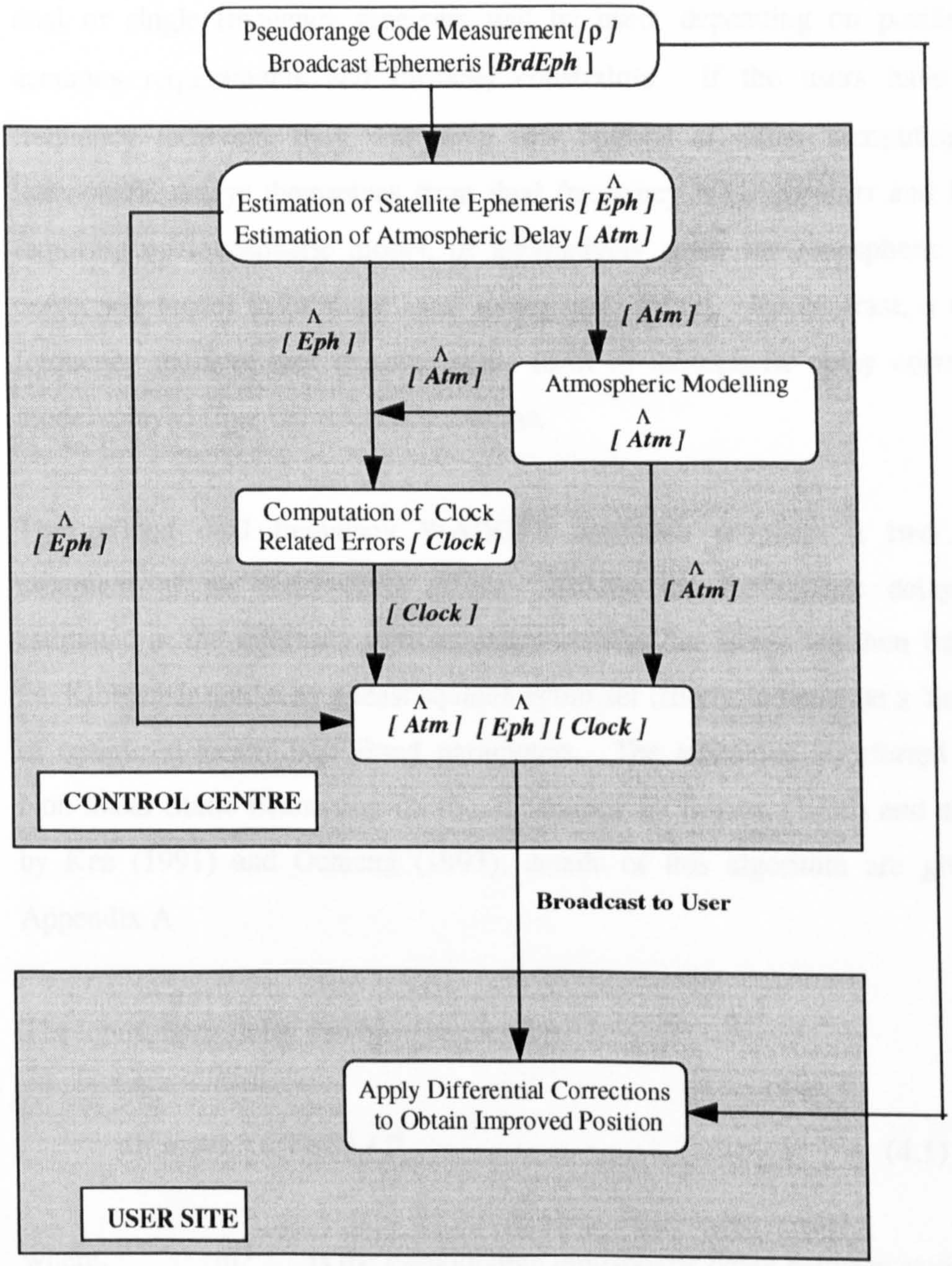

Figure 4.1 The Refined Nottingham WADGPS Scenario

4.2 Dual Frequency Ionospheric Error Estimation and Modelling

The treatment of the ionospheric error depends on the type of receiver available, in terms of accessibility to the second frequency. Currently (April 1996), it may be assumed that the reference stations may be equipped with either single or dual frequency receivers. As far as users are concerned, either dual or single frequency receivers will be used, depending on positioning accuracy requirements and financial constraints. If the users have dual frequency receivers, they will have two options of either computing the ionospheric delays themselves from dual frequency measurements and hence requiring no ionospheric model, or alternatively apply the ionospheric error correction model to estimate local ionospheric delays. By contrast, a single frequency receiver user requires some form of ionospheric delay correction model relayed from the reference stations.

The refined dual frequency WADGPS approach proposes a two stage treatment of the ionospheric errors. Firstly, the ionospheric delays are estimated at the reference stations and secondly, the delays are then fitted to the Klobuchar model by a least squares optimiser (filter), to generate a 'new' set of optimised locally best fitted parameters. The technique is referred to as Non-linear Static Estimation (NSE), developed by Bryson (1989) and applied by Kee (1991) and Ochieng (1993), details of this algorithm are given in Appendix A.

The ionospheric delay can be expressed by,

$$dI_i^j = 40.3 * TEC_i^j / f^2 \qquad (4.1)$$

where, dI_i^j is the pseudorange ionospheric delay between station i and the observed satellite j

f is the signal frequency

TEC_i^j is the total electron content

The equation is actually a first order expression, where the higher order terms are neglected. This truncation can cause up to 5 cm error in pseudorange code measurements (Spilker, 1979). The various linear combinations of the two frequencies L1 and L2 can be used to provide either the 'ionospherically-free' observable or the actual delays. The derivations of the ionospherically-free observable and the value of the ionospheric delay are given in this section.

The observed pseudorange can be expressed as,

$$P^j_{iL1} = \rho_i^j + dI^j_{iL1} \tag{4.2}$$

$$P^j_{iL2} = \rho_i^j + dI^j_{iL2} \tag{4.3}$$

where
P^j_{iL1} is the observed L1 pseudorange
P^j_{iL2} is the observed L2 pseudorange
ρ_i^j is the 'ionospherically-free' range
dI^j_{iL1} is the L1 ionospheric delay
dI^j_{iL2} is the L2 ionospheric delay

Substituting equation (4.1) into equation (4.2), (4.3), results in,

$$P^j_{iL1} = \rho_i^j + A/ f_{L1}^2 \tag{4.4}$$

$$P^j_{iL2} = \rho_i^j + A/ f_{L2}^2 \tag{4.5}$$

where
$A = 40.3 * TEC_i^j$
f_{L1} is the L1 frequency
f_{L2} is the L2 frequency

Rearranging equation (4.4) and (4.5), equation (4.6) is obtained,

$$(P^j_{iL1} - \rho_i^j)\, f_{L1}^2 = (P^j_{iL2} - \rho_i^j)\, f_{L2}^2 \tag{4.6}$$

Re-arranging for ρ_i^j,

$$(f_{L2}^2 - f_{L1}^2)\, \rho_i^j = P^j_{iL2}\, f_{L2}^2 - P^j_{iL1}\, f_{L1}^2$$

$$\rho_i^j = (-1)\, (P^j_{iL2}\, f_{L2}^2 - P^j_{iL1}\, f_{L1}^2) / (f_{L1}^2 - f_{L2}^2) \tag{4.7}$$

ρ_i^j in equation (4.7) is the ionospherically-free pseudorange derived using the combination of the dual frequency measurements. In order to estimate the ionospheric delay for either the L1 or L2 pseudoranges, the formulae can be further developed to generate the ionospheric delays. The derivation is given as below,

From equation (4.1),

$$dI^j_{iL1} = A / f_{L1}^2 \qquad (4.8)$$

Substituting equation (4.4), into equation (4.8)

$$dI^j_{iL1} = (P^j_{iL1} - \rho_i^j)\, f_{L1}^2 / f_{L1}^2 \qquad (4.9)$$

Substituting equation (4.7), into equation (4.9)

$$dI^j_{iL1} = P^j_{iL1} - [(P^j_{iL2} f_{L2}^2 - P^j_{iL1} f_{L1}^2) / (f_{L2}^2 - f_{L1}^2)] \qquad (4.10)$$

Rearranging equation (4.10)

$$dI^j_{iL1} = (P^j_{iL1} - P^j_{iL2})\, f_{L2}^2 / (f_{L2}^2 - f_{L1}^2) \qquad (4.11)$$

In equation (4.11), dI^j_{iL1}, is the L1 pseudorange ionospheric delay. This is employed in the processing software (§5.2), for the estimation of the ionospheric delays at the reference stations. The ionospheric delays are then fitted to a Klobuchar-like model to generate a new set of local ionospheric parameters, using the NSE algorithm.

In the Klobuchar model (Klobuchar, 1977, 1982), the ionospheric zenith delay is expressed by eight coefficients and is a cosine function with a night-time constant term. The eight coefficients are included in the broadcast message for single frequency users to estimate the ionospheric delay. The delay is given as,

$$T_v = A_1 + A_2 \cos [\, 2\pi(\tau - A_3) / A_4 \,] \qquad (4.12)$$

where, T_v is the ionospheric zenith delay

A_1 is the night-time constant

A_2 is the amplitude term of the cosine function

A_3 is the local time when the delay is at its peak

A_4 is the period term of the cosine wave

τ is the local time when the measurements are made

The night-time constant is based on the assumption that the TEC is relatively small and can be treated as constant at night. The night-time value, A_1, is set to 5 nano-seconds, i.e. about 1.5 m in range (Klobuchar, 1977). The A_2 term in equation (4.12) represents the amplitude of the cosine function. It is represented by a third order polynomial, which is a function of the geomagnetic latitude of the sub-ionospheric point. The sub-ionospheric point is the point at which the line of sight between the satellite and the ground station intersects with the ionosphere. This is approximated to occur at an altitude of 350 km. The polynomial is expressed as,

$$A_2 = \alpha_0 + \alpha_1\phi_m + \alpha_2\phi_m^2 + \alpha_3\phi_m^3 \qquad (4.13)$$

where,

$\alpha_0, \alpha_1, \alpha_2, \alpha_3$ are the coefficients that determine the amplitude of the cosine wave

ϕ_m is the geomagnetic latitude of the sub-ionospheric point

The A_3 term is the local time at which the TEC reaches its peak, usually set to 14:00 hours local time, but can be altered according to the local environment. The terms associated with A_3 represent the phase of the cosine wave.

In equation (4.12), A_4 represents the period of the cosine wave, which may also be expressed as a third order polynomial, expressed as,

$$A_4 = \beta_0 + \beta_1\phi_m + \beta_2\phi_m^2 + \beta_3\phi_m^3 \qquad (4.14)$$

where,

$\beta_0, \beta_1, \beta_2, \beta_3$ are the coefficients that determine the period of the cosine wave

The local time, τ is given in seconds as follows,

$$\tau = 4.32 * 10^4 + \text{GPS time}$$

if $\tau > 86{,}400$ then,

$$\tau = \tau - 86{,}400 \qquad (4.15)$$

The geomagnetic latitude, ϕ_m, in units of semi-circles of the sub-ionospheric point is given as,

$$\phi_m = \phi_I + 0.064 \cos(\lambda_I - 1.617) \qquad (4.16)$$

where,

ϕ_I is the longitude of the sub-ionospheric point

λ_I is the latitude of the sub-ionospheric point

The cosine function, part of equation (4.12), needs to be modified, since only the positive part of the cosine wave is used in the model. Therefore the first two terms of the cosine expansion are used instead of the actual function. Then from equation (4.12), model is then expressed as,

$$T_v = A_1 + A_2 \ [1 - x^2/2 + x^4/24] \qquad (4.17)$$

where,

$x = [\, 2\pi(\tau - A_3) / A_4 \,]$, as for equation (4.12)

Due to the physical property of the ionosphere, the TEC is sensitive to the magnetic activities of the ionosphere. Therefore, the ionospheric delays are better represented by geomagnetic latitude than geographic latitude. Consequently, the geomagnetic latitude is used in the model instead of the geographic latitude, and the ionospheric delays are computed at the sub-ionospheric point, rather than at the observer.

In order to calculate the geomagnetic latitude, the geographic latitude and longitude of the sub-ionospheric point, ϕ_I and λ_I, must be calculated first. The errors caused by the difference between the latitude of the sub-ionospheric point and the ground point can be large. For an observer located near to the Earth's surface, looking at a satellite at 5 degrees elevation, the ionospheric intersection location is approximately 14 degrees of earth-centred angle from the observer (Klobuchar, 1982). The earth centred angle, ψ, is given as,

$$\psi = [\, 0.0137 / (E + 0.11) \,] - 0.022 \qquad (4.18)$$

where,

E is the elevation angle of the satellite given in the units of semi-circles

The sub-ionospheric latitude and longitude are estimated, assuming a flat Earth approximation as follows,

$$\phi_I = \phi_u + \psi \cos A \qquad \text{when} \quad |\phi_u| < 0.416, \qquad (4.19a)$$

$$\phi_I = 0.416 \qquad \text{when} \quad |\phi_I| \geq 0.416 \qquad (4.19b)$$

$$\lambda_I = \lambda_u + [\, (\psi \sin A) / \cos \phi_I \,] \qquad (4.20)$$

where,

A is the azimuth of the GPS satellite in semi-circle unit

ϕ_u is the latitude of the observer in semi-circles

λ_u is the longitude of the observer in semi-circles

The ionospheric zenith delays are mapped to the slant values according to the satellite elevation. The mapping function (F), given by Klobuchar (1982), is expressed as,

$$F = 1.0 + 16.0\,(0.53 - E)^3 \qquad (4.21)$$

The L1 pseudorange ionospheric delay (T_i) is then expressed as,

$$T_i = F * c * [\, 5 * 10^{-9} + (\alpha_0 + \alpha_1\phi m + \alpha_2\phi m^2 + \alpha_3\phi m^3) (1 - x^2/2 + x^4/24) \,]$$

when $|x| < 1.57$ (day-time) (4.22a)

$T_i = F * c * 5 * 10^{-9}$ when $|x| \geq 1.57$ (night-time) (4.22b)

where, $x = [\, 2\pi(\tau - 50{,}400) / (\beta_0 + \beta_1\phi m + \beta_2\phi m^2 + \beta_3\phi m^3) \,]$

4.3 Tropospheric Error Estimation and Modelling

As the ionospheric delays are modelled by dual frequency measurements, it is then possible to separate the tropospheric errors from the ionospheric errors and model them individually. Consequently, investigations were concentrated on the estimating, modelling and transmission of the tropospheric delays in the dual frequncy WADGPS. The treatment of the tropospheric errors can be classified into two phases, namely (i) the estimation of the tropospheric delay at the reference station (or at both reference and user stations), and (ii) the modelling of the tropospheric delay.

4.3.1 Estimation of the Tropospheric Delay

The approach employed in this research for the estimation of the tropospheric delays is that of using local scale factors together with a standard tropospheric model as part of the orbit determination process. The tropospheric model used to provide the initial approximate values in this research was the Magnet model (Curly, 1988). The initial approximate value, Z_{trop}, is expressed as,

$$Z_{trop} = 0.002276 \times P \tag{4.23}$$

and,

$$P = (1015.0 - 1.75 \cos\phi) e^{-hx} \tag{4.24}$$

$$x = 0.113 + 0.001h + 0.017 \sin[1+0.382 \mathrm{Cos}(0.0174 (JD-30))] \tag{4.25}$$

where, P, is the atmospheric pressure

ϕ, is the station latitude

JD, is the Julian Day

h, is the height

In fact, the initial approximate tropospheric zenith delay, Z_{trop}, can be given by an empirical value or by any tropospheric model. Tests have been carried out to show that different initial values only result in different scale factors but do not affect the final estimated tropospheric delays (§6.2.1). The initial tropospheric zenith delay is then mapped down to the slant value according to the satellite elevation angle (E). The mapping function (F), used in this research is given as,

$$F = 1/[\sin(E)] + [0.00143\cos(E)/\sin(E) + 0.0445\cos(E)] \qquad (4.26)$$

The mapped value, Z_c, representing the slant tropospheric delay is given by,

$$Z_c = Z_{trop}/[\sin(E)] + [0.00143\cos(E)/\sin(E)+ 0.0445\cos(E)] \qquad (4.27)$$

Any deficiencies in the estimated initial zenith delays are compensated for by introducing a scale factor as an extra unknown to be solved as part of satellite orbit determination in a least squares adjustment. The orbit determination process requires a long span of data to generate a reliable ephemeris (e.g. 48 to 72 hours). However, due to the time varying tropospheric behaviour, one single tropospheric delay scale factor over this entire period cannot properly represent the variation of the tropospheric delays. The approach adopted is to estimate different scale factors at shorter regular periods. The intervals were chosen based on the balance between the precision and the computational complexity caused by introducing by extra unknowns. Ochieng (1993) suggested that 90 minute intervals would provide sufficient accuracy for a WADGPS system. The actual zenith delay, Z, after the least squares

adjustment, can be estimated by the initial value, Z_c (equation 4.27), and the estimated scale factor, α, given by,

$$Z = (1 + \alpha) \times Z_c \tag{4.28}$$

4.3.2 Modelling of theTropospheric Delay

Due to the variability of the tropospheric behaviour over very long baselines, typically hundreds to thousands of kilometres between the reference and user stations, the tropospheric errors become less and less correlated. In the limit, they may be considered as station unique. Consequently, the proposed modelling of tropospheric delays is divided into two parts, one for the reference stations and another for the user sites. At the reference stations, the tropospheric delays are estimated, and hence removed from the data as part of the orbit determination process. At the user site, a standard tropospheric model is used to estimate the user's own tropospheric delay.

Other methods for the modelling of tropospheric delays were also investigated, such as treating the tropospheric errors as system noise at reference and/or user stations, or generating a tropospheric error correction model by the Klobuchar-like parameters.

The process of modelling the tropospheric error as system noise, employed by Kee *et al* (1991) and Casewell (1994) in the WADGPS approach, has been investigated in this research by simulation data and is presented in Section 6.3. The conclusion drawn from these tests is that the tropospheric errors needed to be modelled properly in order to obtain good positional accuracy.

If the user does not apply any existing tropospheric model to estimate local tropospheric effects, the tropospheric errors estimated at the reference stations must be modelled and transmitted in a form suitable for the user to apply. The

approach investigated was the possibility of modelling and transmitting the tropospheric correction, in a similar manner to the ionospheric Klobuchar parameters. Although the physical properties of the ionosphere and troposphere are different, which could cause the tropospheric errors being mis-modelled, the accuracy achievable by this modelling process is investigated. Furthermore the similar type of Klobuchar-like parameters provides the benefit of easy transmission, by the well established RTCM-SC104 recommended DGPS format. As a result, two sets of Klobuchar-like parameters, notably one for ionospheric errors and the other for tropospheric errors are transmitted to users. Consequently, this approach allows single frequency receiver users to apply the locally best fitting ionospheric Klobuchar parameters, to estimate the ionospheric error corrections, and the tropospheric Klobuchar-like parameters to estimate the tropospheric error corrections.

The 'two sets of Klobuchar-like parameters' approach, provides an alternative way of estimating tropospheric delays at the user site without measuring the surface meteorological data and can be easily adopted by the popular DGPS transmission format. The user positioning accuracy is expected to be slightly better than the single frequency combined atmospheric delay approach due to the similar deficiency in the tropospheric modelling, but the ionospheric errors were properly modelled in this approach.

Several problems arise when trying to apply Klobuchar-like models for tropospheric error modelling, including, (i) the point where the delays are calculated is brought down from the sub-ionospheric point (about 350 km altitude) to ground level, since the troposphere is the lower part of atmosphere and is generally considered to extend to an altitude of about 10 km, (ii) the geographic latitude is used in the formulae instead of the geomagnetic latitude, (iii) the mapping functions are different for the tropospheric and ionospheric models and (iv) the night-time constant value present in the ionospheric model is not present in the tropospheric model. These problems were investigated using the simulation data, the details of which are presented in Section 6.3.

4.4 Satellite Orbit Estimation

The refined WADGPS algorithm incorporates a complete dynamic orbit determination by using pseudorange data from a fiducial tracking network. A frequently updated satellite state vector (position and velocity) is transmitted to the user at regular intervals to replace the broadcast ephemeris totally. This orbit determination approach, sophisticated in concept and computation, has some advantages compared with the other approaches (§ 3.3.1). The broad principle of the process of dynamic orbit determination is illustrated in Figure 4.2.

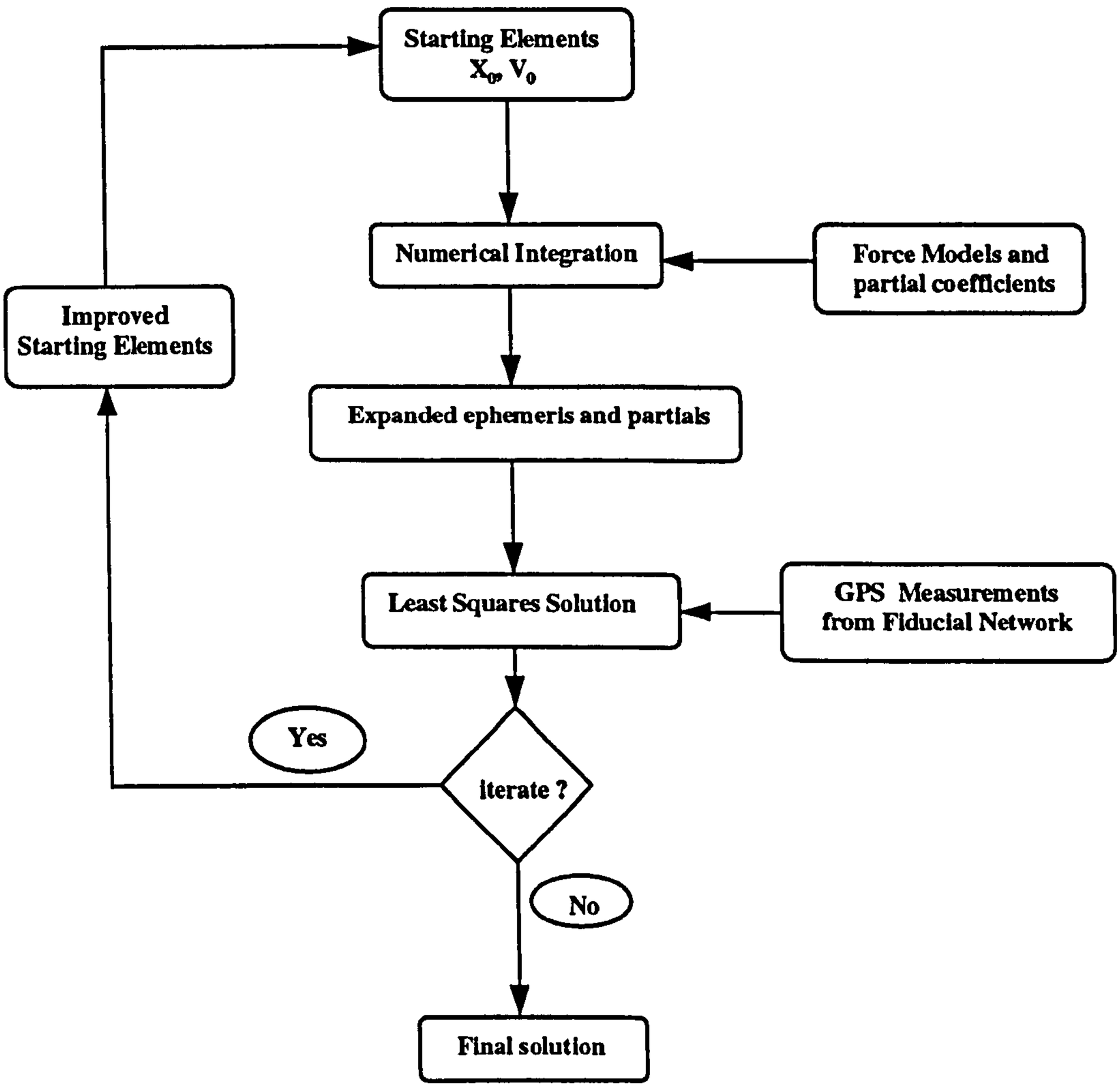

Figure 4.2 Dynamic Orbit Determination Flow Diagram (after Ochieng, 1993)

The approximate starting elements, at an initial time t_0, are generated by integrating the acceleration acting on the satellites once with respect to time to give the velocity, V_0, and twice to give the position, X_0, by the orbit integration program. The corresponding partial coefficients of the satellite position and velocity, with respect to the initial state vector and other orbital unknowns, are also generated. These partials are applied in the least squares adjustment to form the observation equations. GPS data from a tracking network are then used to improve the initial state vector and hence the integrated orbit in a least squares adjustment.

The numerical integration has to be carried out in an inertial (non-rotating) reference frame (IF), $\ddot{\underline{r}}_{IF}$. Consequently, it is necessary to transform the coordinates of the tracking stations and the force model components, given in Earth fix (EF), $\ddot{\underline{r}}_{EF}$, reference frame to IF. The transformation is carried out by the use of rotation matrices, comprising coefficients for polar motion, Earth rotation, nutation and precession. This transformation can be expressed as,

$$\ddot{\underline{r}}_{IF} = Q^T N^T E^T P^T \ddot{\underline{r}}_{EF} \tag{4.29}$$

where, P, E, N and Q are polar motion, earth rotation, nutation and precession rotation matrices, respectively (Moore, 1986).

The precision of the force model acting on the satellites has direct influence on the accuracy of the satellite orbits generated. The force models are described in Section 4.4.1. The numerical integration technique is highlighted in Section 4.4.2. The processing algorithm, including the problems encountered in large network such as the size of WADGPS, is discussed in section 4.4.3.

4.4.1 The Force Model

In order to determine an accurate orbit, all the forces acting on the satellite must be modelled. The force model required for a GPS satellite is mainly made

up of the Earth's gravity field, third body gravitational effects, tidal effects, solar radiation and other minor forces, such as the atmospheric drag.

- **Gravitational Force**

The major component of the total force model is the attraction of the Earth. The Earth's gravitational attraction is generally described by a geopotentional expansion in terms of spherical harmonics (Agrotis, 1984; Moore, 1986).

$$U = \frac{GM}{R}\left[1+\sum_{n=2}^{\infty}\sum_{m=0}^{n}\left(\frac{a}{R}\right)^{n} P_n^m(\sin\phi)[C_{n,m}\cos(m\lambda)+S_{n,m}\sin(m\lambda)]\right] \quad (4.30)$$

where,

G : the universal gravitational constant

M : the mass of earth

R : the radius of the Earth

n, m : the degree and order of spherical harmonic expansion,

a : the earth's equatorial radius,

P_n^m : the associated Legendre polynomial of degree n and order m

$C_{n,m}$,$S_{n,m}$: the spherical harmonic coefficients.

In theory, there is an infinite series for the expansion of the spherical harmonic expression of the gravitational potential. In practice, the series is truncated, depending on the accuracy required. Since the GPS satellite is at an altitude of about 20,200 km, the Earth's gravitational model needs only the spherical harmonic expansion terms up to degree and order 8 (Whalley, 1990). The Goddard Earth Model T1 (GEM T1) is used in this research for the Earth's gravity field.

The acceleration of the satellite due to the gravitational attraction is then given by the gradient of the potential field, U, at the satellite. As the potential is expressed in terms of spherical polar coordinates (Φ, λ and R for latitude,

longitude and radius respectively), the chain rule is used to relate this to the EF Cartesian components by,

$$\underline{\ddot{r}}_{EF} = \frac{\partial U}{\partial R}\left(\frac{\partial R}{\partial R_i}\right) + \frac{\partial U}{\partial \lambda}\left(\frac{\partial \lambda}{\partial R_i}\right) + \frac{\partial U}{\partial \Phi}\left(\frac{\partial \Phi}{\partial R_i}\right) \tag{4.31}$$

where R_i is the vector of the satellite position (X, Y, Z) in the EF reference system

$\underline{\ddot{r}}_{EF}$ is the vector of the satellite instantaneous EF acceleration $(\ddot{X}, \ddot{Y}, \ddot{Z})$.

Since the acceleration is in EF frame, rotation matrices (equation 4.29) are needed to transform it to IF frame to perform the orbit determination process.

The gravitational attractions of the sun, moon and other planets ('third body') are also modelled. The resulting acceleration vector $\underline{\ddot{r}}_s$ of the satellite towards the 'third body', P_j, is illustrated in Figure 4.3. The Earth is similarly attracted towards the third body P_j, resulting in the acceleration vector $\underline{\ddot{r}}_E$. The maximum effect of the resulting acceleration is reached when the three bodies in Figure 4.3 are collinearly arranged.

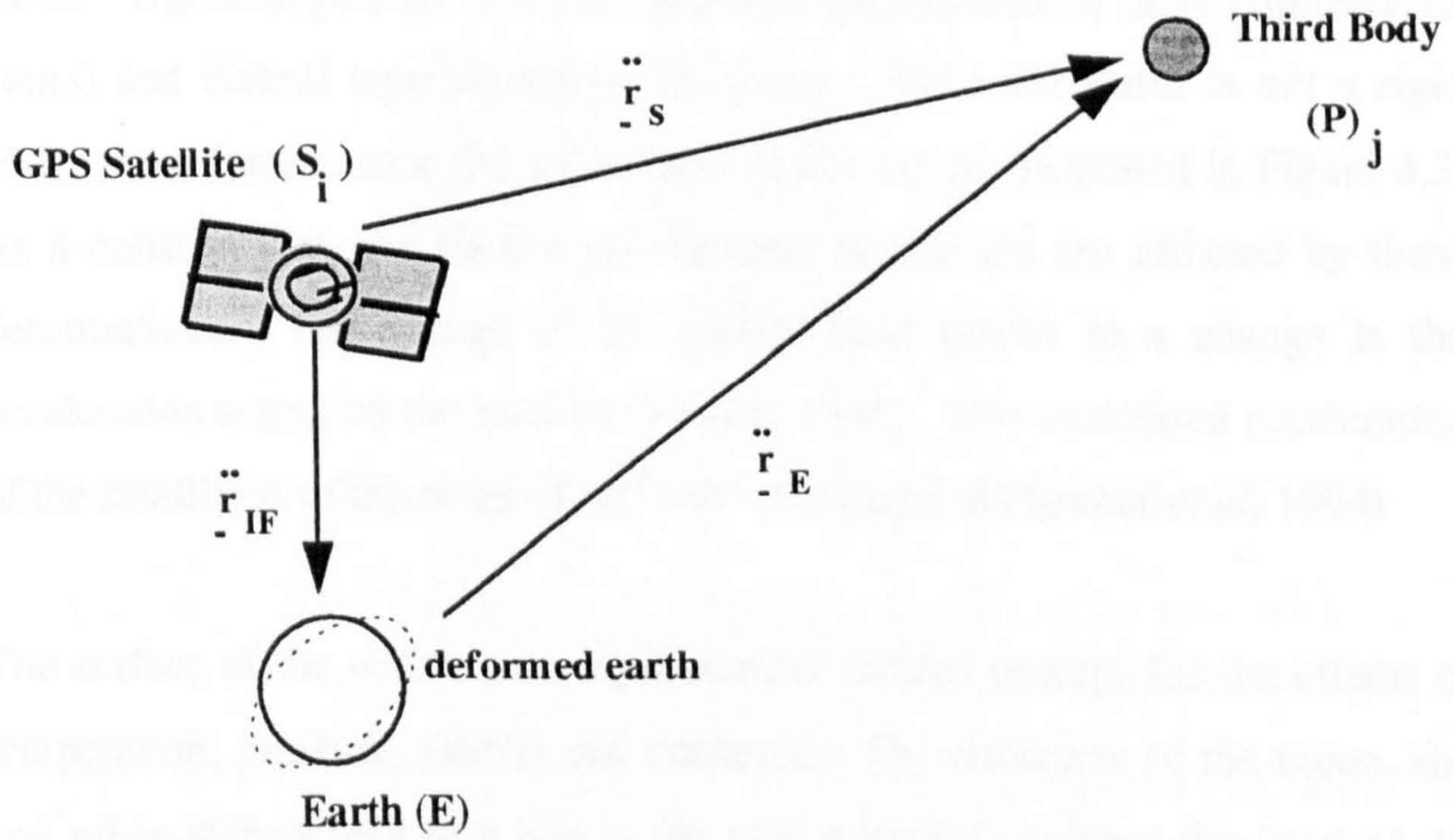

Figure 4.3 Earth Tides Caused by the 'Third Body'

The coordinates of these planets are determined from the JPL Development Ephemeris DE200/LE200 planetary and lunar ephemeris (Kaplan, 1981). This gives the daily positions of the moon and planets in a heliocentric inertial frame, together with the masses of the planets and the constants associated with the ephemeris. The coordinates in the heliocentric inertial frame have to be converted to a geocentric inertial frame in order to apply these positions. This is done by subtracting the coordinates of the Earth from those of the other planets and the moon. The geocentric position vector of the sun is equal but oppositely directed to the heliocentric position vector of the Earth. The coordinates of the moon, sun and planets in an IF frame at the required epoch may be obtained by interpolation between daily vectors. The resulting accelerations acting on a GPS satellite are of the order of 2×10^{-6} m/s^2 for the sun and 5×10^{-6} m/s^2 for the moon (Hofmann-Wellenhof *et al*, 1994).

- **Tidal Effects**

The gravitational attraction of the sun and the moon cause the Earth and the oceans to deform, the effects are referred to as solid Earth tides and ocean tides. The tidal effects vary with time as a function of the position of sun and moon. The main periods of these variations are semidiurnal (approximately 12 hours) and diurnal (approximately 24 hours). Since the Earth is not a rigid body, these forces cause the solid Earth to deform as illustrated in Figure 4.3. As a consequence, the Earth's gravitational attractions are affected by these deformations. The change of the gravity field results in a change in the acceleration acting on the satellite (Moore, 1986). The associated acceleration of the satellite is of the order of 10^{-9} m/s^2 (Hofmann-Wellenhof *et al*, 1994)

The surface of the ocean is an equipotential surface (except for the effects of temperature, pressure, salinity and currents). The attraction of the moon, sun and other planets lead to a rise in the tidal potential, causing the level of the ocean to fluctuate with time. This causes the Earth's mass to be re-arranged

periodically, resulting in a change in the gravitational field of the Earth. Therefore a similar change occurs in the acceleration of the satellites (Moore, 1986). For GPS satellites, the associated acceleration of the satellite caused by the ocean tide effects is again of the order of $10^{-9}m/s^2$, corresponding to less than 1 m after 2 days (Seeber, 1993).

- **Solar Radiation Pressure and Atmospheric Drag**

The solar radiation pressure, caused by the particles continuously emitted by the sun, generates an extra acceleration on the satellites. The resulting acceleration due to the direct solar radiation pressure has two components. These are the principal component, which is directed away from the sun, and the smaller component which acts along the satellite's y-axis, usually referred to as y-bias (Fliegel, 1985). The y-axis is along the solar panel beam, usually defined by a body-fixed spacecraft coordinate system as shown in Figure 4.4 (Seeber, 1993)

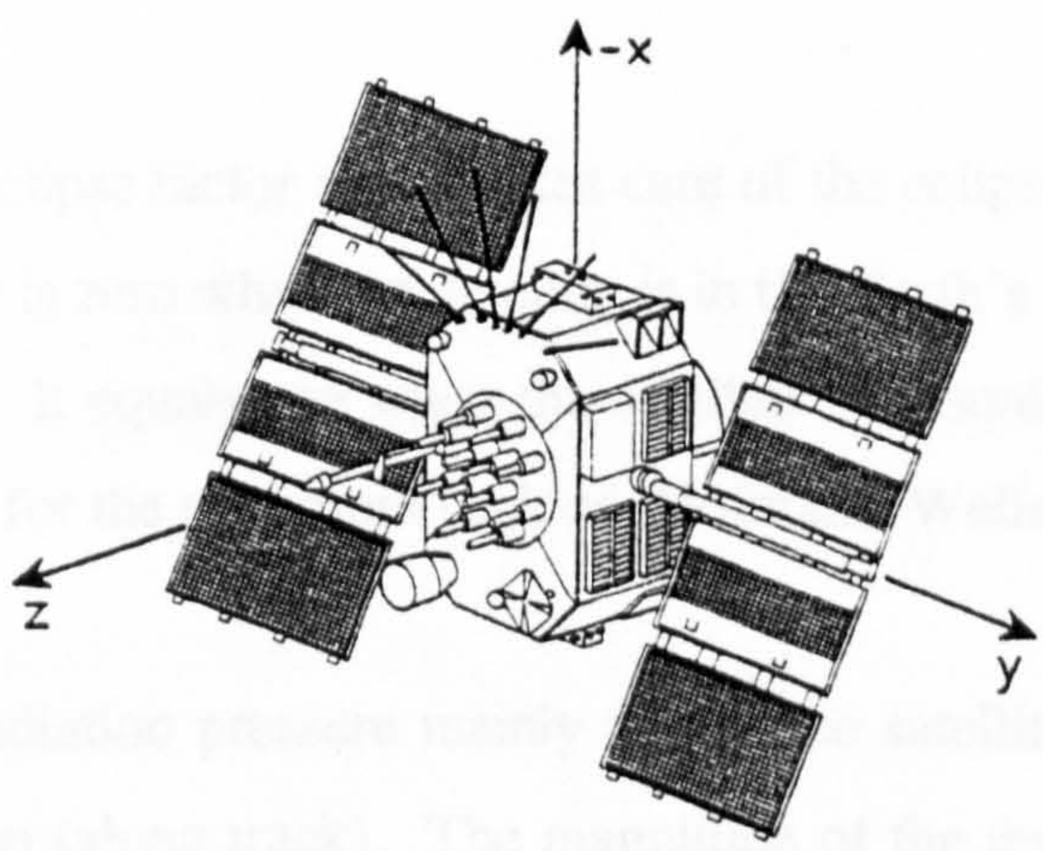

Figure 4.4 The Satellite-Fixed Coordinate System (Seeber, 1993)

The intensity of the solar radiation varies in inverse proportion to the speed of light and to the square of the distance between the satellite and the sun. It is also proportional to the reflectivity of the surface, the effective satellite surface

area and the solar flux (Caperllari *et al* 1976). The resulting acceleration, $\ddot{\underline{r}}_{SR}$, in the direction away from the sun, the principal component, is given as,

$$\ddot{\underline{r}}_{SR} = VC_R(\frac{I_0}{c})\left[\frac{A}{|\underline{r}_S - \underline{r}_j|}\right]^2(\frac{a}{m})\vec{e}_{ss} \qquad (4.32)$$

where C_R is the solar radiation reflectance coefficient, which will absorb certain deficiencies in the model and it can be determined as an unknown in the adjustment process,

V is an eclipse factor

I_0 the intensity of the radiation at a distance A nominally equal to 1367.2 W/m^2, but depending of the solar activity,

c is the speed of light in a vacuum,

A is the Astronomical unit (1.4959787 10^{11}m),

$\underline{r}_S$ is the satellite position vector in an inertial frame,

$\underline{r}_j$ is the sun position vector in an inertial frame,

a/m is the area to mass ratio of the satellite,

$\vec{e}_{ss}$ is the unit vector in the direction of the satellite from the sun.

The V is an eclipse factor which takes care of the eclipsing of the satellite. The eclipse factor is zero when the satellite is in the Earth's shadow, which happens twice a year. It equals one when the satellite is in sunlight and varies between zero and one for the penumbra regions (Hofmann-Wellenhof *et al*, 1994).

The direct radiation pressure mainly affects the satellite in the direction of the orbital motion (along track). The magnitude of the resulting acceleration is of the order of 10^{-7} m/s^2, corresponding to 10 m and more may be expected after a few hours (Hofmann-Wellenhof *et al*, 1994, Seeber, 1993). However, the modelling of the radiation pressure is rather difficult, due to the complicated shape of the satellite. Further concerns are the modelling of the penumbra region which leads to the determination of the eclipse factor. The ROCK 4 and ROCK 42 model, developed by the GPS satellite manufacturer, Rockwell

International, are tailored for BLOCK I and BLOCK II GPS satellites respectively (Fliegel *et al*, 1989). Refined models, referred to as ROCK 4 S 10, ROCK 4 T10, ROCK 42 S20 and ROCK 42 T20 have also been developed (Fliegel *et al*, 1992).

Since the y-bias force varies slowly, it can be treated as a constant for a few weeks. This constant is usually introduced as an extra unknown to be determined in the orbit determination process. The combination of misalignments of the solar panels and the thermal radiation along the y-axis is believed to be the main cause of the y-bias. The resulting acceleration is two orders of magnitude smaller than the principle component (Feltens, 1988).

The indirect solar radiation pressure is the result of the portion reflected back from the Earth's surface, called the *albedo effect* (Wells *et al*, 1986). The albedo portion of the solar radiation is very difficult to model but counts for less than 10 % of the direct radiation in most cases (Seeber, 1993). In the case of GPS satellite, the estimate lies between 1% and 2% and is usually neglected (King *et al*, 1985).

The effect of atmospheric drag is due to the interaction between the atmospheric particles and the satellite. However, as the GPS satellites are at such a high altitude, the atmospheric drag effect is negligible.

4.4.2 Numerical Integration

Satellite motion is expressed by a second order differential equation with six integration constants, usually six Keplerian orbital parameters are used. The accelerations acting on the satellite due to all the forces mentioned in Section 4.2.1, form an extended equation of motion as a function of position, velocity and time, in IF frame, which is given as,

$$\ddot{\underline{r}} = f(\dot{\underline{r}}, \underline{r}, t) \tag{4.33}$$

where $\ddot{\underline{r}}$ is the resultant acceleration vector in the inertial frame

$\dot{\underline{r}}$ is the satellite velocity vector in the inertial frame

$\underline{r}$ is the satellite position vector in the inertial frame

t is the time

The basic idea is to integrate the equation motion stepwise. Therefore, with the initial starting values, such as position, $\underline{r}(t_0)$, and velocity, $\dot{\underline{r}}(t_0)$, at a reference epoch, t_0, the desired satellite state vector (position and velocity) can be obtained by numerical integration.

The numerical integration basically fits a polynomial through a series of consecutive points, in order to create extra points through extrapolation of the polynomial. The coefficients of the polynomial are derived from the given points and their partial derivatives, based on the equation of motion. Two methods are generally used, namely single-step and multi-step methods. The single-step methods, such as the Runge-Kutta method, employ only the value from the last integration step to predict the following point. By contrast, the multi-step methods, also called predictor-corrector methods, such as the Adams-Bashforth predictor-corrector method, basically predict the value at the following epoch and then correct the value in an iterative approach. The predicted value X_{n+1} is obtained from X_n, and then evaluated using the previous n values. If the differences between the predicted and corrected values exceed the specified criteria, the process is iterated by applying the corrected value until the requirements are satisfied (Moore, 1986; Seeber, 1993). Details of the formulae of the two methods can be found in Moore (1986).

The multi-step methods have the advantage of generally producing better results than single-step methods using the same integration step length, but require information of the previous n values and are more time consuming. The integration step length has to be chosen based on the compromise of two error sources, notably the round-off and truncation errors. Round-off errors are characteristic of the computer hardware or the algorithms used. The

sophistication of computer hardware available today is such that round-off is usually due to the algorithms used. The effects of round-off errors can be minimised by using a large step lengths in the process. By contrast, the truncation errors, which arise due to the higher terms of approximation polynomial are cut off, can be reduced by using a rather small step length.

The Nottingham orbit integration program, GPSORBIT, applies a 4^{th} order Runge-Kutta single-step integrator, to provide sufficient integration steps for a more precise 8^{th} order Adams-Bashforth multi-step predictor-corrector integrator to take over. The step length of 30 seconds for Runge-Kutta scheme and 300 seconds for Adams-Bashforth scheme is employed (Ochieng, 1993).

4.4.3 The Observable

The observables used in the refined approaches are the double difference pseudorange code measurements. Pseudoranges are robust for real-time navigation applications, since they are easy to lock on to and there are no integer ambiguity and cycle slip problems. The double difference observable has the advantage that common errors such as SA 'dither', satellite and receiver clock errors are largely eliminated. Also, atmospheric propagation and ephemeris errors are reduced by the double differencing process. As the atmospheric delays are not entirely eliminated by the double differencing, the modelling, estimation and removal of the atmospheric delays are essential for achieving high precision satellite orbits.

The double difference process usually involves the 'base satellite' concept in the processing software. The base satellite is the satellite relative to which double differences are formed at a certain epoch. If a base satellite is not present at an epoch, then the observations at that epoch will be rejected. This concept therefore restricts the size of the network as common satellites are required for this approach. However, it is impossible to have the same constellation over a global area, which eventually results in no double difference pairs being formed

at some of the stations using the base satellite concept. Since orbit determination requires a global network (or a fairly wide regional network), the conventional baseline processing, which requires the same base satellite over the entire network, is obviously not possible for WADGPS.

An alternative technique applied by Ochieng (1993) to counter this problem is the use of *'unconnected double difference baseline approach'*. The baselines are formed by linking pairs of receivers together, resulting in the number of baselines equating to half the number of stations. This technique enables the double difference pseudorange observable to be used in satellite orbit determination and allows different base satellites to be chosen for different baselines. Since the baselines formed are treated as uncorrelated, the network geometry has to be carefully designed otherwise a weak network results.

In order to apply all the measurements available to strengthen the satellite geometry for the orbit determination, a refined approach has been developed and referred to as *'global independent double difference baseline approach'*. This approach allows different base satellites to be specified for each baseline, while the correlation between the baselines is still taken into account. This results in the number of baselines equating to the number of reference stations minus one. This technique is described in the following section and has been successfully implemented in the processing software for the purpose of WADGPS (§ 5.7).

4.4.4 Processing Algorithms

The *'global independent double difference baseline approach'* aims to break the network size limitation caused by the base satellite concept, so as to process a network of independent baselines over a global scale. This is done by allowing different base satellites to be specified for each baseline while the correlations between the baselines are still taken into account. This results in the number of baselines to be processed equating to the number of reference

stations minus one. The main difficulty occurs in the processing software for the computation of the inverse of the covariance matrix (C_D), due to its size. Many techniques have been developed to compute the weight matrix (W), i.e. the inverse of the covariance matrix (C_D^{-1}), efficiently.

The undifferenced observables are assumed to be mathematically uncorrelated in space and time. The differenced observables induce correlations by the differencing process. The differencing operator (D) is introduced as the operator which is applied to the original undifferenced observables to form the differenced observables. The D matrix can be expressed in different ways, two main expressions are used extensively, namely the sequential and the reference satellite differencing (Talbot, 1991). The D matrix at one station has the following pattern in the sequential differencing form,

$$D=\begin{bmatrix} 1 & -1 & 0 & \dots & 0 & 0 \\ 0 & 1 & -1 & 0 & \dots & 0 \\ \dots & & & & & \\ 0 & \dots & & 0 & 1 & -1 \end{bmatrix} \tag{4.34}$$

In the reference satellite differencing method, the pattern of the D matrix depends on the reference (base) satellite. Assuming the first satellite is selected to be the base satellite, the D matrix is given by,

$$D=\begin{bmatrix} 1 & -1 & 0 & 0 & \dots & 0 \\ 1 & 0 & -1 & 0 & \dots & 0 \\ \dots & & & & & \\ 1 & 0 & 0 & & \dots & -1 \end{bmatrix} \tag{4.35}$$

The covariance matrix of the double difference measurement (C_D) can be represented by the covariance matrix of the undifferenced observables (C_l), and the D matrix as,

$$C_D = \overline{D}\, C_l\, \overline{D}^{\mathrm{T}} \tag{4.36}$$

with $\overline{D} = [D, -D]$ and

$C_l = \sigma_0^2\, I$

where,

I is an identity matrix and

σ_0^2 is the variance of the undifferenced observable

Since the double difference observations are not correlated between epochs, the covariance matrix for multiple epochs is comprised of similar diagonal blocks. Therefore, only the inverse of the covariance matrix at a particular epoch needs to be computed. This is given as (Hofmann-Wellenhof *et al*, 1994),

$$W = (2)^{-1}\frac{1}{n}\begin{bmatrix} (n-1) & -1 & -1 & \dots \\ -1 & (n-1) & -1 & \dots \\ \dots & & & \\ -1 & \dots & -1 & (n-1) \end{bmatrix} \tag{4.37}$$

where, n-1 is the number of double difference observations at the epoch considered

In the case of a network of m stations, the correlations between the baselines are defined by a (m-1)×(m) matrix (Λ). The elements of this matrix only consist of 0s and ± 1s. There are only one +1 and one -1 per row, which identify the stations from which the baseline is formed. The double difference covariance matrix for a network can be given by (Ffoulkes-Jones, 1990).

$$C_D = [\Lambda\Lambda^T] \otimes [\overline{DD}^T] \tag{4.38}$$

where,

$\otimes$ stands for Kronecker product

The weight matrix is then given by

$$W = C_D^{-1} = \sigma_0^2 (\Lambda\Lambda^T)^{-1} \otimes (\overline{D}\,\overline{D}^T)^{-1} \quad (4.39)$$

The $(\overline{D}\,\overline{D}^T)^{-1}$ matrix can be computed as a function of the number of double differences (equation 4.37). Therefore, the advantage of forming the weight matrix in this pattern is that only a matrix of the order of m-1 needs to be inverted (inverse of $\Lambda\Lambda^T$), instead of the full weight matrix of the dimension (n-1) × (m-1). To employ equation (4.39), which saves a lot in computation time, it is assumed that each station simultaneously tracks the same satellites. This assumption makes it possible for the double differences formed at each baseline to involve the same satellites, i.e. the D matrix is the same for each baseline. However, this is a rare occurrence, since the satellite constellation would not be the same for each station when large area are invloved. Therefore, in order to take advantage of this technique, the baseline network is restricted to a regional area over which the satellite constellation is the same.

To overcome this problem, the D matrix is forced to be the same for each baseline by assuming that each station observed all the satellites visible anywhere in the network. The observations to those satellites which were not tracked were therefore assumed to be 'missed observations'. The vector of double differences actually observed, ρ_{DD_R}, different for each baseline, can be expressed by applying a linear transformation, L_R, to the double differences, ρ_{DD}, which includes all possible double differences, given by,

$$\rho_{DD_R} = L_R \rho_{DD} \quad (4.40)$$

All of the elements, except for the diagonal of the L_R matrix are zero. The diagonal has only 1s which represent the actual observed double differences. The covariance matrix of ρ_{DD_R} is given as,

$$C_{DD_R} = L_R \, C_{DD} \, L_R^{\mathrm{T}} \tag{4.41}$$

where,

C_{DD_R} is the covariance matrix of the actual observed double differences

C_{DD} is the covariance matrix of the complete set of all possible double differences

One of the methods for computing the weight matrix is by inverting the full covariance matrix. This requires a lot of computational time due to the large dimension of this matrix. The other technique, proposed by Beutler *et al*, (1986), makes further use of the results given by equation (4.39). The vector, ρ_{DD_A}, which consists of the 'missed' and the actual observed double differences can be rearranged to have the form,

$$\rho_{DD_A} = \left[\rho_{DD_R}, \quad \rho_{DD_m}\right]^T \tag{4.42}$$

where,

ρ_{DD_R} is the vector of actual observed double differences

ρ_{DD_m} is the vector of the 'missed' double differences

Thus, equation (4.42) can be rewritten as,

$$\rho_{DD_A} = L\rho_{DD} \tag{4.43}$$

where

$$L = \left[L_R, \quad L_M\right]^T$$

The rows of L_M are rows of a unit matrix. The covariance matrix of ρ_{DD_A} may be written as,

$$C_{DD_A} = LC_{DD}L^T \tag{4.44}$$

The weight matrix can be computed as

$$W_A = (L^T)^{-1} W L^{-1} \tag{4.45}$$

By substituting equation (4.43) into (4.44), the covariance matrix can be rewritten as,

$$C_{DD_A} = \begin{bmatrix} L_R C_{DD} L_R^T & L_R C_{DD} L_M^T \\ L_M C_{DD} L_R^T & L_M C_{DD} L_M^T \end{bmatrix} = \begin{bmatrix} N_{11} & N_{12} \\ N_{21} & N_{22} \end{bmatrix} \tag{4.46}$$

The weight matrix (equation 4.45) can also be expressed in a similar way as,

$$W_A = \begin{bmatrix} W_{11} & W_{12} \\ W_{21} & W_{22} \end{bmatrix} \tag{4.47}$$

The required weight matrix is finally given by Beutler *et al* (1986) as,

$$W_R = W_{11}\left[I_r + \underbrace{L_R C_{DD} L_M^T}_{N_{12}} \right]\left[W_{22} \underbrace{L_M C_{DD} L_M^T}_{N_{22}} \right]^{-1} W_{21} \tag{4.48}$$

where I_r is an identity matrix of dimensions equal to the actual number of double difference observations.

The apparent advantage of this method is that only the matrix $W_{22}N_{22}$, which has dimensions of the number of 'missed' observations (usually a few), instead of the complete covariance matrix, has to be inverted. However, a large amount of multiplication has to be carried out to obtain the final required weight matrix, which may make the algorithm unattractive.

Alternatively, the above equation (4.48) can be modified to a much simpler form, referred to as the modified algorithm, given by Monico (1995) as,

$$W_R = W_{11} - W_{12} W_{22}^{-1} W_{21} \tag{4.49}$$

In order to take advantage of the properties of the Kronecker product in the computation of the weight matrix, the techniques described above can be summarised as,

1) assuming all the observations are available and that the weight matrix is computed using the properties of Kronecker products (equation 4.38)
2) if there are some missing observations, the actual weight matrix is obtained by applying a linear transformation to the original set of observations.

Monico (1995) had reported that when there is no 'missing' observation, the algorithm proposed by Beutler *et al* (1986) and the modified algorithm proposed by Monico (1995) performed far better than the full inversion method. When the number of missing observations reached approximately half of the total number of the original observations, the full inversion method required less than half of the computation time required by the other two algorithms (Monico, 1995).

In the case of a global network, or a large network as involved with WADGPS, if the properties of the Kronecker product (equation 4.38) are to be applied, the D matrix has to be assumed to contain all the satellites in the constellation, i.e. 24 satellites. In fact, only a few satellites can be observed at each station, which results in the number of 'missing' observations being much higher than the actual number of observations. It is therefore clear that the use of the Kronecker product for the purpose of computational efficiency, fails to reduce the size of matrix to be inverted and introduces a lot of multiplication. Consequently, the most efficient method of computing the covariance matrix of a global network is the full inversion method.

4.5 Clock Related Error

The proposed approach for the estimation of clock related errors is based on the assumption that, if the ephemeris and atmospheric errors have been modelled correctly and hence eliminated, then the only remaining errors may be assumed to be clock related. This is based on the premise that the residual errors remaining after correcting the measurements for ephemeris and atmospheric errors are very small compared with the 'true' clock related errors

(which includes SA 'dither') and can therefore be absorbed by the latter, without significant differential error.

The 'total' clock related error is made up of the satellite clock, the receiver clock and SA 'dither' error. The satellite clock and SA 'dither' errors are position independent, and have a common effect on all observers (reference stations and users), regardless of location, as long as all the observations to the satellites are made simultaneously. However, range errors resulting from the receiver clock errors are different for every reference station receiver. In conventional DGPS, all the errors are bundled together to generate one differential correction per satellite, from a single reference station. This is clearly not the case in WADGPS, where a reference network is used to generate the corrections. In order to have a single differential correction for each satellite, the results from the different reference stations have to be aggregated. This is done by selecting one of the reference stations to act as a master clock and then having all the clock errors referenced to it by propagating the clock errors round the network through common view satellites (Ochieng, 1993).

The resulting (aggregated) differential corrections consist then of one reference receiver clock error, and an averaged satellite clock error for each satellite visible from the WADGPS network. This combined clock correction is broadcast to the user, who corrects the observed pseudoranges accordingly. The only remaining clock error is now that corresponding to the user's own receiver, which is modelled and solved for by an independent point positioning computation, using the corrected pseudoranges. However, the resulting clock correction is not just that corresponding to the user's own clock, but the sum of the reference station clock error and the user clock error. This is an important conceptual point, which has no practical implication and should not affect the user. As a result, relatively inexpensive, less accurate clocks can be used as reference clocks without degrading the navigation accuracy.

4.6 Data Pre-Processing and Validation

The data pre-processing includes the detection and removal of the outliers and may involve a certain amount of filtering to improve the accuracy of the observables. The detection and removal of the outliers is an important issue in terms of the integrity of a WADGPS system.

The outliers are usually detected by the use of the residuals of a least squares computation, commonly referred to as the 'data snooping' (Cross, 1990). The value of the test statistic $\hat{w}_i$ is given as,

$$\hat{w}_i = \hat{v}_i / \sigma_{\hat{v}_i} \tag{4.50}$$

where,

$\hat{v}_i$ is the residual of the i^{th} observation

$\sigma_{\hat{v}_i}$ is the estimated standard deviation of the i^{th} residual

The 'data snooping' involves the detection, removal and re-computation of the observations. It is obvious that this procedure is not appropriate for real-time applications due to the batch least squares post-processing. Although in theory, this technique can be applied in the process of the estimation of satellite orbit and atmospheric errors since these two errors are estimated by batch least squares adjustment. The re-computation procedure, which is a time consuming process does not make it favourable for WADGPS.

In practice, the character of the reference stations in a WADGPS system themselves can be employed to detect the outliers. As the coordinates of the reference stations are well known, the outliers can easily be detected by checking the observations based on epoch by epoch comparisons. A simple polynomial fit to the previous observations can predict the approximate measurements in the near future. If an observation exhibits difference that exceeds a specified threshold, the measurement is identified as an outlier and rejected in all processing. This kind of process can be employed in the pre-

processing software to perform an effective detection of outliers. At the user site, the outliers can be detected using the RAIM (Receiver Autonomous Integrity Monitoring) approach, which is basically a measure of the consistency of the measurements (IESSG, 1995).

The data pre-processing may also involve a filtering technique to improve the accuracy of the raw observations. The noisy pseudorange code measurements can be improved, by the combination of code and carrier phase observations with proper weighting, in a recursive process to generate a 'phase smoothed code'. The use of recursive filter to generate the phase smoothed pseudorange was first proposed by Hatch (1982) and similar algorithms were proposed by Lachapelle *et al* (1989, 1991). The general form of the phase smoothed pseudorange can be represented as,

$$\hat{P}_k = w_p P_k + w_\Phi [\hat{P}_{k-1} + (\Phi_k - \Phi_{k-1})] \tag{4.51}$$

where, $\hat{P}_k$ is the phased smoothed pseudorange at time t_k

P_k is the raw observed pseudorange at time t_k

Φ_k is the observed carrier phase at time t_k

w_p is the weight of the raw pseudorange at t_k

w_Φ is the weight of the term, $[\hat{P}_{k-1} + (\Phi_k - \Phi_{k-1})]$

$$w_p = (1.0 - w_\Phi)$$

w_p = 1.0, at the first epoch (4.52)

At the first epoch, the measurement is a pure raw pseudorange observation, and the weight of the pseudorange is set equal to 1.0. From the second epoch, the difference between the two successive carrier phase measurements is used to form part of the phase smoothed code. The weight of the raw pseudorange is progressively decreased as the weight of the carrier phase measurements increased correspondingly, according to time.

The highly accurate carrier phase measurement, with smaller multipath effects and lower measurement noise, improves the accuracy of the phase smoothed code substantially (Hatch, 1982, Lachapelle 1991, Casewell *et al*, 1994). However, there are potential problems in applying this approach, such as cycle slips, code and carrier divergence and multipath effects. If a cycle slip occurs during the process, the algorithm has to be reset. The ability to detect the cycle slips is therefore essential for the success of this process, as undetected cycle slips will introduce a bias in the observables. Depending on the receiver used, the tolerance for the cycle slip detection is generally set to 8 to 10 cycles, i.e. 1.6 m to 2.0 m in range, to avoid too many false alarms (type I errors) (Cannon *et al*, 1990). The code and carrier divergence is caused by the effects of the ionospheric delay, which affect the code and carrier phase by the same magnitude but of different sign. The problem with the code and carrier divergence can be reduced by re-initialising the algorithm regularly at a short period (Lachapelle, 1991). The use of dual frequency ionospherically free observables is another method to counter this problem (Casewell *et al*, 1994). The multipath effect could also bias the results which can also be minimised by re-initialisation.

An alternative method proposed by Lachapelle (1986) to reduce the effects of multipath, code and carrier divergence and undetected cycle slips, is referred to as the 'dual ramps' algorithm. Two parallel filters are set to work together, each one resets at a certain interval alternately. The first filter starts the process on its own, the second filter does not start until the first one reaches its half cycle. The first filter is reset after its cycle is completed, and then the second filter, which has reached its half cycle, takes over the process. The iterative process proceeds until a cycle slip occur which requires both filters to be reset and the process re-start from the beginning.

Since this research was concentrated on the modelling of the error sources and the achievable user navigation accuracies by different algorithms. The Nottingham GPS data pre-processing program, FILTER (§ 5.2), was used to

pre-process both the simulated and real field data. The filtering techniques have not been implemented in the software and is suggested for future research.

4.7 Single Frequency WADGPS

At the time of writing (April, 1996), Selective Availability and Anti-Spoofing were still in place. The necessity of developing a WADGPS system which would be of use to the civilian user community, and therefore able to operate with both dual and single frequency reference stations is highlighted. The principle of the processing algorithms of the WADGPS technique, which is based entirely on the use of single frequency GPS receivers is described in this section. Obviously, the key issue in this scenario is the modelling of the ionospheric delay, by using exclusively single frequency pseudorange (code) measurements.

Broadly speaking, the estimation of the ephemeris and clock related errors remains unchanged from the dual frequency approach. The main difference between the single and dual frequency scenarios is in the modelling of atmospheric propagation errors. In this context, the direct estimation of corrections for ionospheric delay is a luxury restricted to dual frequency receivers. For single frequency receivers, the atmospheric errors need to be estimated and modelled differently. Two algorithms designed for the single frequency receiver environment have been developed at Nottingham. A simple method which bundles together the tropospheric and ionospheric delays as one single atmospheric error, which is estimated as part of the orbit determination process, is further investigated and described in Section 4.7.1. A more refined approach for estimating the ionospheric delay for single frequency receivers has now been developed and is described in Section 4.7.2. The use of the code and carrier phase measurement divergence for the estimation of the ionospheric delays for single frequency receivers, is for completeness also described.

4.7.1 The Combined Atmospheric Propagation Error Approach

The combined atmospheric propagation error approach was designed specifically for a single frequency receiver environment. The atmospheric propagation delay is estimated as part of the orbit determination process and optimised through a NSE algorithm to generate a local best fitting atmospheric model for onward transmission. As the effects of the ionosphere and troposphere are combined together as one single atmospheric delay, modifications in the models are necessary to adopt this combined delay.

The Klobuchar model used in the NSE algorithm was originally designed for ionospheric error estimation only (§ 4.2). To be able to accommodate this approach, the sub-ionospheric point, where the signal intersects the ionosphere, is virtually brought down to the observer. The model is then further simplified by replacing the geomagnetic latitude, ϕ_m and the sub-ionospheric latitude, ϕ_I, by the observer's latitude, ϕ_u. The longitude of the sub-ionospheric point, λ_I, is also replaced by the observer's longitude, λ_u. As a result, the computation of the geomagnetic latitude, sub-ionospheric latitude and longitude, expressed in equation 4.16, 4.19 and 4.20 respectively, are no longer executed. The mapping function is also changed from that in equation (4.21), an ionospheric mapping function, to a tropospheric mapping function (equation 4.26). The night-time constant value of 1.5 m is obviously not realistic for the combined atmospheric delays, where the tropospheric error is included in the combined atmospheric delay.

The achievable satellite orbit accuracy is expected to be slightly worse than that obtained from the dual frequency approach, especially due to the potentional mis-modelling of the atmospheric errors. The user position is determined in a similar manner as used in the dual frequency approach: using a local best fitting atmospheric correction model, the differential correction and the improved integrated ephemeris to perform a point positioning.

4.7.2 The Ionospheric Scale Factor Approach

A unique approach for the estimation of the ionospheric delay by the use of single frequency measurements has been developed during this research and is referred to as the *'Single Frequency Ionospheric Scale Factor Approach'*. The procedure of this approach can be summarised as:

- Removal of the tropospheric errors by standard tropospheric model
- Calculation of the ionospheric errors by broadcast Klobuchar parameters
- Generation of the ionospheric scale factor as part of the orbit determination process
- Generatiuon of the local best fitting ionospheric model
- Transmission of the optimised ionospheric model to the user

The success of this approach is based on the fact that the 'dry' part of the tropospheric delay, which is responsible for about 90% of the total tropospheric delay, and can be very precisely modelled using surface meteorological data. As a result, the 'dry' part of the tropospheric error at the reference stations can be estimated by one of the existing tropospheric models and hence largely removed from the data, leaving only the 'wet' part of the tropospheric errors and ionospheric errors.

The approximate ionospheric delay can be initially obtained from the broadcast Klobuchar parameters for the estimation process. The difference between the truth and the approximate delays are assumed due to a scale error. An extra unknown is then added for each reference station as part of the orbit determination process in a least squares adjustment.

The local scale factors are then applied to the approximate ionospheric delays at each reference station. The scaled ionospheric delays from all the reference stations are then fitted through the Klobuchar model by the NSE algorithm to generate a regional best fit ionospheric delay model. The improved local best

fitting ionospheric correction model, estimated tropospheric delays and the integrated ephemeris, are then applied to form the clock related error, which is transmitted to the user. The user then applies the same tropospheric model and the optimised ionospheric error correction model, to estimate local delays and uses the clock corrections to obtain an improved position.

As the ionospheric scale factors are solved together with the orbit determination process, it is obvious that one single ionospheric scale factor throughout the period, typical 48 to 72 hours, is not enough to accommodate the variation of the ionospheric delays. The approach of estimating different local scale factors at shorter intervals is therefore adopted.

The choice of the mapping function encountered by the combined atmospheric approach, in which one mapping function is applied for combined ionospheric and tropospheric delays, is not a problem with the ionospheric scale factor approach. The ionospheric and tropospheric mapping function (equations 4.21 and 4.26) are used to map down the ionospheric and tropospheric delays respectively.

4.7.3 Ionospheric Delay Estimation by Code and Carrier Phase Divergence

The ionospheric delay has the same effect but of opposite sign on pseudorange and carrier phase observables. The pseudorange is delayed by the ionosphere while the carrier phase is advanced. This property, referred to as code and carrier phase divergence, is used to derive the ionospheric errors for single frequency observations.

The observation equation for the pseudorange and carrier phase observables is given in equations (2.1) and (2.3), respectively. These equations can be rewritten, based only on L1 measurements, for the purpose of describing code and carrier divergence technique.

$$\rho_{L1} = \rho + d\rho + c(dt - dT) + d\rho^{L1}_{ion} + d\rho_{trop} + \Delta(\rho_{L1}) \quad (4.53a)$$

$$\lambda_1\Phi_{L1} = \rho + d\rho + c(dt - dT) - \lambda_1 d\Phi^{L1}_{ion} + d\rho_{trop} + \lambda_1 N_{L1} + \Delta(\Phi_{L1}) \quad (4.53b)$$

where,

ρ_{L1}	:	observed L1 pseudorange measurement
ρ	:	true range
$d\rho$	:	ephemeris error
c	:	speed of light in a vacuum
dt	:	the offset of the satellite clock from GPS time
dT	:	the offset of the receiver clock from GPS time
$d\rho^{L1}_{ion}$, $d\Phi^{L1}_{ion}$	:	ionospheric error on L1 code and carrier measurements
$d\rho_{trop}$	:	tropospheric error
λ_1	:	L1 carrier wavelength
N_{L1}	:	integer ambiguity
$\Delta(\rho_{L1})$	:	receiver internal measurement noise and multipath of L1 pseudorange
$\Delta(\Phi_{L1})$	:	receiver internal measurement noise and multipath of L1 carrier phase

On inspecting equations 4.53a and b, it can be seen that the difference between the code and carrier phase measurements can be used to isolate the ionospheric error. This expression is given by,

$$\rho_{L1} - \lambda_1\Phi_{L1} = d\rho^{L1}_{ion} + \lambda_1 d\Phi^{L1}_{ion} - \lambda_1 N_{L1} + \Delta(\rho_{L1}) - \Delta(\Phi_{L1}) \quad (4.54)$$

The last two terms on the right hand side of the equation are the receiver internal noise and multipath errors. The effects of multipath and measurement errors on carrier phase observables are generally much smaller than pseudorange code measurements. If the sites are carefully chosen to minimise multipath effects, and high precision receivers which provide accurate code measurements, are used, the last two terms will be insignificant compared with the real ionospheric errors and can hence be truncated. Consequently, equation 4.54 can be rewritten as,

$$\rho_{L1} - \lambda_1\Phi_{L1} = d\rho^{L1}_{ion} + \lambda_1 d\Phi^{L1}_{ion} - \lambda_1 N_{L1} \quad (4.55)$$

Since the ionosphere generates identical magnitude of errors on the code and carrier phase measurements, the difference between the code and carrier phase measurements are twice the ionospheric errors plus an integer ambiguity. To obtain the ionospheric errors, equation 4.55 can be rearranged as,

$$\rho^{L1}{}_{ion} = \frac{1}{2}(\rho_{L1} - \lambda_1\Phi_{L1} - \lambda_1 N_{L1}) \qquad (4.56)$$

It is clear now, from equation 4.56, that in order to estimate the ionospheric error, the integer ambiguity has to be separated from the ionospheric errors. A least squares adjustment approach is applied using the observables ($\rho_{L1} - \lambda\Phi_{L1}$), over the observation period for the estimation of the ionospheric error and the integer ambiguity. The ionospheric error, $\rho^{L1}{}_{ion}$, is represented by the vertical error and a mapping function, as described in equation (4.21), as,

$$\rho^{L1}{}_{ion} = \rho_v F \qquad (4.57)$$

where,

$$F = 1.0 + 16.0\,(0.53 - E)^3$$

ρ_v is the ionospheric vertical error

The ionospheric vertical delay, ρ_v, is separated into an approximate correction, I_0, and residual error, dI_0, given as,

$$\rho^{L1}{}_{ion} = (I_0 + dI_0)\,F \qquad (4.58)$$

On substituting 4.56 into 4.58 and rearranging,

$$(\rho_{L1} - \lambda_1\Phi_{L1}) = 2\,(I_0 + dI_0)\,F + \lambda_1 N_{L1} \qquad (4.59)$$

The approximate correction, I_0, can be an empirical value or calculated from the broadcast Klobuchar parameters. As the ionospheric error is modelled in the least squares adjustment, the approximate value does not have to be very accurate. Rearranging equation 4.59 so that all the unknowns are located on the right hand side of the equation as,

$$(\rho_{L1} - \lambda_1\Phi_{L1}) - 2I_0 = 2dI_0\,F + \lambda_1 N_{L1} \qquad (4.60)$$

Assuming the ionospheric errors are constant during the observation period, the residual error may be approximately represented by a polynomial. As the ionospheric error is a function of factors such as, local time, magnetic latitude, sunspot cycle, a polynomial which is a function of the same factors is suitable for approximating the ionospheric errors. Therefore the residual error can be approximated by a polynomial which is a function of the sub-ionospheric point. Many functions can provide the required polynomial, depending on the observation period, generally, a higher order polynomial can serve for longer intervals. The coefficients of the polynomial, along with the integer ambiguity are then estimated using the difference between the code and carrier phase measurements over the observation period in a least squares adjustment. With a carefully chosen receiver site, P code and narrow correlator spacing C/A code receiver, 90% of the ionospheric errors recovered had been demonstrated (Qiu *et al*, 1995).

The property of the code and carrier divergence provides a technique for ionospheric error estimation for single frequency receivers. However, several assumptions must be made to ensure the success of this technique. Firstly, the assumption of the multipath and receiver internal noise is negligible, results in the truncation of the last two terms of equation 4.54, must hold. This may be achieved by a carefully selected receiver site, antenna design and some other devices to reduce the effects of multipath, together with highly accurate pseudorange observables. Secondly, the cycle slips have to be detected and recovered properly, otherwise the technique fails. Thirdly, the TEC is assumed to be constant during the observation period, which is not true especially during day time. The observation period has to be short to accommodate the variation of the ionospheric effect.

4.7 Data Latency and Data Transmission

The period between the reception of data and application of differential corrections at the user is referred to as data latency. Data latency degrades the user position accuracy, since the corrections are not applied at the same epoch as the observations are made at the reference sites, typically being a few seconds late. Therefore, the temporal variation of the errors introduces extra errors to the system. Data latency is a common problem to all differential systems, notably conventional DGPS, NDGPS and WADGPS. In the condition when the temporal variation is rapid, such as the SA 'dither' component, the increased error due to the data latency has to be taken into account in order to achieve accurate user positioning.

To overcome the problem, the range correction rate (§ 3.1.2), in addition to the range correction, is applied at the user site to reduce the effect. The observed pseudorange is therefore corrected by the range correction, as well as the range correction rate multiplied by the data latency, to obtain the improved position. The correction algorithm is given in equation (3.2). The processing software provides an option to implement the range rate correction as an option in the user positioning process, whilst real filed data test results are described in Chapter 7.

Various WADGPS algorithms have been proposed, based on the use of either dual frequency or single frequency receivers. In practice, WADGPS requires data transmission systems to transmit data from the reference stations to control centre and from control centre to users. Research on the capacity of the data transmission system used in WADGPS had been carried out by IESSG and BAe (1992). The suggested format and information to be transmitted are still applicable for the proposed WADGPS algorithms, therefore only a brief summary of the proposed data transmission is given in Appendix B.

Chapter 5

Software

The WADGPS algorithms are distinct from the conventional DGPS in the way that the error sources inherent in GPS are more gracefully handled. The separation and modelling of the errors in the pseudorange signals from the satellites, allow the system to provide a consistent user navigation accuracy over a wide area, with fewer reference stations than the conventional DGPS to cover the same area. In order to investigate the performance of these algorithms, the proposed processing algorithms had to be implemented in computer programs. The computer software developed and applied in this study is described in this chapter.

The consideration of the software design strategy is described in Section 5.1. The structures and functions of the software applied or developed for this research are described in Sections 5.2 to 5.6. The GPS Analysis Software (GAS) is a software package developed in-house at the Institute of Engineering Surveying and Space Geodesy (IESSG), University of Nottingham, over the last ten years (Steward *et al*, 1994). GAS performs the pre-processing, post-processing and analysis of GPS data which is described in Section 5.2. The DATa SIMulator (DATSIM) used for the simulation studies is described in Section 5.3. The DIFFerential CORRection (DIFFCORR) software performs the task of modelling the atmospheric and clock related errors is described in Section 5.4. The DIFFerential POSitioning (DIFFPOS) software, described in Section 5.5, is designed for the user to apply all the error correction models transmitted from the control centre in order to compute an improved position. The analysis software, CONVERT, for the purpose of position error computation, is also described in Section 5.6. The model implementation is detailed in Section 5.7.

5.1 Software Design Strategy

The variety of the WADGPS algorithms proposed in this research, classified by the type of receiver available and the way the error components are separated and modelled, have to be accommodated by the software to perform tests consistently for both simulation and real filed data. Since the software was developed during the progress of this research, it was essential to design the software in such a way that the use of the software would be flexible, efficient and user-friendly.

The first software design consideration was the flexibility. The software was developed through the modular organisation. The main program was kept as concise as possible, performing as the central control of the software. The functions were operated by the use of subroutines which enabled the programs to have the ability to switch between different options smoothly and to allow additional routines to be added to the software easily.

The second factor that was taken into account was the efficiency. The efficiency is particularly critical to real time navigation applications. This was achieved through the use of vector storage, pointers and manipulation of the matrices. The vector storage acts by replacing the multi-dimensional matrix subscriptions to corresponding vector subscripts through the use of pointers, which reduce the physical number of computations required during matrix manipulation (Bierman, 1977).

The use of dynamic memory allocation within the software further reduced the computer storage problem. The dimensions of arrays were determined dynamically by relevant variables during the program execution by the amount exactly required for the process. This greatly reduced the amount of storage required, as traditionally the dimensions of arrays are over-estimated for the maximum values at the time of compilation.

Finally, for the benefit of the operator, the software was activated together with a user-friendly ASCII format control file, whereby the general information, such as the names and coordinates of reference stations, processing modes and options could be defined by the user clearly.

5.2 The GPS Analysis Software (GAS)

GAS software was used in this research for the purpose of orbit determination and atmospheric error estimation. The software was written in FORTRAN 77 computer language, to operate on MS-DOS compatible PCs and UNIX systems. The modified version applied in this research was based on the Silicon Graphics UNIX system. The main programs involved are described as follow,

1) Pre-processing - CON2SP3, FILTER

- **CON2SP3**

The program CON2SP3 (CONvert to SP3 format) was used to convert the RINEX (Receiver INdependent Exchange) format broadcast ephemerides into SP3 format ephemerides, which is the format used in the GAS module. The SP3 format ephemeris is the format used by the US National Geodetic Survey (NGS) to distribute precise ephemeris (Remondi, 1989). The International GPS Geodynamics Service (IGS) also provides precise ephemerides in SP3 format.

When no satellite clock correction values are contained in the SP3 format ephemeris file, CON2SP3 also performs the task of inserting these clock correction values using the clock coefficients from the broadcast ephemeris. The integrated orbit generated by GPSORBIT, the GAS module for orbit determination, does not have satellite clock corrections. Hence the clock correction values have to be inserted by the use of CON2SP3.

- **FILTER**

FILTER converts RINEX format GPS data into the GAS NOTT2 (NOTTingham 2) format. NOTT2 format is an ASCII format which is similar to RINEX format but is tailored for GAS processing. FILTER is capable of removing data from unhealthy or unwanted satellites, removing the epochs with less than a specified number of satellites and reporting all these changes in a log file. FILTER also detects 'bad' data and cycle slips by comparing the change in the phase and pseudorange measurements for adjacent epochs and approximately corrects large cycle slips. An epoch by epoch pseudorange point positioning solution, as well as an accumulated pseudorange solution can be obtained, to provide the approximate receiver coordinates and useful information about the quality of the data set. The user also has the options to reduce the amount of data by changing the epoch separation and may specify the period of data to be converted.

2) Main-Processing : PANIC, GPSORBIT, FILTER

- **PANIC**

The Program for the Adjustment of Networks by Interferometric Carrier phase (PANIC) is the main program in the GAS software. It is designed for GPS data processing with a variety of modes to serve different requirements. PANIC was used in this research for two purposes. Firstly, the initial state vectors of each satellite were obtained using the 'network processing' mode and, secondly the updated satellite state vectors and the atmospheric delays, were obtained using the 'fiducial network processing' mode.

The PANIC 'network processing' mode basically carries out the network solution, without involving the orbit improvement, by fixing the coordinates of known stations and solving for the unknown positions in a least squares

adjustment. However, the PANIC 'network processing' mode was only used in this research for the purpose of creating the initial satellite state vector file.

The PANIC 'fiducial network processing' mode was used to carry out the orbit determination, as well as the atmospheric delays estimation, in a least squares network adjustment. To run PANIC in 'fiducial network processing' mode, two more GAS modules, GPSORBIT and MKGAF had to be called.

- **GPSORBIT, MKGAF**

More information than the PANIC 'network processing' model is required in order to run the PANIC 'fiducial network processin'g mode. The first program involved is GPSORBIT, one of the GAS modules, which is used to generate the integrated ephemeris and corresponding partial derivatives of the orbital unknown parameters. A 4th order Runge-Kutta single-step integrator is applied in GPSORBIT to provide sufficient integration steps for a more precise 8th order Adams-Bashforth multi-step predictor-corrector integrator to take over. The step lengths of 30 seconds for the Runge-Kutta scheme and 300 seconds for the Adams-Bashforth scheme have been adopted in this research, based on the research by Ochieng (1993).

An integrated satellite ephemeris, satellite state vector file and its associated partial derivatives, with respect to the orbital unknowns, has to be generated before the fiducial network adjustment may be activated to improve the satellite orbits. The satellite initial state vector file contains the start time of the orbit integration for each satellite, the initial state vectors of the satellites (position and velocity) and the corresponding rotation matrices, necessary for the transformation of the initial state vectors from Inertial Frame (IF) to Earth Fixed (EF) reference frames (§ 4.4). In order to run GPSORBIT, a global gravity model, a tidal model and GAF file are also required in advance.

The second program involved is the MKGAF (MaKe Gas Ancillary File) GAS module, for generating the GAS Ancillary File (GAF). GAF is required for both the computation of the integrated orbit and to implement the Earth body tide model used in PANIC. The GAF contains the information about the positions of the sun, moon and planets which is used by PANIC to compute the Earth body tide corrections (§ 4.4.1). The GAF also provides the Earth rotation and polar motion information in the form of the coefficients of the Chebyshev polynomial, which is necessary for the transformation between IF and EF reference frames.

One of the geopotentional models of the Earth's gravity field, the Goddard Earth Model T1 (GEM T1) is used in the software with an expansion of order and degree 8.

Modifications have been made to PANIC to accommodate different requirements specified by the proposed WADGPS algorithms for the purpose of the estimation of the orbit and atmospheric errors.

3) Analysis - EPHDIFF

The EPHemeris DIFFerence (EPHDIFF) program was developed during this research in order to assess the accuracy of the recovered orbit. The recovered satellite orbit was compared with the *truth* (in the simulation tests) or, with an independent precise ephemeris, such as IGS precise ephemeris (in the real field data tests). The program is capable of comparing the discrete satellite positions over the specified arc. The orbit accuracy is expressed in root mean square (RMS) values for each satellite in total orbit error as well as the three individual components, namely the along track, cross track and radial error and also the total errors. To summarise the process of the estimation of the satellite orbit and atmospheric delays, the procedure of the fiducial network processing is shown in Figure 5.1.

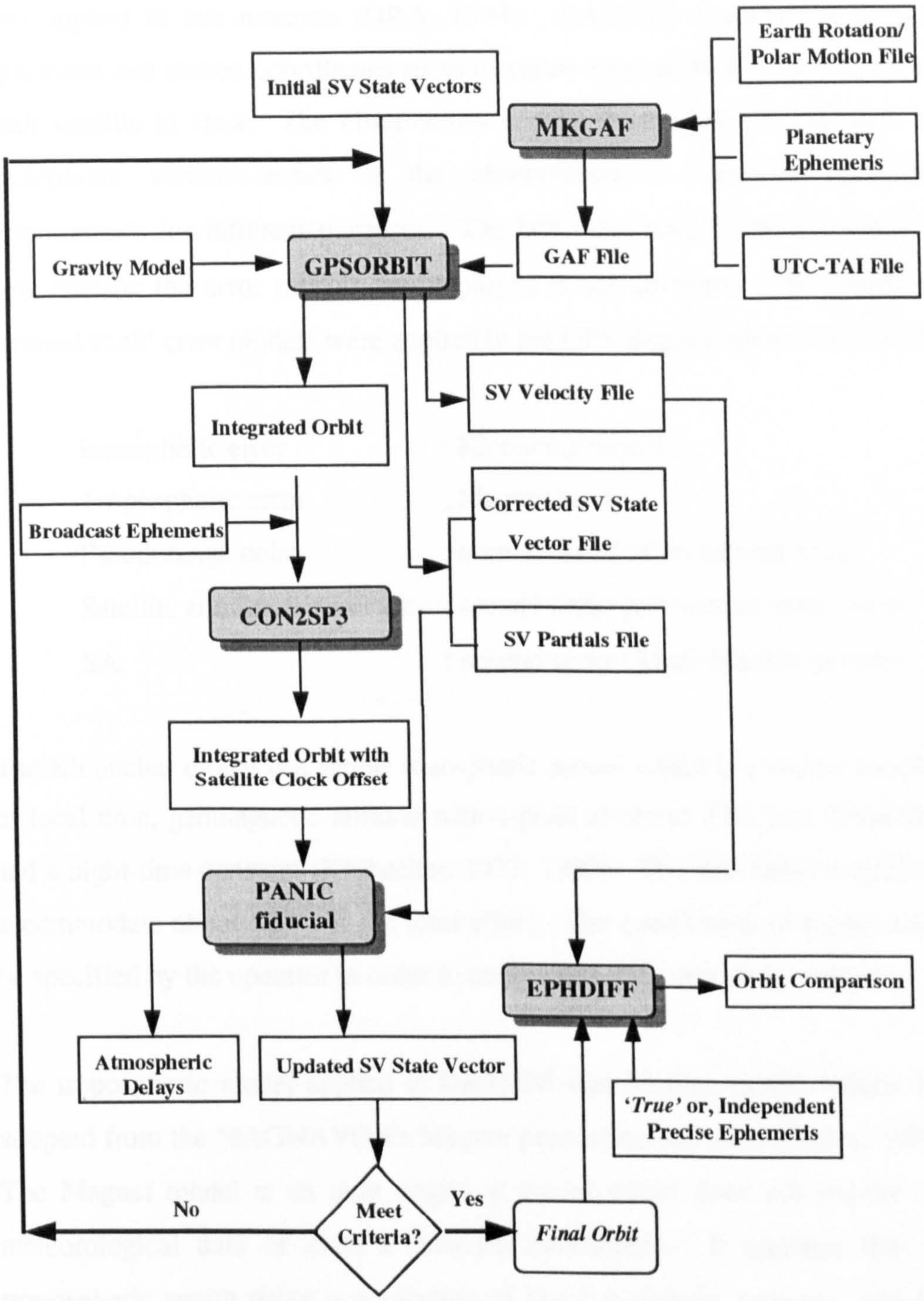

Figure 5.1 Fiducial GAS Flow Diagram

5.3 The DATa SIMulator (DATSIM) Software

The DATa SIMulator (DATSIM), developed at the University of Nottingham was applied in this research (DRA, 1994). DATSIM employs the known ephemeris and station coordinates so as to create time-tagged observations for each satellite in view. The observations can be manipulated by the user to incorporate various errors in the observations to simulate particular environments for different purposes. The key issue need to be addressed is how realistic the error models are employed in the software. The following 'ground truth' error models were applied in the GPS data simulator, DATSIM.

Ionospheric error	: Klobuchar model
Tropospheric error	: Magnet model
Pseudorange noise	: normal distribution random noise
Satellite and Receiver clock	: second order polynomial, white noise
SA	: second order Gauss-Markov process

The Klobuchar model is a simple ionospheric model which is a cosine function of local time, geomagnetic latitude with a peak at about 2:00 p.m. local time and a night-time constant (Klobuchar, 1977, 1982). The Klobuchar model can accommodate about 50 % of the total effect. The coefficients of model could be specified by the operator in order to manipulate the ionospheric delays.

The tropospheric model applied in DATSIM was Magnet model, which was adopted from the MAGNAVOX's Magnet processing software (Curley, 1988). The Magnet model is an pure empirical model which does not require any meteorological data or even a standard atmosphere. It assumes that the tropospheric zenith delay is a function of the atmospheric pressure, which is based on the Julian Day (JD), station latitude and height. Since it is purely empirical model, the wet part of the tropospheric delay is not included in the mode. The Chao's mapping function, given in Section 4.3.1, equation (4.26), was applied to map the zenith delays according to the satellite elevation angle.

The receiver hardware and measurement noise is modelled as pseudorange noise which is simulated by a normal distribution random white noise. The standard deviation and mean values can be specified by the operator to simulate different types of receivers.

The satellite and receiver clock errors are all simulated by a second order polynomial with white noise, which are described by the general expression,

$$Error = a + b\,(T - T_{oc}) + c\,(T - T_{oc}) + R \qquad (5.1)$$

where, a is the offset term (seconds),
b is the drift term (seconds/second),
c is the ageing term (seconds/second^2),
T is the time indicated by the clock,
T_{oc} is the time of the last calibration,
R is the white noise term with zero mean and an operator specified standard deviation.

The coefficients in equation (5.1) are created by the standard random number generator available on the computer system, which vary for different runs of the program. The coefficients are then output as a clock coefficient file for future use. In case new stations were to be simulated to be incorporated with an existing network, the software read the clock coefficient file instead of randomly creating the clock errors to be consistent with the other simulated data.

SA 'epsilon' is simulated as part of the satellite ephemeris error. SA 'dither' is simulated based on an SA model proposed by Chou (1990), where a second order Gauss-Markov process is used. The model had been evaluated using the simulated and real field data, and the magnitude and period of the estimated SA 'dither' show similar pattern as the observed SA 'dither' effects (Chou, 1990).

In summary, the software provides the operator with the options of manipulating the simulated data by switching on or off individual error components , which include the ionospheric, tropospheric and SA errors. The magnitude of the satellite and receiver clock errors, as well as the pseudorange noise, can also be specified by the operator. The operator also has options to alter the Klobuchar parameters to simulate required ionospheric delays.

5.4 The DIFFerential CORRection (DIFFCORR) Software

Both software DIFFCORR and DIFFPOS were developed in the FORTRAN 77 computer language in order to be compatible with the existing GAS software. The software is operated on the Silicon Graphics UNIX system in the consideration of the requirements of the data storage and processing capability for the WADGPS system.

DIFFCORR was developed to perform the atmospheric error modelling and clock related error formation at the control centre. The software is capable of handling different algorithms in the proposed WADGPS, namely the dual frequency, single frequency combined atmospheric delay and refined single frequency *ionospheric scale factor* approaches. The DIFFCORR processing procedure is shown in the flow diagram in Figure 5.2.

The main functions of DIFFCORR, as illustrated in Figure 5.2 are:

1) atmospheric delay modelling
2) clock related error computation

Depending on the approach chosen to perform WADGPS, the inputs and outputs and the modelling procedure are different. In all three approaches, the clock related errors are computed in a similar manner by removing the satellite ephemeris and atmospheric propagation errors from the pseudorange

measurement. The difference appears in the way that the improved satellite ephemeris and the atmospheric delays were estimated.

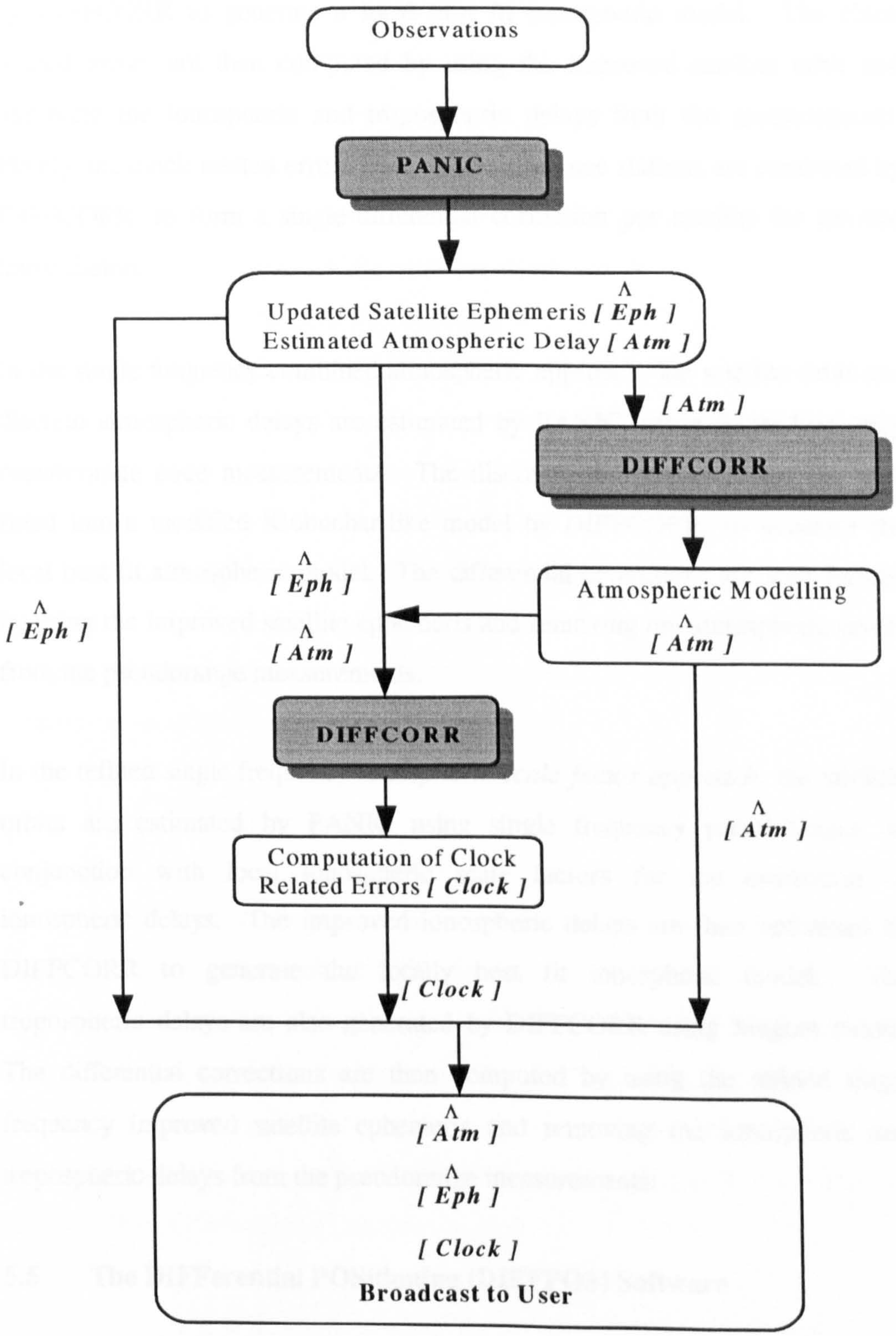

Figure 5.2 DIFFCORR Diagram

In the dual frequency approach, the satellite orbit and tropospheric delay are estimated by PANIC using the ionospherically-free observable. The ionospheric delays estimated by the dual frequency measurements are modelled by DIFFCORR to generate a local best fit ionospheric model. The clock related errors are then computed by using the improved satellite orbit and removing the ionospheric and tropospheric delays from the measurements. Finally, the clock related errors from all the reference stations are combined by DIFFCORR, to form a single differential correction per satellite for onward transmission.

In the single frequency combined atmospheric approach, the satellite orbit and discrete atmospheric delays are estimated by PANIC, using single frequency pseudorange code measurements. The discrete atmospheric delays are then fitted into a modified Klobuchar-like model by DIFFCORR, to generate the local best fit atmospheric model. The differential corrections are then formed by using the improved satellite ephemeris and removing the atmospheric errors from the pseudorange measurements.

In the refined single frequency *ionospheric scale factor approach*, the satellite orbits are estimated by PANIC using single frequency pseudoranges, in conjunction with local ionospheric scale factors for the estimation of ionospheric delays. The improved ionospheric delays are then optimised by DIFFCORR to generate the locally best fit ionospheric model. The tropospheric delays are also generated by DIFFCORR using Magnet model. The differential corrections are then computed by using the refined single frequency improved satellite ephemeris and removing the ionospheric and tropospheric delays from the pseudorange measurements.

5.5 The DIFFerential POSitioning (DIFFPOS) Software

DIFFPOS is able to perform the task of user positioning in three different modes, namely stand-alone, conventional DGPS and WADGPS. In the stand-

alone mode, the observed pseudorange is taken directly to perform the stand-alone single point position determination. In the conventional DGPS mode, all the the error sources are bundled together to be treated as the differential corrections. In the WADGPS mode, the precise ephemeris produced at the control centre using PANIC in various approaches, replaces the broadcast ephemeris. The corresponding optimised atmospheric model (depending on the approach applied) generated at the control centre by DIFFCORR, removes the atmospheric propagation errors. DIFFPOS employs the updated precise ephemeris, optimised atmospheric model and the differential corrections from the control centre for WADGPS positioning.

Since the differential corrections are always behind the current epoch, due to the computation/transmission time required, the data latency (temporal variation) is another problem for the WADGPS system. Data latency is the time difference between the reception of data and the application of differential corrections at the user station. This difference is a result of the computation and transmission time required. DIFFPOS applies the range rate corrections to counter the error introduced by data latency.

5.6 The Analysis Software

The CONVERT software has been developed at the University of Nottingham (Ochieng, 1993) and later modified for this research by the author to assess the user positioning quality. The user's positions estimated by DIFFPOS is output in an appropriate format to be used as an input file for CONVERT. CONVERT computes the RMS of the differences between the estimated user coordinates and the *truth* in the WGS84 Cartesian coordinate system (dX, dY and dZ). The difference can be represented as,

$$dX = X_c - X_t \tag{5.2}$$

$$dY = Y_c - Y_t \tag{5.3}$$

$$dZ = Z_c - Z_t \tag{5.4}$$

where,	dX, dY and dZ	are the Cartesian coordinate errors
	X_e, Y_e, Z_e	are the estimated user Cartesian coordinates
	X_t, Y_t, Z_t	are the *true* user Cartesian coordinates

A transformation from the Cartesian coordinate to the corresponding geodetic WGS84 coordinates, has to be carried out.

5.7 Model Implementation

The large reference network in a WADGPS system causes some problems in the data processing which restrict the size of the network to a regional area. The refined '*Global Independent Double Difference Baseline Approach*' was developed to allow baseline processing extend to a global network. The problems caused by the base satellite concept formerly implemented in the software and the technique for large matrix inversion in a WADGPS environment, are discussed in the following section.

- **Global Independent Double Difference Baseline Approach**

GAS applies the base satellite concept in the double difference process which requires a common satellite observed by all the stations in the network. The base satellite is the satellite relative to which double differences are formed at a certain epoch. If a base satellite is not present, then the observations will be rejected in GAS processing. This concept, therefore restricts the size of the baseline network processing to a regional area, where common satellites can be viewed throughout the region. However, it is impossible to have the same constellation over a global area, which eventually results in no double difference pairs can be formed by the base satellite concept when the size of the network increases. Since the orbit determination requires a global network (or, a fairly wide regional network), the conventional baseline processing which

requires the same base satellite over the entire network is obviously not possible for WADGPS.

An alternative technique applied was proposed by Ochieng (1993), and referred to as the *'unconnected baseline approach'* (§ 4.4.3). A refined approach has been developed and referred to as the *'Global Independent Double Difference Baseline Approach'* (§ 4.4.4). This approach allows different base satellites to be specified for each baseline while the correlations between the baselines are still taken into account. The approach enables the number of baselines processed in the network to be equal to the number of reference stations minus one.

To allow the refined approach to be carried out using GAS, the restriction of using the same base satellite for all baselines needs to be removed in the software. The technique implemented in the software which allows a different base satellite for each baseline is referred to as the '*base satellite per baseline*' option. The difference between the two base satellite selections can be illustrated by the differencing operator (D) (§ 4.4). The D matrix applied in GAS at one station, assuming the first satellite is selected to be the base satellite, has the following pattern in reference station differencing form as given in equation (4.35),

$$D=\begin{bmatrix} 1 & -1 & 0 & 0 & \ldots & 0 \\ 1 & 0 & -1 & 0 & \ldots & 0 \\ \ldots & & & & & \\ 1 & 0 & 0 & & \ldots & -1 \end{bmatrix} \qquad (4.35)$$

To allow different base satellites for different baseline, the D matrix should be structured in the sequential differencing form, as given in equation (4.34),

$$D=\begin{bmatrix} 1 & -1 & 0 & \dots & 0 & 0 \\ 0 & 1 & -1 & 0 & \dots & 0 \\ \dots & & & & & \\ 0 & \dots & & 0 & 1 & -1 \end{bmatrix} \qquad (4.34)$$

The concept of Kronecker product applied in GAS to solve the inversion of the double difference covariance matrix, i.e. the weight matrix, requires identical D matrices for each baselines. To overcome this problem, the D matrix is forced to be the same for each baseline by assuming 'missing observations' at different baselines, so that the same observations are observed at each station. The vector of double differences actually observed can be expressed as a linear transformation of all the possible double differences in the network (§ 4.4.4).

One of the methods for computing the weight matrix is by inverting the full covariance matrix. This would require a lot of computation time since the dimensions of this matrix are rather large. The technique applied in GAS, proposed by Beutler *et al*, (1986), manipulates the matrix in the way that only the dimension of the number of 'missing observations' (usually a small number in a regional network) need to be inverted and the final results are obtained by a lot of matrix multiplication.

In the case of a global network, such as the WADGPS network, the D matrix has to be assumed to contain all satellites in the sky, i.e. 24 satellites. In fact, only a few satellites can be observed at each station which results in the number of 'missing observations' being much higher than the actual number of observations. It has been demonstrated that in such a case, it is more efficient to make use of the full inversion of the covariance matrix than to handle the 'missed observations' (Monico, 1995). The reason is that the matrices to be inverted are approximately of the same dimension for all algorithms but extra multiplication is needed except in the full inversion method.

The *base satellite per baseline* option was implemented in PANIC for WADGPS and is able to handle a maximum of 27 satellites and 30 stations in a global network. The potential base satellites for each baseline have to be specified by the user. Among those specified satellites, the satellite with the highest elevation angle at the middle point of the baseline is then chosen as the base satellite.

Chapter 6

Refined WADGPS Approach : Simulation

Simulation studies are necessary to provide rigorous tests for the proposed algorithms, both in terms of sensitivity of the error modelling and efficiency of the software. To design a WADGPS algorithm, it is essential to understand the behaviour of individual error components. This is because the key success of the WADGPS concept depends on the error separation and modelling. It is only through simulation that the errors which affect the system can be precisely controlled and manipulated, in order to study the capability of different algorithms to recover the errors. With knowledge of all the error sources whose *true* values are precisely defined in the simulation, the behaviour of these error components in the system could be studied and analysed properly. This is provided that the models applied in the simulation are realistic i.e. approximate closely those arising in practice. In the simulation tests, error components which included satellite and receiver clock, atmospheric, pseudorange noise, SA and ephemeris errors, were separately imposed on the data set to enable detailed studies of individual and combined effects of these errors on the WADGPS system.

The simulation data and the test strategy are described in Section 6.1. The recovery of the satellite orbit error by both single and dual frequency observables are detailed in Section 6.2. The estimation of atmospheric delays, including the single frequency combined atmospheric delays and the dual frequency separated tropospheric and ionospheric delays, is given in Section 6.3. Section 6.4 details the corresponding user positioning results.

6.1 The Simulated Data Set and Test Strategy

A WADGPS network covering the North Atlantic region, defined by the dotted line in Figure 6.1, was used for the simulation tests. A network of 12 reference and 5 user stations was generated within the region using the GPS data simulator SIMDAT. A further 6 reference stations outside this region were also used for the purpose of orbit determination. In order to compare the WADGPS user positioning accuracy with those from conventional DGPS, the user stations were selected to have a distance ranging from 0.05 to 1,000 km to one of the reference stations (Richmond). The data was generated for a 72 hour period. The input station coordinates and the satellite orbit were used to simulate data and hence treated as *truth* for future analysis. Details of the errors applied in the simulated data are given below.

6.1.1 Satellite and Receiver Clock Errors

The satellite and receiver clock errors were always included in all the simulated data sets. Both the satellite and receiver clock errors are generated using equation 2.5. The coefficients for satellite clock error were generated randomly, in accordance with the expected accuracy of the satellite clock errors, i.e. 10^{-12} over one day (Hofmann-Wellenhof *et al*, 1994). The receiver clock errors were simulated in a similar manner as the satellite clock errors were generated. The receiver clock errors of the level of 10^{-10} over one day were simulated, in accordance with the quartz crystal clock used in most receivers (Hofmann-Wellenhof *et al*, 1994).

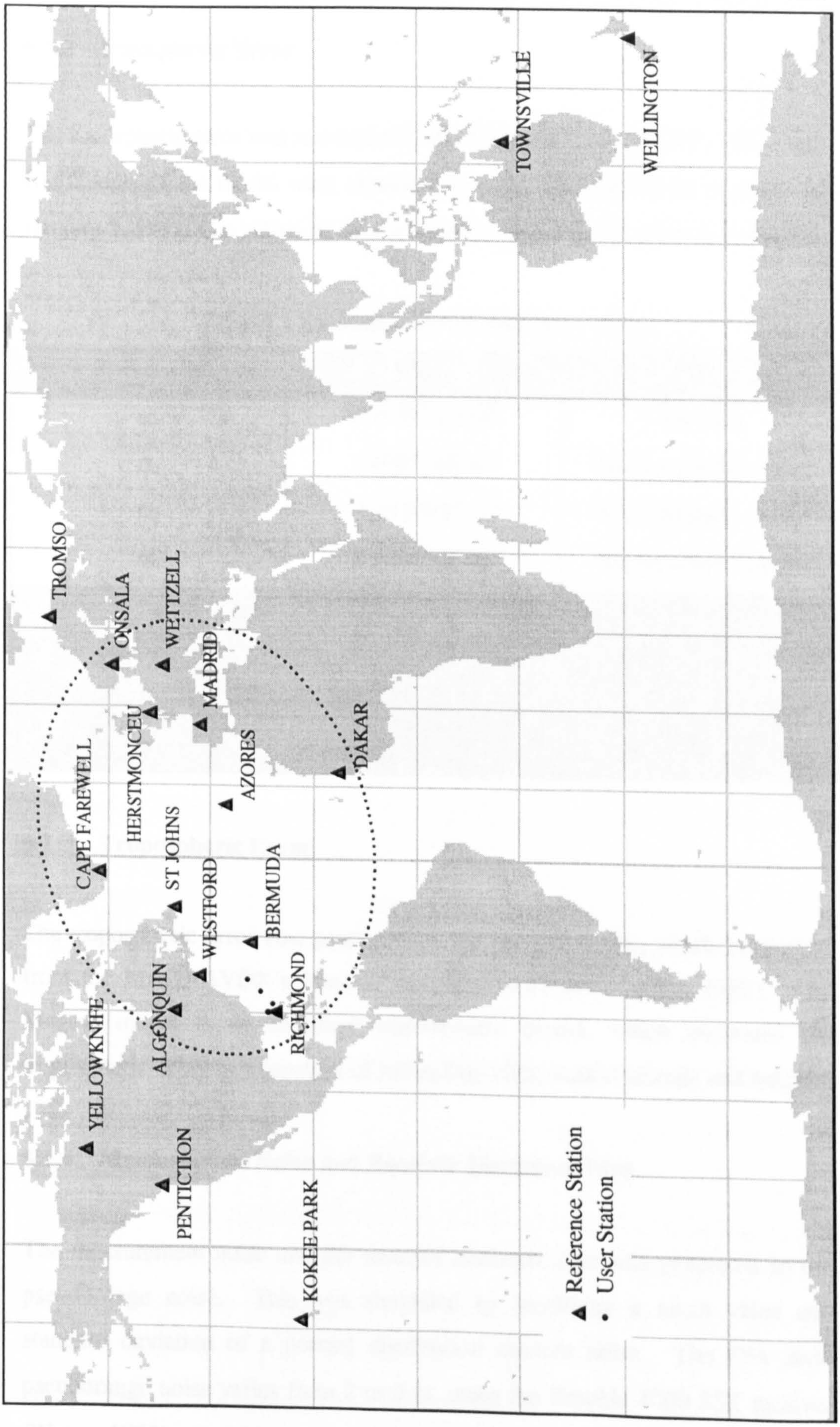

Figure 6.1 Simulation Network Configuration

6.1.2 Ionospheric Error

The ionospheric error was simulated by the Klobuchar model (§4.2). The eight coefficients of the model were obtained from the GPS broadcast message on January 1, 1991. The values of the coefficients, α and β, are given in Table 6.1.

Table 6.1 Klobuchar Model Parameter Value

Parameter	Value	Unit
α_0	2.793938E-08	Seconds
α_1	1.490116E-08	Seconds/Semi-circle
α_2	-1.192093E-07	Seconds/Semi-circle^2
α_3	5.960464E-08	Seconds/Semi-circle^3
β_0	1.515520E+05	Seconds
β_1	-1.966080E+05	Seconds/Semi-circle
β_2	0.000000E+00	Seconds/Semi-circle^2
β_3	3.276800E+05	Seconds/Semi-circle^3

6.1.3 Tropospheric Error

The tropospheric error was generated by the Magnet model, which is adopted from the MAGNAVOX's Magnet processing software (Curley, 1988). The Magent model is an empirical tropospheric model, which estimates the tropospheric delay as a function of Julian Day (JD), station latitude and height.

6.1.4 Measurement Noise and Receiver Hardware Bias

The measurement noise and the receiver hardware bias was generated as the pseudorange noise. This was simulated by specifying a mean value and standard deviation of a normal distribution random noise. The C/A code pseudorange noise varies from 2 to 3 m, using the Trimble 4000 SST receiver (Wang, 1992), to 10 cm, obtained using the NovAtel GPSCard™ receiver

(Chao, 1993; Lachapelle, 1992). In this research, three levels of the standard deviation of the pseudorange noise, namely 0.2 m, 0.5 m and 1.0 m, with zero mean value, were applied to investigate the effect of the random noise.

6.1.5 Selective Availability

The error due to Selective Availability (SA) effects has two parts, 'epsilon' and 'dither'. The 'epsilon' error was treated as part of the ephemeris error. SA 'dither' was simulated based on the model proposed by Chou (1990). The model applies a second order Gauss-Markov process. The two parameters required for the model, the variance, σ, and the correlation time, β, were identified based on the statistics of actual data provided by Chou (1990), as 14.3m for σ and 0.01129 sec^{-1} for β.

6.1.6 Satellite Ephemeris Error

The satellite orbit errors were introduced by altering some of the *true* initial state vectors by small amounts, i.e. ± 10 to 100 m in position and ± 0.001m/sec in velocity. This was in accordance with the worst case scenario of the broadcast ephemeris as a result of the SA error being employed in the 'epsilon' component. This corrupted initial state vector was then applied in the orbit integration software, GPSORBIT, to generate satellite orbits to be treated as the 'broadcast ephemeris'.

6.1.7 Test Strategy

The strategy of the simulation tests was designed to verify the ability of the algorithms to recover the satellite orbit and atmospheric propagation errors (including ionospheric and tropospheric error) in WADGPS system, and to assess the corresponding user positioning accuracy. Intensive simulation tests were carried out for the single frequency combined atmospheric effects approach and also the refined dual frequency approach. The refined single

frequency *ionospheric scale factor approach* was not tested by the simulated data since the simulation process would not have been effective for this approach. This technique relies on the use of standard tropospheric model for tropospheric error modelling, therefore no conclusion can be drawn from simulation tests involving the use of the similar models for generating and recovering the tropospheric errors. As a consequence, it was only assessed using real filed data.

6.2 Estimation of Satellite Orbit Errors

The recovery of the satellite orbit depends on several factors, such as the observable applied, the span of the observation data, the interval at which the atmospheric scale factor is solved for, the number of reference stations and the size of the network. In this research, only the code pseuodorange observable was used, due to the problems of cycle slips and integer ambiguity resolution associated with the carrier phase observable.

The data span and the interval for the atmospheric scale factor were held fixed throughout the tests. 72 hours of continuous data and a 90 minute interval for the atmospheric scale factor estimation were used throughout the tests for this study. This selection was based on a compromise between accuracy and efficiency, as concluded from previous work at Nottingham (Ochieng, 1993).

The capability of the algorithm to model the satellite orbit error was analysed by comparing the *true* ephemeris with the recovered ephemeris. The *true* satellite ephemeris, also used to create the simulation data, was an integrated ephemeris generated from the original satellite initial state vectors. The recovered ephemeris was obtained by employing the fiducial network concept, in conjunction with the orbit integration technique in an iterative process.

Several methods exist for the evaluation of the satellite orbit accuracy. The use of *a posteriori* standard deviations of the orbital parameters, in conjunction

with the comparison of the improved satellite initial state vector with the *truth* is one of the methods. The method adapted in this study was to compare the discrete satellite positions produced by the two ephemerides over the entire period. The RMS value of the total orbital error which consists of the radial, along track and cross track errors was used as an indication of the achievable accuracy of the recovered satellite orbit.

In order to analyse the effects of individual errors on the capability of the proposed algorithm to recover the satellite orbit, a number of tests were conducted by applying various combinations of errors in the system. The combinations of the error components investigated in the system, along with the satellite orbit error included,

(i) only satellite and receiver clock errors simulated

(ii) ephemeris and SA 'epsilon' error introduced to case (i)

(iii) tropospheric error added to case (ii)

(iv) ionospheric error added to case (ii)

(v) tropospheric and ionospheric errors added to case(ii)

(vi) pseudorange noise introduced in case (v)

(vii) pseudorange noise introduced in case (ii)

All the above error combinations were investigated for the single frequency combined atmospheric delay WADGPS approach. These are described on a case by case basis in section 6.2.1. Based on the conclusions from the single frequency approach, more tests were conducted for the refined dual frequency approach, which is described in Section 6.2.2.

6.2.1 Single Frequency Pseudorange Analysis

- **Case (i)**

The first step in any simulation study involving algorithm assessment is to ensure the internal consistency and correct implementation of the algorithm i.e.

to ensure that the algorithm has been designed correctly and that the resulting software has been coded as per the design of the algorithm. It is only after this that proper simulation studies involving error recovery can be carried out.

The 'self-check' test was designed to 'recover' the *true* satellite orbit, using simulation data in which no errors apart from the satellite and receiver clock errors were included. During the adjustment process, although no atmospheric error was simulated in the data, the atmospheric error was still estimated. Since the receiver and satellite clock errors are cancelled out by double differencing, there were therefore no error sources left in the data. As such, if the modelling and software implementation have been carried out properly, the *true* satellite orbits should be recovered with zero atmospheric delay values. Furthermore, since the data simulator and the processing software were developed independently, this analysis provided a rigorous independent 'self-check' for the GPS data processing algorithm.

Results of the analysis showed that the original satellite orbit errors were accurately recovered. The estimated atmospheric delay was found to be negligible. The small but insignificant differences may due to computer round off error. These results proved that the software was actually consistent within itself and therefore ready for further testing. However, before any other error components were introduced to the data, it was necessary to introduce satellite errors and to assess the satellite orbit error recovery capability of the algorithm.

- **Case (ii)**

The second test was conducted by introducing the satellite orbit error, which included SA 'epsilon' as well as the satellite and receiver clock errors, into the simulated data. The satellite orbit error was introduced by corrupting the initial position and velocity of the satellites in accordance with the worst case SA 'epsilon' scenario and then integrating to obtain a representative *broadcast ephemeris*. This *broadcast ephemeris* was then used during the data processing, generating corrections to the corrupted satellite orbit as well as the

atmospheric delays. In this test, the expectation was that the corrections generated for the initial state vectors should be very close to the values by which the original state vector was corrupted or altered. Atmospheric delay errors were expected to be almost zero since no apriori errors were introduced.

The results indicated a successful recovery of the orbit and the atmospheric delays. The difference between the initial satellite position and velocity of the recovered satellite orbit and the *truth* was at millimetre level. The atmospheric zenith delay was estimated to be at the sub-millimetre level. Other error components were then added to the simulated data for further investigations. The data sets used in the following tests were all simulated with satellite and receiver clock and SA 'dither' errors, plus specific errors mentioned in the actual tests. The satellite orbit errors were simulated by manipulating the initial state vectors as described previously.

- **Case (iii)**

The first error component added to the simulation data was the tropospheric error. In the adjustment process, the atmospheric scale factor was solved for at 90 minutes intervals. The initial approximate tropospheric delays (for the purpose of least squares adjustment) can either be provided by an empirical value or generated by a suitable model e.g. Magnet model. In fact, if the errors in the system are all properly modelled, the initial approximate value should not affect the final estimated atmospheric delay, the only difference would show on the resulting scale factors. This conclusion was reached by comparing the effects of generating the approximate atmospheric delays by each of the two methods. The results showed that the delays obtained were exactly the same, the different approximate values resulted in different scale factors but did not affect the final estimated delays.

The recovered satellite orbit was assessed by comparing the discrete satellite positions over a specified period using the program EPHDIFF, the software for the orbit accuracy evaluation developed for this research (§ 5.2). In this test,

the recovered satellite orbit was compared with the *true* satellite orbit, and the RMS total orbital errors were found to be at the 10 cm level. The main conclusion of this test was that the atmospheric scale factor approach is a realistic technique for recovering the tropospheric error.

- **Case (iv)**

Another new data set was then simulated which included the ionospheric error only. The same procedure as in previous test (**case(iii)**) was adopted. The RMS total orbital error was of the order of 2 to 3 m. Compared with **case (iii)**, the level of the errors were much higher here, indicating that the scale factor approach applied for tropospheric error recovery was not so suitable as for modelling the ionospheric error. The reason for the poorer orbit recovery was mainly due to the deficiency of the model to handle ionospheric errors (§ 4.6.2).

There are several factors which may contribute to the poorer satellite orbit recovery. Firstly, the atmospheric scale factor is estimated as constant over a period of time, which is based on the assumption that the zenith delays are constant during this period. However, the ionospheric delays, simulated by the Klobuchar model, essentially took the form of a cosine wave which changed rapidly during day time. Secondly, the model applied in the optimiser was modified to accommodate the combined tropospheric and ionospheric error. The main modifications involved bringing down the computation point from sub-ionospheric point to ground and the use of tropospheric mapping function, which was obviously not suitable for data with only ionospheric errors.

- **Case (v)**

In this test, both tropospheric and ionospheric errors were introduced to the simulated data. The satellite orbit recovered by this set of data produced an RMS total orbit error of the order of 10 m. This was much higher than both **case (iii)**, the tropospheric error only data, and **case (iv)**, the ionospheric error only data. This shows that the approach of solving for one scale factor every

90 minutes, for the combined troposphere and ionosphere error may not be adequate. Therefore further investigation of the modelling of atmospheric propagation effects was necessary. The recoveries of the satellite orbit error in terms of the RMS of the total orbit errors are shown in Figure 6.2 for **cases (iii), (iv)** and **(v)**, the tropospheric error only data, the ionospheric error only data and both the tropospheric and ionospheric error data, respectively.

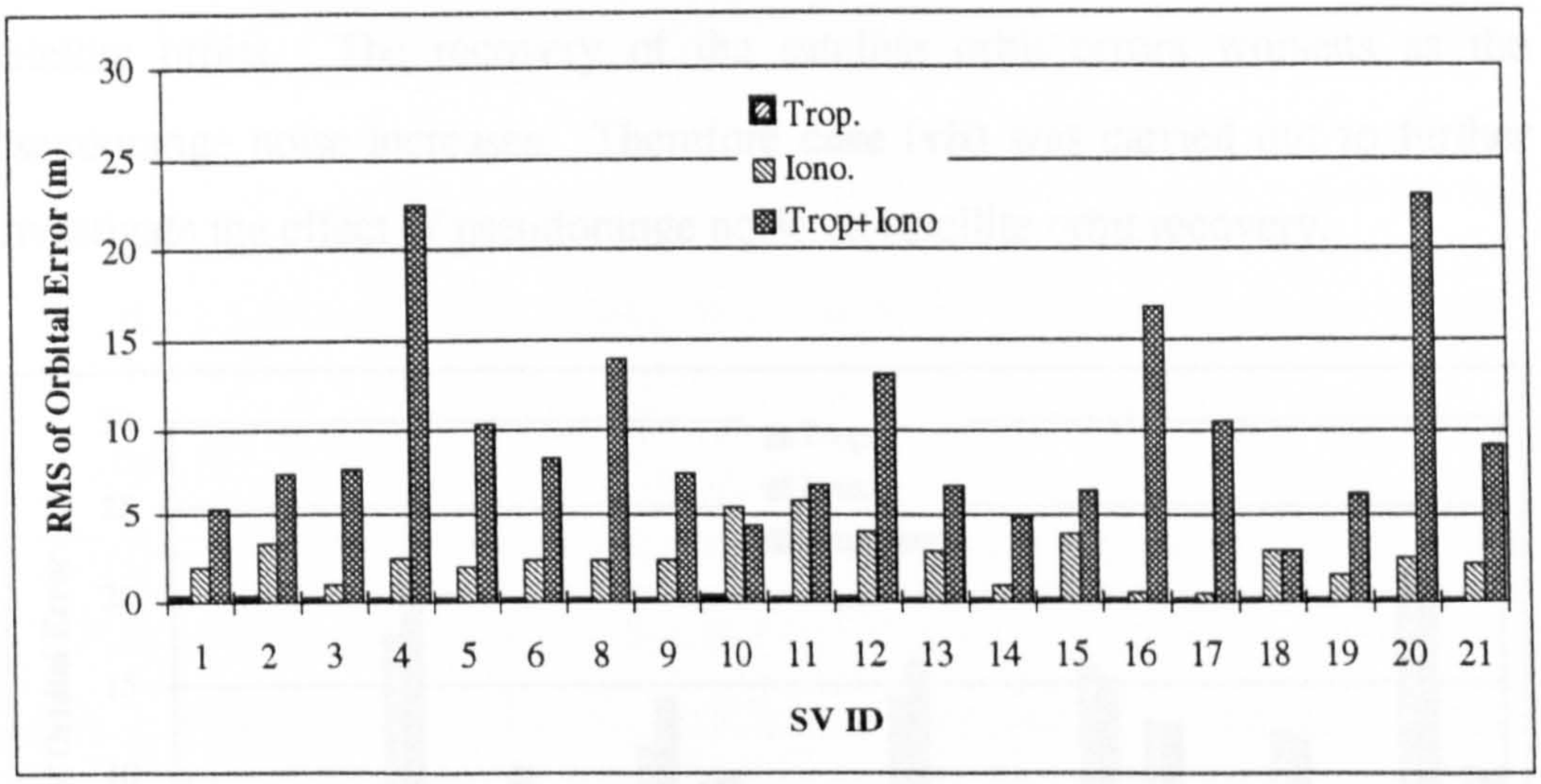

Figure 6.2 Single Frequency Satellite Orbit Recovery : (i), Tropospheric ii) Ionospheric, (iii) Ionospheric and Tropospheric Errors Applied

- **Case (vi)**

The pseudorange noise was introduced into the data used in this case. Three different levels of pseudorange noise were used in the generation of the simulated data. The statistical characteristics used were zero mean and standard deviations of 0.2 m, 0.5 m and 1 m. Each level of pseudorange error was then added to **cases (iii)**, **(iv)** and **(v)** for the purpose of analysing the system sensitivity to noise in terms of the satellite orbit recovery. The results of this analysis are given in Figures 6.3 to 6.5 for all satellites. Each figure shows the satellite orbit accuracy obtained using three different data sets. These data sets are distinguished by the types of errors included during the simulation process, i.e. tropospheric error for **case (iii)**, ionospheric error for **case (iv)** and both tropospheric and ionospheric errors for **case (v)**.

Several points can be noted regarding the results given in Figures 6.2 to 6.5 (Figure 6.2 can be treated as a similar test as **case (vi)** with 0.0 m (SE) pseudorange noise). It is clear that the tropospheric error was well recovered, especially when the pseudorange noise is low. However, the ionospheric error was not so well recovered. The worst result was obtained when both tropospheric and ionospheric errors were included in the data. The tests also show that the pseudorange noise has a significant effect on the recovery of the satellite orbits. The recovery of the satellite orbit errors worsens as the pseudorange noise increases. Therefore **case (vii)** was carried out to further investigate the effect of pseudorange noise on satellite orbit recovery.

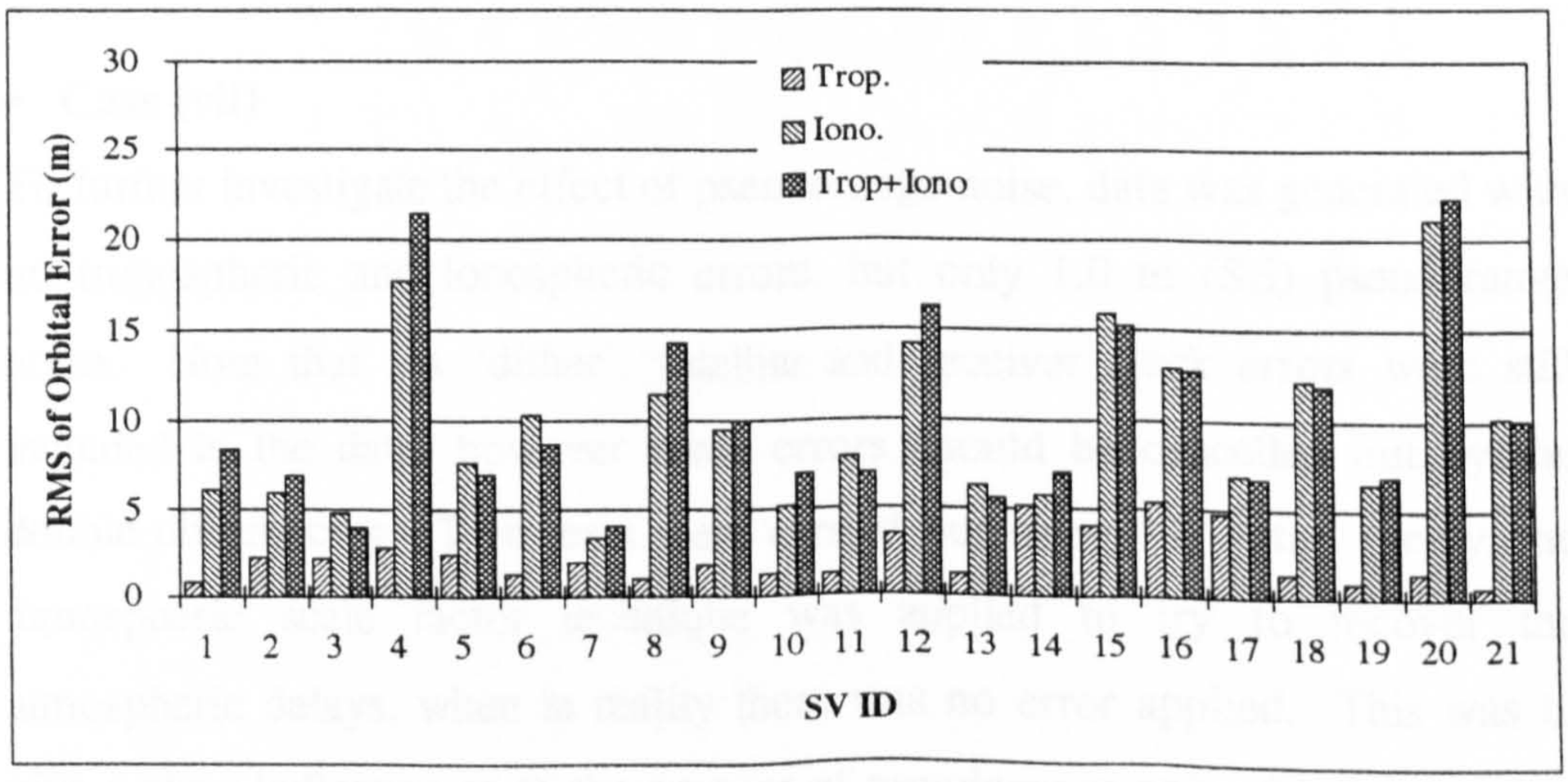

Figure 6.3 Satellite Orbit Recovery with 0.2m (SE) Pseudorange Noise

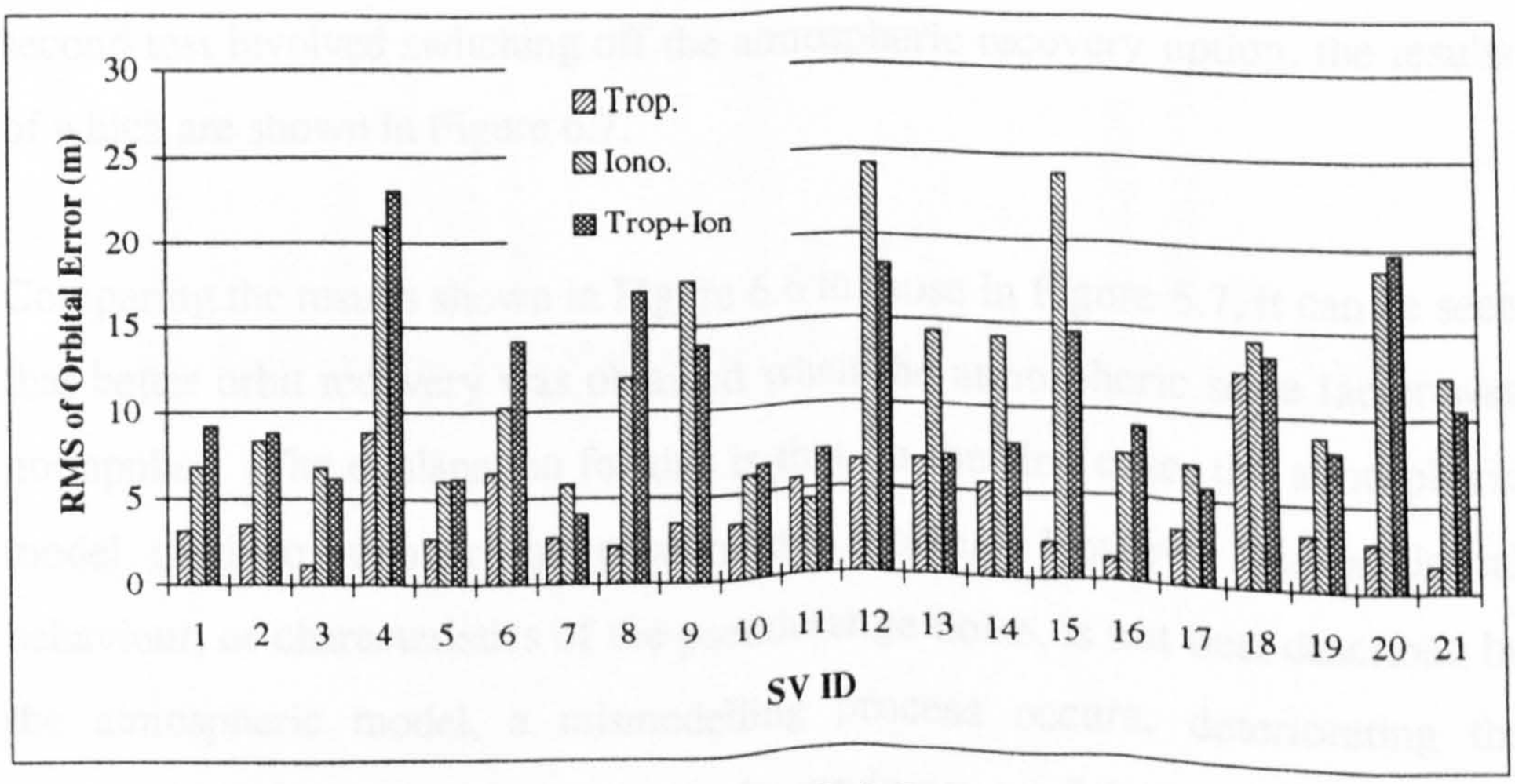

Figure 6.4 Satellite Orbit Recovery with 0.5m (SE) Pseudorange Noise

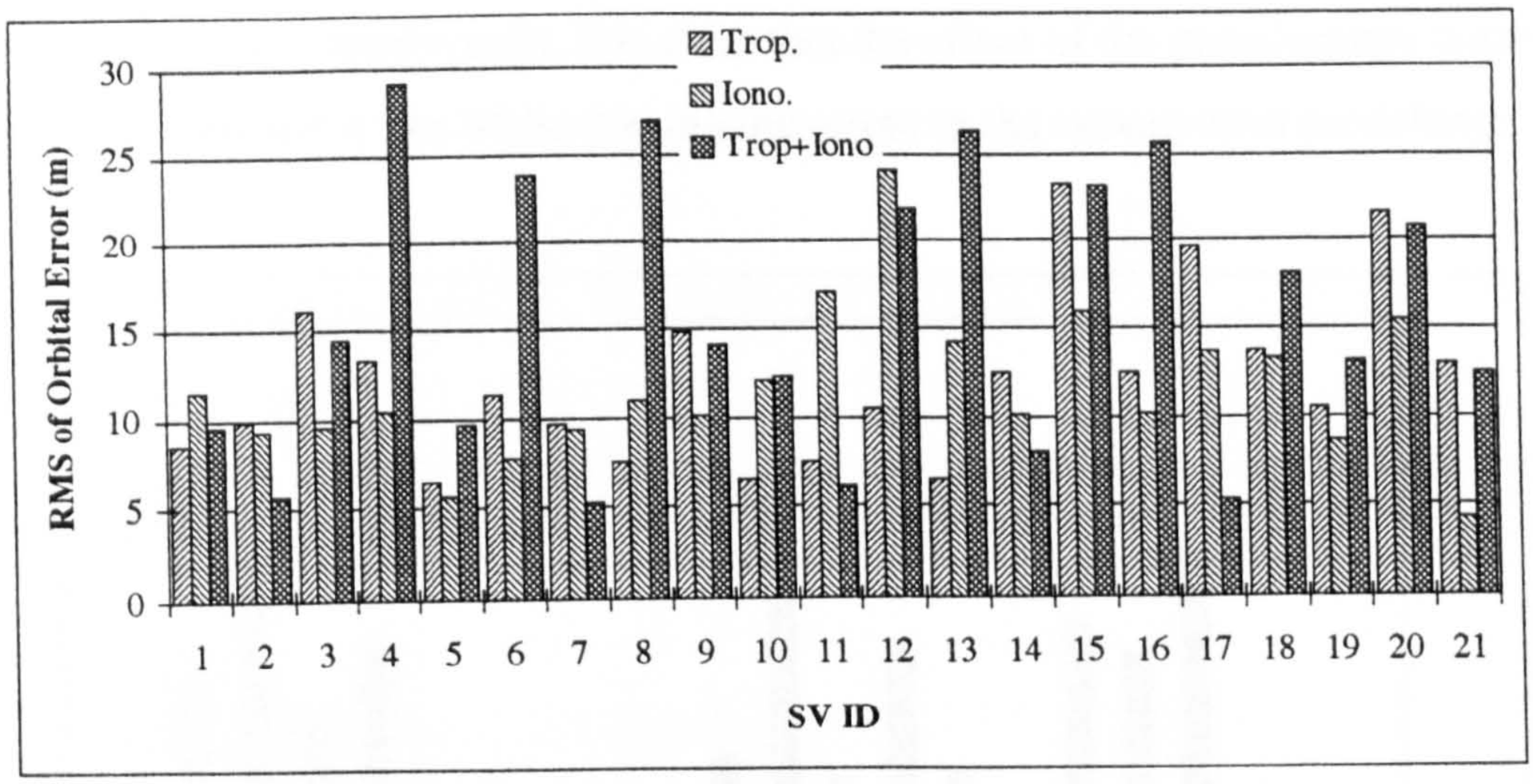

Figure 6.5 Satellite Orbit Recovery with 1.0m (SE) Pseudorange Noise

- **Case (vii)**

To further investigate the effect of pseudorange noise, data was generated with no tropospheric and ionospheric errors, but only 1.0 m (SE) pseudorange noise. Note that SA 'dither', satellite and receiver clock errors were still included in the data, however these errors should be cancelled out by the double differencing. Two tests were carried out using this data. Firstly, the atmospheric scale factor technique was applied to try to recover the atmospheric delays, when in reality there was no error applied. This was to give a clear indication as to the amount of pseudorange noise falsely absorbed by the atmospheric model, the results of which are shown in Figure 6.6. The second test involved switching off the atmospheric recovery option, the results of which are shown in Figure 6.7.

Comparing the results shown in Figure 6.6 to those in Figure 6.7, it can be seen that better orbit recovery was obtained when the atmospheric scale factor was not applied. The explanation for this is that, in the first case, the atmospheric model tried to recover the pseudorange noise. However the statistical behaviour, or characteristics of the pseudorange noise, is not best described by the atmospheric model, a mismodelling process occurs, deteriorating the results. However, in the second case, the randomness of the pseudorange noise

results in an averaging process, culminating in better overall orbit accuracy recovery. From these results, it is clear that the effect of the pseudorange noise is significant and is one of the dominating errors in the system error modelling.

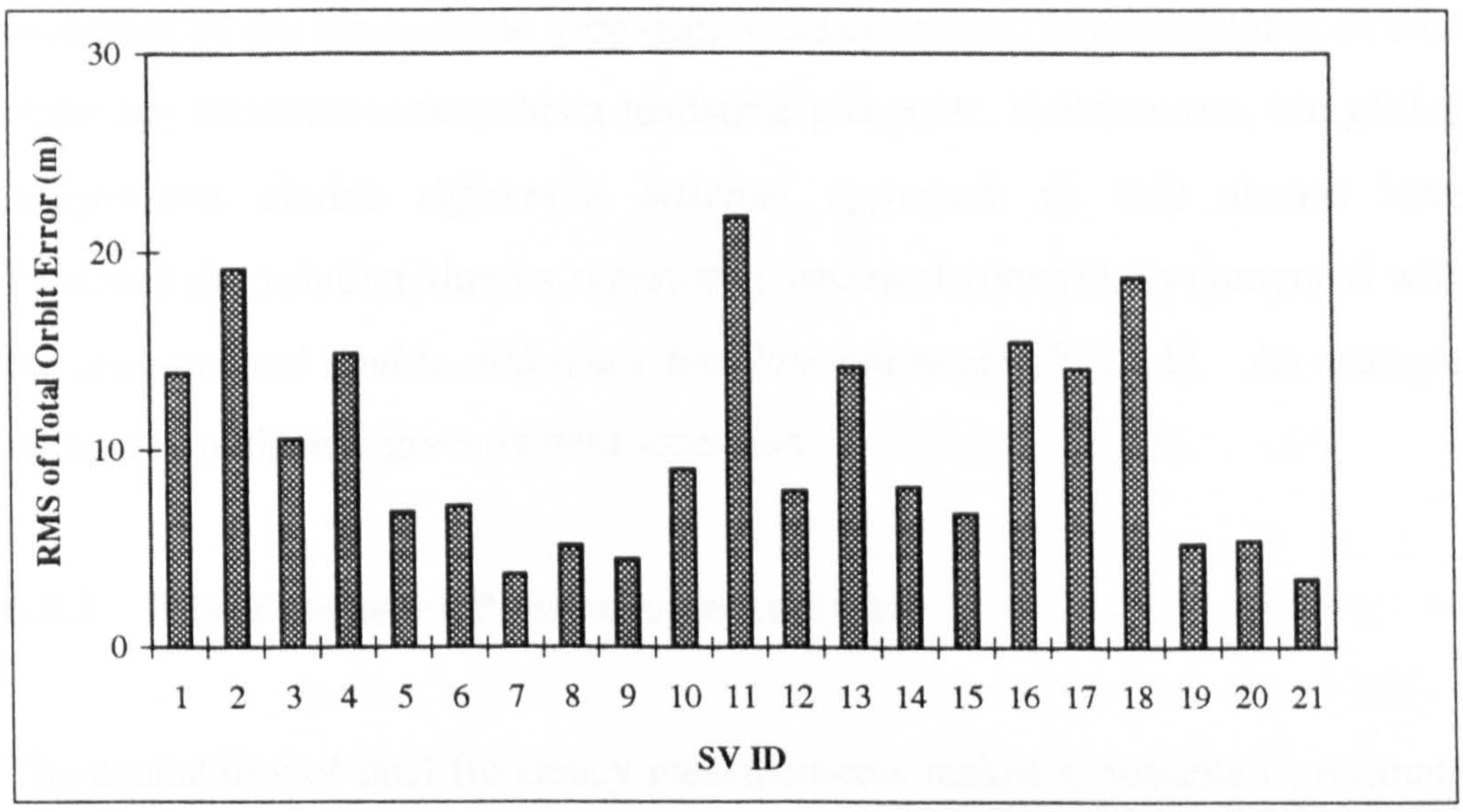

Figure 6.6 Satellite Orbit Recovery with 1m Pseudorange Noise (Scale Factor On)

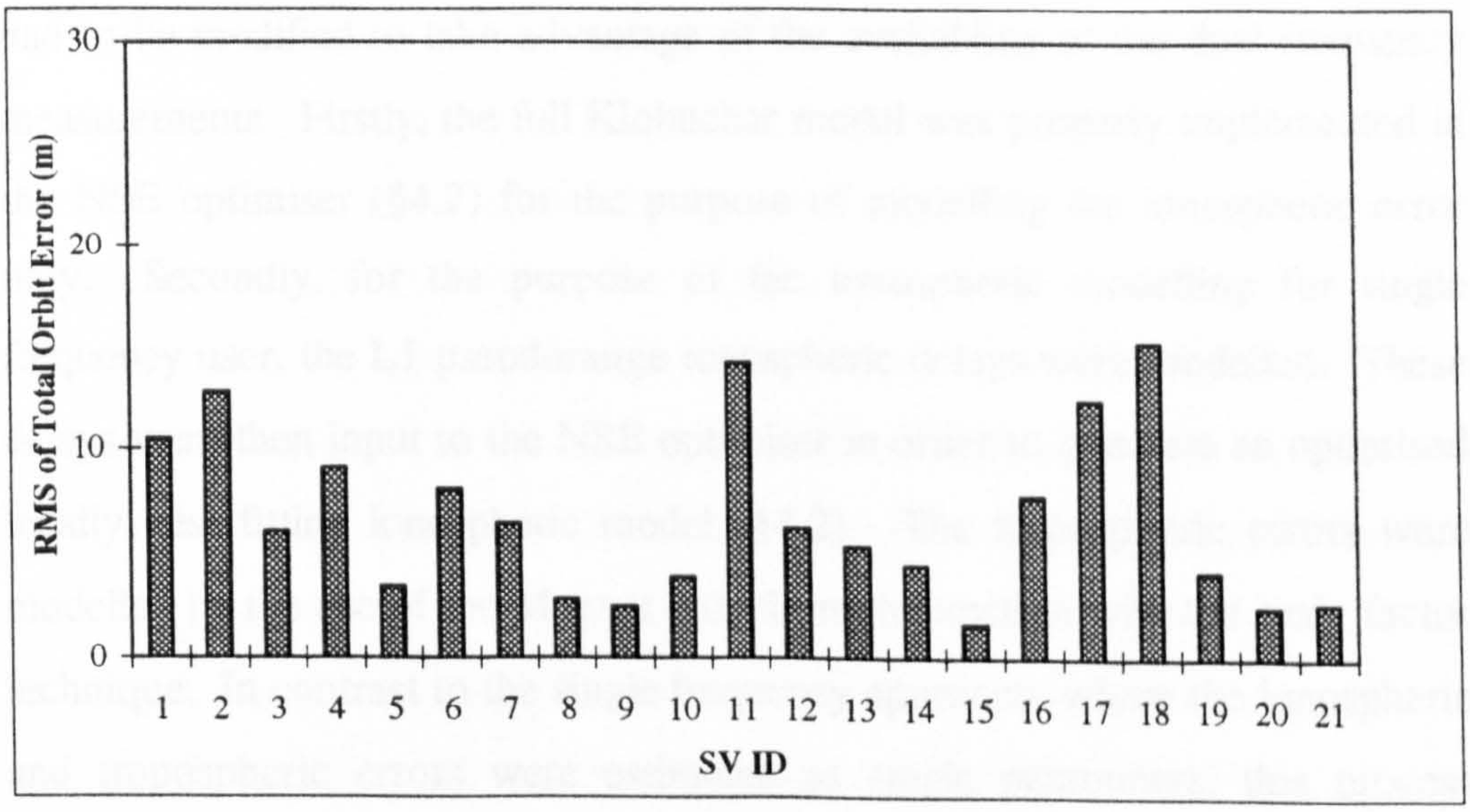

Figure 6.7 Satellite Orbit Recovery with 1m (SE) Pseudorange Noise (Scale Factor Off)

The analysis carried out so far enabled the deficiencies in the single frequency technique to be highlighted. There is very little that can be done regarding the pseudorange noise currently except for the availability of low noise receivers. The improvement of the WADGPS concept must therefore rely on better modelling of the atmospheric propagation delay errors. The availability of dual frequency receivers makes this a realisable prospect. Furthermore, the *global independent double difference baseline approach* (§ 4.4) should have improved the solution, due its superior geometrical strength, as compared with the *unconnected double difference baseline approach* (§ 3.4.1). An example of the comparison is given in next secession.

6.2.2 Dual Frequency Pseudorange Analysis

The availability of dual frequency measurements makes it possible to estimate and hence eliminate first order ionospheric delay effects by the use of the ionospherically-free observable. Therefore the dual frequency ionospherically-free observable was applied in the refined Nottingham WADGPS approaches, as one of the options for the orbit determination process. The related software had to be modified to take advantage of the availability of the dual frequency measurements. Firstly, the full Klobuchar model was properly implemented in the NSE optimiser (§4.2) for the purpose of modelling the ionospheric error only. Secondly, for the purpose of the ionospheric modelling for single frequency user, the L1 pseudorange ionospheric delays were modelled. These delays were then input to the NSE optimiser in order to generate an optimised locally best fitting ionospheric model (§4.2). The tropospheric errors were modelled by the use of the Magnet model, in conjunction with the scale factor technique. In contrast to the single frequency approach, where the ionospheric and tropospheric errors were estimated as single parameters, this process separated the two and hence, the appropriate mapping functions could be employed.

Based on the conclusion drawn from previous section (§ 6.2.1), three sets of data were simulated in order to investigate the effect of using the ionospherically-free observable during the estimation of the satellite ephemeris. All the test data were corrupted with receiver and satellite clock (including SA 'dither') errors along with the corrupted *broadcast ephemeris*. In addition, the other error sources were simulated and added to the data as given below,

(a) 0.2 m (SE) pseudorange noise

(b) all error sources excluding pseudorange noise

(c) all error sources including 0.2m (SE) pseudorange noise

The recovered orbits were then assessed using the *true* ephemeris by comparing the discrete satellite positions over a 72 hour period. The RMS of the total orbital errors for each satellites are shown in Figures 6.8 to 6.10 for cases (a), (b) and (c) respectively.

- **Case (a)**

In this test, although only pseudorange noise was included in the data, all the error recovery models for the orbit determination were activated. Since both ionospheric and tropospheric errors were absent and the double difference process eliminates all the other common errors, this test investigated the effect of pseudorange noise on the recovery of the satellite orbit. It should be noted that due to error propagation, the formation of the ionospherically-free observable introduces to the system three times the noise level than the L1 observable does. The benefit of the dual frequency ionospherically-free observable could therefore be shadowed by the increase in noise level which has been shown to be a significant error source in the orbit determination process. The RMS of the total orbital error of the recovered satellite orbit was of the order of 5 m, which is shown in Figure 6.8.

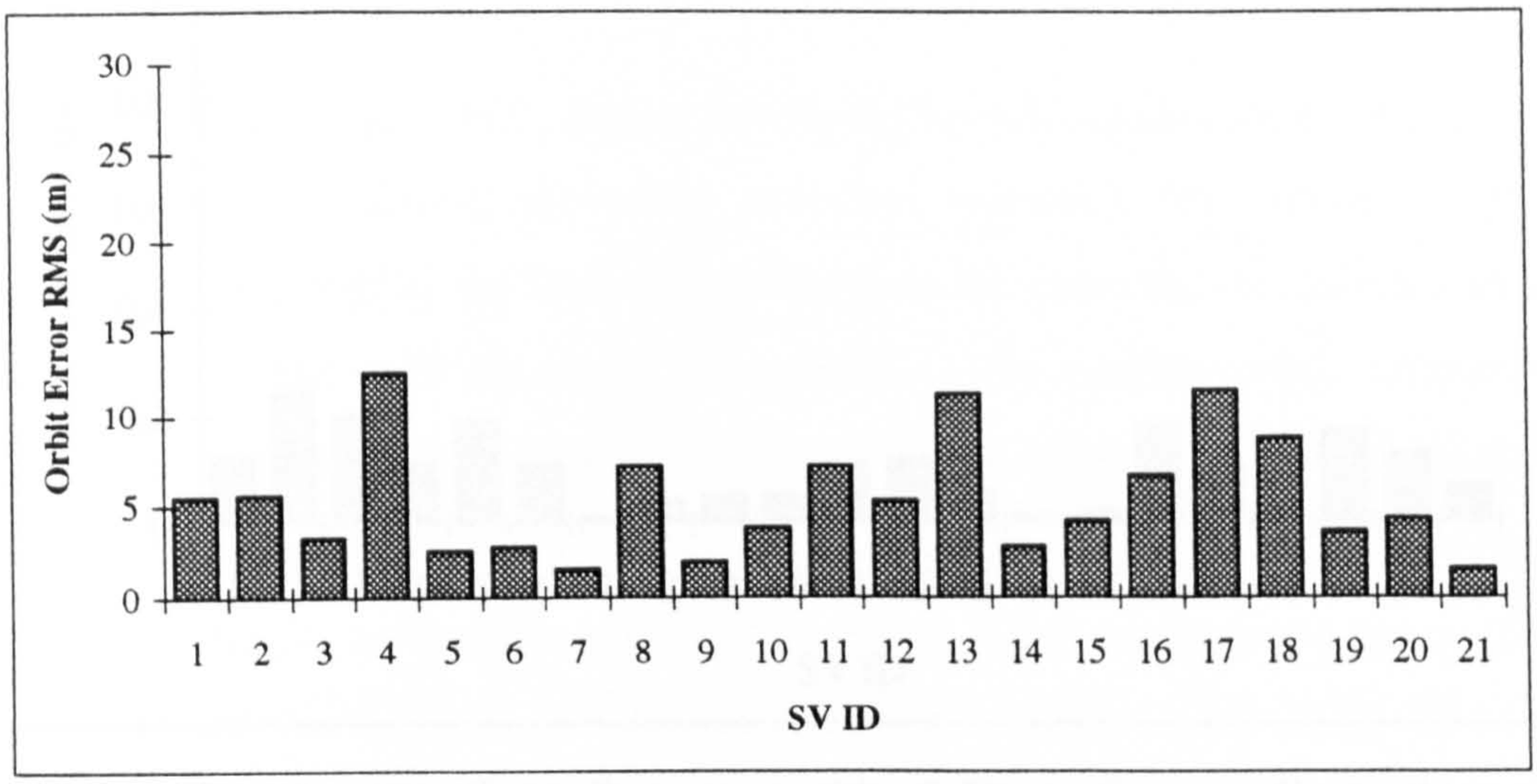

Figure 6.8 Satellite Orbit Recovery with 0.2 m (SE) Pseudorange Noise

- **Case (b)**

In this test, all the error sources except the pseudorange noise were applied to the data. The tropospheric error was modelled by the Magnet model in conjunction with the scale factor technique. The ionospheric error was eliminated by the use of dual frequency observables and the receiver and satellite clock errors (including S-A 'dither') were eliminated by the double differencing process. Since no random noise is left after the double difference processing, the remaining errors should all be properly treated by the proposed models. It is therefore a good test to show how well the models and algorithms were applied. The results of this test are shown in Figure 6.9, the RMS of the recovered satellite orbit accuracy being of the order of 0.1 m. This represents a very significant improvement over the single frequency test (10 m level), shown in Figure 6.2 in Section 6.2.1, **case (v)**. It is clear that the models applied in the dual frequency approach perform much better than those applied in the single frequency approach which again, highlights the importance of the modelling of the atmospheric error. The next step was then to include the pseudorange noise in the simulated data.

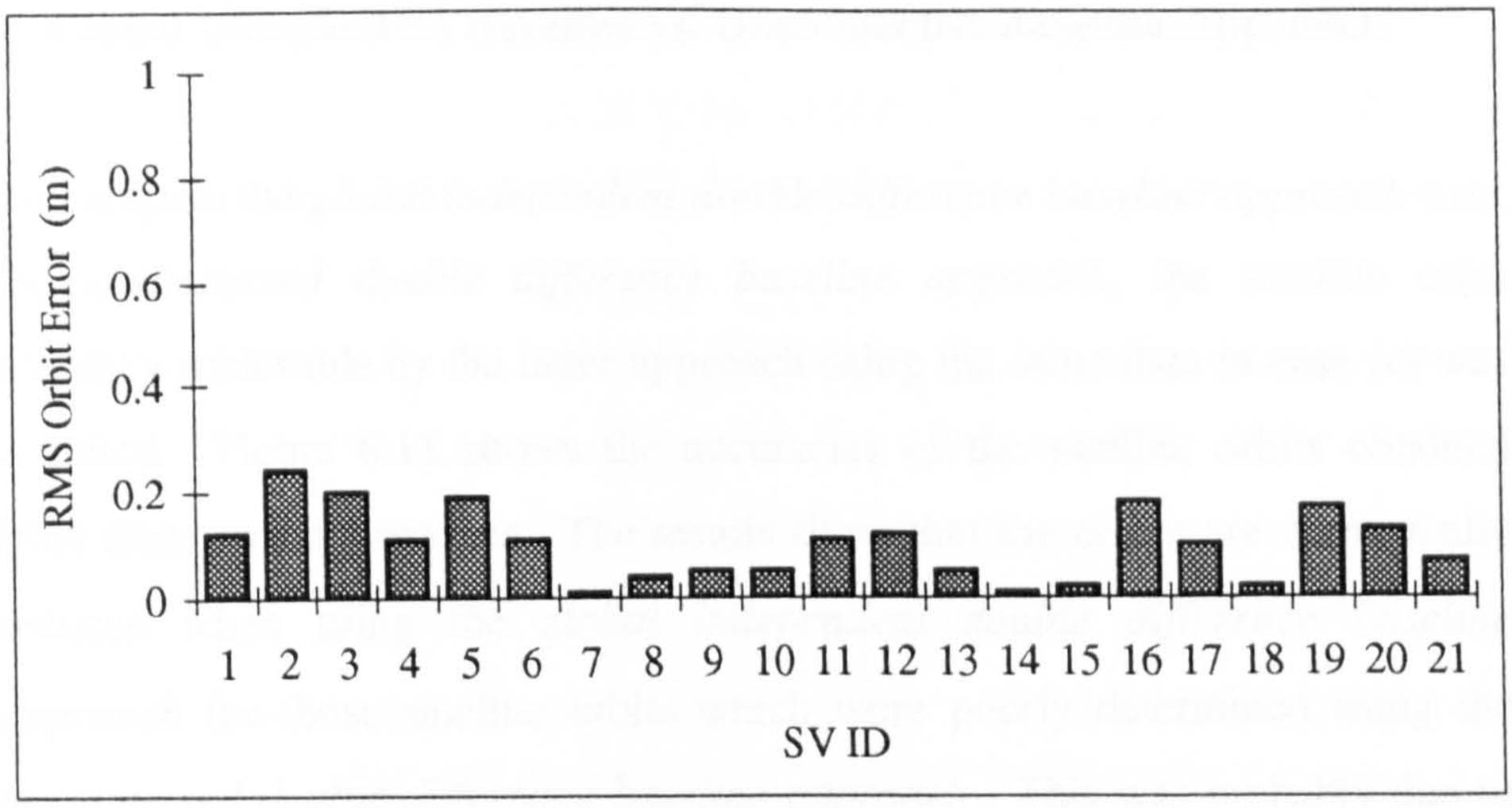

Figure 6.9 Satellite Orbit Recovery with all Error Sources Excluding Pseudorange Noise

- **Case (c)**

This case represented the situation in which all the known error sources were applied to the data. The RMS error of the recovered satellite position was of the order of 5 m (see Figure 6.10). Compared with the similar case of the single frequency approach (Figure 6.3), where RMS errors of about 10 m level were obtained, it is clear that the dual frequency measurements improve the accuracy of the orbit determination.

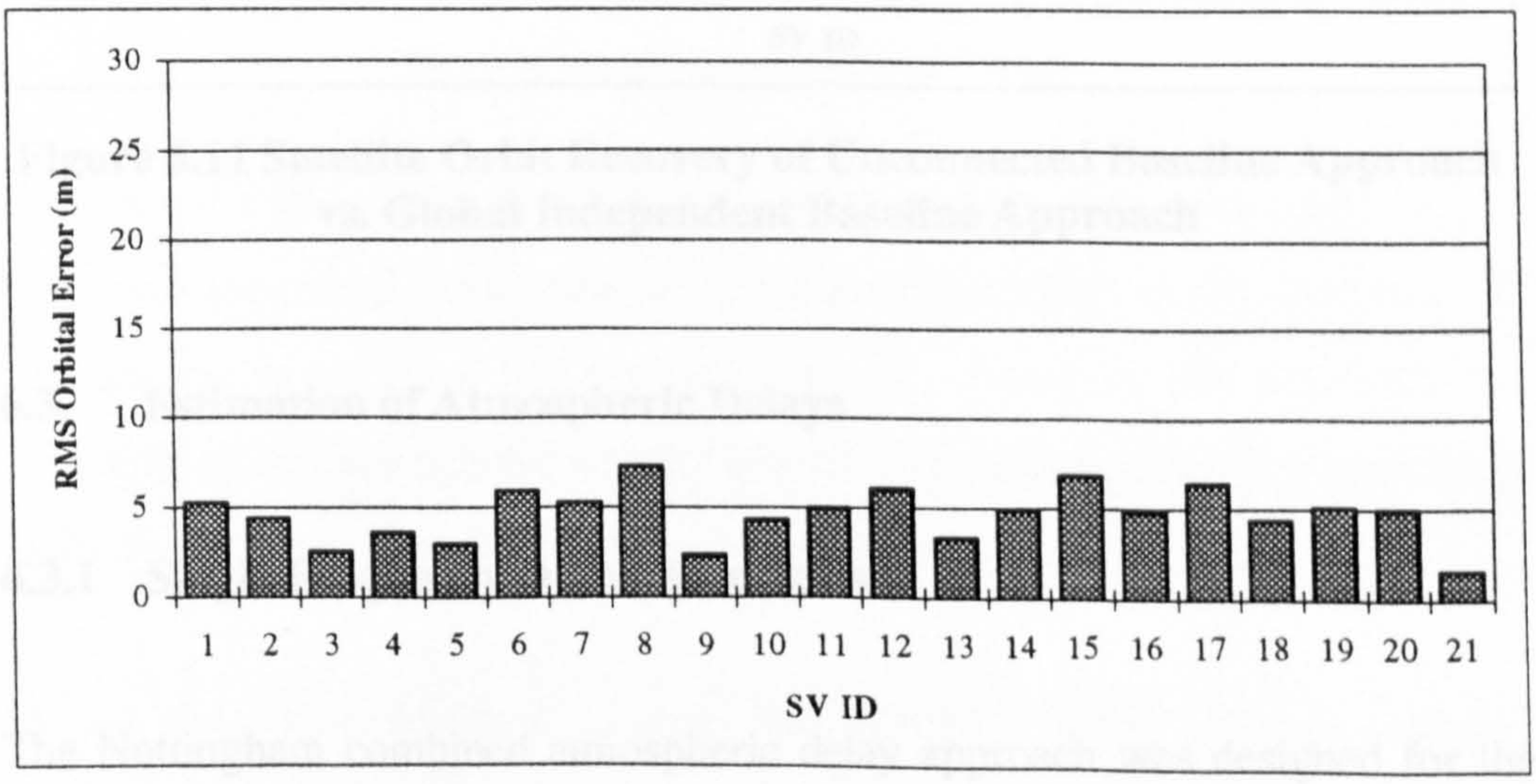

Figure 6.10 Satellite Orbit Recovery with All Error Sources and 0.2 m Pseudorange Noise

- **Global Independent Baseline vs. Unconnected Baseline Approach**

To compare the *global independent double difference baseline approach* over the *unconnected double difference baseline approach*, the satellite orbit accuracy achievable by the latter approach using the same data in **case (c)** was acquired. Figure 6.11 shows the accuracies of the satellite orbits obtained from these two approaches. The results show that the errors are dramatically reduced when using the *global independent double difference baseline approach* for those satellite orbits which were poorly determined using the *unconnected double difference baseline approach*. This was probably due to the increased geometric strength afforded by the *global independent double difference baseline approach*.

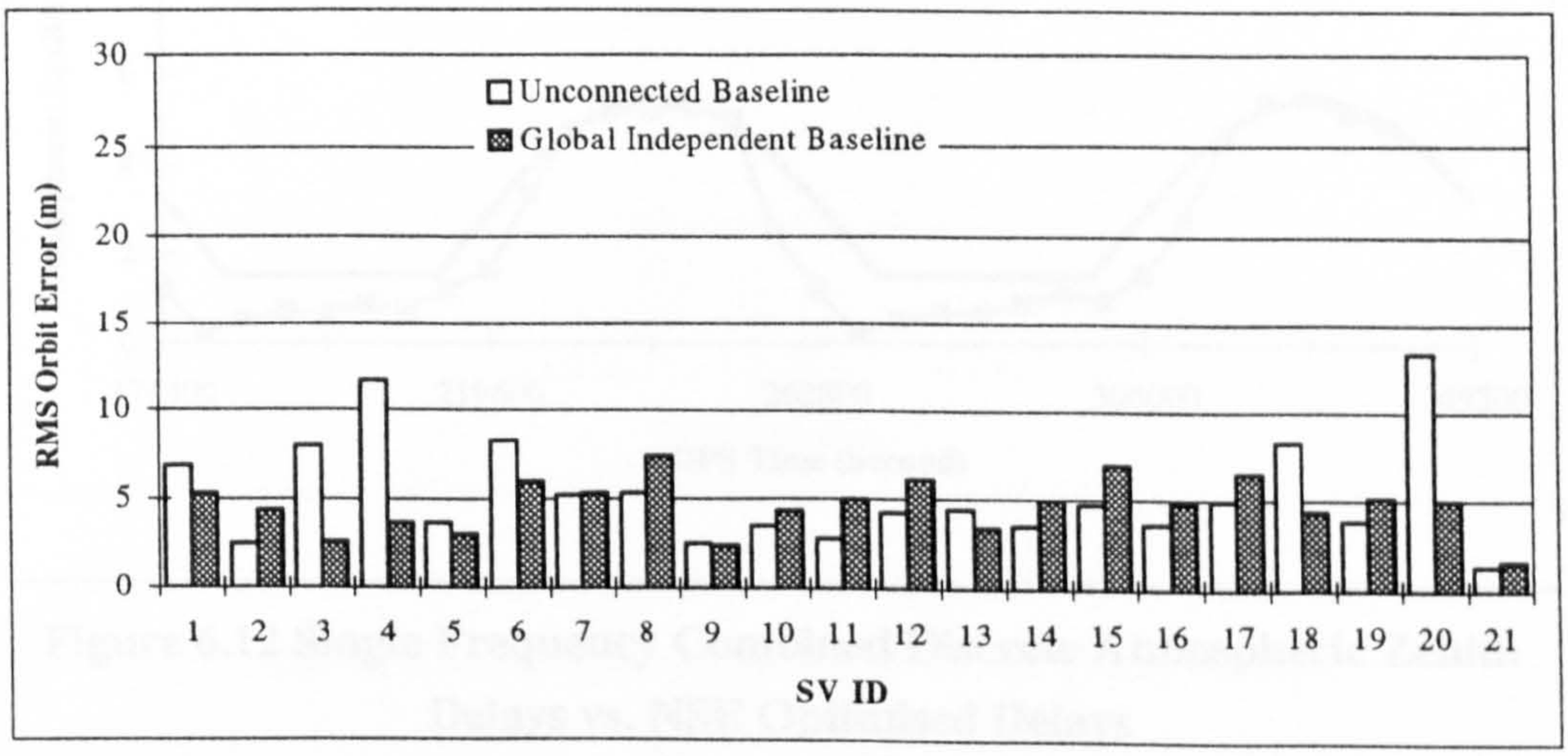

Figure 6.11 Satellite Orbit Recovery of Unconnected Baseline Approach vs. Global Independent Baseline Approach

6.3 Estimation of Atmospheric Delays

6.3.1 Single Frequency Observable Tests

The Nottingham combined atmospheric delay approach was designed for the single frequency receiver environment (Ashkenazi *et al*, 1993). The combined atmospheric delays are estimated at regular intervals as part of the orbit

determination process. These delays are then fitted to the modified Klobuchar model by the NSE optimiser to generate a 'new' set of atmospheric parameters which can be transmitted to users for the estimation of the atmospheric delays.

In order to analyse the power of the process of the optimisation for the atmospheric error correction model, a comparison between the discrete atmospheric delays estimated over a 72 hour period, and those resulting from the optimisation process is shown in Figure 6.12. The results show a close agreement between the discrete delays and those resulting from the optimiser.

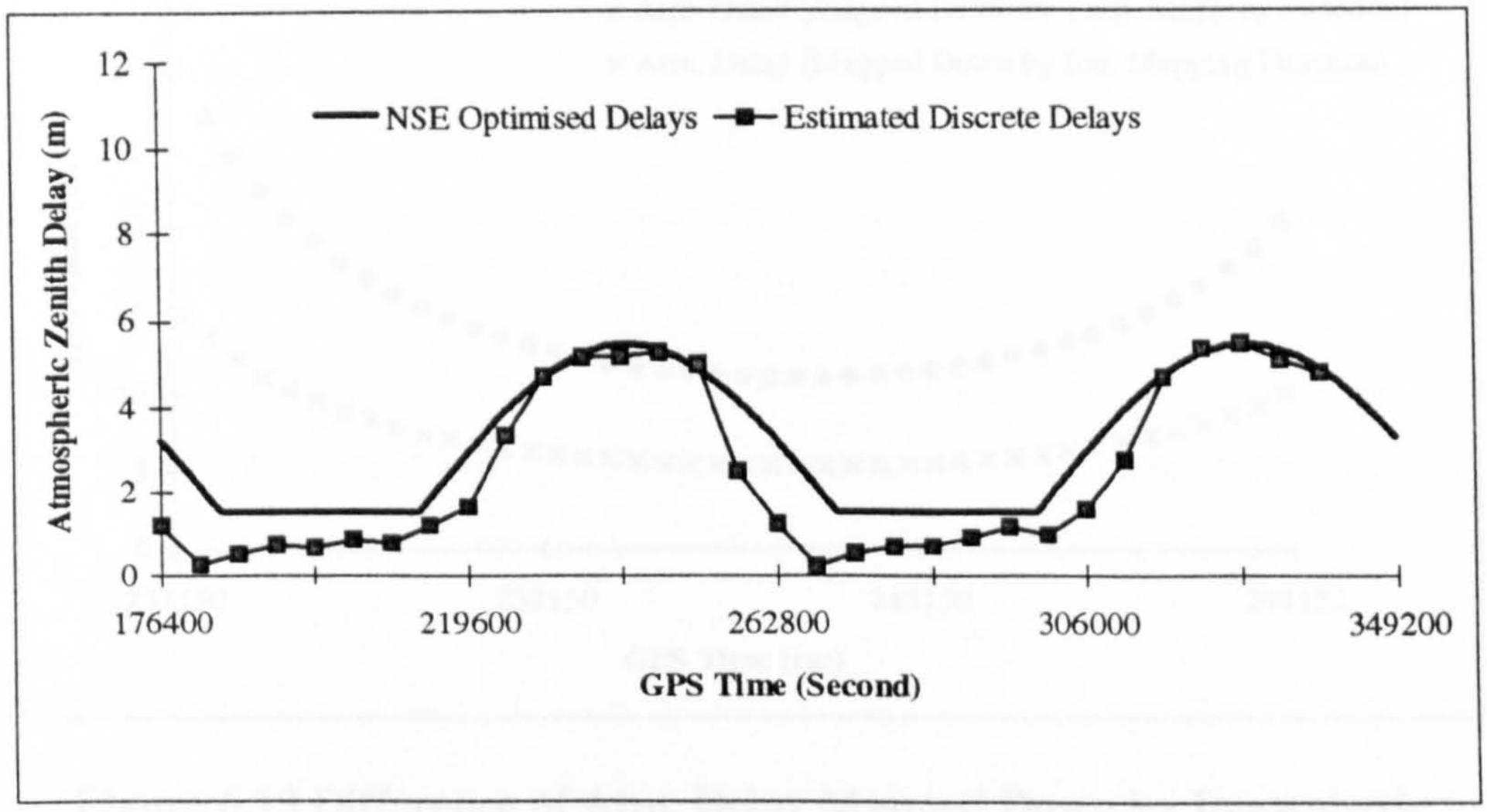

Figure 6.12 Single Frequency Combined Discrete Atmospheric Zenith Delays vs. NSE Optimised Delays

The second step is then to obtain the corresponding slant delays that can be applied to the actual measurements and assess the delays at the user site. In this process a mapping function is required. Since in this approach the tropospheric and ionospheric delays have been combined, either a tropospheric or ionospheric mapping function can be employed.

Special tests were designed to study the effects of using different mapping functions for the combined atmospheric delays. Firstly, the *true* tropospheric and ionospheric zenith delays, obtained from the data simulator, were mapped

down individually using appropriate mapping functions. These two mapped down delays were then added together to be treated as the *true* atmospheric delays. Secondly, two different mapping functions were applied to map down the estimated atmospheric zenith delays in order to compare with one another. Figure 6.13 shows the slant atmospheric delays of a particular satellite mapped down by the ionospheric and tropospheric mapping functions at one of the user stations. It is clear that the tropospheric mapping function appears to produce a much larger slant value than the ionospheric one.

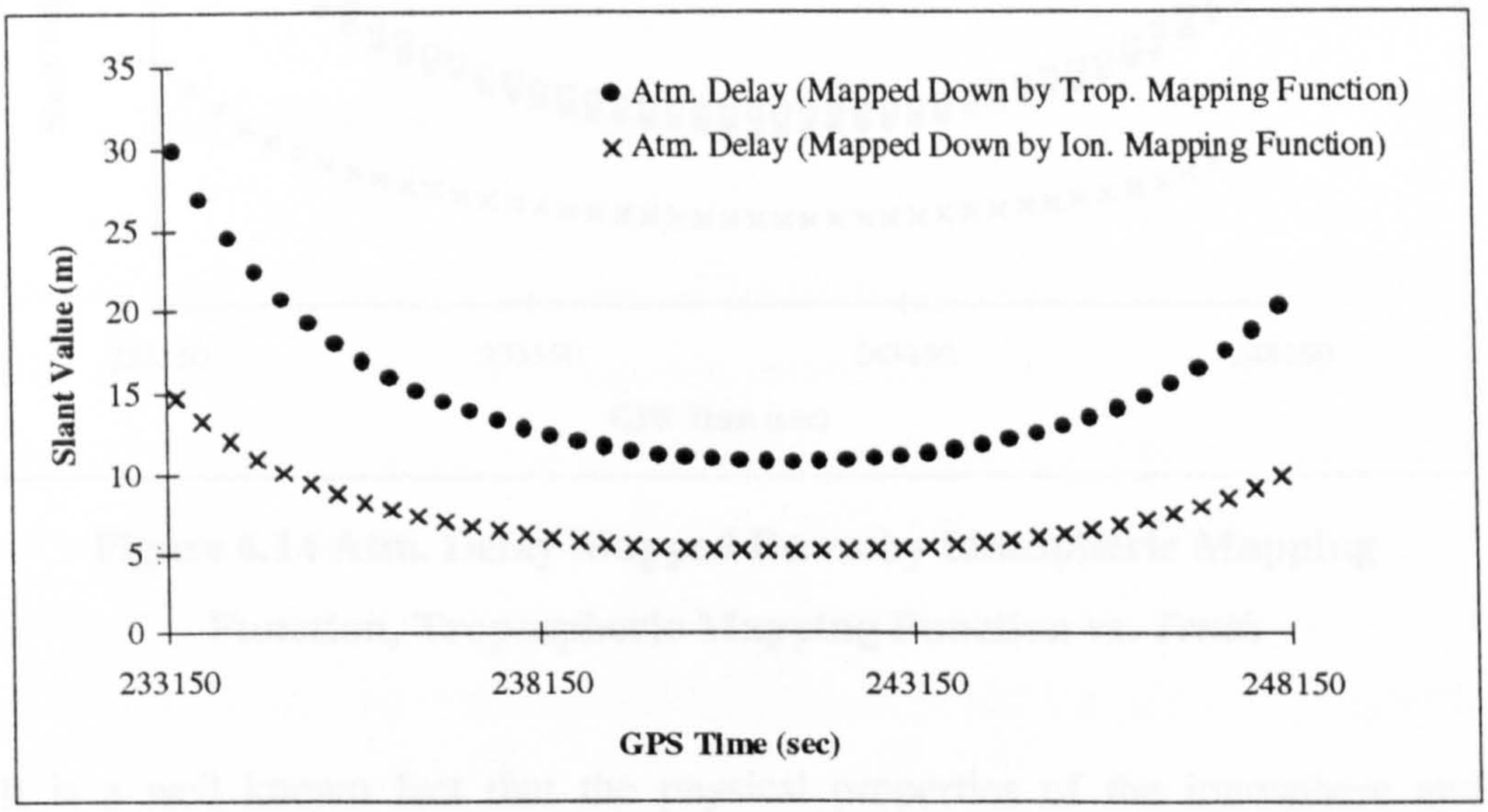

Figure 6.13 Difference of Atm. Delay Mapped Down by Ionospheric Mapping Function vs. Tropospheric Mapping Function

Since the tropospheric mapping function was applied in the modified Klobuchar model, the estimated atmospheric zenith delays were therefore expected to be less than the *truth*, due to the ionospheric and tropospheric errors being treated together. However the under-estimated zenith delays should be compensated by the tropospheric mapping function, resulting in the slant atmospheric delays estimated by the user being close to the *truth*, if the scale factor technique is powerful enough to model the atmospheric errors. The expectation for the use of the ionospheric mapping function is that the slant atmospheric delays should be under-estimated. Figure 6.14 shows the agreement of the mapped down delays between the *truth* and the delays

mapped down by the ionospheric and tropospheric mapping functions at one of the user stations. It clearly shows that the atmospheric delays mapped down by the tropospheric mapping function agree with the *truth* more closely than those mapped down by the ionospheric mapping function for this period.

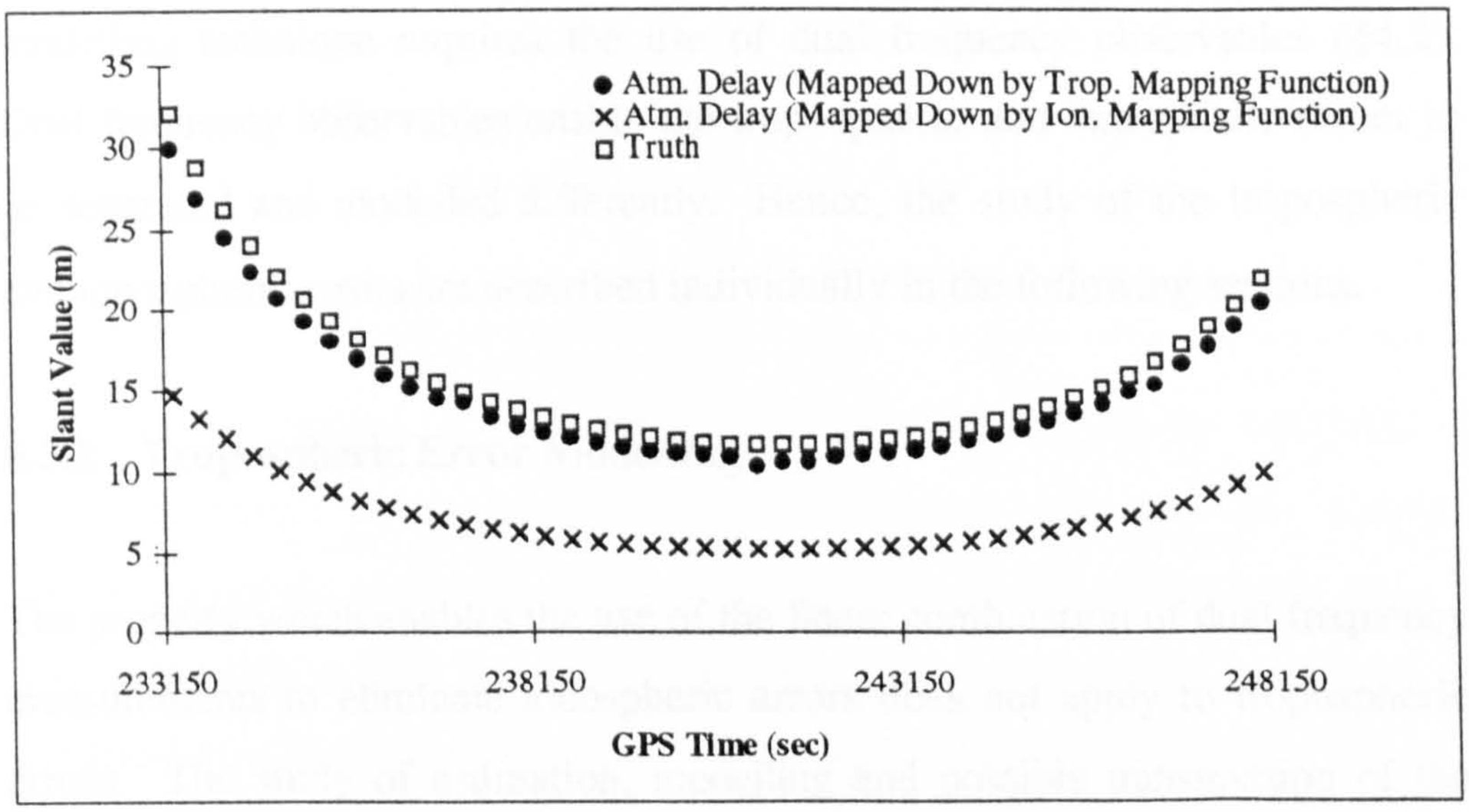

Figure 6.14 Atm. Delay Mapped Down by Ionospheric Mapping Function, Tropospheric Mapping Function vs. *Truth*

It is a well known fact that the physical properties of the ionosphere and troposphere are different, which raises the question of the validity of the combined atmospheric delay approach. In terms of the implementation of this approach, questions regarding the modification of the atmospheric model have to be answered. The questions arising are, for example, (a) what is the night time constant value to be used in the modified model, (b) whether the computation should be based on the ground (for troposphere) or the sub-ionospheric point (for ionosphere), (c) whether the geometrical (troposphere) or geomagnetic (ionosphere) latitude should be used, and (d) which mapping function should be used? Based on these problems, it is probably unwise to combine the ionospheric and tropospheric delay into one atmospheric delay, as the estimation process may not be robust enough.

The above tests indicate the deficiencies in the modelling of the atmospheric propagation errors using the single frequency combined atmospheric delay approach. Therefore in this research, it was essential that the ionospheric and tropospheric errors were separated modelled. For the ionospheric error, either single or dual frequency modelling techniques can be used. However, the best modelling technique requires the use of dual frequency observables (§4.2). Dual frequency observables enable the tropospheric and ionospheric errors to be separated and modelled differently. Hence, the study of the tropospheric and ionospheric errors are described individually in the following sections.

6.3.2 Tropospheric Error Modelling

The property which enables the use of the linear combination of dual frequency measurements to eliminate ionospheric errors does not apply to tropospheric errors. The study of estimation, modelling and possible transmission of the tropospheric delays are described in this section. Tests were conducted at two levels namely, (i) the estimation of tropospheric delay at reference stations (or at both reference and user stations) and (ii) the modelling of the tropospheric errors.

- **The Estimation of Tropospheric Delay**

The use of the Magnet model in conjunction with the scale factor technique was applied in the dual frequency WADGPS approach. Data was simulated with all error sources included, and dual frequency measurements were used for the processing. Since the ionospheric errors were eliminated by using the dual frequency measurements, the tropospheric errors remained, to be estimated by the scale factor technique as part of the orbit determination process. The tropospheric delays estimated by this technique were compared with the *true* tropospheric delays generated by the data simulator. Results show that the two zenith delays agree at the decimetre level for all reference

stations, indicating that the scale factor technique is suitable for the estimation of the tropospheric delays.

- **The Modelling of Tropospheric Delay**

The modelling of the tropospheric errors at the reference and/or user stations was investigated. The proposed approaches are described below,

(a) Treat tropospheric error as noise at both reference and user stations

There are two stages of processing involved in this case for the modelling of the tropospheric errors, namely the orbit determination and user position determination stage. At the orbit determination stage, the tropospheric error is still estimated in the rigorous way using the scale factor technique in conjunction with the Magnet model. This is the attempt to determine the best possible orbits. Afterwards, the delays are neither modelled nor applied in any form for the reference (during the generation of the differential corrections) and user stations (for the user position determination). The tropospheric error is therefore simply treated as a kind of noise in the system.

(b) Treat tropospheric error as noise at the user station only

At the orbit determination stage, the tropospheric error is properly estimated in the same manner as in case (a). At the user position determination stage, the estimated delays are applied for the formation of the differential corrections at the reference stations. For the users, the tropospheric error is still not modelled in any form for application to the measurements.

(c) Treat the tropospheric error in a similar way to that of the ionospheric error, by estimating a different set of Klobuchar-like parameters

The tropospheric delay is fitted to a Klobuchar-like model to generate another set of optimised coefficients, for the user to estimate his tropospheric delay at

his site. The idea of applying another set of Klobuchar-like parameters to model the tropospheric delay, which is apparently different from the ionospheric delay, is supported by two factors. Firstly, the success of applying the Klobuchar-like model to estimate the combined ionospheric and tropospheric delays in the single frequency observable case. Secondly, the existing transmission format for the Klobuchar parameters will make the transmission of the tropospheric error an easy task.

The software was modified to adapt the physical property of the tropospheric delays. The basic modifications were similar to those made for the single frequency combined atmospheric model (§ 4.2), the major difference being the dropping of the night-time constant. The night-time constant is included in the ionospheric model due to the ionospheric activity (TEC) being general quieter at night than day time. Since the tropospheric error does not have this kind of behaviour, the night-time constant was dropped in this test.

The precision of the fit of the Klobuchar-like model in estimating the tropospheric delay was then investigated. Figure 6.15 shows examples of the fit between the discrete tropospheric delays, estimated by the scale factor technique (in the orbit determination stage), and the delays generated by the optimised Klobuchar-like parameters. The form of a periodical waves shown in the optimised delay pattern is not seen in the delays estimated by the scale factor approach. This suggests that the precision of the fit of the tropospheric error by the Klobuchar model is inappropriate for the tropospheric delay, due to the fact that the troposphere and ionosphere behave differently. The effects of the proposed tropospheric error modelling were further investigated by the corresponding user positioning accuracy achievable (§ 6.4.2).

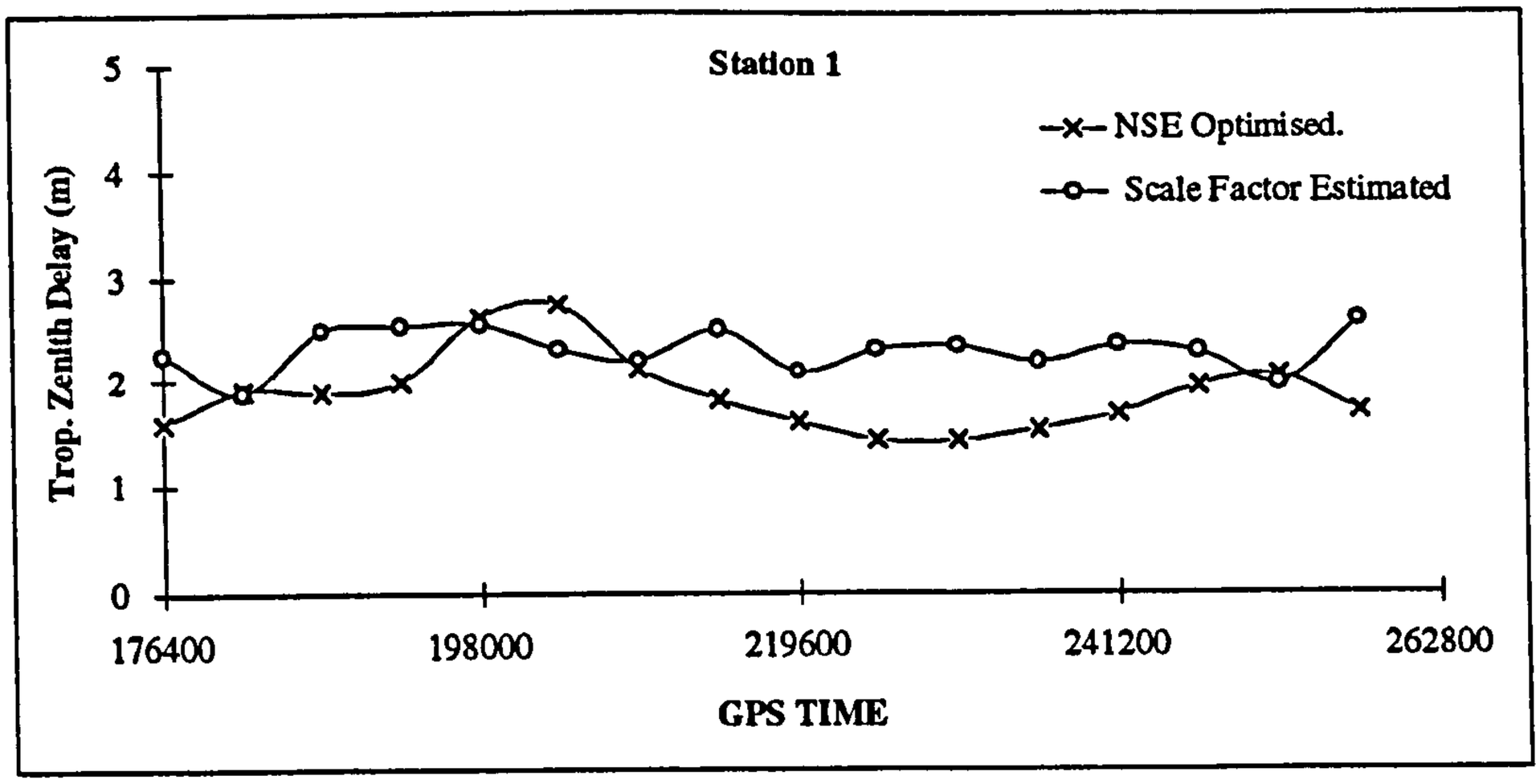

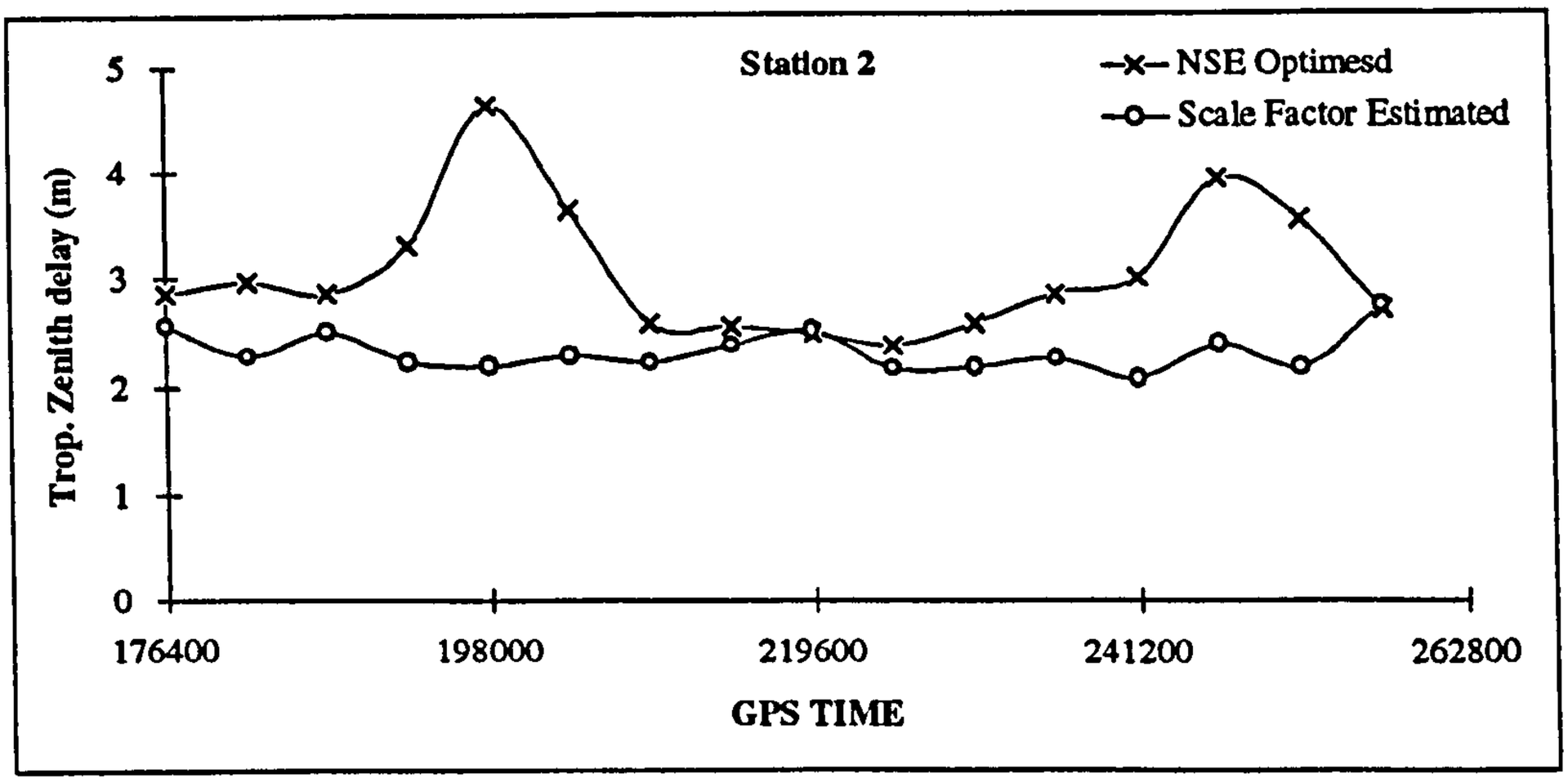

Figure 6.15 The Fit of the Tropospheric Zenith Delay to the Simplified Klobuchar-like Tropospheric Model

6.3.3 Ionospheric Delay Modelling

There are five steps involved in the investigation of the dual frequency ionospheric delay modelling, namely :

(i) simulate the ionospheric delays (treat as *truth*)

(ii) estimate the delays using dual frequency measurements

(iii) optimise the delays to generate a locally best fitting ionospheric model

(iv) estimate the ionospheric delays using the optimised ionospheric model

(v) compare the estimated delays at the user with the *truth*

Figure 6.16 shows the results of a comparison between the *true* delay and those estimated from the locally best fitting model for a typical user site. The two sets of delays agreed at decimetre level.

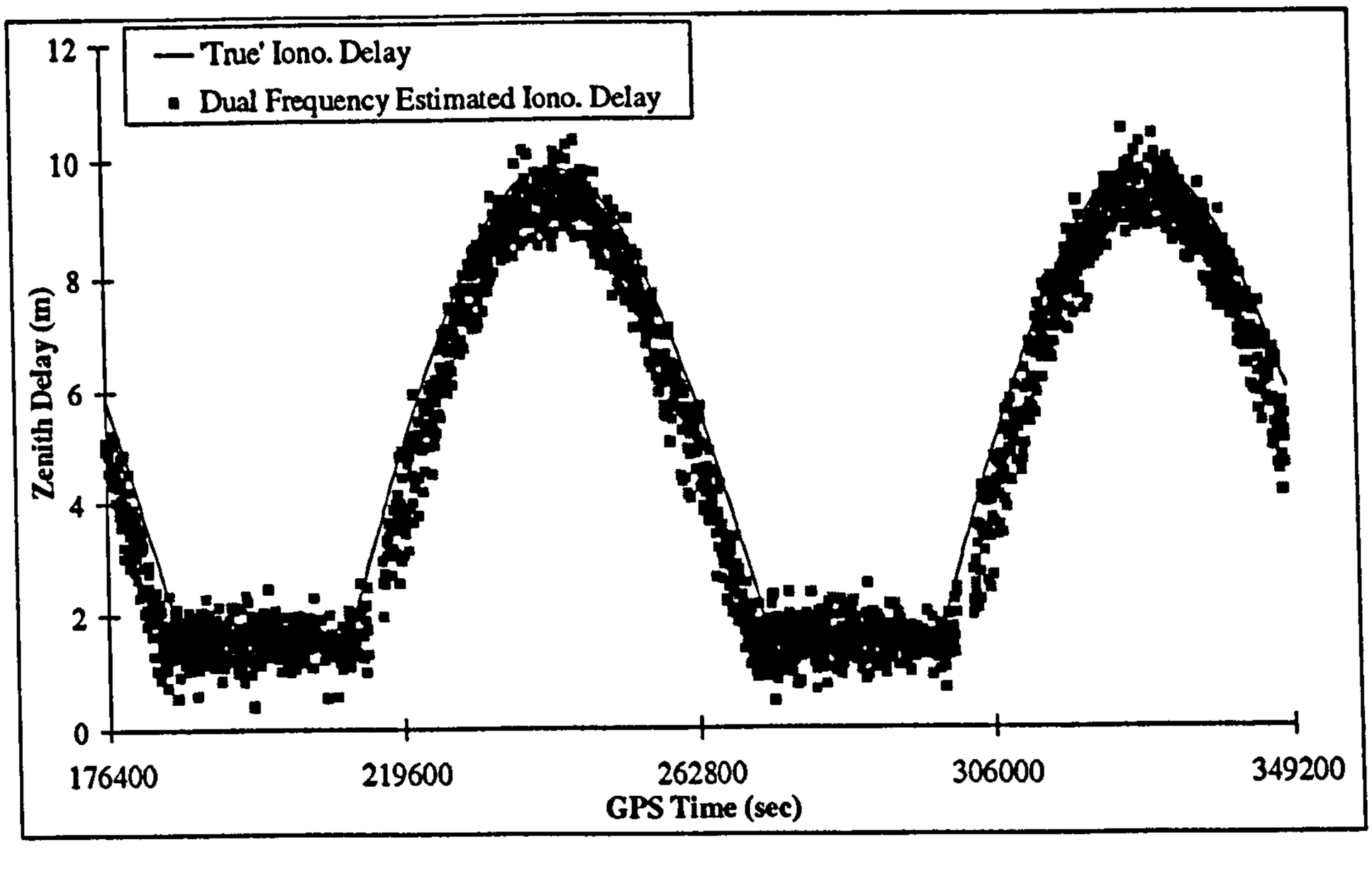

Figure 6.16 The Fit of Dual Frequency Estimated Ionospheric Zenith Delays vs. 'Truth'

6.4 User Positioning Accuracy

Five user stations were simulated to analyse the user position accuracy. In order to enable a comparison to be made with the conventional differential GPS, the stations were designed to have distances ranging from 0.05 to 1,000 km from one of the reference stations, Richmond in the USA. The precisely known coordinates of these stations were treated as *truth*, to compare with the user positions obtained from the simulated measurements. Various sets of data containing different combinations of error sources were simulated and processed, to provide a thorough analysis of WADGPS performance. The user data was simulated at a sampling interval of 1 second for a period of 1 hour. The error sources, including those due to the satellite orbit, satellite and receiver clocks, atmosphere and SA were applied in the way described in

Section 6.1. Pseudorange noise of zero mean and standard deviation of 0.2 m was also included in the data in line with the noise level of a modern receiver.

The situation where only single frequency receivers are available is described in Section 6.4.1. This is assuming that both the reference and user stations are occupied by single frequency receivers. Section 6.4.2, on the other hand, presents a case where the reference stations are occupied by dual frequency receivers. In this case, the user station can either be occupied by a single or dual frequency receiver.

6.4.1 Single Frequency Observable

The Nottingham single frequency approach combines tropospheric and ionospheric delays together as a single atmospheric delay and estimates it together with the orbit determination process. Though the combined treatment of the two components, which obviously have different physical properties, has caused some concern. However, the previous tests for the estimation of the satellite orbit and atmospheric errors have shown reasonable results. The effects of the deficiency of this modelling approach on the user positioning accuracy is described in the next section.

The user position accuracy was evaluated by comparing the *true* coordinates (used to simulate the data) with the coordinates obtained by applying the WADGPS error correction models over the one hour period. The orbit was generated from three days of single frequency observations, and the atmospheric zenith delays during the one hour period were optimised to produce a new set of Klobuchar-like parameters. The RMS errors of the user positioning accuracies are given in Table 6.2, showing RMS values of 1.05m, 1.89m and 2.16m for plan, height and total respectively.

Table 6.2 User Position Accuracy of the Single Frequency Case

	Reference Site	User Site	Position Accuracy (rms)	
Atm.	Single Freq. Combined Atmosphere	Single Freq. Optimised Klob.-like Parameters	1.05 m	Plan
			1.89 m	Height
			2.16 m	Total

The user position accuracy obtained from applying the conventional DGPS approach, with user sites ranging from 0.05 to 1,000 km to one of the reference stations (Richmond), were compared with the WADGPS approach. Figure 6.17 shows the comparison of the positioning accuracies between conventional DGPS and WADGPS. It can be seen that the WADGPS approach provides better positioning accuracy than conventional DGPS when the user-reference separation exceeds approximately 250 km and 700 km in plan and height component, respectively.

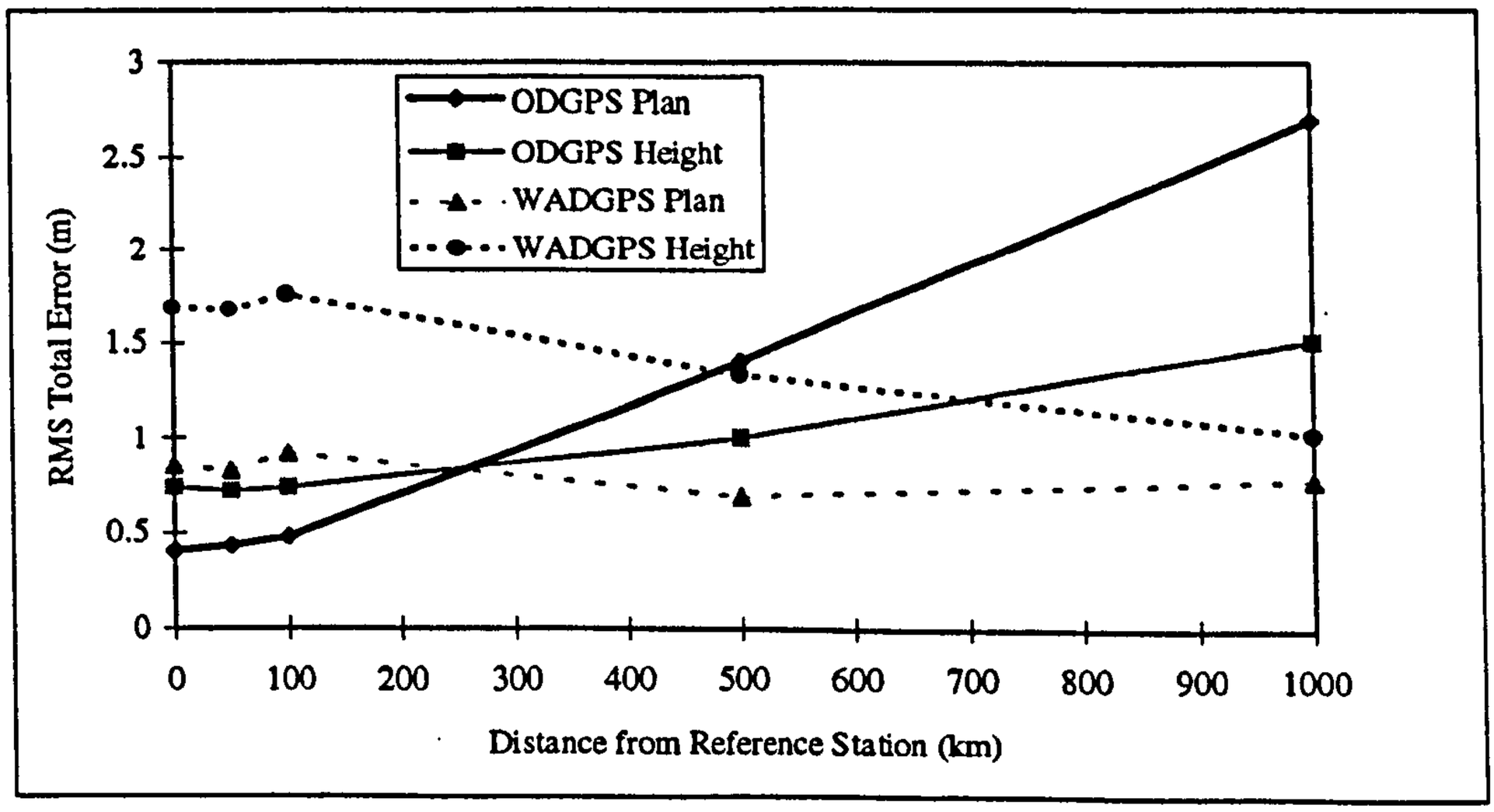

Figure 6.17 WADGPS vs. Conventional (Ordinary) DGPS

6.4.2 Dual Frequency Observable

It has been shown in Section 6.2 that the best recovery of the satellite orbit is produced using the dual frequency observable when the ionospheric and tropospheric delays were separated and modelled individually. The user

positioning accuracy however, is a result of all the error correction models applied in the system interacting with each other. The error sources can be modelled and transmitted in various ways, achieving different user position accuracies. The algorithms proposed for the modelling and transmission of the ionospheric and tropospheric errors and corresponding user position accuracy are discussed in this section.

For the ionospheric error, the dual frequency measurements can be used to model the ionospheric delays for both reference and user stations. From the user's point of view, if only a single frequency receiver is available, the optimised ionospheric model has to be transmitted from the control segment to enable the estimation of the ionospheric delay to be carried out at the user stations. If the user is equipped with a dual frequency receiver, then he has the choice of applying the transmitted ionospheric model or relying on his own ionospherically-free measurements. In this research, the user positions were obtained by assuming the worst case, when the users were only equipped with single frequency receivers.

The tropospheric error can be well recovered using the Magnet model in conjunction with the scale factor technique at the reference stations. The difficulty occurs in how to model and transmit the recovered tropospheric delays for the user. Several approaches have been proposed in Section 6.3.2, and the corresponding user positioning accuracies were investigated and presented here.

The user positioning accuracy was evaluated by comparing the *true* coordinates (used in the data simulation) and the calculated coordinates, obtained from different algorithms. The tests conducted are discussed below from case (a) to case (g), depending on the way that the errors were estimated and modelled.

- **Case (a)**

Ionospheric Error	**Tropospheric Error**
• ionospheric delays generated by the linear combination of dual frequency measurements • optimised by the NSE algorithm • 'new' locally optimised Klobuchar parameters applied to estimate the ionospheric error at both reference and user stations	• neither estimated nor modelled at both reference and user stations

The first test carried out involved the modelling of the ionospheric errors, but ignoring the errors due to the troposphere i.e. treating it as system noise. No attempt was made to model or transmit the tropospheric errors at neither reference nor user sites. The ionospheric delay estimated by the optimised Klobuchar model is applied at the user site. The ionospheric errors at the reference stations may be modelled by two methods, namely the use of ionospherically-free observables, or the optimised ionospheric model. Both methods were tested in this test, while in the following tests, optimised ionospheric model was applied at the reference stations in all cases.

Since the orbit and ionospheric errors are properly recovered, the tropospheric and clock related errors are the main contributors to the pseudorange differential correction to be transmitted to the user. If the tropospheric error is highly correlated between the reference and user site, it should be largely cancelled out after the application of the differential correction. If this is not the case, a poorly determined user positioning accuracy would reveal the necessity of tropospheric modelling. The test conducted here provides an indication of whether the modelling of the tropospheric error should be carried out.

The RMS positioning accuracies achieved are shown in Table 6.3. The RMS plan, height and total positioning accuracies of 1.71 m, 2.61 m and 3.12 m respectively, were achieved. Compared with the single frequency combined atmospheric delay approach described in § 6.4.1 (RMS total error of 2.16 m), it is clear that the treatment of the tropospheric delays as noise gives a worse result. Thus it is better to model the tropospheric error as part of the ionospheric error than treat it as noise. It also points out the fact that in order to achieve higher positioning accuracy, the tropospheric error needs to be modelled properly.

The test of using the ionospherically-free observable for eliminating ionospheric errors at the reference stations was also carried out. The results showed that the use of these two different methods for obtaining ionospheric error corrections, resulted in decimetre level differences in user positioning accuracies. The close agreement of these results indicated that the optimisation process was performing correctly, and the level of the pseudorange noise, 0.2 m (SE), applied in the simulated data, did not corrupt the solutions.

Table 6.3 User Position Accuracy for Case (a)

		Reference Site	User Site	Position Accuracy (RMS)	
(a)	Ion.	D.F.* Optimised Klobuchar Parameters	D.F. Optimised Klobuchar Parameters	1.71 m	Plan
				2.61 m	Height
	Trop.	Not modelled	Not modelled	3.12 m	Total

D.F.* : Dual Frequency

- **Case (b)**

Ionospheric Error	**Tropospheric Error**
• ionospheric delays generated by the linear combination of dual frequency measurements • optimised by NSE algorithm • 'new' locally optimised Klobuchar parameters applied to estimate the ionospheric error at both reference and user stations	• estimated by the Magnet model in conjunction with the scale factor technique • applied at the reference station • neither modelled nor transmitted to the user

In this test, the ionospheric error was recovered in the same way as in **case (a)**. The tropospheric error was estimated as part of the orbit determination process, using the Magnet model in conjunction with the scale factor approach. The estimated tropospheric delays were then applied at the reference station to remove the effects of tropospheric delays. The differential corrections, in the form of the composite clock error, were formed after the ionospheric, tropospheric and orbital errors were modelled and removed. No attempt was made to transmit any form of tropospheric error model to the user. Therefore, the tropospheric error-free differential corrections were applied to the user measurements, which contain tropospheric errors. This was equivalent to treating the tropospheric error as noise at the user stations. As the GPS heighting accuracy is more sensitive to the atmospheric errors than the horizontal component (Shardlow, 1994), it is expected that the height component of the user position would be less well determined.

The RMS positioning accuracy achieved was of the order of 0.64 m, 6.04 m and 6.07 m in plan, height and total error respectively (Table 6.4). The poor height positioning accuracy emphasises the need for accurate tropospheric delay modelling.

Table 6.4 User Position Accuracy for Case (b)

		Reference Site	User Site	Position Accuracy (rms)	
(b)	Ion.	D.F. Optimised Klobuchar Parameters	D.F. Optimised Klobuchar Parameters	0.64 m	Plan
				6.04 m	Height
	Trop.	Scale Factor + Magnet Model	Not modelled	6.07 m	Total

- **Case (c)**

Ionospheric Error	**Tropospheric Error**
• ionospheric delays generated by the linear combination of dual frequency observables • optimised by NSE algorithm • 'new' locally optimised Klobuchar parameters applied to estimate the ionospheric error at both reference and user stations	• estimated by the Magnet model in conjunction with the scale factor technique • applied at reference stations • neither modelled nor transmitted to the user • user data simulated with no tropospheric error included

In the previous test, the tropospheric error was treated as noise at the user station, the result of which was a poor user height position determination. In order to provide a base against which tropospheric error modelling can be compared, user data can be simulated with no tropospheric errors. This would represent a perfect tropospheric error modelling at the user station. Therefore, this test would clearly indicate the importance of tropospheric modelling and set the best possible user position accuracy of the designed WADGPS system, with regards to tropospheric error modelling.

It should be mentioned that the data at the reference station still contains all error sources including the tropospheric delays. The error components were all catered for as for **case (b)**.

The RMS position accuracy achieved was of the order of 0.35 m, 0.73 m and 0.81 m for the horizontal, vertical and total errors respectively (Table 6.5). Compared with case (b), the position accuracy in every component is improved significantly, especially the height component.

Although, the situation simulated in this test would not happen in practice, where the tropospheric errors would be present in all measurements, valuable conclusions can still be drawn from the results. The main conclusion from this test is that if the tropospheric errors were modelled correctly, the WADGPS positioning accuracy can be improved significantly.

Table 6.5 User Position Accuracy for Case (c)

		Reference Site	User Site	Position Accuracy (rms)	
(c)	Ion.	D.F. Optimised Klobuchar Parameters	D.F. Optimised Klobuchar Parameters	0.35 m	Plan
				0.73 m	Height
	Trop.	Scale Factor + Magnet Model	Not Modelled, No Trop. Error	0.81 m	Total

- **Case (d)**

Ionospheric Error	**Tropospheric Error**
• ionospheric delays generated by the linear combination of dual frequency observables • optimised by NSE algorithm • 'new' locally optimised Klobuchar parameters applied to estimate the ionospheric error at both reference and user stations	• estimated by the Magnet model in conjunction with the scale factor technique • fitted into a Klobuchar-like model to form a regional best fit tropospheric model • applied at both reference and user stations

In this test, the data included all the system errors. Efforts were made to recover the tropospheric error at both the reference and user sites using a similar approach to that of the ionosphere (i.e. generating a new set of optimised Klobuchar-like parameters). The estimated tropospheric error was optimised by an NSE algorithm, resulting in a 'new' set of Klobuchar-like tropospheric parameters. The fit of the tropospheric error to the tropospheric style Klobuchar model is presented in § 6.3.2, **case (c)**.

The locally generated Klobuchar-like parameters for the tropospheric error modelling, were employed to estimate the tropospheric errors at both the reference and user stations. The user therefore received two sets of Klobuchar-like parameters, one set for the ionospheric and the other set for the tropospheric errors. The ionospheric and tropospheric parameters were applied at the user station, to estimate the respective ionospheric and tropospheric errors.

The RMS position accuracy achieved was of the order of 0.91 m, 1.91 m and 2.13 m for plan, height and total error respectively (Table 6.6). This accuracy is very similar to that from the single frequency combined atmospheric delays approach where corresponding values of 1.05 m, 1.89 m and 2.16 m were obtained (§ 6.4.1). This agreement in the position accuracy determination indicates that the atmospheric error is the main cause of the degradation of the position accuracy in the proposed WADGPS system. Hence, further research was concentrated on the tropospheric delay modelling.

Table 6.6 User Position Accuracy for Case (d)

		Reference Site	User Site	Position Accuracy (rms)	
(d)	Ion.	D.F. Optimised Klobuchar Parameters	D.F. Optimised Klobuchar Parameters	0.91 m	Plan
				1.91 m	Height
	Trop.	Optimised Klobuchar-like Trop. Para.	Optimised Klobuchar-like Trop. Para.	2.13 m	Total

- **Case (e)**

Ionospheric Error	**Tropospheric Error**
• ionospheric delays generated by the linear combination of dual frequency observables • optimised by NSE algorithm • 'new' locally optimised Klobuchar parameters applied to estimate the ionospheric error at both reference and user stations	• estimated by the Magnet model in conjunction with the scale factor technique • applied at reference stations • fitted into a Klobuchar-like model to form a regional best fit tropospheric model • parameters transmitted to users to apply

The ionospheric error was treated in the same manner as for **case (a)**, in which dual frequency measurements were applied to estimate and model the ionospheric delays. The tropospheric errors were estimated and modelled in the same way as is in **case (d)**. However, the tropospheric parameters were only applied at the user station, but not the reference site. The reference stations applied their own tropospheric delays, estimated by the scale factor technique during the orbit determination process. Therefore the differential corrections transmitted to the user were derived without introducing the errors from the modelling process. However, the user received the Klobuchar-like tropospheric error model from the control segment, to estimate the local tropospheric errors.

The RMS user position accuracy achieved was of the order of 0.58 m, 2.72 m and 2.79 m for plan, height and total error components respectively (Table 6.7). The results show some discrepancies with the previous test, in which both the reference and user sites used the same tropospheric model. The previous test benefited from the application of the same model at both the reference and user sites, which enabled the errors due to the deficiency in the tropospheric model to behave in a similar manner. The residuals left were

channelled into the differential correction, which was more likely to be partly cancelled out at the user site. In this test, though the reference stations correctly recovered the tropospheric delays (decimetre level), but the user employed a modified tropospheric error correction model, which weakened the differential effect. The slightly worse height determination accuracy again indicates the importance of the atmospheric modelling.

Table 6.7 User Position Accuracy for Case (e)

		Reference Site	User Site	Position Accuracy (rms)	
(e)	Ion.	D.F. Optimised Klobuchar Parameters	D.F. Optimised Klobuchar Parameters	0.58 m	Plan
				2.72 m	Height
	Trop.	Scale Factor + Magnet Model	Optimised Klobuchar-like Trop. Para.	2.79 m	Total

- **Case (f)**

Ionospheric Error	**Tropospheric Error**
• estimated by the linear combination of dual frequency measurements	• estimated by the Magnet model in conjunction with the scale factor technique

This test was designed to take advantage of the dual frequency measurements in estimating the ionospheric and tropospheric errors separately at the reference stations, but combined them together to transmit only one atmospheric error correction model for the single frequency user.

The ionospheric and tropospheric delays were estimated separately, i.e. dual frequency linear combination for the ionospheric delays and the Magnet model with scale factor approach for tropospheric delays. These two delays were mapped from the zenith values by appropriate mapping functions and then

combined together to form a single 'atmospheric delay'. These atmospheric delays were then optimised by an NSE algorithm to form Klobuchar-like parameters to produce a 'new' set of atmospheric parameters. These parameters were then applied at both the reference and user stations to estimate the atmospheric delays

The difference between the tests conducted here and the single frequency combined case (§ 6.4.1) was in the way that the combined atmospheric delays were estimated. In the single frequency combined atmospheric delay case, the atmospheric (ionospheric and tropospheric) delay was estimated as a discrete value by the scale factor technique as part of orbit determination process. However in this case, the ionospheric and tropospheric delays were estimated separately and combined afterwards.

The effects of using different mapping functions have been shown in § 6.3.1, Figure 6.13. The RMS user position accuracy, employing the tropospheric mapping function, was of the order of 0.87 m, 3.36 m, and 3.47m for plan, height and total error components respectively (Table 6.8). The reason behind the better estimation of the atmospheric delay but poor user position accuracy is likely due to the mapping function. Since both of the individual error components were correctly estimated and combined, the use of one mapping function for the aggregated delays cannot generate accurate overall slant delays. The slant values of the combined atmospheric delays would either be over-estimated (using the tropospheric mapping function) or be under-estimated (using the ionospheric mapping function).

Table 6.8 User Position Accuracy for Case (f)

		Reference Site	User Site	Position Accuracy (rms)	
(f)	Atm.	Dual Frequency Combined Atmosphere	D.F. Optimised Klobuchar.-like Parameters	0.87 m	Plan
				3.36 m	Height
				3.47 m	Total

The RMS of the position accuracy, employing the ionospheric mapping function, was of the order of 1.42 m, 1.76 m and 2.26 m for plan, height and total error components, respectively (Table 6.9). The total user position accuracy was better than that when using the tropospheric mapping function. The explanation for this is that the slant ionospheric delays, generated using the ionospheric mapping function, generally contributes more to the total atmospheric delays than the slant tropospheric delays.

Table 6.9 User Position Accuracy for Case (g)

		Reference Site	User Site	Position Accuracy (rms)	
(g)	Atm.	Dual Frequency Combined Atmosphere	D.F. Optimised Klobuchar-like Parameters	1.42 m	Plan
				1.76 m	Height
				2.26 m	Total

There are several other possible candidates for the modelling and transmission of the tropospheric delays at either the reference or user stations. The model can be some kind of three-dimensional polynomial fitted to the reference network tropospheric delays. The coefficients are then sent to the user for the estimation of the local tropospheric delay. As the dry part of the troposphere is responsible for about 90% of the delay, the user and/or the reference station may apply a standard tropospheric model to estimate the tropospheric delay. It is also possible for the reference station and/or user to measure the meteorological data to apply a more sophisticated model. However, it would not be effective to test such tropospheric modelling against the simulated data.

Enormous knowledge has been gathered from the above simulation tests. Hence an optimal WADGPS system design, taking into account the effects of the individual error components, has been developed. However, the simulation tests has to be accessed using real data to validate the overall system performance. Furthermore the single frequency *ionospheric scale factor* approach, not tested in the simulation studies, also has to be assessed using real data. Therefore the next chapter is dedicated to real data field tests.

Chapter 7

Field Test Results

The feasibility of the proposed WADGPS technique has been investigated and demonstrated by the simulation studies detailed in Chapter 6. The WADGPS algorithms have been shown to be powerful and sensitive to the system errors and hence can be used to recover and model the errors. This resulted in a very high user positioning accuracy. However, it is essential that the real field data is introduced to thoroughly test the effectiveness of the error models. The power and sensitivity of the algorithms, and the performance of the system, could then be assessed under operational condition.

The major disadvantage of using real data to analyse the proposed algorithms is the lack of precise knowledge of the *truth*. As a consequence, some other estimates which also have errors in them, have to be treated as the *truth*, to assess the accuracies of the recovery of individual errors and the final positions. The precise ephemerides provided by IGS, accurate to about 1 to 2 m, were used to evaluate the recovered satellite orbits. The ionospheric delays estimated using the dual frequency pseudorange measurements were compared to the recovered ionospheric delays. However, the pseudorange noise greatly reduces the accuracy and reliability of these values. The coordinates of the reference and user stations, which are part of the reference network used in the Racal SkyFix system, were provided by Racal Survey Ltd., to be treated as the *true* positions.

As with the simulation studies, three approaches were investigated,

- The dual frequency approach
- The single frequency combined atmospheric delays approach
- The refined *single frequency ionospheric scale factor approach*

The dual frequency approach applies dual frequency receivers at the reference stations, while allowing the user to be equipped with either single or dual frequency receiver. The ionospherically-free observable is used for the orbit determination and the estimation of the tropospheric delays at the reference stations. The ionospheric delays estimated from the dual frequency measurements are fitted to the Klobuchar model, to provide a new set of optimised ionospheric parameters to be transmitted to the single frequency users. The single frequency user applies the tropospheric delays estimated by the Magnet model, the ionospheric delays estimated by the optimised Klobuchar-like parameters, the differential corrections and the improved satellite ephemerides for positioning. The dual frequency user may have the choice of applying the ionospherically-free observable or the optimised ionospheric model, transmitted from the control centre. However, the tests mainly concentrated on algorithm design for the single frequency receiver users. Nevertheless, the user positioning accuracy determined by using dual frequency observables at both reference and user sites is also presented.

The single frequency combined atmospheric approach employs single frequency receivers throughout the system. The ionospheric and tropospheric errors are combined together as a single parameter to be estimated as part of the orbit determination process. The atmospheric delays are then fitted to a modified Klobuchar-like model, to generate a locally best fitting atmospheric model for the computation of the differential corrections, and onward transmission to the users. The user then applies the atmospheric model, the differential corrections and the improved satellite ephemerides for positioning.

The refined single frequency *ionospheric scale factor* approach also makes use of single frequency receivers throughout the system. The tropospheric delays at the reference stations are estimated using the Magnet model. The ionospheric delays are estimated by solving for local scale factor as extra unknowns in the orbit determination process of a least squares adjustment, using the broadcast Klobuchar parameter estimated delays as the initial approximate values. The estimated ionospheric delays are then fitted to a Klobuchar model by the NSE algorithm, to generate a locally best fitting ionospheric model, for application at both reference and user stations. The user applies the tropospheric delays estimated by the Magnet model, the ionospheric delays estimated by the optimised Klobuchar-like parameters, the differential corrections and the improved satellite ephemerides for positioning.

The refined single frequency *ionospheric scale factor* approach could not be effectively tested using simulation data. For instance, no conclusion could be drawn from simulation tests involving the use of similar models for simulating and recovering the tropospheric delays. In this case, the use of real data was the only way to obtain realistic and practical results.

In this chapter, the description of the real field data set is given in Section 7.1, followed by the analysis of the recovery of the individual errors for each of the three proposed WADGPS approaches in Sections 7.2 and 7.3. The WADGPS user positioning accuracies are analysed and presented in Section 7.4. The user positioning accuracies obtained from conventional DGPS and multi-station DGPS are detailed in Section 7.5.

7.1 The Field Data

The real data used in this project were kindly provided by Racal Survey Ltd. Data from four sites used for the Racal SkyFix system, Aberdeen, Cadiz, Cyprus and Hammerfest, were collected using Trimble 4000 SSE GPS receivers from May 3 to May 5, 1993. Data were logged at 1 second intervals

for the L1 C/A code pseudorange, L2 (Y2-Y1 cross-correlation + C/A) code pseudoranges, L1 phase and L2 phase. The configuration of the network stations is shown in Figure 7.1. Aberdeen was treated as the user station to assess the positioning accuracy. The baselines between the user (Aberdeen) and the reference stations range from about 2,000 km to 3,500 km.

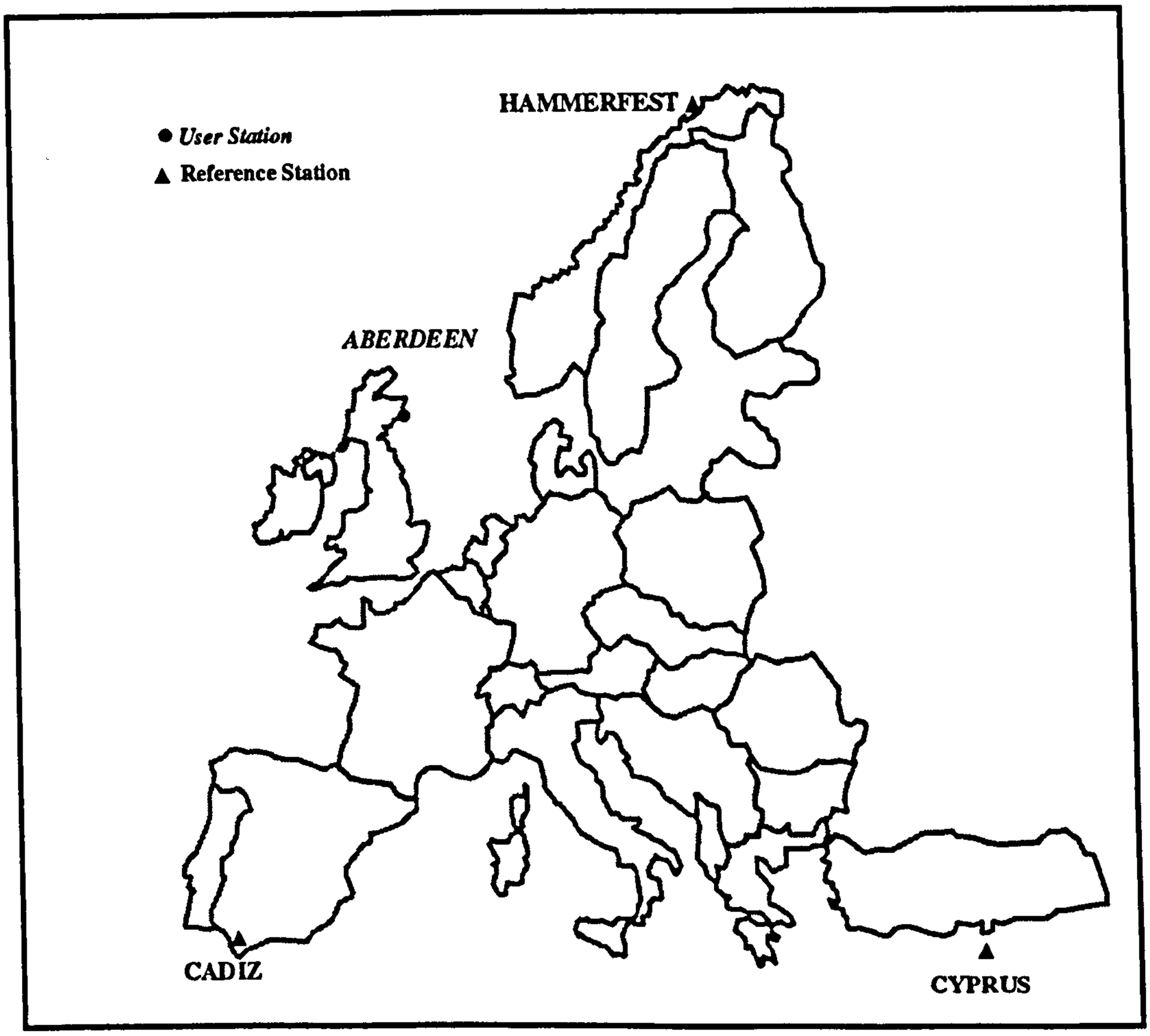

Figure 7.1 Reference Network Configuration

The Trimble 4000 SSE receiver provides the L1 C/A and L2 cross-correlation codes which both have a double difference measurement noise of the level of 0.3 to 0.7 metre (Chao, 1993). This noise level agrees with the pseudorange noise investigated in the simulation studies. From error propagation, the noise level of the double difference dual frequency ionospherically-free observable could be expected to be of the order of 1 to 2 m.

7.2 Recovery of the Satellite Orbit

The satellite orbit was estimated by the full dynamic orbit determination process, in conjunction with the fiducial network concept, using the double difference pseudorange observable. Apart from the type of observable, the satellite orbit accuracy depends on the number and spread of the reference stations as well as the span of data. The sampling interval of the discrete atmospheric propagation zenith delay was set at 90 minutes, based on the experience gained from the simulation studies.

Since field data from only four stations around Europe were available, the tests on satellite orbit recovery were first investigated by using data from all four stations, to evaluate the best possible accuracy. This was followed by excluding data from Aberdeen, which was treated as the user station, in order to investigate the user position accuracy. Data spanning 72 hours were used in the orbit determination process.

The recovery of the satellite orbit was assessed by comparing the recovered orbit with the IGS precise ephemeris. Although the reference network roughly covers the European region, it is still a relatively small portion of the world. The orbit determined using this network should be more accurate over Europe, where tracking data was available, than other areas of the world. Therefore, the comparison should be carried out for only those portions of the arc actually passing over Europe. Hence, a threshold is introduced to the orbit comparison by cutting off the orbit that had not been observed by any of the reference stations. The comparison of the discrete satellite positions over the entire orbit is referred to as 'global comparison'. The restricted comparison over those positions that have been observed by at least one of the reference stations is referred to as 'European comparison'. The satellite orbit recovered by the single frequency combined atmospheric delay, the dual frequency and the refined single frequency *ionospheric scale factor* approaches are presented in the following sections.

7.2.1 Single Frequency Combined Atmospheric Delay Approach

The observable applied for the orbit determination in the single frequency combined atmospheric delay approach was the double difference raw L1 C/A code pseudorange. The tropospheric and ionospheric delays were combined together and estimated every 90 minutes as part of the orbit determination in a least squares process. The recovery of the satellite orbit error, compared with the IGS precise ephemeris, is shown in Figure 7.2, for the orbit recovered by three reference stations. The results for the orbit recovered using four reference stations can be found in Appendix C, Figure C.1.

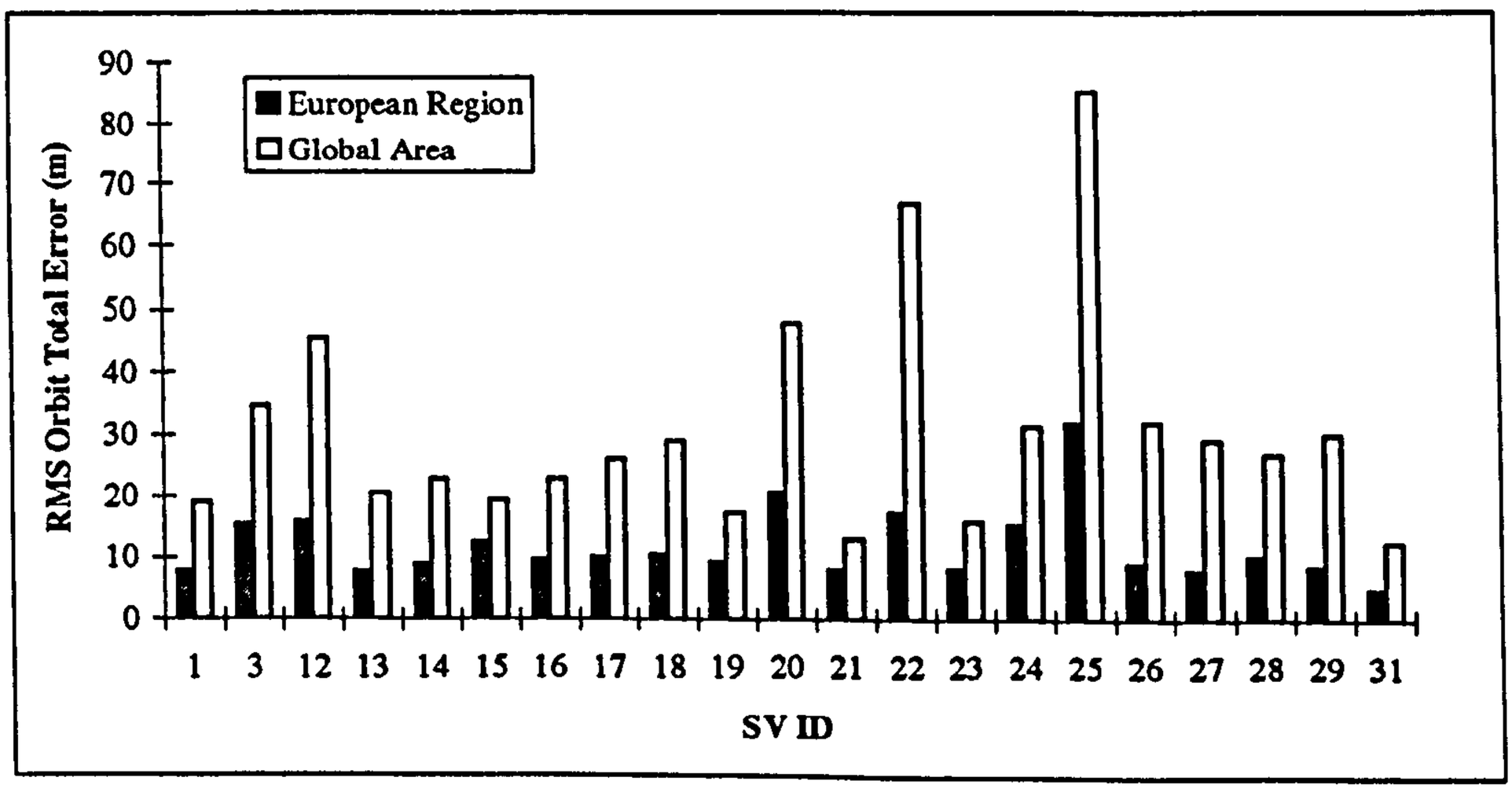

Figure 7.2 Satellite Orbit Recovery using 3 Reference Stations (Single Frequency Combined Atmospheric Delay Approach)

The mean, best and worst RMS satellite orbit errors are listed in Table 7.1, for the three and four reference stations cases respectively. Satellite orbit accuracies of the order of 12 m and 9 m from the use of three and four reference stations respectively, were achieved for the European region.

Table 7.1 Orbit Recovery by the Single Frequency Approach

RMS (m)	Europe		Globe	
	3 stations	4 stations	3 stations	4 stations
Mean	12.0	9.2	30.9	23.6
Best	5.1	3.5	12.6	7.0
Worst	32.0	17.7	85.3	55.2

It can be seen from Table 7.1 that the orbits recovered from using 4 reference stations are better than 3 reference stations due to the geometrical strength of the reference network. The significant difference between the orbits recovered for the 'European' and 'global' area indicate that the reference network is not large enough to provide accurate orbits world-wide. It is vital to have tracking stations uniformly spread across the globe in order to obtain consistently high accuracies. Though results show that the satellite orbit accuracies were higher in the European region than the global area, this was adequate since the system is designed to cater for users within or close to the reference network.

The validity of the satellite orbit predicted from the satellite initial state vectors depends on the force model applied in the orbit integration approach. Thus the accuracy of the satellite orbit degrades gradually with time from the initial starting point. Figure 7.3 shows the orbit error, compared with IGS precise ephemeris, for one of the satellites in radial, cross track and along track components over a three day period. The along track component diverges much quicker than the other two components which is due to the difficulty of modelling the satellite velocity. The radial components of the satellite orbit, which can be treated as part of the satellite clock error, diverges in a slower gradient than the other two components.

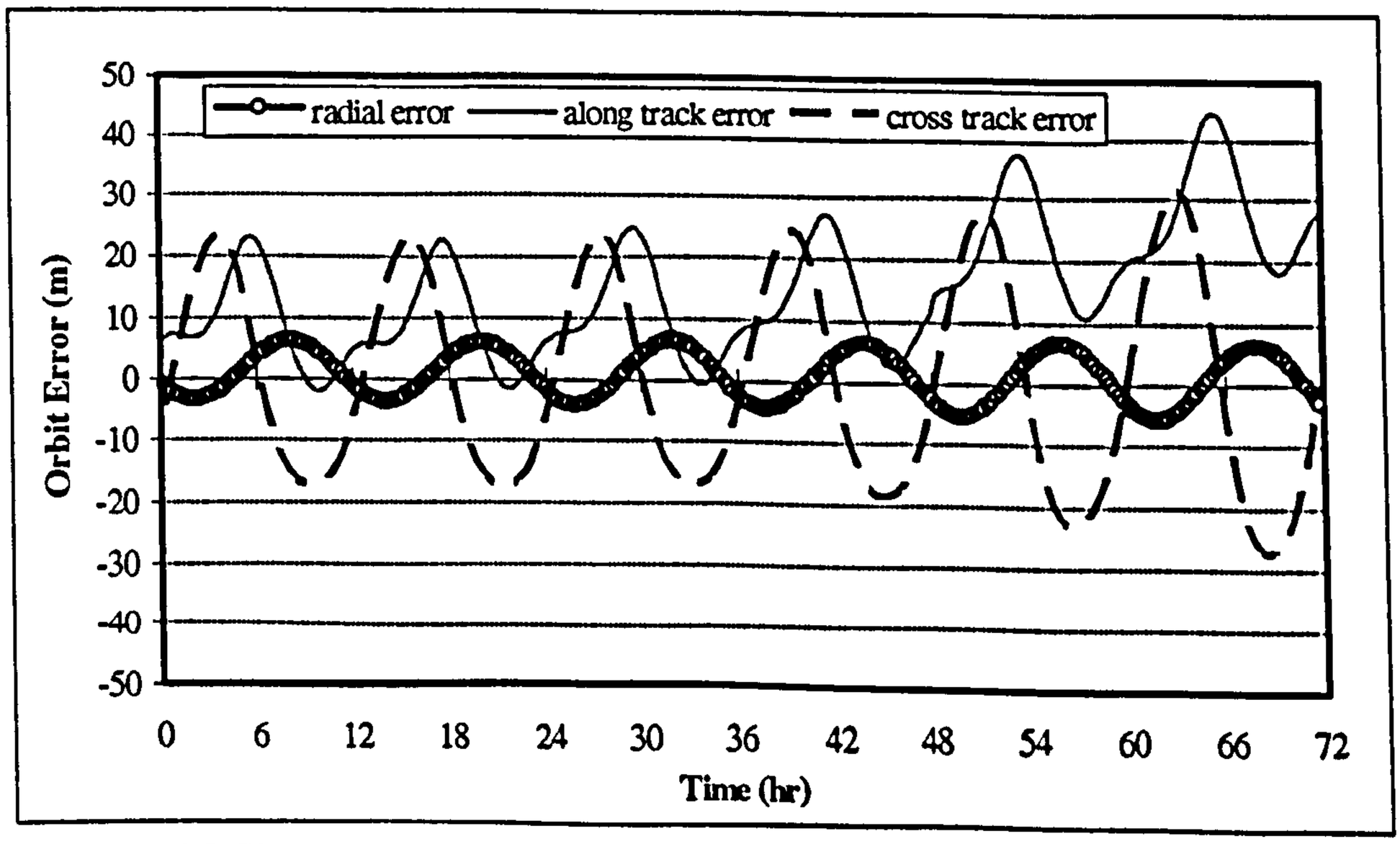

Figure 7.3 Single Frequency Approach Individual Orbit Error vs. Time

7.2.2 Dual Frequency Approach

The second approach tested involved the use of dual frequency pseudorange measurements. Results of the satellite orbit recovered using the dual frequency ionospherically-free observable are presented in Table 7.2. The recoveries of the individual satellite orbits obtained using three reference stations are shown in Figure 7.4 The recovery of the satellite orbit obtained using four reference stations can be found in Appendix C, Figure C.2. Satellite orbit accuracies of the order of 10 m and 5 m from using three and four reference stations respectively were achieved for the European region. This represents an improvement in accuracy compared with the results from the single frequency combined atmospheric delay approach.

Table 7.2 Orbit Recovery by Dual Frequency Approach

RMS (m)	Europe		Globe	
	3 stations	4 stations	3 stations	4 stations
Mean	10.0	5.1	25.9	13.3
Best	2.0	1.6	14.9	3.3
Worst	18.6	9.0	39.1	28.1

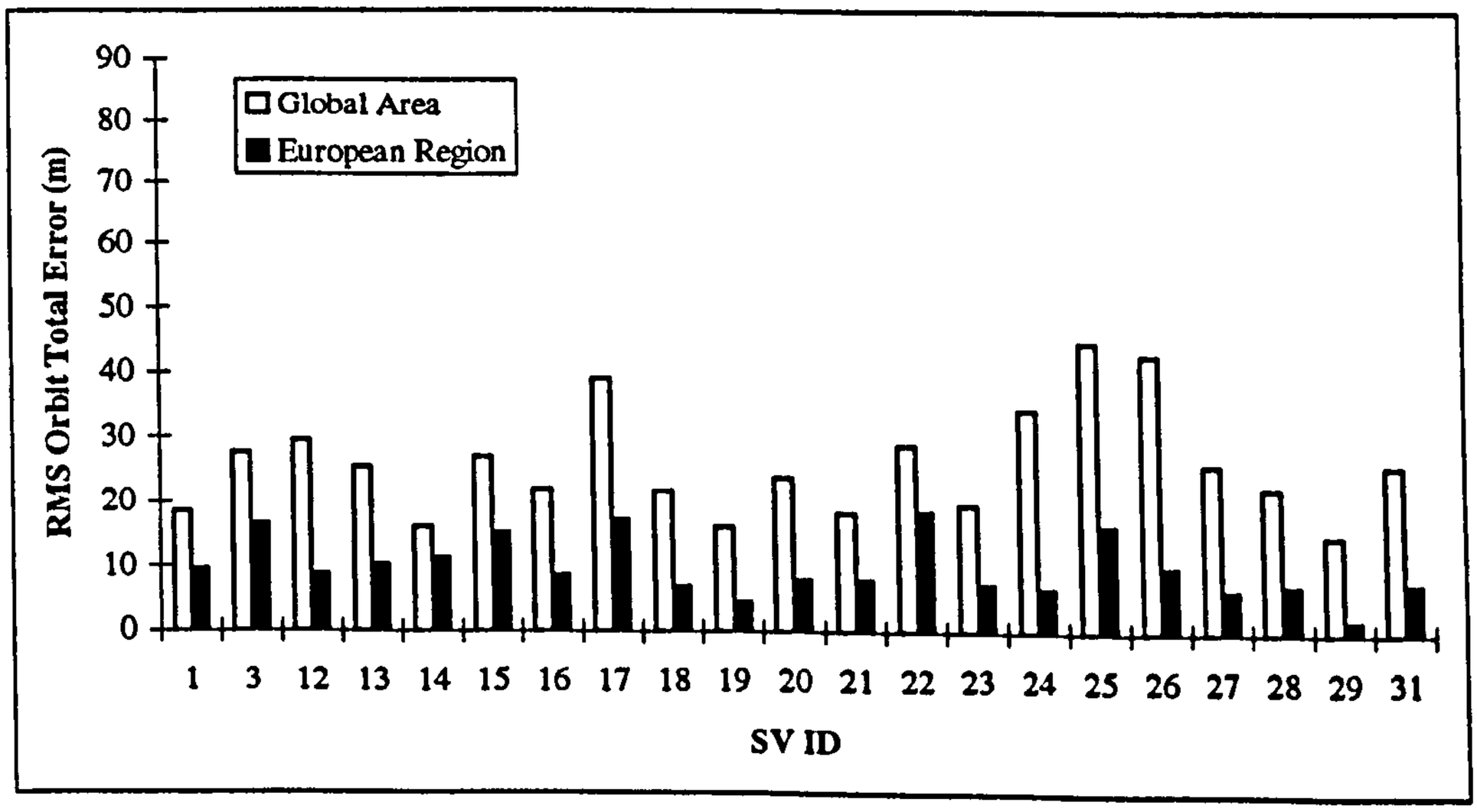

Figure 7.4 Dual Frequency Observable Satellite Orbit Accuracy

The predicted satellite orbits also degrade as the validity of the force models decreases with time. The effects of the accuracy degradation are shown in

Figure 7.5, by the mean RMS of the total orbit errors for both 'European' and 'global' comparisons. The errors of the individual components are very similar in pattern and magnitude as those from the single frequency approach, which can be found in Appendix C, Figure C.3

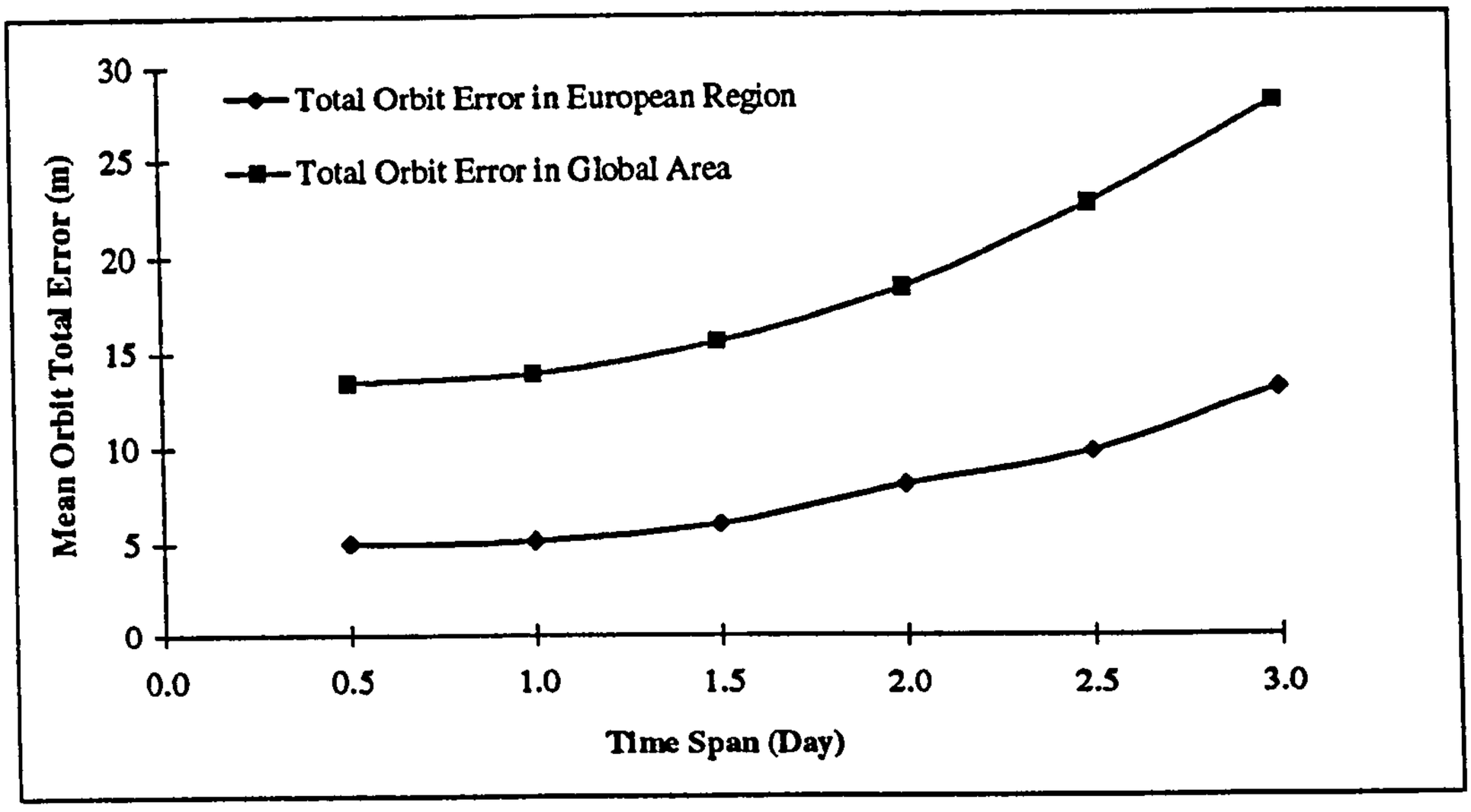

Figure 7.5 Orbit Accuracy vs. Time by Dual Frequency Approach

7.2.3 Refined Single Frequency Ionospheric Scale Factor Approach

The observable applied in estimating the satellite orbit for the refined single frequency *ionospheric scale factor* approach was the double difference L1 C/A code pseudorange. The difference between the single frequency combined atmospheric delay approach and the refined single frequency *ionospheric scale factor* approach occurred in the modelling of the atmospheric errors. In the single frequency combined atmospheric delay approach, the tropospheric and ionospheric errors were combined and estimated as one single delay per station at 90 minute intervals. The refined single frequency *ionospheric scale factor* approach estimated the tropospheric delays using the Magnet model. The ionospheric delays were then left to be estimated by solving for local scale factor as extra unknowns in the orbit determination process. The broadcast Klobuchar parameter estimated delays are used as the initial approximate values of a least squares adjustment.

The results of the satellite orbit generated using the refined single frequency *ionospheric scale factor approach* are listed in Table 7.3 for the three and four reference station cases. The individual RMS errors of the satellite orbit obtained from using three reference stations are shown in Figure 7.6. The results of those obtained from four reference stations can be found in Appendix C, Figure C.4. Satellite orbit accuracies of the order of 9 m from the use of both three and four reference stations were achieved for the European region.

Table 7.3 Orbit Recovery by Refined Single Frequency Approach

RMS (m)	Europe		Globe	
	3 stations	4 stations	3 stations	4 stations
Mean	9.3	8.6	25.4	22.5
Best	4.8	2.7	8.3	6.9
Worst	18.9	17.7	68.6	51.8

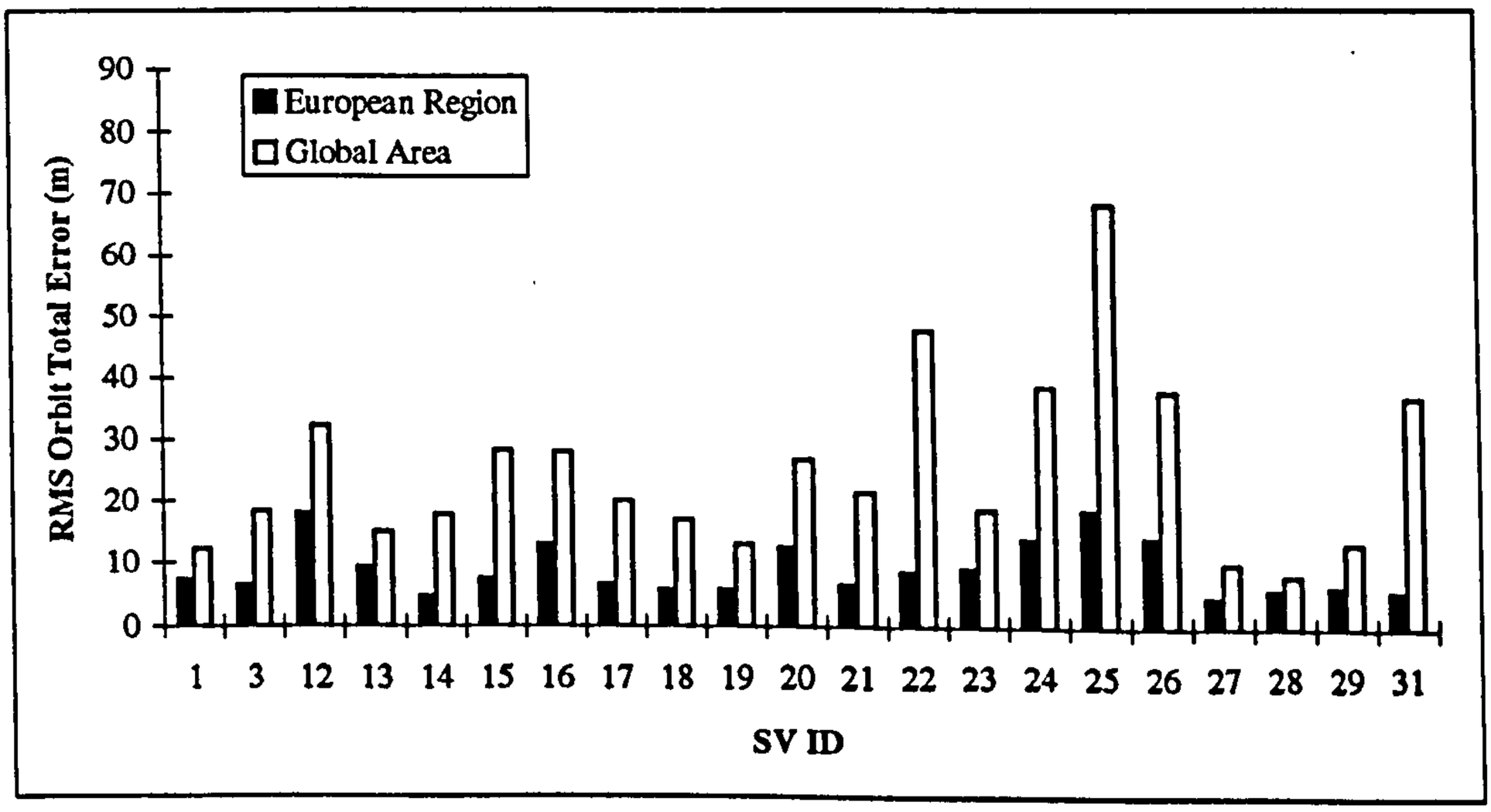

Figure 7.6 Recovery of Satellite Orbit by Refined Single Freq. Approach

From the results above , it can be concluded that the dual frequency approach, using the ionospherically-free observable, generates the best orbit accuracy in the European area (5m and 10m orbit accuracies from the use of four and three reference stations respectively). The problem imposed by the increased noise level is partly solved by averaging over long periods. The satellite orbit

accuracy provided from the refined *ionospheric scale factor* approach (9 m orbit accuracies from the use of both four and three reference stations respectively) was slightly better than the single frequency combined atmospheric approach (9 m and 12 m orbit accuracies from the use of four and three reference stations respectively).

7.3 Atmospheric Delay Estimation

7.3.1 Single Frequency Combined Atmospheric Delays Approach

The proposed single frequency combined atmospheric delay approach, as the name suggests, combined the ionospheric and tropospheric delay together as a single atmospheric delay, estimated at 90 minute intervals as part of the orbit determination process. The *true* atmospheric delay is not available due to the unavailability of meteorological data to estimate the tropospheric delays. Therefore the assessment of the estimation of the atmospheric delays is described in the next section, along with the dual frequency approach.

7.3.2 Dual Frequency Approach

The ionospheric delays estimated using the dual frequency measurements were fitted to the Klobuchar model by the NSE algorithm, to generate a locally best fitting Klobuchar-like ionospheric model. The analysis of the fit of the ionospheric delays to the Klobuchar model by the NSE algorithm at the reference stations had been studied by simulation. However, this test had to be verified using real data. The reason for this test was that in the simulation studies, the ionospheric delays were estimated by the use of the Klobuchar model and then optimised by the NSE algorithm. Therefore, this technique would fail if the real ionospheric delays did not behave in a similar manner to the Klobuchar model estimated delays. Hence the ionospheric zenith delays estimated by the optimised Klobuchar-like parameters at one of the reference stations, Cadiz, were compared with the *truth* provided by the dual frequency

measurements. Figure 7.7 shows the fit of the model against the *truth* for all satellites in view. It can be seen that the model fits the delays reasonably well, the mean error of the zenith delays being of the order of 0.7 m.

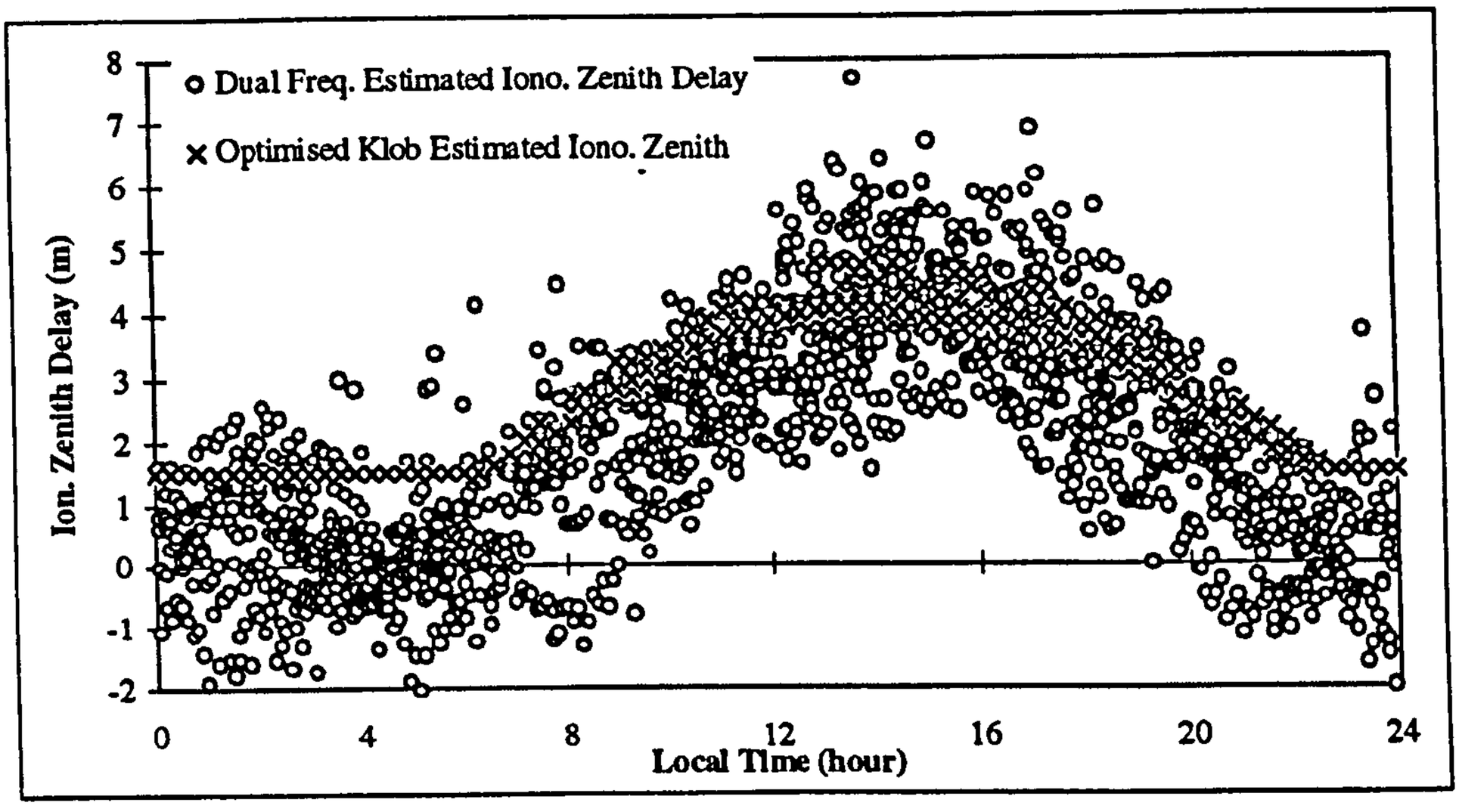

Figure 7.7 Ionospheric Delay Model vs. *Truth*, Reference Site : Cadiz

Problems were observed for the night-time period, which was constrained by the night-time constant assumed in the Klobuchar model. The modelling of the ionospheric delays was affected by the pseudorange noise and the receiver interchannel bias, resulting in the *true* ionospheric delay scatter being widely distributed within a band of several metres. As a consequence, some unrealistic negative ionospheric delays were estimated during the night-time, when the ionospheric activities were generally quieter. The mean errors of the recovered ionospheric zenith delays at reference stations were of the order of 0.7 to 0.9 m.

The recovery of the ionospheric delays at the user site were assessed by comparing the delays estimated using the optimised Klobuchar-like parameters, with the dual frequency *truth* model. The recoveries of the ionospheric delays are shown graphically in Figure 7.8. The results show that the optimised parameters were capable of estimating the ionospheric delays at the user stations. The mean error of recovered ionospheric zenith errors was of the order of 1.3 m.

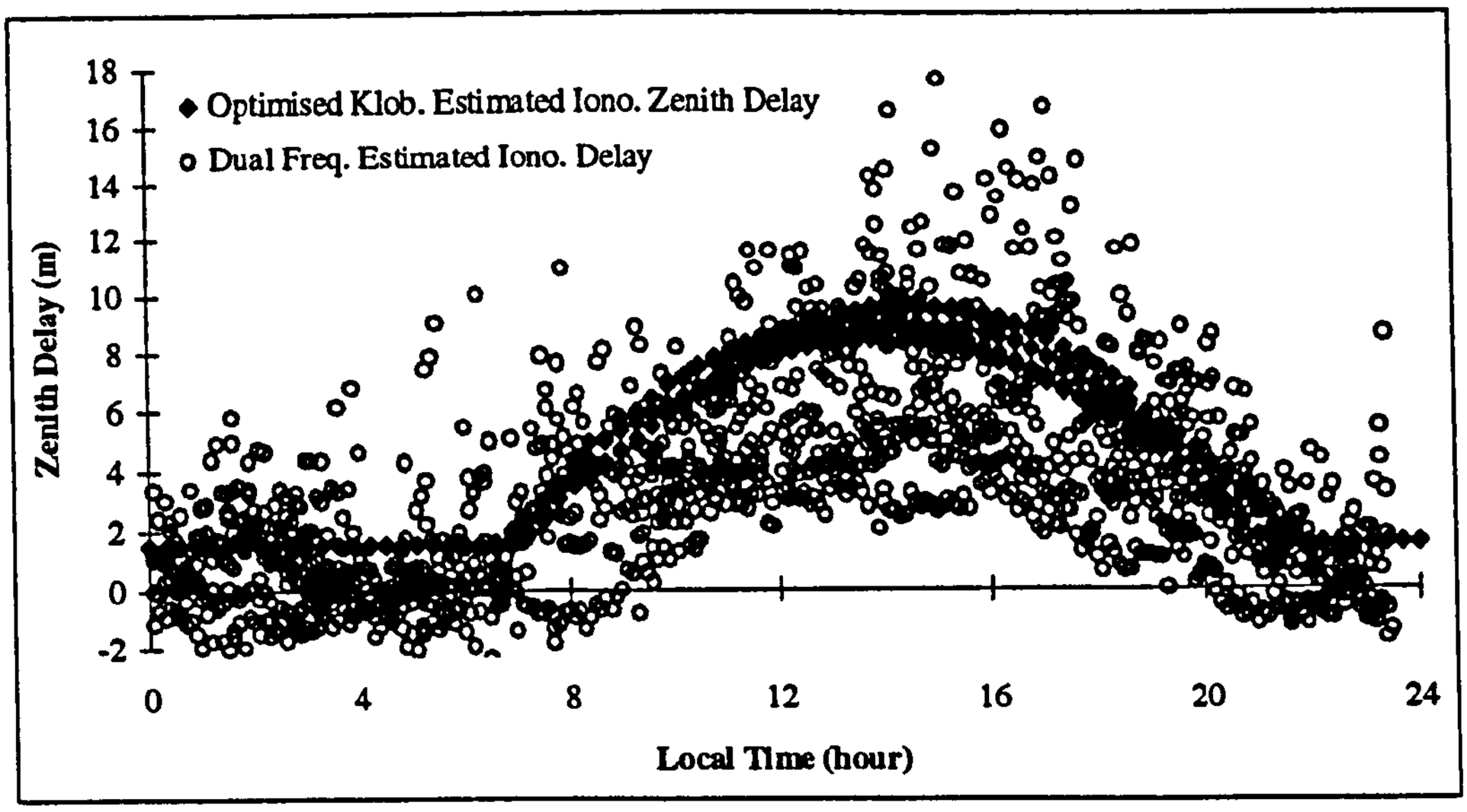

Figure 7.8 Ionospheric Delay Model vs. *Truth*, User Site : Aberdeen

Since, in this case, the ionospheric delays were removed by the use of dual frequency measurements, the errors remaining after the double differencing process were the tropospheric and residual errors. The tropospheric delays were estimated using local scale factors, together with the Magnet model, as part of the orbit determination process. There was no *truth* model available to assess the accuracy of the tropospheric delays. However, the tropospheric delays estimated by this technique were compared with the single frequency combined atmospheric delay approach.

The atmospheric delays estimated by the single frequency combined atmospheric delay approach, contained both ionospheric and tropospheric contributions. If the tropospheric delays from the dual frequency approach were subtracted from the discrete atmospheric delays from the single frequency approach, the remainder should represent the ionospheric delays plus the errors introduced by the modified atmospheric model (§ 4.7.1). The tropospheric delays estimated by the scale factor technique and the combined atmospheric delays estimated from the single frequency combined atmospheric delay approach, are shown in Figure 7.9 for a 72 hour period. The differences between these two delays are also presented in the same figure. The diurnal

pattern of the continuous line in Figure 7.9, which has a peak at about 14:00 local time every day, strongly suggests the behaviour of ionospheric delay.

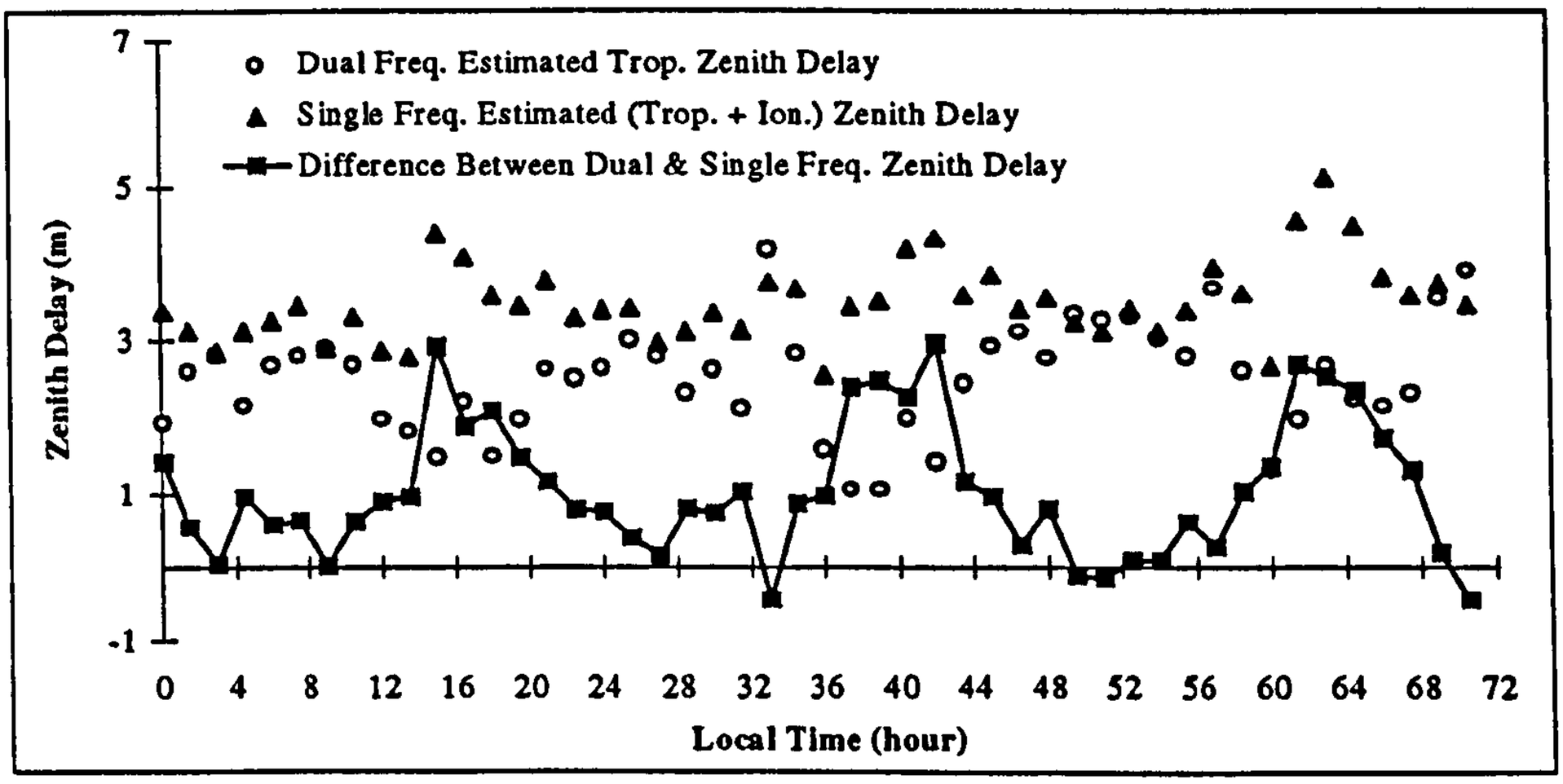

Figure 7.9 Atmospheric Zenith Delays

The values represented by the squares in Figure 7.9, referred to as 'pseudo-ionospheric zenith delays' were superimposed on the ionospheric *truth* model for the first 24 hours and shown in Figure 7.10. The ionospheric delays, estimated by the broadcast Klobuchar parameters and the optimised dual frequency Klobuchar-like parameters, are also shown in Figure 7.10.

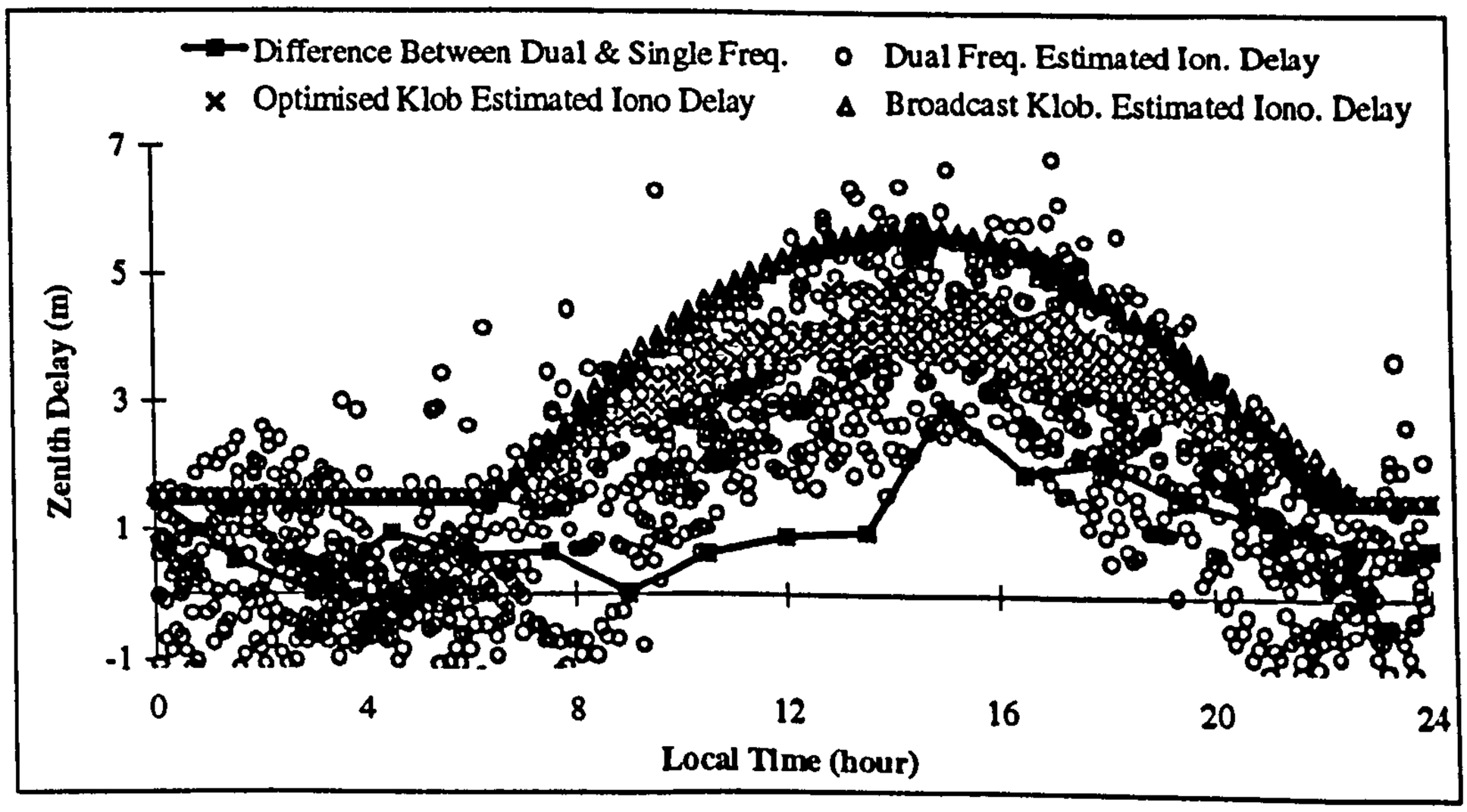

Figure 7.10 Ionospheric Zenith Delays

The results show that the 'pseudo-ionospheric zenith delays' have a pattern close to the *truth* model but were always under-estimated. This can be explained using the results obtained in the simulation studies. As described in Section 4.7.1, the tropospheric mapping function was applied in the single frequency combined atmospheric approach. The tropospheric mapping function generated a much higher slant value than the ionospheric mapping function, if applied to the same zenith delay. Therefore the under-estimated 'pseudo-ionospheric zenith delays' were the result of the tropospheric mapping function. However, the slant value should be compensated by the tropospheric mapping function.

The ionospheric zenith delays estimated by the broadcast Klobuchar parameters represented the worst fit to the *truth* model. The mean error of the ionospheric delays estimated by the broadcast Klobuchar parameters was of the order of 2.2 m, much worse than those obtained from the dual frequency approach (0.7 to 0.9 m)

The pattern of the 'pseudo-ionospheric zenith delays' implicitly demonstrated the successful estimation of the tropospheric delays using the local scale factor technique. This was because only if the tropospheric delays were estimated properly and removed from the combined atmospheric delays, then the remaining errors should behave as ionospheric delays. The next question was then whether it was possible to employ the scale factor technique to estimate the ionospheric delays in a similar manner to the tropospheric delays. This is described in the following section.

7.3.3 Refined Single Frequency Ionospheric Scale Factor Approach

The *single frequency ionospheric scale factor approach* used a similar idea to the tropospheric estimation employed in the dual frequency approach, but was modified to apply scale factors together with the broadcast Klobuchar model. The meteorological data required for the estimation of the tropospheric delays

were not available for this project. Therefore an alternative empirical tropospheric model, which did not require meteorological data to estimate the delays, was employed in this test. This empirical Magnet model, which does not account for the wet part of the tropospheric delay, degrades the recovery of the tropospheric zenith delays at the level of 20 cm (Shardlow, 1994).

In order to assess the accuracy of the ionospheric delays estimated by the *ionospheric scale factor* technique, the *truth* model needed to be re-defined. The ionospheric delays estimated by the dual frequency pseudorange measurements are shown in Figures 7.7 and 7.8. It can been seen that the delays are spread over a wide band. If the truth model is only accurate to several metres, no conclusion of statistical significance can be drawn from the delays estimated from the different approaches. Therefore, it was decided that the estimation of the ionospheric delays, by the help of the dual frequency carrier phase measurements should be carried out for one satellite at the user station.

The dual frequency carrier phase measurements, with unknown integer ambiguities, can be used to estimate the changes of the ionospheric delays very precisely. By combining the ionospheric delay changes from the carrier phase measurements and the absolute ionospheric delay (much noiser) from the pesudorange measurements, the initial ionospheric delay at the starting epoch can be estimated accurately as long as no cycle slip occurs. Therefore it is essential that the process of the detection and repairing of cycle slips is carried out correctly for the carrier phase measurements to avoid introducing biases in the estimation. This process had been carried out for a single satellite at the user station, and the resulting carrier phase ionospheric delays were then treated as *truth* to assess the achievable accuracies of the ionospheric delays estimated by different techniques in this particular analysis.

Figure 7.11 shows the ionospheric delays estimated by (i) the broadcast Klobuchar parameters, (ii) the refined single frequency *ionospheric scale factor*

approach, (iii) the dual frequency approach and (iv) the *truth* model for satellite PRN 21 at the user site. The discrete delays were estimated at 90 minute intervals. The results show that the ionospheric delays calculated by the broadcast Klobuchar parameters provided a poor fit to the *truth*. The delays estimated from the dual frequency optimised Klobuchar-like parameters provided the best fit to the *truth*. The single frequency *ionospheric scale factor* approach performed only slightly worse than the dual frequency approach, and was much better than the broadcast Klobuchar model. The RMS errors of the ionospheric delays for satellite PRN 21 at the user site were of the order of 0.2 m, 0.8 m and 4.2 m, from the dual frequency, refined single frequency *ionospheric scale factor* approach and broadcast Klobuchar parameters, respectively (Table 7.4).

Table 7.4 Recovery of Ionospheric Delays at User Station

Ionospheric Model	RMS (m)
Dual Frequency Optimised Klobuchar-like Parameters	0.2
Single Frequency *Ionospheric Scale Factor* Approach	0.8
Broadcast Klobuchar Model	4.2

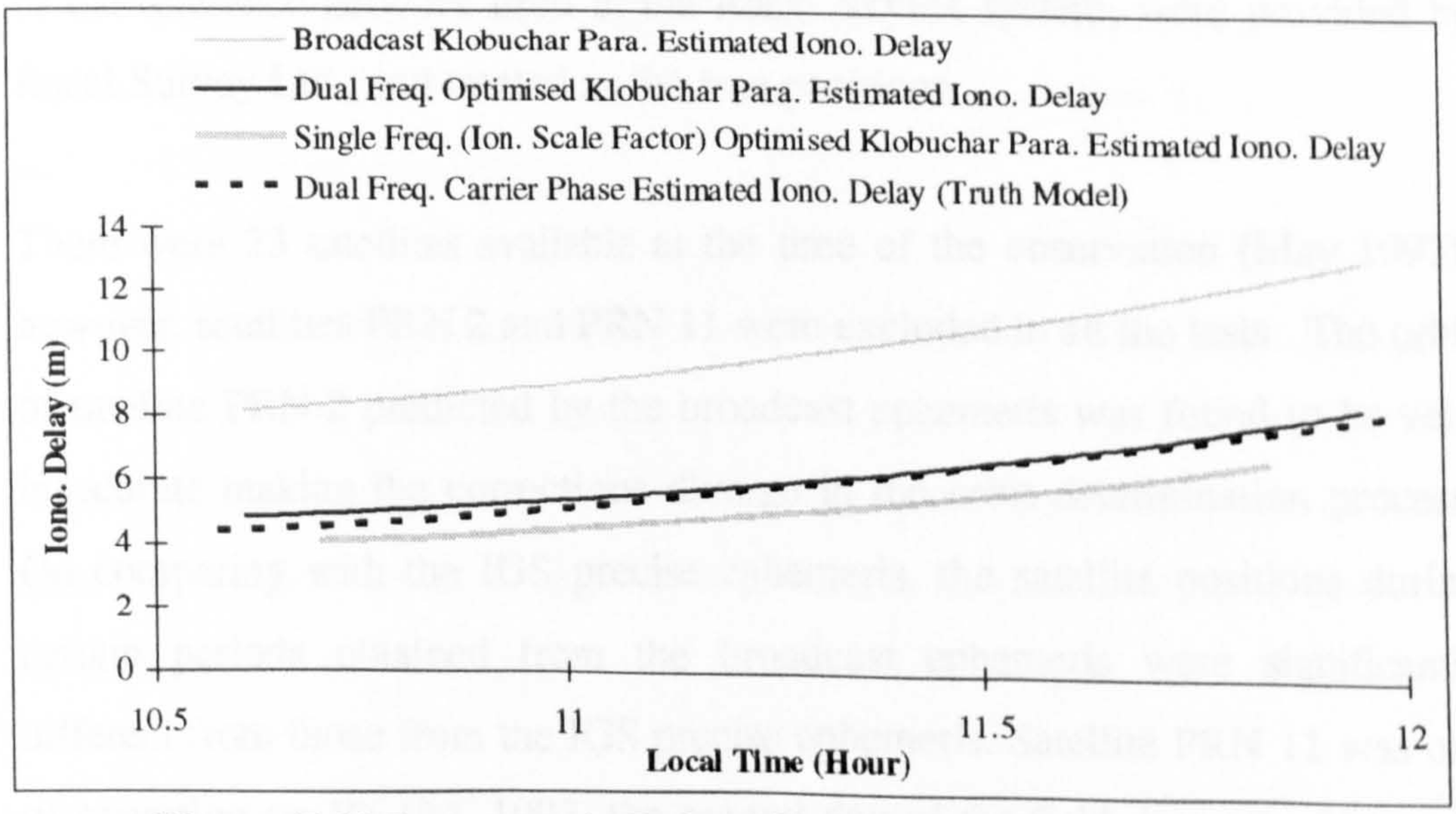

Figure 7.11 Ionospheric Delays from Different Approaches

The delays estimated by the broadcast Klobuchar model appear to have a large bias away from the *truth*, which was probably due to the deficiency of the model for the estimation of local ionospheric effects. The RMS error of 0.2 m achieved from the dual frequency approach indicated that the optimised ionospheric model is capable of estimating the local ionospheric delays accurately. The accuracy obtained by the single frequency *ionospheric scale factor* approach, with a RMS error of 0.8 m, is encouraging. It shows that the *ionospheric scale factor* technique has successfully compensated for the deficiencies of the approximate initial ionospheric delays by the use of local scale factors in a least squares adjustment process.

7.4 WADGPS User Positioning Accuracy

The user positioning accuracy is the final indication of the combined effects of all the individual error sources. The corrections derived from the WADGPS error correction models were applied to the observations to perform a WADGPS point positioning on an epoch-by-epoch basis. The coordinates of the reference stations were held fixed in all the processes. Aberdeen was treated as the user station to assess the user positioning accuracy. The coordinates of the reference and user stations, which were established as part of the reference network used in the Racal SkyFix system, were provided by Racal Survey Ltd., and treated as the *true* positions.

There were 23 satellites available at the time of the observation (May 1993), however, satellites PRN 2 and PRN 11 were excluded in all the tests. The orbit of satellite PRN 2 predicted by the broadcast ephemeris was found to be very inaccurate making the corrections diverge in the orbit determination process. On comparing with the IGS precise ephemeris, the satellite positions during certain periods obtained from the broadcast ephemeris were significantly different from those from the IGS precise ephemeris. Satellite PRN 11 was out of operation on JD 124, 1993, the second day of the field data set. Hence in order to control the consistency of the tests, PRN 11 was also dropped from

the tests. The constellation of 21 out of 23 available satellites created some periods of poor geometry and gaps, when less than 4 satellites were visible from some stations.

The user position was computed based on the all-in-view satellite approach without the selection of a low PDOP constellation. An elevation mask of 15° and a minimum of four visible satellites were used as minimum requirements for positioning. User positions were determined every 30 seconds over a 24 hour period, to represent a realistic performance of the proposed WADGPS.

The user positioning accuracy obtained from the three proposed WADGPS algorithms, namely the dual frequency, single frequency combined atmospheric delay and the refined single frequency *ionospheric scale factor* approaches, were investigated. The availability of real data made it possible to verify the conclusions drawn from the simulation studies and provided an assessment of the effects of the errors on the positioning accuracy.

User positioning accuracies were obtained by using the first day's orbit from three different ephemerides, namely (i) the IGS precise ephemeris, (ii) the integrated ephemeris improved by the proposed WADGPS algorithms and (iii) the broadcast ephemeris. Although IGS precise ephemeris is a post processed ephemeris, not available in real-time, it has been used to show the orbit effects on user positioning accuracy.

The user positioning accuracies achieved by (i) the dual frequency approach, (ii) the single frequency combined atmospheric approach and (iii) the refined single frequency *ionospheric scale factor* approach, each with three different ephemerides are shown in Table 7.5, in the forms of 95 % probability level and RMS errors.

Table 7.5 Orbit Effects vs. WADGPS Positioning Accuracy

	Ephemeris Type	Plan (95%, RMS)	Height (95%, RMS)
Dual Freq. at Ref. Single Freq. at User	Broadcast Eph.	5.9m / 2.7m	6.7m / 3.1m
	Integrated Eph.	4.5m / 2.2m	6.6m / 2.6m
	IGS Precise Eph.	4.4m / 1.9m	5.1m / 2.5m
Single Freq. at Both Ref. & User (Combined Atm.)[*1]	Broadcast Eph.	7.3m / 3.1m	7.8m / 3.3m
	Integrated Eph.	5.4m / 2.4m	6.7m / 3.0m
	IGS Precise Eph.	5.2m / 2.3m	6.2m / 2.7m
Single Freq. at Both Ref. & User (Ion. Scale Factor)[*2]	Broadcast Eph.	5.2m / 2.6m	5.9m / 3.0m
	Integrated Eph.	5.0m / 2.3m	6.3m / 2.5m
	IGS Precise Eph.	4.5m / 1.9m	5.3m /2.5m

(Combined Atm.)[*1] single frequency combined atmospheric delay approach

(Ion. Scale Factor)[*2] single frequency *ionospheric scale factor* approach

User position accuracies of the order of 2.2 m (RMS) in the plan component and 2.6 m (RMS) in height were achieved from the dual frequency approach with the integrated ephemeris. The differences between the *truth* and the WADGPS positions derived on an epoch-by-epoch basis are shown in Figures 7.12 and 7.13 for the plan and height components respectively. The corresponding distribution of the position error is shown in Figure 7.14.

User RMS positioning accuracies of 2.3 m and 2.5 m for the plan and height components respectively, were achieved using the refined single frequency *ionospheric scale factor* approach, with the integrated ephemeris. The differences between the user positions determined from this approach and the *truth* are in a similar pattern to those obtained in the dual frequency approach. The corresponding figures can be found in Appendix D, Figures D.1 to D.3.

User RMS positioning accuracies of 2.4 m and 3.0 m for the plan and height components respectively, were achieved using the single frequency combined atmospheric delay approach, with the integrated ephemeris.

It can be seen that there are some periods when no position estimates were computed, due to less than four satellites being visible during those periods. There are also some peaks observed in the figures, which are due to poor satellite geometry.

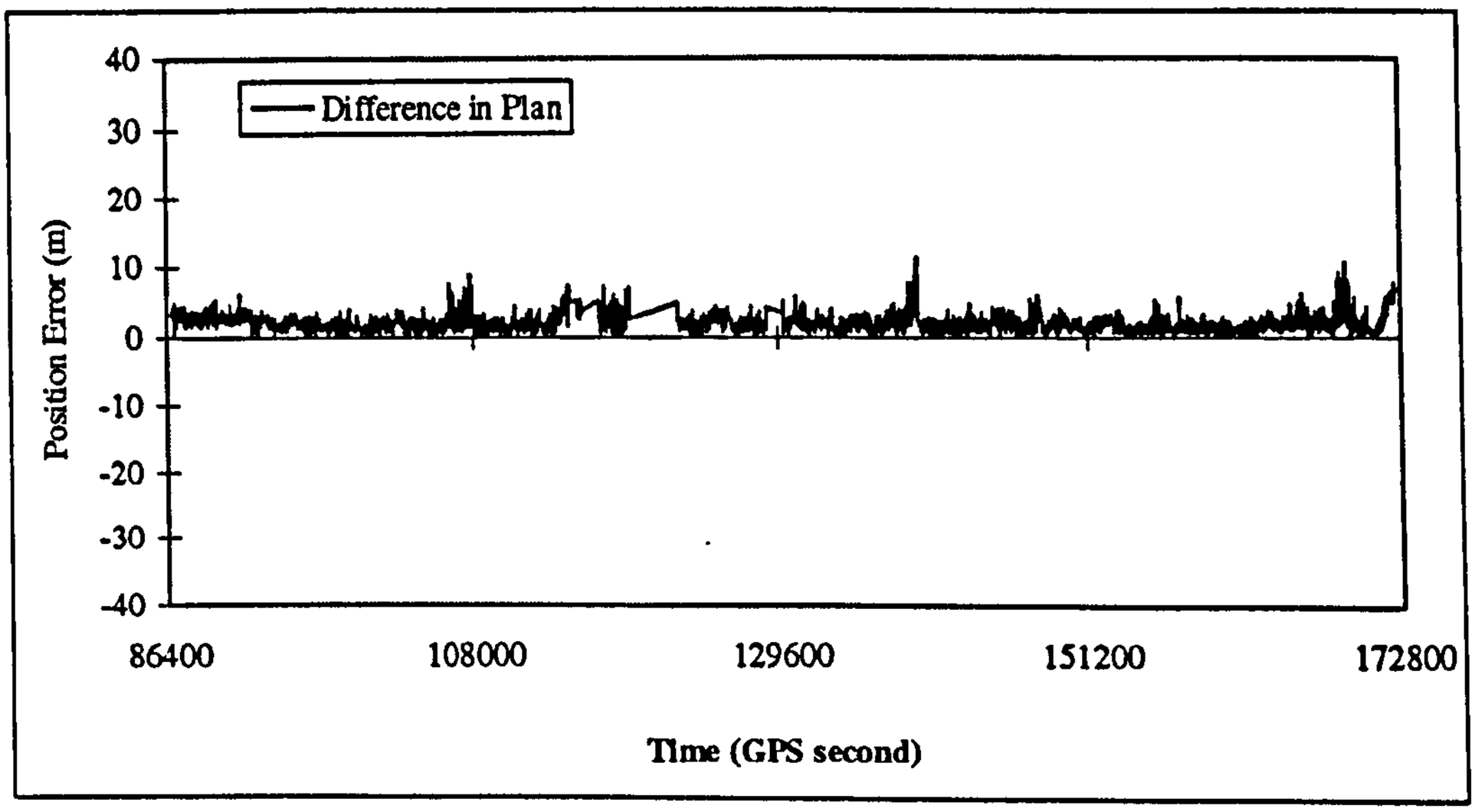

Figure 7.12 WADGPS Positioning by Dual Freq. Improved Ephemeris : (Plan Errors)

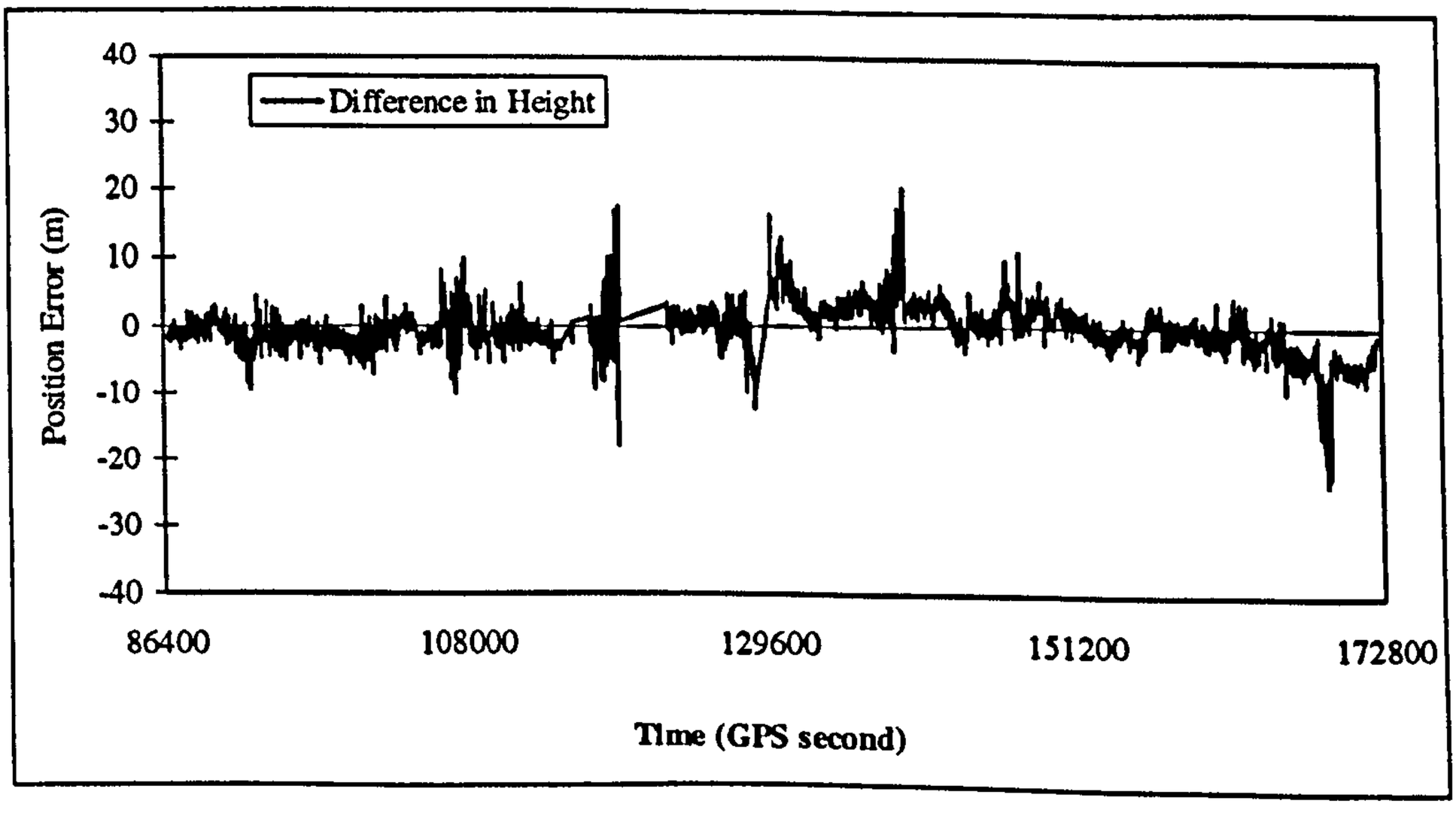

Figure 7.13 WADGPS Positioning by Dual Freq. Improved Ephemeris : (Height Errors)

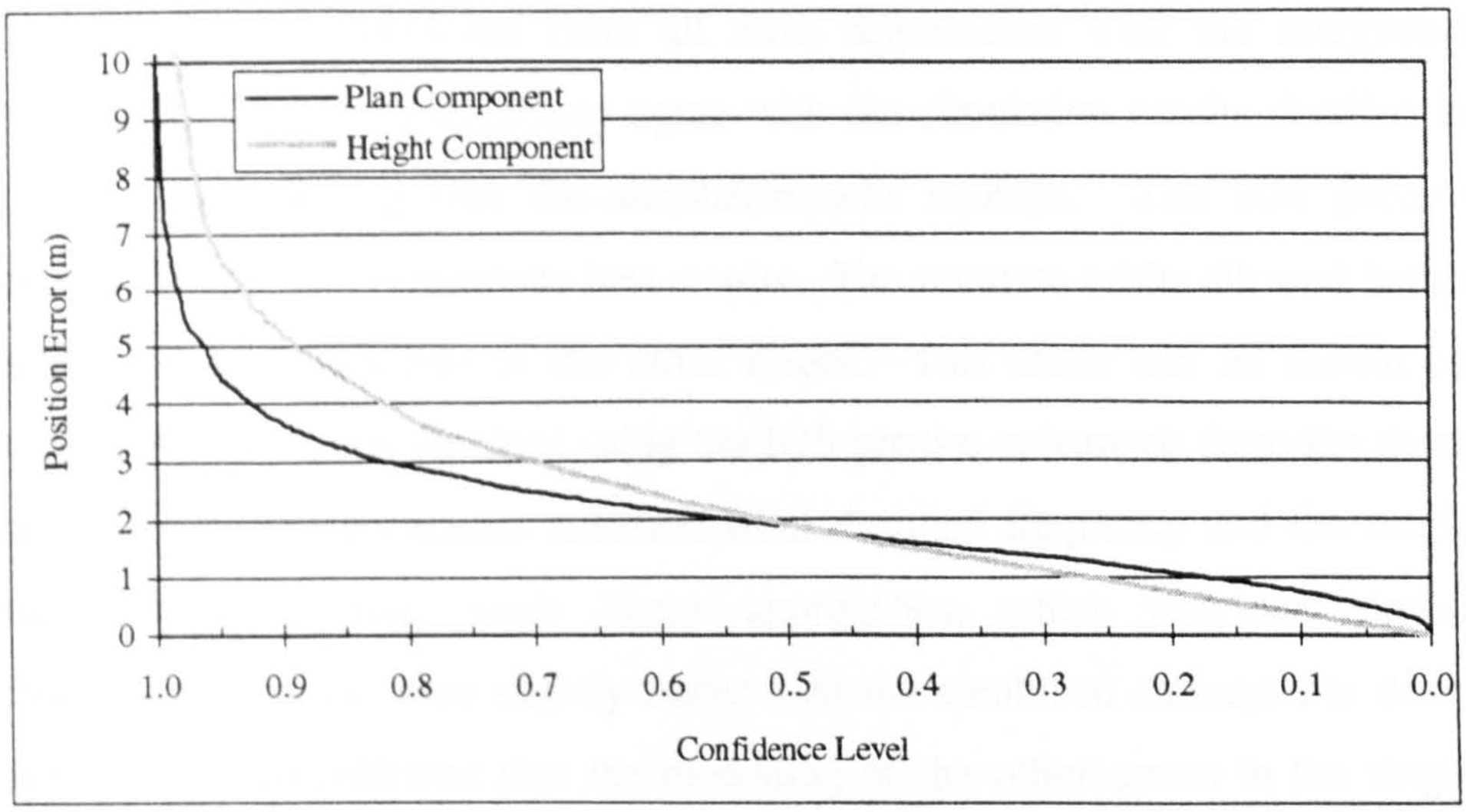

Figure 7.14 Distribution of Positioning Error by Dual Freq. Approach, (Integrated Ephemeris)

The user position accuracies determined by applying the dual frequency ionospherically-free observable at both reference and user sites, with the integrated ephemeris, was also investigated. The RMS errors of the order of 2.7 m and 3.2 m in the plan and height components respectively, were obtained. The results indicate that a better user positioning accuracy was obtained from the single frequency observable than the dual frequency ionospherically-free observable. This was not expected since the ionospherically-free observables should generally give better results than the single frequency observables especially if the baseline involved are very long. Therefore the poor results may be due to the increased noise propagated to the system by the dual frequency ionospherically-free observables. The effect of the increased noise should be minimised by employing the phase smoothed code pseudorange to reduce the noise level of the ionospherically-free observables.

Basically, there were no significant differences found in the user positioning accuracies from the three proposed WADGPS algorithms. The two single frequency approaches both provided similar levels of positioning results as those obtained from the dual frequency approach. User RMS positioning

accuracies of the order of 2 m and 3 m in the plan and height components respectively, were achieved from all three approaches with the integrated ephemeris. These results closely agree with the simulation results detailed in Chapter 6, indicating that the simulation was realistic. The IGS precise ephemeris always produced the best results. The accurate orbits allowed better separation and modelling of the other errors. This effect can be shown by comparing the results obtained using the IGS precise ephemeris from the three approaches. The accuracies achieved from the dual frequency and the single frequency *ionospheric scale factor* approaches, which provided almost identical accuracies, were slightly better than the combined atmospheric delay approach. This indicated that the modelling of the other errors in the single frequency combined atmospheric delay approach was worse than the other approaches.

On the other hand, the broadcast ephemeris always generated the lowest level of accuracy, with the integrated ephemeris somewhere in between. The accuracy of this broadcast ephemeris, compared with the IGS precise ephemeris, was similar to the integrated ephemeris, which was of the order of 5 to 10 m. This explains the similar user position accuracy achieved from the broadcast ephemeris and the integrated ephemeris. However, the broadcast ephemerides received at the different stations may have been different, and the effects of SA 'epsilon' error may have degraded the accuracy. As a result, the integrity, which is essential to the system users, provided by the integrated ephemeris is a deficiency of the broadcast ephemeris.

In order to provide a basis comparison for the WADGPS positioning, the user position was computed using the stand-alone point positioning, using pseudorange measurements on an epoch-by-epoch basis. The stand-alone point positioning RMS errors at Aberdeen, over a 24 hour period were 52 m and 54 m in plan and height respectively, which is well in line with the SPS accuracy of 100 m (2DRMS) in plan and 156 m (95%) in height. This level of accuracy

agrees closely with the RMS errors of the simulation data, which were of the order of 50 to 60 m in plan and 60 to 70 m in height.

- **Data Latency and Real Time Positioning Accuracy Analysis**

The data latency is the duration from data collection, processing and transmission to the user. As a result, the user always applies the differential correction which is late by a few seconds. This problem is overcome by predicting the corrections ahead, using the differential correction rate (§ 4.7). Tests were conducted to investigate the effects of data latency upon the user positioning accuracy, the results of which are shown in Table 7.6. Latencies of 6 seconds and 10 seconds were tested over a 24 hour period. The results indicated that a degradation of 0.2 m (RMS) and 0.2 m (RMS) in plan and height components respectively, can be expected when 6 seconds latency is applied. When there is a latency of 10 seconds, a degradation of 0.5 m (RMS) in plan and 0.4 m (RMS) in the height components may be expected.

Table 7.6 Data Latency Increased Error

Latency	Increased Error in Plan (RMS)	Increased Error in Height (RMS)
6 seconds	0.2 m	0.2 m
10 seconds	0.5 m	0.4 m

The user positioning results obtained using the best possible orbit (the first day), with no data latency, is not a realistic scenario. To simulate real-time positioning, the orbit and the atmospheric models need to be predicted ahead and data latency needs to be added, to allow for the time required for processing and transmission.

As a result, the orbit was estimated using data from three reference stations using 48 hours of data. This orbit was then predicted ahead for a further hour and transmitted to the users. The atmospheric models were predicted using the

previous 90 minutes of data. A data latency of 6 seconds was also applied to simulate the real time positioning. The user positioning accuracies based on the averaged RMS of 1 hour at night and 1 hour from the daytime are listed in Table 7.7. User RMS positioning accuracies of the order of 2.6 m and 3.0 m for the plan and height components respectively, were achieved using the dual frequency approach. The corresponding values for the single frequency *ionospheric scale factor* approach were 2.7 m and 3.0 m respectively. These results represented an increased error of 0.4 to 0.5 m in both plan and height components, than those obtained using zero latency and the best possible ephemeris. The increased errors for the single frequency combined atmospheric delay approach, were larger than for the other two approaches. This may due to the validity of the combined atmospheric error correction model degrading faster than for the other approaches. These results demonstrated that the proposed WADGPS techniques were capable of performing real time positioning.

Table 7.7 Real Time User Positioning Accuracy

	Plan (95%, RMS)	**Height (95%, RMS)**
Dual Frequency Approach	5.0 / 2.6	6.9 / 3.0
Single Freq. Combined Atm. Delay Approach	6.5 / 3.0	7.8 / 3.5
Single Frequency Iono. Scale Factor Approach	5.6 / 2.7	6.7 / 3.0

The number of the unknowns for orbit parameters and atmospheric scale factors are accumulated over a period of time, resulting in a large size of normal equation matrix to be solved for. For future development, the investigation of a stochastic model is recommended. The use of some kind of filtering technique, such as Kalman filtering, should be able to facilitate the computation process involving a large number of unknowns, enabling a substantial saving in computation time.

7.5 Conventional DGPS and NDGPS User Positioning Accuracy

7.5.1 Conventional DGPS

To highlight the superiority of WADGPS over conventional DGPS over long distances, the positioning accuracy achievable by conventional DGPS was investigated. Tests were conducted whereby Aberdeen was treated as the user station, and each one of the reference stations were treated as the reference station in turn. The distance between the reference stations and Aberdeen ranged from about 2,000 to 3,500 km. The user position was then determined by conventional DGPS every 30 seconds over a 24 hour period. The position errors and the distances between the reference stations and Aberdeen are shown in Table 7.8. The RMS user positioning accuracies achieved were of the order of 5.3 m, 7.9 m and 14.1 m in the plan component from reference station Hammerfest, Cadiz and Cyprus respectively. The corresponding RMS values for the height component were of the order of 5.1 m , 4.4 m and 7.1 m respectively.

Table 7.8 Conventional DGPS positioning accuracy

Ref. Stn.	Range to Aberdeen	Plan (95%, rms)	Height (95%, rms)
Hammerfest	1,933 km	10.8 / 5.3 m	11.8 / 5.1 m
Cadiz	2,298 km	13.5 / 7.9 m	8.6 / 4.4 m
Cyprus	3,551 km	22.4 / 14.1 m	17.5 / 7.1 m

The graphical displays of the positioning results using Cadiz as the reference station are shown in Figures 7.15 and 7.16 for the plan and height components respectively. The results using Cyprus as reference station can be found in Appendix E, Figures E.1 and E.2.

The conventional DGPS user positioning accuracy relies on the correlation of the system errors between the reference and user sites. The results clearly

show that the user positioning accuracy degrades as the reference-user distance increases, due to the effects of spatial decorrelation. Since only one user station was available, it was difficult to relate these results with distance from the reference stations directly. The reference stations were located far apart (about 4,000 km between each of the reference stations), and hence the satellites geometry and the atmospheric delays experienced may have been different from one reference station to the others. However the distance between the reference and user sites could still be used as an indicator for the positioning accuracy degradation of the conventional DGPS results.

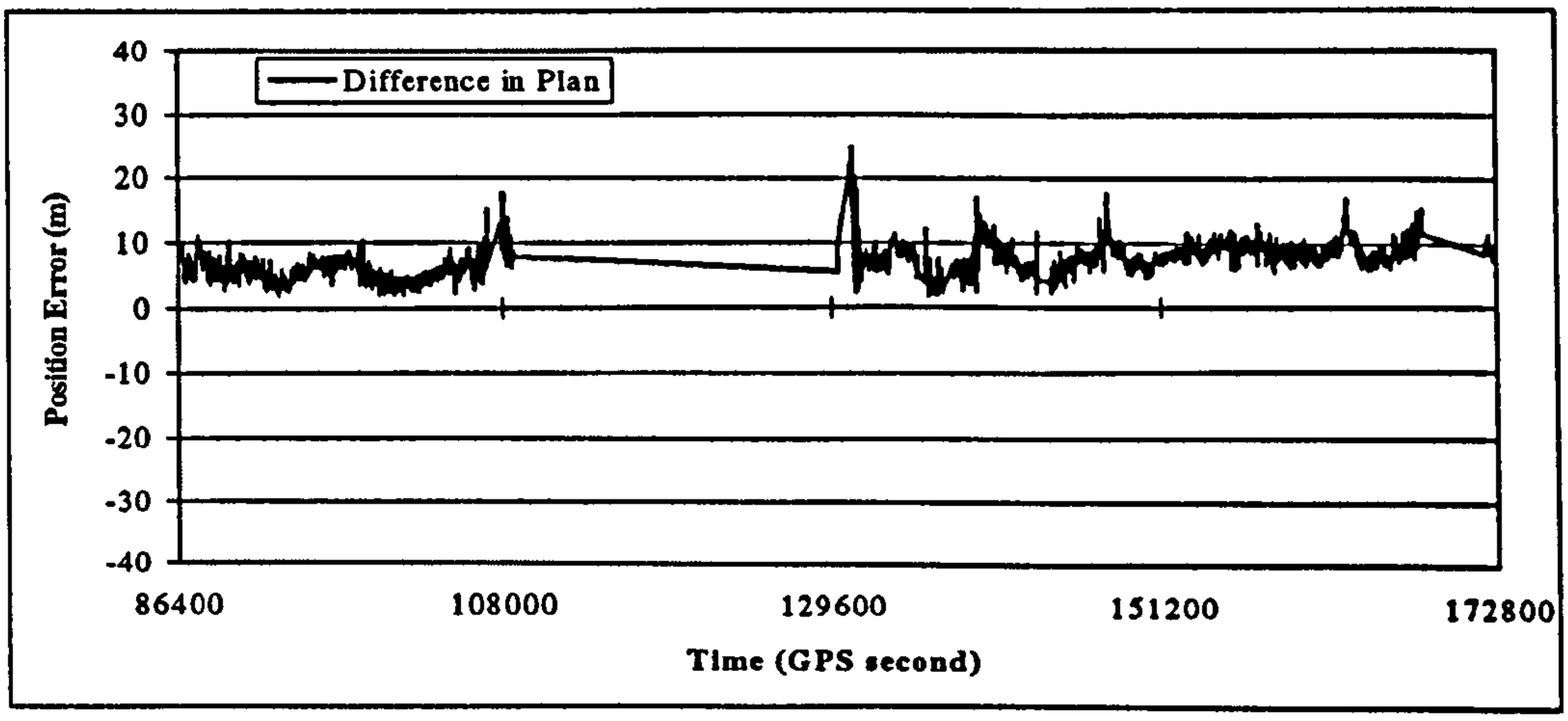

Figure 7.15 Conventional DGPS Positioning - Plan Error
Reference Station : Cadiz

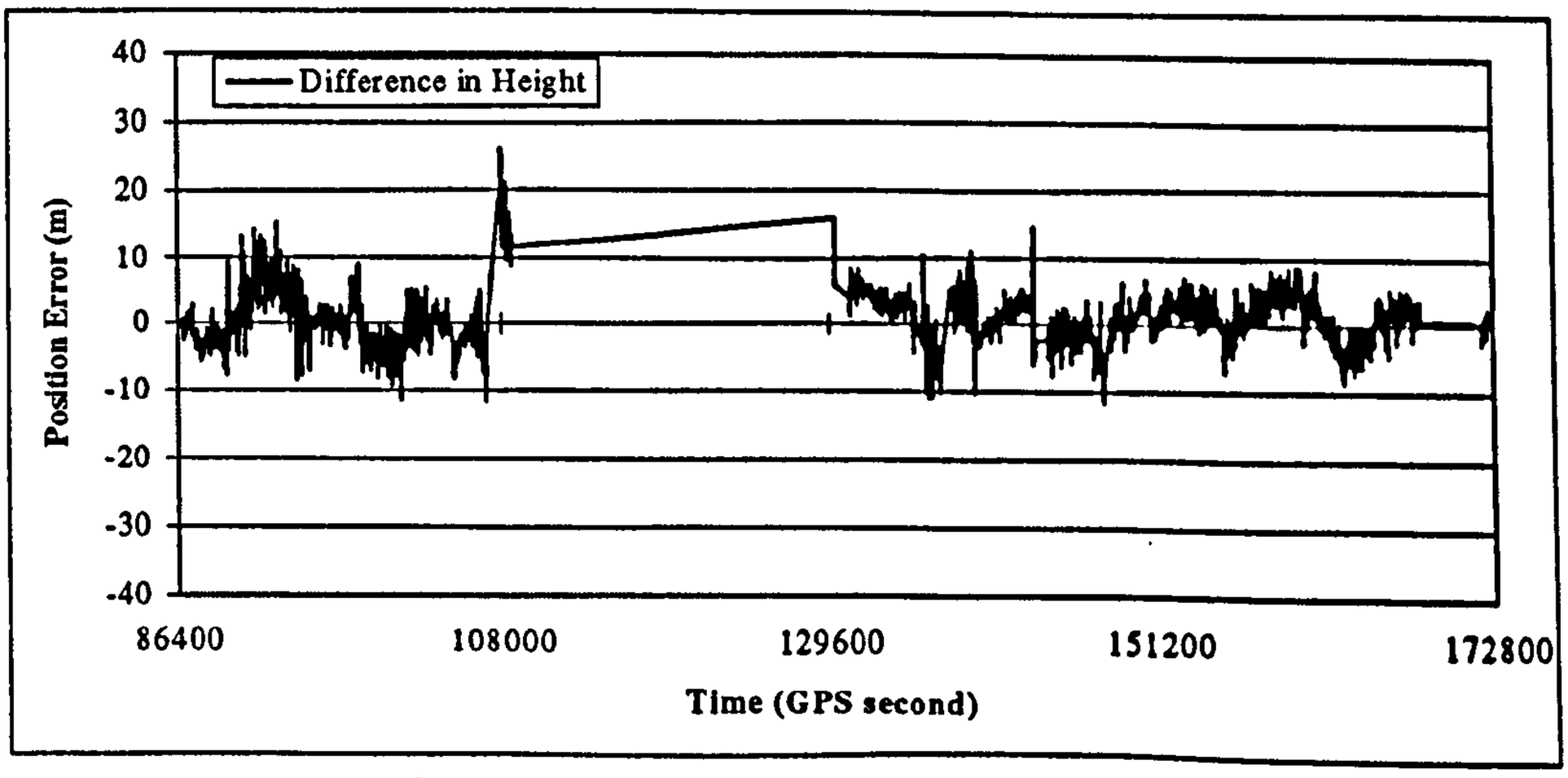

Figure 7.16 Conventional DGPS Positioning - Height Errors
Reference Station : Cadiz

The gaps observed in the figures indicate that either there was data missing or less than four satellites were available for positioning. More gaps exist from the DGPS approach than from the WADGPS case. The requirement of the conventional DGPS, that a minimum of four satellites are observed at both reference and user sites, becomes more and more difficult when the distance between them increases to several thousand kilometres. However, the improvement of conventional DGPS over stand-alone positioning (52 m and 54 m for plan and height components respectively) is still significant.

7.5.2 NDGPS

The conventional DGPS concept is based on one reference station providing one set of differential corrections whereas the WADGPS concept is based on a network of reference stations providing corrections to large areas without loss of accuracy. In the process of moving from conventional DGPS to WADGPS, the NDGPS concept can be defined (§ 3.2). This concept attempts to extend the area of applicability of the differential corrections by applying weighting parameters based on the distance between the reference and user stations. This should represent an improvement over the conventional DGPS concept, without the need for actual separation of the error components, as is the case with WADGPS.

The rigorous NDGPS applies various weight matrices, usually involving the relative geometry of the reference and user stations, in the user position determination. However, a simplified NDGPS, referred to as the averaged NDGPS, in which no complicated weight matrices are employed in performing the computation of the user position, has been tested using the real data.

The differential corrections generated from each of the three reference stations were properly combined through the network via common view satellites, to provide a unique differential correction for the user (§ 3.2). The positioning accuracy achievable was tested against the broadcast ephemeris, the recovered

integrated ephemeris and the IGS precise ephemeris. The RMS user accuracies achieved were of the order of 4.1 m, 3.9 m and 3.9 m in plan, and 7.3 m, 7.1 m and 7.3 m in the vertical component from the use of broadcast, integrated and IGS precise ephemerides respectively (Table 7.9).

Table 7.9 Averaged DGPS User Positioning Accuracy

Ephemeris Type	Plan (95%, RMS)	Height (95%, RMS)
Broadcast Ephemeris	8.9 / 4.1 m	13.5 / 7.3 m
Integrated Ephemeris	8.1 / 3.9 m	13.1 / 7.1 m
IGS precise Ephemeris	8.8 / 3.9 m	13.5 / 7.3 m

There was no significant difference found in the user positioning accuracy obtained using different ephemerides. The orbit errors were bundled together with atmospheric propagation and clock related errors, which diluted the direct effect of the individual error components. Consequently, the user positioning accuracy was a function of the averaged errors amongst the reference stations. The graphical displays of the positioning errors in plan and height components over a 24 hour period, are given in Figures 7.17 and 7.18 respectively.

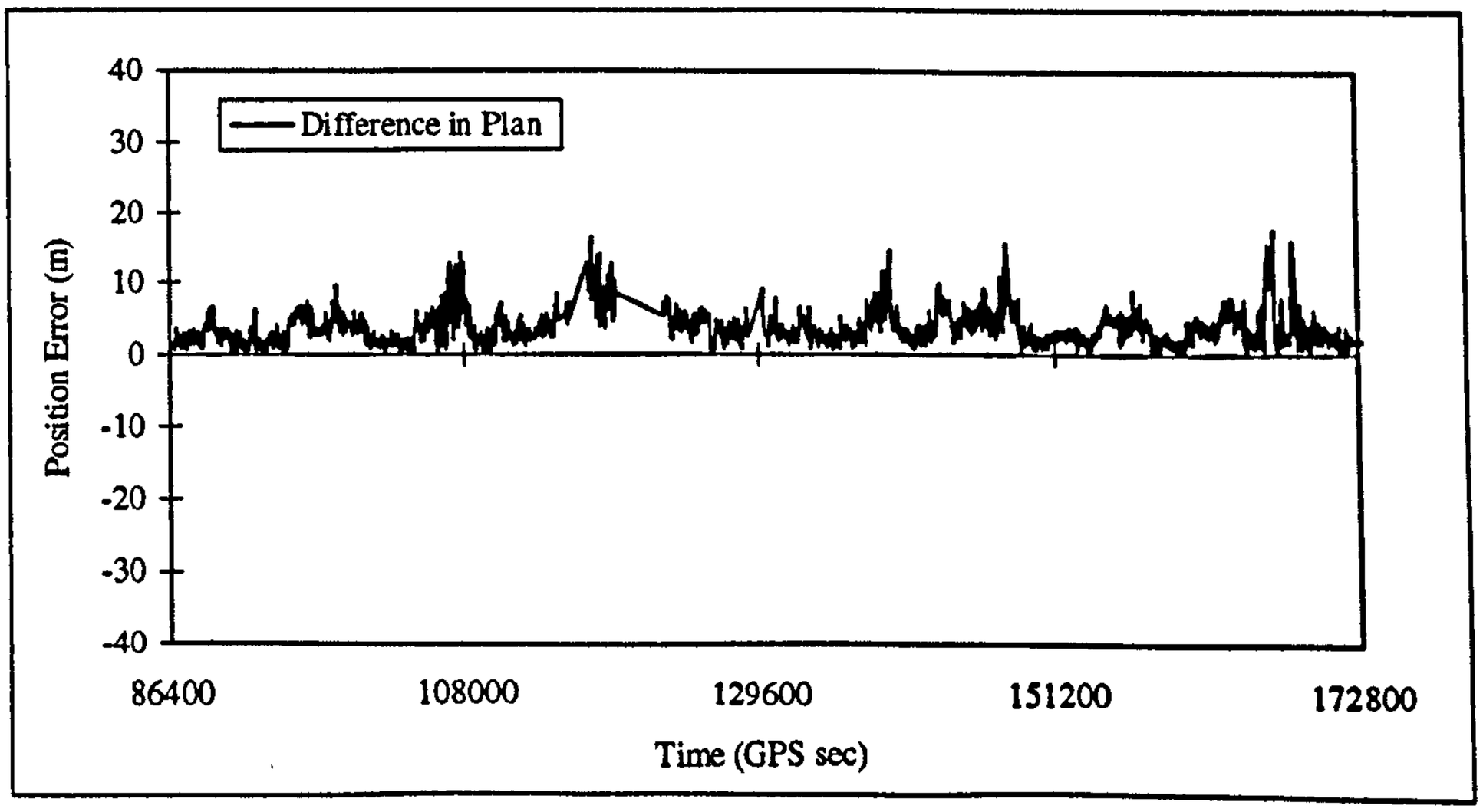

Figure 7.17 Averaged DGPS Positioning by Integrated Ephemeris - (Plan Error)

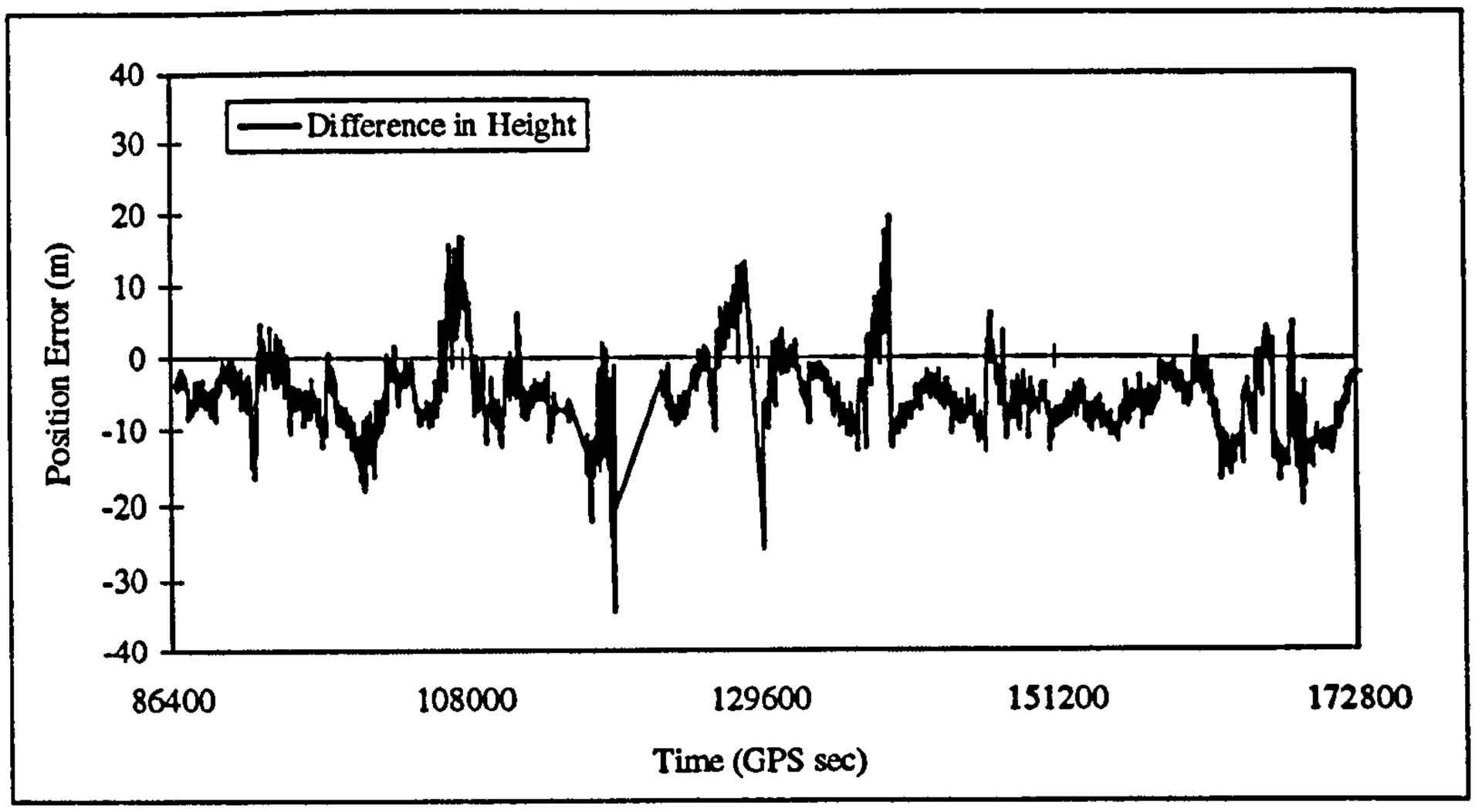

Figure 7.18 Averaged DGPS Positioning by Integrated Ephemeris - (Height Error)

It can be seen that the periods when no positions were computed were greatly reduced than those from the conventional DGPS technique. The NDGPS technique generates differential corrections for all the satellites visible in the network, which virtually overcomes the problem of the availability of common satellites faced by conventional DGPS. As long as the satellite has been observed by any of the reference stations, differential corrections can be computed and then transmitted to the user.

The user positioning accuracy in the plan component was improved using the averaged NDGPS compared with those obtained from using the conventional DGPS. Since the user was far away from the reference stations, the spatial decorrelation of the atmospheric errors degraded the positioning accuracy, especially in the vertical component, which is more sensitive to atmospheric error effects. The application of weighting matrices to the differential corrections should be able to extend the applicability of the differential corrections. However, the correlation of the system errors, especially the atmospheric errors, over such long baselines (2,000 to 3,500 km) is less. Therefore the effects of weighting parameters over such a long baseline should be minor.

Tests using real data had been carried for the WADGPS, conventional DGPS and averaged NDGPS concepts. The RMS user position accuracies achieved were of the order of 2 m, 4 m and 5 to 14 m in the plan component, and 3 m, 7 m and 4 to 7 m in the height component, from the WADGPS, averaged NDGPS and conventional NDGPS technique respectively. The results have highlighted the need for WADGPS in order to achieve high positioning accuracies over a wide area, typically a communication satellite's entire footprint. Results have shown that a WADGPS system, comprising only three reference stations separated about 4,000 km from each other, is capable of providing a user RMS position accuracy of the order of 2 to 3 m, for users with either single or dual frequency receivers, within most of the European area.

The dual frequency WADGPS approach provides the best performance in the system errors modelling and the corresponding user positioning accuracy, using dual frequency receivers at the reference stations and allowing the users to be equipped with either single or dual frequency receivers. The development of the refined single frequency *ionospheric scale factor* approach, has provided a new technique which would be important for a civilian WADGPS system. This approach demonstrates a robust scenario to build a WADGPS system which is capable of modelling system errors based entirely on the use of single frequency measurements. Results from the real field data have demonstrated that this approach is capable of providing accurate orbit determination and ionospheric error modelling and hence resulting in high precision user positioning. The advantage of this approach is highlighted by its ability to operate solely on single frequency receivers in the event that second frequency is rendered entirely unavailable to the civilian community.

Chapter 8

Conclusions and Suggestions for Further Work

8.1 Conclusions

1. The WADGPS system is aimed at providing consistently high positional accuracy over a large area, typically a communication satellite's entire coverage region, with a less dense distribution of reference stations in the network than the conventional DGPS or NDGPS. This is achieved by modelling the error sources separately, in a way that breaks the spatial correlation of the system errors.

2. The bundled differential correction in conventional DGPS is broken down into (i) an independent ephemeris (not affected by the SA 'epsilon' part) and transmitted to the user to replace the broadcast ephemeris, (ii) regional optimised atmospheric parameters, transmitted to the user to estimate local atmospheric delay and (iii) the remaining errors, assumed to be clock related, transmitted to the user for all satellites in view of the reference network.

3. The combined atmospheric delay WADGPS approach, designed for the single frequency receiver environment (Ashkenazi *et al*, 1993), was further investigated. The tests on the dual frequency approach, using both simulation and real field data, were carried out in the light of the availability of dual frequency measurements, irrespective of whether A-S is activated or not. Another refined single frequency approach, referred to as the *'single frequency ionospheric scale factor approach'*, was developed during this research and tested using real field data.

4. The processing software, including GPS and WADGPS processing and analysis software, was developed/modified to be able to implement the proposed algorithms. The *'Global Independent Double Difference Baseline Approach'* was developed and implemented in the GAS software, to enable network adjustment for a global network using the double difference observables. This approach allows different base satellites to be used for different baselines, which removes the restriction of the size of network previously limited by the single base satellite concept for the entire network employed in the GAS software.

5. The software was tested by simulation data to ensure the internal consistency and correct implementation of the algorithms. The 'self-check' was carried out by recreating the 'ground truth' of the ephemeris and atmospheric errors simulated in the GPS data, which included only satellite ephemeris and clock related (satellite and receiver clock and SA 'dither') errors. The recovered errors were found to be consistent with the applied errors, proving that the software was internally consistent.

SIMULATION

- **Satellite Ephemeris Error**

6. The method of ephemeris error computation used in this research involves the use of pseudorange data from a network of reference stations, to perform a complete orbit determination using the fiducial technique, in conjunction with an orbit integration method. The accuracies of the recovered satellite orbits were of the order of 10 m (RMS) and 5 m (RMS) for the single frequency combined atmospheric delay and dual frequency approaches respectively, using data simulated with all error sources and 0.2 m (SE) pseudorange noise.

7. The RMS errors of the recovered satellite orbit using the single frequency combined atmospheric delay approach with tropospheric errors only, ionospheric errors only and both ionospheric and tropospheric errors, were of the order of 0.1 m, 2 to 3 m and 10 m respectively. These results highlight the need for modelling the ionospheric and tropospheric errors separately.

8. The pseudorange noise was found to be one of the main dominating error sources in the orbit determination process. The accuracies of the recovered satellite orbits, obtained using the single frequency combined atmospheric approach using data with only 1 m (SE) pseudorange noise, were of the order of 10 to 15 m (RMS). Satellite orbit accuracies of the order of 5 to 10 m (RMS) were achieved with data simulated with all error sources except pseudorange noise.

9. The dual frequency approach generated satellite orbits with RMS errors of the order of 5 m, using data simulated with 0.2 m (SE) pseudorange noise as

the only error source. This result is similar to that obtained from data simulated with all error sources and 0.2 m (SE) pseudorange noise, which again highlights the significant effects of the pseudorange noise in the error modelling process.

10. When data was simulated with all error sources excluding pseudorange noise, satellite orbit accuracies of the order of 0.1 m (RMS) were achieved by the dual frequency approach. Compared with the similar case of the single frequency combined atmospheric delay approach (RMS values of 5 to 10 m), the importance of the atmospheric modelling is clear.

- **Atmospheric Propagation Errors**

11. The approach of combining the ionospheric and tropospheric delays as one single atmospheric parameter, proposed by Ashkenazi *et al* (1993), was designed specifically for a single frequency receiver environment. This combined atmospheric delay was estimated using local scale factors together with a standard tropospheric model, in a fiducial network adjustment process. Tests carried out for this thesis demonstrated the deficiencies of this approach in recovering the atmospheric delays.

12. In the dual frequency approach, the atmospheric propagation errors are separated into two components, namely the ionospheric and tropospheric delays. The dual frequency measurements were used to recover the ionospheric errors. The tropospheric delays were then solely estimated by the scale factor technique in conjunction with the Magnet model, as part of the orbit determination process. Simulation tests have shown that the recovered ionospheric and tropospheric delays at the reference stations agree with the *truth* (obtained from the data simulator) at the decimetre level.

13. The ionospheric delays estimated from the dual frequency measurements are optimised by a Non-linear Static Estimation (NSE) algorithm, which is a kind of least squares optimisation technique, to generate a locally best fitting Klobuchar-like ionospheric model. These parameters are then used to estimate the local ionospheric delays. The simulation tests show that the ionospheric delays estimated by the optimised parameters at a typical user station agree with the *truth* at the decimetre level.

14. Two tests were carried out in order to investigate the effect of the tropospheric delays on the positioning accuracy capability of WADGPS. In the first case, perfect tropospheric error recovery at the user was simulated by generating user data free from the effects of troposphere. The positioning accuracy achievable was of the order of 0.4 m (RMS) and 0.7 m (RMS) for horizontal and vertical components respectively. The second case represents the situation where correct modelling at the reference stations was undertaken but with no tropospheric model being sent or applied at the user. In this case the user data was generated with all error sources. Positioning accuracy of the order of 0.6 m (RMS) and 6.0 m (RMS) for plan and vertical components respectively, was achieved. Comparing the first and second test results, it can be concluded that the effects of the tropospheric error should be modelled and estimated in order to obtain a high positioning accuracy.

- **Clock Related Errors**

15. The estimation of the clock related errors relies on the assumption that if the satellite ephemeris and atmospheric propagation errors have been modelled and eliminated, then the only remaining errors are those associated with the reference station receiver and satellite clocks. In order to have a single differential correction for each satellite, the clock related errors from the different reference stations have to be aggregated. This is done by selecting

one of the reference stations to act as a master clock and then having all the clock errors referenced to it, by propagating the clock errors through the network via common view satellites. The resulting differential corrections then consist of one reference receiver clock error, and an averaged satellite clock error, for each satellite visible from the WADGPS network. As a result, relatively inexpensive, less accurate clocks could be used as reference clocks without degrading the navigation accuracy.

- **User Positioning Accuracy**

16. Five user stations were simulated to analyse the user positioning accuracy. In order to enable a comparison to be made with conventional DGPS, the stations were designed to be located at distances from 0.05 to 1,000 km from one of the reference stations. The stand-alone absolute point positioning accuracies of the order of 50 to 60 m (RMS) and 60 to 70 m (RMS) in the plan and height components respectively, were obtained. They are in accordance with the SPS specified accuracy (100 m (2DRMS) and 156 m (95% probability level) for the plan and height components respectively). In this case, the conventional DGPS produces better position accuracies than WADGPS within about 250 km and 700 km from the reference station, in the plan and height components respectively. However the DGPS accuracies degrade as the user-reference station distance increases. In contrast, the WADGPS provides consistently high positional accuracies regardless of reference station location.

17. The positioning accuracies achieved using the single frequency combined atmospheric delay approach were of the order of 1.1 m (RMS) and 1.9 m (RMS) for the plan and height components respectively. The test results proved that this approach is realistic and is capable of providing a high user positioning accuracy. However these accuracies are not as good as those

obtained when the perfect tropospheric modelling was assumed in the dual frequency approach (0.4 m (RMS) and 0.7 m (RMS) for the plan and height components respectively). This highlights the deficiencies of the atmosphere modelling in the single frequency combined atmospheric delay approach.

18. The use of two sets of Klobuchar-like model parameters (one for the ionospheric and the other for tropospheric delays) to recover the atmospheric errors in the dual frequency approach, provided user positioning accuracies of the order of 0.9 m (RMS) and 1.9 m (RMS) for the plan and height components respectively. This is remarkably similar to the level of accuracy achieved with the single frequency combined atmospheric delay approach. The agreement in the positioning accuracy determination indicates that the technique of combining the ionospheric and tropospheric delays is a realistic approach.

19. When no attempt was made to model the troposphere at both reference and user sites, i.e. the tropospheric errors were treated as system noise, the user positioning accuracies achieved were of the order of 1.7 m (RMS) and 2.6 m (RMS) in the plan and height components respectively. Compared with the single frequency combined atmospheric error case (corresponding values of 1.1 m (RMS) and 1.9 m (RMS)), it is clear that the tropospheric errors need to be modelled properly to achieve higher positioning accuracy.

TESTS WITH REAL FIELD DATA

20. The real field data was provided by Racal Survey Ltd., which consisted of the raw data at one user and three reference stations. The baseline lengths between the user and the reference stations range from about 2,000 km to 3,500 km. The stand-alone positioning accuracy achieved was of the order of 52 m and 54 m (RMS) for the plan and vertical components respectively.

21. The single frequency *ionospheric scale factor approach* recovers the tropospheric errors by Magnet model, and the ionospheric delays are estimated by the local scale factors, in conjunction with the broadcast ionospheric model, to generate a locally best fitting ionospheric correction model. This approach provides a new technique to build a WADGPS which is based entirely on the use of single frequency receivers, both at the reference stations and user end. Results from real data have proved that this approach is capable of providing similar user positioning accuracy as that from the dual frequency approach. The advantage of this approach is highlighted by its ability to operate solely on single frequency receivers in the event that second frequency is rendered entirely unavailable to the civilian community.

22. Satellite orbit accuracies of the order of 12 m (RMS) and 9 m (RMS) from three and four (three reference plus the user stations) reference stations respectively, were achieved with the L1 C/A code pseudorange for the European region, using the single frequency combined atmospheric delay approach. These results agree with those orbit accuracies obtained using the same approach from the simulation tests (of the order of 10 m (RMS)), which indicates that the simulation tests are realistic.

23. Satellite orbit accuracies of the order of 10 m (RMS) and 5 m (RMS) from three and four reference stations respectively, were achieved for the European region using the dual frequency approach. These accuracies are also similar to those obtained from the dual frequency approach from the simulation tests (of the order of 5 m (RMS)), which again proves the validity of the simulation tests.

24. Satellite orbit accuracies of the order of 9 m were achieved for the European region, using data from three as well as four reference stations, by using the single frequency *ionospheric scale factor* approach.

25. The RMS errors of the recovered ionospheric delays for one of the satellites at the user station, were of the order of 0.2 m (RMS), 0.8 m (RMS) and 4.2 m (RMS), obtained from the dual frequency approach, single frequency *ionospheric scale factor* approach, and the broadcast ionospheric (Klobuchar) parameters respectively.

26. Three ephemerides, namely the broadcast, WADGPS recovered and IGS precise ephemeris were used to estimate user positioning accuracies. Results showed that the IGS precise ephemeris always produced the best results. The user position accuracies of the order of 2 m (RMS) in plan and 3 m (RMS) in height had been achieved using the single frequency, dual frequency and single frequency *ionospheric scale factor* approaches, with the recovered ephemeris. No significant difference was found among the three WADGPS approaches. This level of user positioning accuracy agreed with the simulation results, indicating that the simulation was realistic.

27. Data latency tests using real data showed that there is an increase of 0.2 m (RMS) error in both the plan and height components when a data latency of 6 seconds is applied, and an increased error of 0.5 m (RMS) and 0.4 m (RMS) in the plan and height components respectively, when a data latency of 10 seconds was applied.

28. Tests were conducted to investigate the real-time positioning, using the predicted satellite orbit and atmospheric models, together with a data latency of 6 seconds. The user positioning accuracies achieved were of the order of 2.6 m (RMS) and 3.0 m (RMS) for the plan and height components

respectively, using the dual frequency approach, with corresponding values of 2.7 m (RMS) and 3.0 m (RMS) using the single frequency *ionospheric scale factor* approach.

29. Since only one user station was available, the effect of the user-reference station separation on positioning accuracies was investigated by computing the user station position based on different reference stations. The RMS errors of the user positions obtained from three different reference stations, in ascending order of the distances between the user and reference stations, were of the order of 5.3 m, 7.9 m and 14.1 m for plan, and 5.1 m, 4.4 m and 7.1 m for the vertical component.

30. The user positioning accuracies achieved by the averaged multi-station DGPS were of the order of 3.9 m (RMS) and 7.1 m (RMS) for plan and height components respectively.

8.2 Suggestions for Further Work

1. The carrier phase measurements should be incorporated with the code pseudorange measurements in the WADGPS technique, for the estimation of satellite orbit, atmospheric delay and clock related errors, in order to investigate the possibility of generating more accurate error correction models than those generated using the pseudorange data.

2. The orbit determination technique, based on the use of the full dynamic orbit determination process should be further developed, in an attempt to perform the orbit determination process almost in real-time, to provide the most up to date ephemeris.

3. A careful re-evaluation of the force models used with the orbit integration program, GPSORBIT, should be carried out to ensure that precise up-to-date models are used and that the different type of satellites (GPS Block IIA, IIF, GLONASS etc.) are accommodated, effectively developing a GNSS orbit program.

4. The development of a stochastic model is recommended, in order to refine the technique of estimating the discrete atmospheric delay by local scale factors in a least squares process. The use of some kind of filtering techniques, such as Kalman Filtering, should be able to facilitate the computation process involving a large number of unknowns, enabling a substantial saving in computation time.

5. More real field data should be collected in different areas of the world in different seasons, so as to include various effects of the tropospheric and ionospheric delays, in order to investigate the feasibility of the single frequency *ionospheric scale factor* approach, especially during periods of high ionospheric activity.

6. The issues of transmission, integrity and possible integration with other systems, to incorporate the proposed WADGPS technique as part of the GNSS network, should be investigated.

References

Agrotis, L.G. (1984) Determination of Satellite Orbits and the Global Positioning System. *PhD Thesis, University of Nottingham, United Kindom.*

Ashjaee, J. (1993) An Analysis of Y-code Tracking Techniques and Associated Technologies. *Geodetical Info Magazine, 7(7).*

Ashjaee, J. and Lorenz, R. (1992) Precision GPS Surveying after Y-code. *Proceedings of ION GPS-92, The 5th International Technical Meeting of the Satellite Division of the Institute of Navigation, Albuquerque, New Mexico, September.*

Ashkenazi, V. (1993) An Introduction to GPS. *Lecture Notes, IESSG, University of Nottingham U.K.*

Ashkenazi, V. (1993) Kinematic GPS. *Lecture Notes, IESSG, University of Nottingham.*

Ashkenazi, V. and Dodson, A.H. (1992) Positioning with GPS. *Mapping Awareness & GIS In Europe, Vol.6, No.7, September,1992.*

Ashkenazi, V., Gough, R.J. and Sykes, R.M. (1980) Doppler Translocation and Orbit Relaxation Techniques. *Phil Trans Royal Society, London A294, pp357-364.*

Ashkenazi, V., Moore, T., Ffoulkes-Jones, G., Whalley, S and Aquino, M (1989a) High Precision GPS Positioning by Fiducial Techniques. *International Association of Geodesy Symposia 102, Edinburgh, Scotland.*

Ashkenazi, V., Moore, T., Whalley, S and Aquino, M (1989b) Orbit Determination for GPS Satellites. *International Association of Geodesy Symposia 102, Edinurgh, Scotland.*

Ashkenazi, V. and Summerfield, P.J. (1989c) Rapid Static and Kinematic GPS Surveying: With or Without Cycle Slips. *2nd International Seminar on the Global Positioning System, IESSG, University of Nottingham.*

Ashkenazi, V., Hill, C.J. and Ochieng, W.Y (University of Nottingham, Nottingham, United Kindom), **Nagle, J.** (Inmarsat, London, United Kindom) (1993) Wide-Area Differential GPS : A Performance Study. *Navigation : Journal of the Institute of Navigation, USA, Vol.40, No.3, Fall.*

Ashkenazi, V., Ochieng, W.Y., Hill, C., Moore. T. and Chao, C.H. (1995) An Improved Wide Area Differential GPS. *The 4th International Conference on Differential Satellite Navigation Systems. Bergen, Norway, April, 1995.*

Barbous, J.P. (1993) Data Links for Real Time Differential GPS. *2nd International Conference on Differential Satellite Navigation Systems, 30 March to 2 April, 1993, Amsterdam, The Netherlands.*

Basker, S. and Caswell, I.E. (1994) Time and Clock Issues within WADGPS. *3rd International Conference on Differential Satellite Navigation Systems 18-22, April, London, U.K.*

Bate, R.R.,Mueller, D.D. and White, J.E. (1971) Fundamentals of Astrodynamics. *Dover Publications, New York.*

Beutler, G., Gurtner, W., Bauresima, I. and Rothacher, M. (1986) Efficient Computation of the Inverse of the Covariance Matrix of Simultaneous GPS Carrier Phase Difference Observations, *Manuscripta Geodaetica (1986) 11, p.249-255.*

Beutler, G., Brockmann E., Gurtner, W., Hugentobler, U., Mervart, L., Rothacher M., and Verdun A. (1994) Extended orbit modeling techniques at the CODE processing center of the international GPS service for geodynamics (IGS): theory and initial results, *Manuscripta Geodaetica (1994) 19, p.367-386.*

Bierman, G.J. (1977), Factorization Methods for Discrete Sequential Estimation. *Mathematics in Science and Engineering, Vol. 128. ISBN 0-12-097350-2.*

Blanchard, W. (1989) GPS for Marine and Air Navigation. *2nd International Seminar on the Global Positioning System, IESSG, University of Nottingham.*

Boucher C., Altamimi Z. and Duhem L. (1992) ITRF 91 and other realizations of IERS Terrestrial Referene System for 1991. *IERS Technical Note 12, October 1992, Observatoire de Paris.*

Boucher C., Altamimi Z. and Duhem L. (1993) ITRF 92 and Its Associated Velocity Field. *IERS Technical Note 15, October 1993, Observatoire de Paris.*

Brown, A. (1989) Extended Differential GPS. *Journal of the Institute of Navigation, USA, Vol 36, No.3.*

Brown, A. (1990) A Multi-sensor Approach to Assuring GPS Integrity. *GPS World 1(2), 44-48.*

Brown, R.G. (1992) A Baseline RAIM Scheme and a Note on Equivalence of Three RAIM Methods. *Journal of the Institute of Navigation, USA, Vol 39, No.3. Fall 1992.*

Bryson, A. (1989) Lecture Notes on Optimal estimation and Control Logic in the Presence of Noise. *Stanford Course AA278B.*

Cannon, M.E. and Lachapelle, G. (1990) High Accuracy GPS Semi-kinematic Positioning: Modelling and Results. *Journal of the Institute of Navigation, Vol. 37, No.1.*

Cannon, M.E., Lachapelle, G., Falkenberg, B., Ford, T., Neumann, J and Fenton, P. (1992a) Precise Real-time Kinematic Differential GPS Using a Cellular Radio Modem. *IEEE Position Location And Navigation System PLANS 92, Moterey, Ca. 1992.*

Cannon, M.E. and Lachapelle, G. (1992b) Analysis of a High Performance C/A Code GPS Receiver in Kinematic Mode. *National Technical Meeting, U.S. Institute of Navigation, San Diego, 1992.*

Casewell, I., Basker, S., Johnson, G., Hakegard, O.,Forssell. B., Hein, G and Oskam, D. (1994) A European Wide Area DGPS Experiment : Final Results. *Proceeding of ION GPS-94, 7th International Technical Meeting of the Satellite Division of the Institute of Navigation, Salt Lake City, Utah, U.S.A.*

Cross, P.A. (1990) Advanced Least Squares Applied to Position Fixing. Reprint with Corrections Version. *Working Paper No6, Polytechnic of East London.*

Curley, R.A. (1988) The Use of TI 4100 GPS Receivers and MAGNET Software to determine Height Differences. *MSc Dissertation, University of Nottingham, U.K.*

DMA (U.S. Defense Mapping Agency) (1987) Methods, Techniques and Data Used in WGS84 Development, Supplement to Department of Defense World Geodetic System 1984. *DMA Technical Report, Part 1, December, DMA TR 8350.2-A.*

DOD and DOT (1992) 1992 Federal Radionavigation Plan. *DOT-VNTSC-RSPA-92-2/DOD-4650.5.*

DOD and DOT (1994) 1994 Federal Radionavigation Plan. *DOT-VNTSC-RSPA-95-1/DOD-4650.5*

Dodson, A.H. (1986). Refraction and Propagation Delays in Space Geodesy. *International Journal of Remote Sensing, Vol. 7, No. 4, pp515-524*

Dodson, A.H., Hill, C.J. and Shardlow, P.J. (1992) The Effects of Propagation Errors on GPS Measurements. *5th Seminar on the Global Positioning System, University of Nottingham, U.K.*

El-Arini, M.B., Kellam, P.M., O'Donnel, P.A., Klobuchar, J.A., Wisser, T.C., and Doherty P. H. Ionospheric Experimentation for Wide Area Differential GPS (WADGPS) with Implications on Algorithm and System Design. *Proceeding of the 1993 National Technical Meeting of the Institute of Navigation, San Fransico, USA, January, 1993.*

El-Arini, M.B., Hegarty, C.J., Fernow, J.P. and Klobuchar, J.A. (1994) Development of an Error Budget for a GPS Wide Area Augmentation System (WAAS). *Proceeding of ION 1994 National Technical Meeting, San Diego, California, USA, January 24-26, 1994.*

Erickson, C., Lachapelle, G. and She B. (1991) Precise Rapid Static Survey Using a Combination of Code and Carrier Measurements. *Processing of ION GPS'91, The Institute of Navigation, Wash. D.C. USA.*

Federal Aviation Administration (FAA) (1996) *FAA Technical Centre Home Page: http://www. http://155.178.236.56/Home.html.*

Ffoulkes-Jones, G.H. (1990) High Precision GPS Surveying by Fiducial Techniques. *PhD Thesis, University of Nottingham, U.K.*

Goad, C.C. (1990) Optimal Filtering of Pseudorange and Phases from Single Frequency GPS Receivers. *Journal of the Institute of Navigation, Vol. 37, No.2.*

Graviss, L.P. (1992) GPS Development Program Status. *Proceedings of ION GPS-92, Fifth International Technical Meeting of the Satellite Division of the Institute of Navigation, Albuquerque, New Mexico, September.*

Gurtner, W. (1990) Receiver Independent Exchange Format Version 2. *GPS Bulletin Commission VIII, International Co-ordination of Space Techniques for Geodesy and Geodynamics, Vol.3, No.3, September-October, 1990.*

Hatch, R. (1982) The Synergism of GPS Code and Carrier Measurements. *In: Proc. of the Third International Geodetic Symposium on Satellite Doppler Positioning, Las Cruces, Mexico.*

Hatch, R. (1986) Dynamic Differential GPS at the Centimetre Level. *Proceeding of the 4th International Geodetic Symposium on satellite Positioning, Austin, Texas, USA, April 28-May 2, Vol 2 : 1287-1298.*

Hein G.W. (1990) Kinematic Differential GPS Positioning : Applications in airborne Photogrammetry and Gravimetry. *In : Crosilla F, Mussio L (eds) : II Sistema di Posizionamento Globale Satellite GPS. International Centre for Mechanical Science (CISM), Collana di Geodesia e Cartografia, Udine, Italy.*

Heiskanen, W and H Moritz (1984), Physical Geodesy, Reprint. *Institute of Physical Geodesy, Technical University Graz, Austria.*

Hill, C.J. (1989) Satellite Laser Ranging and Some Geophysical Applications. *PhD Thesis, University of Nottingham, U.K.*

Hofmann-Wellenhof, B., Lichtenegger, H. And Collins, J. (1994) Global Positioning System Theory and Practice. Third, Revised Version. *Springer-Verlag, Wien, New York.*

IESSG and BAe (1992) Wide Area Differential Corrections R & D Study *Project Report, University of Nottingham and British Aerospace (Systems) Ltd, England.*

IESSG (1995) The Integrity of GNSS for Civil Aviation. *Project Report, University of Nottingham, U.K.*

Catania, G (1995) Status Update for Block IIR Block IIF. *Proceeding of the 26th Meeting of Civil GPS Service Interface Commitee, Palm Spring, Califoria, USA, Stptermber, 1995.*

Kalafus, R. (1992) RTCM SC-104, Differential GPS Standards. *In : Summary Record of the 20th Meeting of the Civil GPS Service Interface Committee, Albuquerque, New Mexico, USA, Septermber 14-15.*

Kee, C., Parkison, B.W. and Axelrad, P. (1991). Wide Area Differential GPS. *Journal of the Institute of Navigation, Vol. 38, No.2.*

Kee, C. and Parkison, B.W. (1994) Wide Area Differential GPS as a Future Navigation System in the U.S. *IEEE PLANS'94.*

King, R.W., Masters, E.G., Rizos, C., Stolz, A. and Collins, J. (1987) : Surveying with Global Positioning System. *University of New South Wales, Australia, 1985. F Dummler, Bonn, 1987.*

Klobuchar, J.A. (1977) Ionospheric Time Delay Corrections for Advanced Satellite Ranging Systems. *Propagation Limitations of Navigation and Positioning Systems, AGARD-CP-209*

Klobuchar, J.A. (1982) Ionospheric Corrections for Single Frequency User of the Global Positioning System. *National Telesystems Conference NTC'82, System for the 80s, Galveston, Texas, 7-10 November, 1982 (New York : IEEE, 1982).*

Klobuchar, J.A. (1986) Design and Characteristics of the GPS Ionospheric Time Delay Algorithm for Single Frequency Users. *IEEE PLANS, Las Vegas, pp 169-176.*

Kouba, J. (1995) Analysis Coordinator Report. *In : Zumberger, J.F., Liu, R. And Neilan, R.E. (eds) IGS 1994 Annual Report. September, 1995.*

Kremer, G.T., Kalafus, R.M., Loomis, P.V.W. and reynolds, J.C. (1990) The Effect of Selective Availability on Differential GPS corrections. *Journal of the Institute of Navigation, USA, Vol. 37, No.1.*

Lachapelle, G. (1991) GPS Lecture Notes. *ENSU 629, University of Calgary, Canada.*

Lachapelle, G., Kielland. P. And Casey, M. (1991) GPS for Marine Navigation and Hydrography. *Proceedings of Fourth Biennal canadian Hydrographic Conference. Rimouski, April, 1991.*

Lachapell, G., Cannon, M.E., Erickson, C. and Falkenberg, W. (1992) High Precision C/A Code Technology for Rapid Static DGPS Surveys. *Proceedings of the Sixth International Geodetic Symposium on Satellite Positioning, Columbus, Ohio, March 17-20, Vol 1.*

Lanigan, C.A., Pflieger K. and Enge P.K. (1990) Real-Time Differential Global Positioning System (DGPS) Data Link Alternatives. *Proceedings of ION GPS-90, Third International Technical Meeting of the Satellite Division of the Institute of Navigation, Colorado Springs, Colorado, USA, September 19-21.*

Langley, R.B. (1994) RTCM SC-104 DGPS Standards. *GPS World, 5(5) 48-53.*

Lee, Y. (1995) New Technique Relating fault detection and exclusion Performance to GPS primary Means Integrity requirements. *Proceedings of ION GPS-95, The 8th International Technical Meeting of the Satellite Division of the Institute of Navigation, Palm Springs, California, USA, September 12-15, 1995.*

Leick, A. (1990) GPS Satellite Surveying. *John Wiely & Sons, New York.*

Liu, R., Gurtner, W., Zumberge, J. F and Neilan, R.E. (1994) Introducing the Central Bureau Information System of the International GPS Service for Geodynamics. *UKGA'94, Liverpool, U.K., March 1994.*

Llewellyn, S.K. and Bent, R.B. (1973) Documentation and Description of the Bent Ionospheric Model. *IAFCRL-tr-73-0657, AD772733.*

Loh, R., Wullschleger, V. and Butler, R. (1995) FAA's Wide Area Augmentation System (WAAS) for GPS-Concepts and Test Results. *The 4th International Conference on Differential Satellite Navigation Systems. Bergen, Norway, April, 1995.*

Loomis, P.V.W., Denaro, R.P. and Saunders P. (1990) Worldwide Differential GPS for Space Shuttle Landing Operations. *IEEE PLANS, Las Vegas, USA.*

Loomis, P.V. Sheynblatt, L. and Mueller, T. (1991) Differential GPS Network Design. *4th International Technical Meeting of the Satellite Division of the Institute of Navigation, september, 1991, Albuquerque, New Mexico, U.S.A.*

Michalson, W., Bernick,. J., Levin, P. and Enge., P. (1994) RAIM Availability for Augumented GPS-Based Navigation Systems. *Proceeding of ION GPS-94, 7th International Technical Meeting of the Satellite Division of the Institute of Navigation, Salt Lake City, Utah, U.S.A.*

Milliken, R.J. and Zoller, C.J. (1980) Principles of Operation of NAVSTAR and System Characteristics. *In: The Institute of Navigation : Global Positioning System, Vol. 1: 3-14.*

Monico, J.F.G. (1995) High Precision Inter-Continental GPS Network. *PhD Thesis, University of Nottingham, U.K.*

Montgomery, H. (1991) GPS -the Next Generation. *GPS World 2(10), 12-16.*

Moore, T. (1986) Satellite Laser Ranging and the Determination of Earth Rotation Parameters. *PhD Thesis, University of Nottingham, U.K.*

Moore, T (1995) Coordinate Systems and Reference Datums. *Lecture Notes, University of Nottingham, U.K.*

Muller, K.T., Biester, M. and Loomis, P.V.W. (1994) Performance Comparison of Candidate U.S. Coast Guard WADGPS Network Architectures. *Proceeding of the 1993 National Technical Meeting of the Institute of Navigation, San Diego, California, USA.*

Nagle, J. (1996) Inmarsat Services for Navigation. *Fact Sheets from Inmarsat World Wide Web http://www.worldserver.pipex.com/inmarsat/index.htm.*

Neilan, R. (1995) The Organization of the IGS. *In : Zumberger, J.F., Liu, R. And Neilan, R.E. (eds) IGS 1994 Annual Report. September, 1995.*

Ochieng, W. Y. (1993) Wide Area DGPS and Fiducial Network Design. *PhD Thesis, University of Nottingham, U.K.*

Parkinson, B.M. and Axelrad, P. (1988) Autonomous GPS Integrity Monitoring Using the Pseudorange Residual. *Journal of the Institute of Navigation, USA, Vol 35, No.2. Summber 1988.*

Remondi B. W (1991) NGS Second Generation ASCII and Binary Orbit Formats and Associated Interpolation Studies. *Paper presented at the XXth General Assembly of IUGG at Vienna, Austria, August 11-24, 1991.*

Remondi B.W. and Hofmann-Wellenhof B (1989) Accuracy of Global Positioning System Broadcast Orbits for Relative Surveys. *National Information Centre, Rockvill, Maryland, USA, NOAA Technical Report NOS 132, NGS 45.*

RTCM (1992) Radio Technical Commission for martime services Special Committee 104, RTCM Recommended Standards for Differential NAVSTAR GPS Service, Draft Issue 2.1, *RTCM SC-104, Washington, D.C. USA.*

RTCM (1994) Radio Technical Commission for martime services Special Committee 104, RTCM Recommended Standards for Differential NAVSTAR GPS Service, Version 2.1. *RTCM SC-104, Washington, D.C. USA.*

Seeber, G. (1993) Satellite Geodesy. *Walter de Gruyter, Berlin New York.*

Shardlow, P.J. (1994) Propagation Effects on Precise GPS Heighting. *PhD Thesis, University of Nottingham, U.K.*

Smith., K.E. and Weintraub,S. (1953) The Constants in the Equation for Atmospheric Refractivity Index at Radio Frequencies. *Proceeding of Institution of Radio Engineers, 41, 1035.*

Spilker, J.J. (1978) GPS Signal Structure and Performance Characteristics. *Journal of the Institute of Navigation, USA, Vol. 25, No.2.*

Stein, W.L. (1986) NAVSTAR Global Positioning System 1986 Status and Plans. *Proceeding of the 4th International Geodetic Symposium on satellite Positioning, Austin, Texas, USA, April 28-May 2, Vol 1: 37-49.*

Stewart, M.P., Ffoulkes-Jones, G.H. and Ochieng, W.Y. (1994). GAS: GPS Analysis Software User Manual. Version 2.2. *Publication IESSG, University of Nottingham, U.K.*

Sturtz, M.A., and Brown, A.K. (1990) Comparison of Fixed and Variable Threshod RAIM Algorithms. *Proceeding of the Third Internation Technical Meeting (ION-GPS90), Colorado Spring, CO, September 19-21, 1990.*

Takagi, N (1995) Implementation Plan for Multi-functional Transport SATellite (MTSAT) Satellite-based Augmentation System (MSAS). *Working Paper presented in the International Civil Aviation Organization Global Navigation Satellite System Panel (GNSSP), Montreal, 14 to 24 November 1995.*

Tam, D. (1996) Inmarsat-A. *Fact Sheets from Inmarsat World Wide Web http://www.worldserver.pipex.com/inmarsat/index.htm.*

United State Coast Guard (USCG) Differential GPS (1996) *Information from the USCG World Wide Web Site, http://www.navcen.uscg.mil/dgps/dgpsff.htm.*

Walsh, D. (1994) Real Time Kinematic GPS Positioning. *PhD Thesis, University of Nottingham, U.K.*

Watt, A. And Storey, J. (1995) The Technical Implementation of a Common European Programme for Satellite Navigation. *The 4th International Conference on Differential Satellite Navigation Systems. Bergen, Norway, April, 1995.*

Wells, D., Beck, N., Delikaraoglou, D., Kleusberg, A., Krakiwsky, E.J., Lachapelle, G., Langley, R.B., Nakiboglou, M., Schwarz, K-P., Tranquilla, J.M., and Vanicek, P. (1987) Guide to GPS Positioning. *Canadian GPS Associates, Federiction, New Brunswick, Canada.*

Whalley, S. (1990) Precise Orbit Determination for GPS Satellites. *PhD Thesis, University of Nottingham, U.K.*

White H. L., Decker B. L. and Kumar M. (1989) WGS 84 Reference Frame. *Proceeding of 5th International Geodetic Symposium on Satellite Positioning, March 13-17 1989, Las Cruces, New Mexico, pp 127-141.*

The White House. (1996) Fact Sheet. U.S. Global Positioning System Policy. *Office of Science and Technology Policy National Security Council. March 29, 1996.*

Zhu S.Y. and Groten E. (1988) Relativity Effects in GPS. *GPS-Techniques Applied to Geodesy and Surveying. Springer, Berlin Heidelberg New York London Paris Tokyo, 41-46.*

Appendix A

Non-linear Static Estimation (NSE) Algorithm

Given $x = n(\bar{x}, M)$ (A.1)

where,

x is a randon variable with mean $\bar{x}$ and a priori covariance matrix M

The observation equation relating the unknown parameters, x, the observed values, z, and noise, v, is given by,

$$z = h(x) + v,$$
$$v = N(0, w^{-1}) \quad \text{(A.2)}$$

The problem is then to find out the solution of x, which minimise the quadratic form of the least squares functions,

$$J = \frac{1}{2}\{(x-\bar{x})^T M^{-1}(x-\bar{x}) + [z-h(x)]^T w\,[z-h(x)]\} \quad \text{(A.3)}$$

Apply Taylor's series to linearise J,

$$J = J_0 + dJ$$
$$dJ = J'dx + \frac{1}{2}J''dx^2$$
$$= (x-\bar{x})^T \mathrm{M}^{-1}\,dx + \{z-h(x)^T w\,[-h'(x)]\,dx\} \quad \text{(A.4)}$$
$$+ \frac{1}{2}dx^T\{M^{-1} + h'(x)^T w^{-1}h'(x) - [z-h(x)]^T w\,[h''(x)]\}\,dx$$
$$+ \textit{high order terms}$$

Assume the $[z-h(x)]^T w\,[h''(x)]$ and higer order terms are small,

$$dJ = (x-\bar{x})^T \mathrm{M}^{-1}\,dx + \{z-h(x)^T w\,[-h'(x)]\,dx\} + \frac{1}{2}dx^T[M^{-1}+h'(x)^T w^{-1}h'(x)]\,dx \qquad \text{(A.5)}$$

To minimise J is to make $\frac{\partial J}{\partial x}=0$. If the partial derivative with respect to x, is not a linear function, an iterative method for the nonlinear estimation can be used. The method referred to as the 'Newton's Method' was used in this research. Geometrically speaking, this method is to find the tangent to the curve $f(x)$ in the last-found point x_i to find a new approximation x_{i+1}. (Hochstrasser, 1962).

The soultion $g(x)$ is found iteratively by,

$$g(x)=x-\frac{f(x)}{f'(x)} \qquad \text{where, } f(x)\equiv\frac{\partial J}{\partial x} \qquad \text{(A.6)}$$

The numerical steps suggested by Kee *et al* (1991) are given as,

1 find an approximate x

2 evaluate $h(x)$ and $H=h'(x)$

3 evaluate a posteriori covariance matrix p,

$$p=(M^{-1}+H^T w^{-1}H)^{-1}\equiv(\frac{\partial^2 J}{\partial x^2})^{-1}=f'(x)^{-1}$$

4 evaluate the partial derivative

$$GR\equiv\frac{\partial J}{\partial x}=(x-\bar{x})M^{-1}-H^T w^{-1}[z-h(x)]\equiv f(x)$$

5 if $|GR|<\varepsilon$, where ε is a specified criteria,

then set $\hat{x}=x$ and stop, otherwise,

6 replace x by $x-p\cdot GR\equiv x-\frac{f(x)}{f'(x)}$

7 go to (2)

References

Hochstrasser, U.R.S. (1962) Numerical Methods for Finding Solutions of Nonlinear Equations. *In Todd, J. (Eds) Survey of Numerical Analysis. Mcgraw-Hill Book Company, Inc. 1962. New York, San Franciso, Toronto, London.*

Kee, C., Parkison, B.W. and Axelrad, P. (1991). Wide Area Differential GPS. *Journal of the Institute of Navigation, Vol. 38, No.2.*

Appendix B

WADGPS Data Transmission

The feasibility of WADGPS by both simulation and real field data has been investigated in this research. In practice, WADGPS requires data transmission systems to transmit data from the reference stations to control centre and from control centre to users. The capacity of the data transmission system used in WADGPS is briefly identified and analysed here, for more details the reader is referred to IEESG and BAe (1992).

Communication satellites, such as Inmarsat, were proposed to be used as the data transmission system. Communication satellites are able to provide a high data transmission rate, up to 9,600 bps by Inmarsat-A (and with High Speed Data option, up to 64,000 bps), and wide area of coverage, such as the Inmarsat Ocean Region (Tam 1996).

Two types of data-collection and distribution standards, provided by Inmarsat-A, can be used for the delivery of the differential corrections, namely a point-to-multipoint data distribution service and a multipoint-to-point facility (Nagle, 1996). The data from the reference stations is transmitted to the control centre via the multipoint-to-point facility, and the error correction models, generated at the control centre, are sent to an Inmarsat satellite to be transmitted to the users, via the point-to-multipoint service.

The type of information to be transmitted and possible update rates in the proposed WADGPS, based on the test results from both the simulation and real field data, are summarised here. The information required at the control centre to be transmitted from the reference stations includes,

(i) the raw pseudoranges

(ii) Time-tag for pseudorange

(iii) SV ID

This information is required for every satellite in view, and should be updated as often as possible. Reports by IESSG and BAe (1992) suggested an update rate of at least every 6 seconds.

The error correction models information, generated at the control centre, have to be passed to the user via the communication system, which includes,

- **The Improved Satellite Ephemeris**

The independently generated satellite ephemeris is sent to the user to replace the broadcast ephemeris. The satellite positions are given by transmitting eight sets of the satellite positions (X,Y,Z) for each satellite to the user. The user employs an Everret interpolation to obtain the satellite positions at the desired epochs. For each satellite, the following information need to transmitted,

one SV ID

8 satellite X components

8 satellite Y components

8 satellite Z components

8 time-tags

The satellite state vectors (position and velocity) are proposed to be updated every 15 minutes, however, this information should be repeated regularly, in order to keep the warm-up time to reasonable levels, typically 1 to 2 minutes.

- **Atmospheric Error Correction Models**

Though different atmospheric error modelling approaches have been proposed in this research, the required information to be transmitted is of the same manner to the Klobuchar-like parameters. In the single frequency combined atmospheric delay approach, a set of atmospheric Klobuchar-like parameters, which contain the effects of the ionospheric and tropospheric delays, are sent to the user. In the dual frequency and single frequency *ionospheric scale factor* approach, the ionospheric error correction models are both sent to the user, using the Klobuchar parameters. These Klobuchar-like parameters were proposed to be updated every 90 minutes in this research, however, this information should be repeated regularly, to keep the warm-up time reasonable.

- **Clock Related Errors**

The information required to relay the clock related errors to the user for each satellite in view include,

the clock related differential range correction
the rate of change of differential correction (range rate correction)
time-tag of the pseudorange
SV ID
satellite health status

This information is critical to the user position accuracy achievable, and should be updated according to the accuracy requirements. Under the SA activated situation, the update rate needs to be increased, to encounter the rapid variation of SA 'dither' effect.

To show typical examples of the data capacity required for WADGPS, the quantity of data to be transmitted was calculated, based on the report by IESSG and BAe (1992). Assuming all 24 satellites are observed in a WADGPS network, at data transmission capacity of 600 bps, the following information can be transmitted,

improved ephemeris every 2 minute

optimised atmospheric parameters every 1 minute

clock related error corrections every 4 seconds

At 1200 bps, the following information can be transmitted,

improved ephemeris every 1 minute

optimised atmospheric parameters every 1 minute

clock related error corrections every 2 seconds

The above examples indicate that the data transmission capacity required by the proposed WADGPS algorithms can be comfortably met by Inmarsat satellites, which indicates the feasibility of implementing the proposed WADGPS in practice.

Appendix C

Satellite Orbit Recovery Using Four Reference Stations

The satellite orbit accuracies achievable obtained using data from four stations (three reference stations plus one user station) are given graphically in this section. The recovery of the satellite orbit errors, compared with the IGS precise ephemeris, from the single frequency combined atmospheric delay approach and dual freqency approach are shown in Figures C.1 and C.2 respectively.

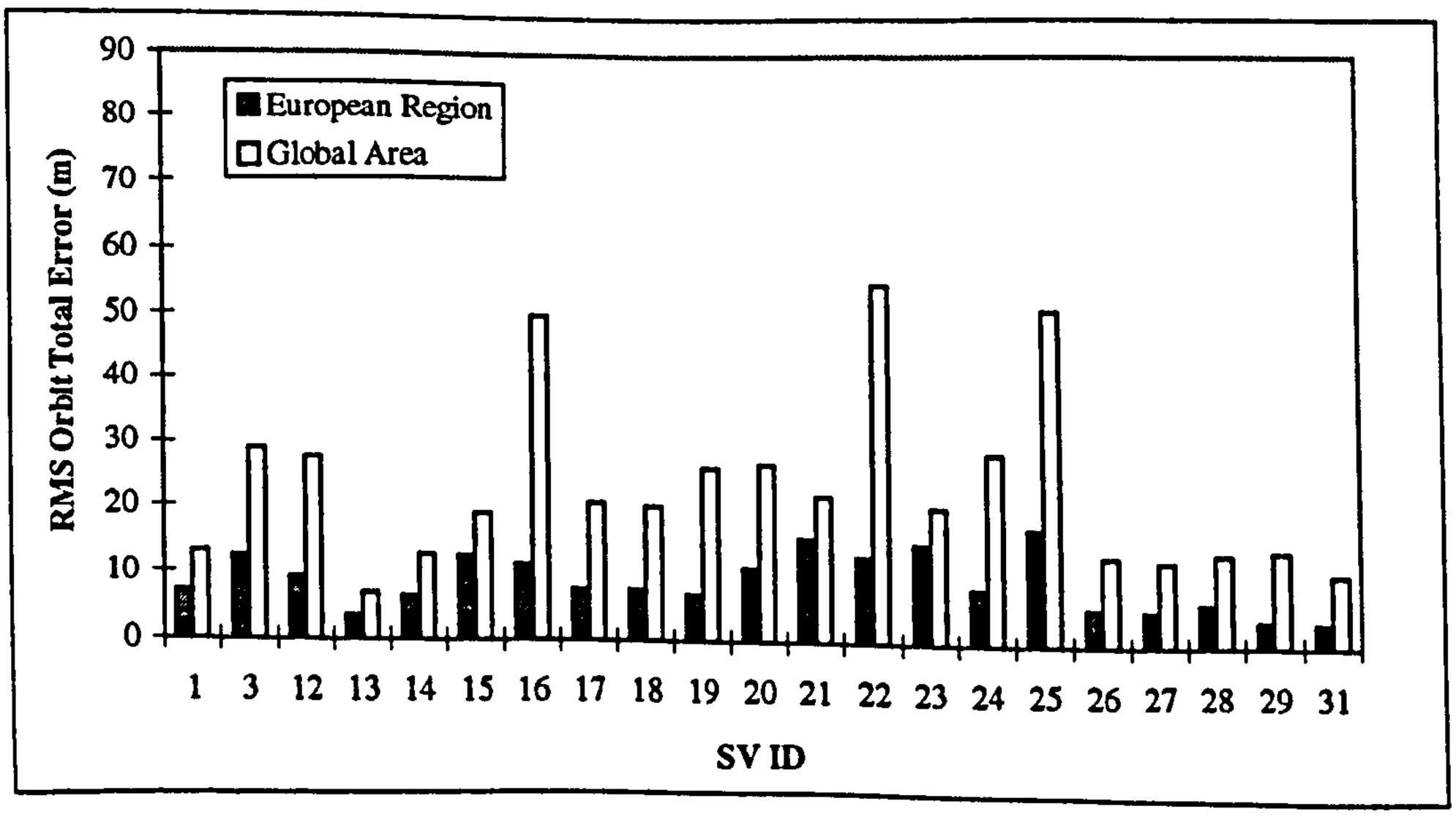

Figure C.1 Satellite Orbit Accuracy by 4 Reference Stations (Single Frequency Combined Atmospheric Delay Approach)

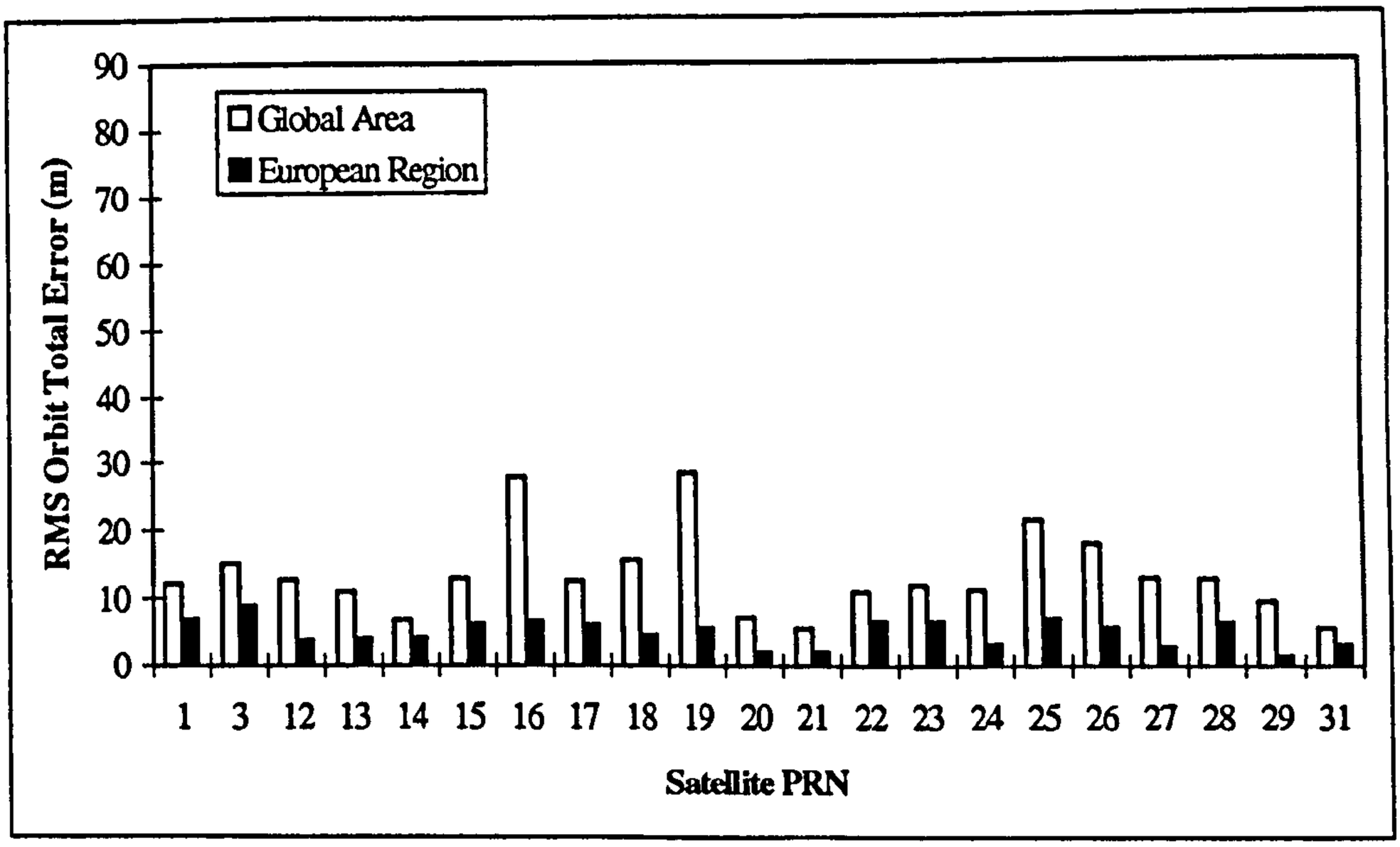

Figure C.2 Satellite Orbit Recovery by 4 Reference Stations (Dual Frequency Approach)

The individual orbit errors, namely along track, cross track and radial errors, recovered from dual frequency approach over a 72 hour period for satellite PRN 12 are shown in Fugure C.3.

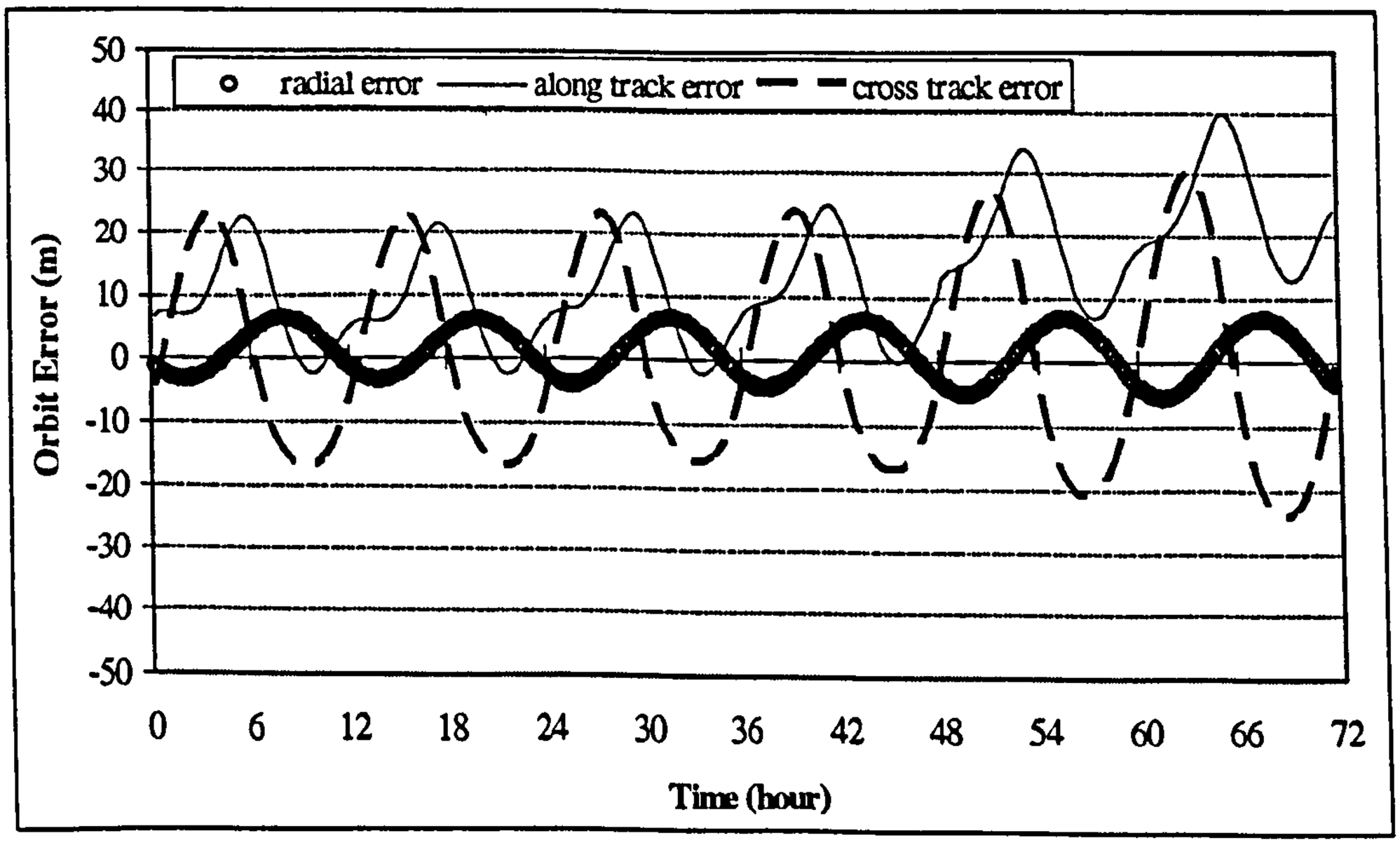

Figure C.3 Individual Orbit Error vs Time (Dual Frequency Observable)

The accuracies achievable of the recovered satellite orbit obtained from the refined single frequency *ionospheric scale factor* approach using data from four stations are shown in Figure C.4.

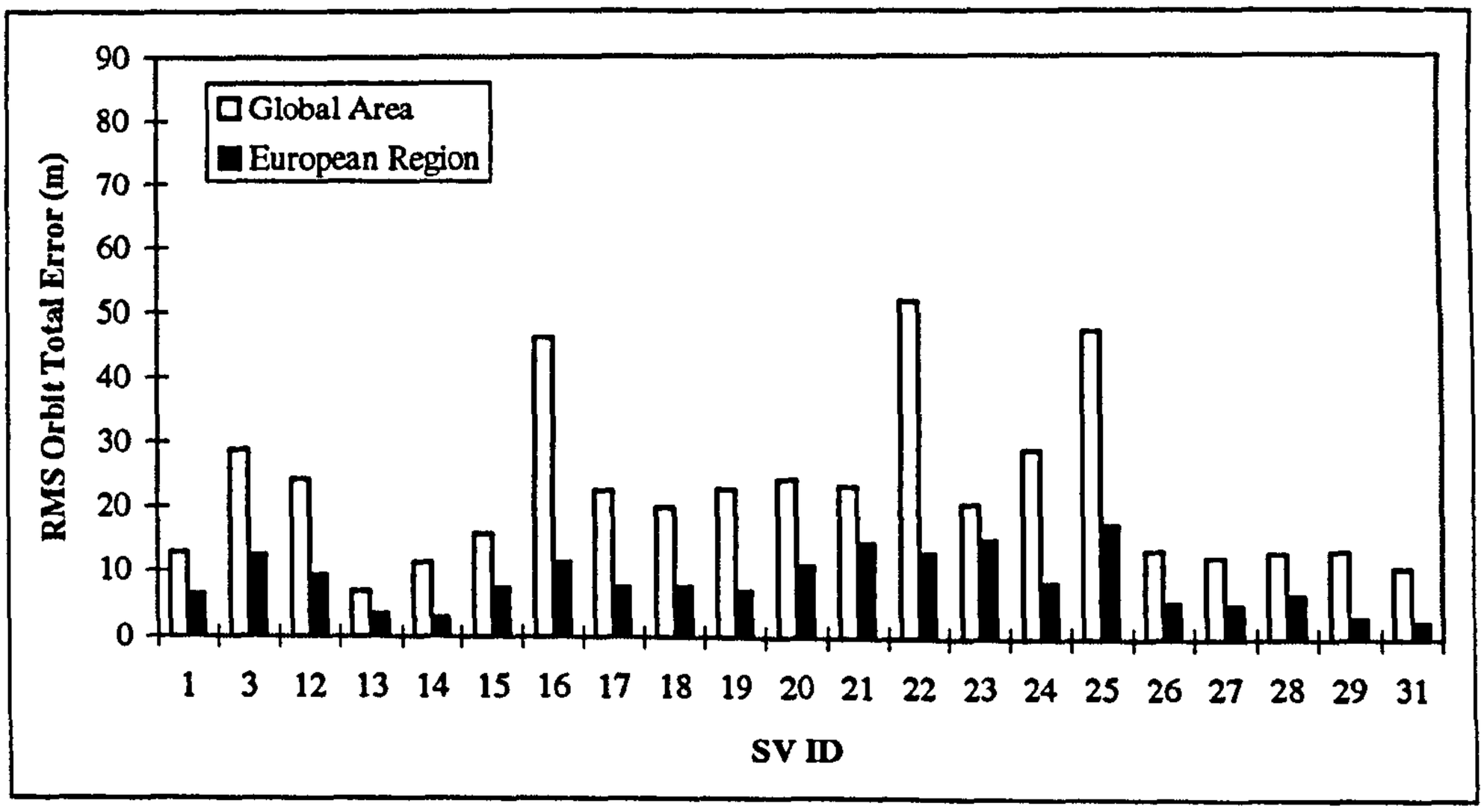

Figure C.4 Satellite Orbit Recovery by 4 Reference Stations

(Refined Single Frequency *Ionospheric Scale Factor* Approach)

Appendix D

WADGPS Positioning Results : Single Frequency *Ionospheric Scale Factor* Approach

This Appendix gives the graphical displays of the WADGPS positioning results over a 24 hour period. The results were obtained from the refined single frequency *ionospheric scale factor* approach using the recovered integrated ephemeris. The RMS results were tabulated in Section 7.4.1, Table 7.5. The positioning results in plan and height components are shown in Figures D.1 and D.2 respectively.

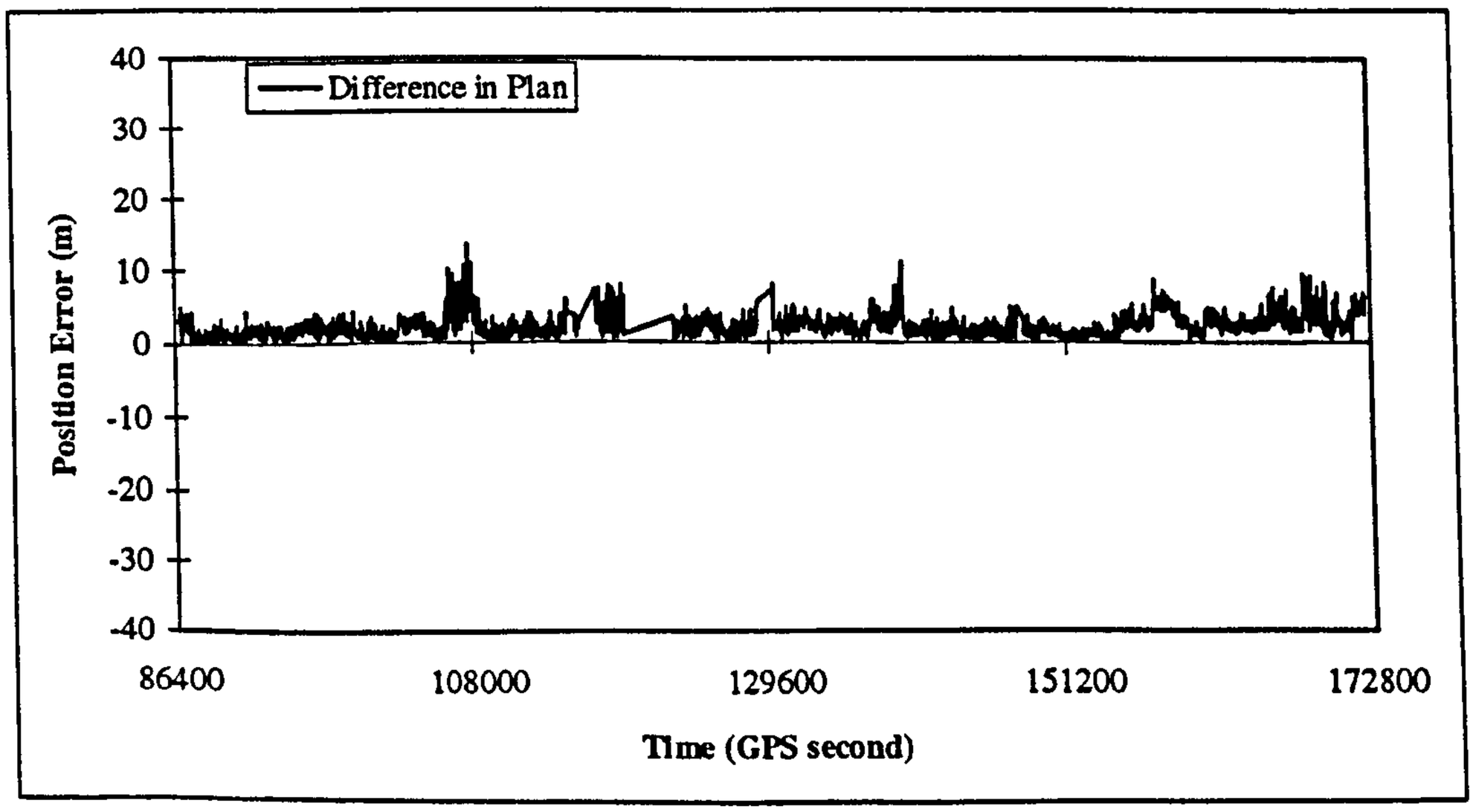

Figure D.1 WADGPS Positioning by Refined Single Frequency Integrated Ephemeris : Plan Errors

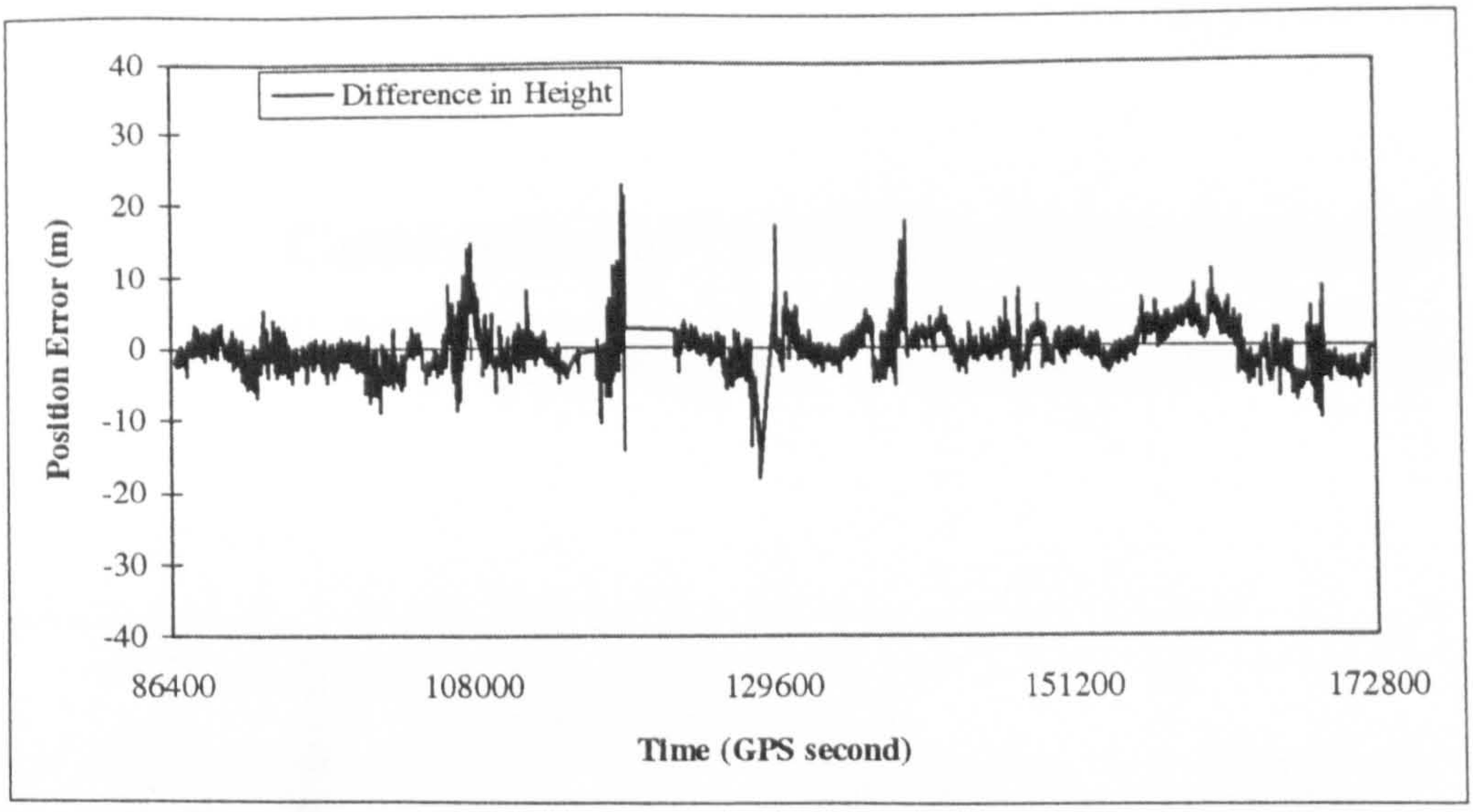

Figure D.2 WADGPS Positioning by Refined Single Frequency Integrated Ephemeris : Height Errors

The distribution of errors are shown graphically in Figure D.3 for both plan and vertical components.

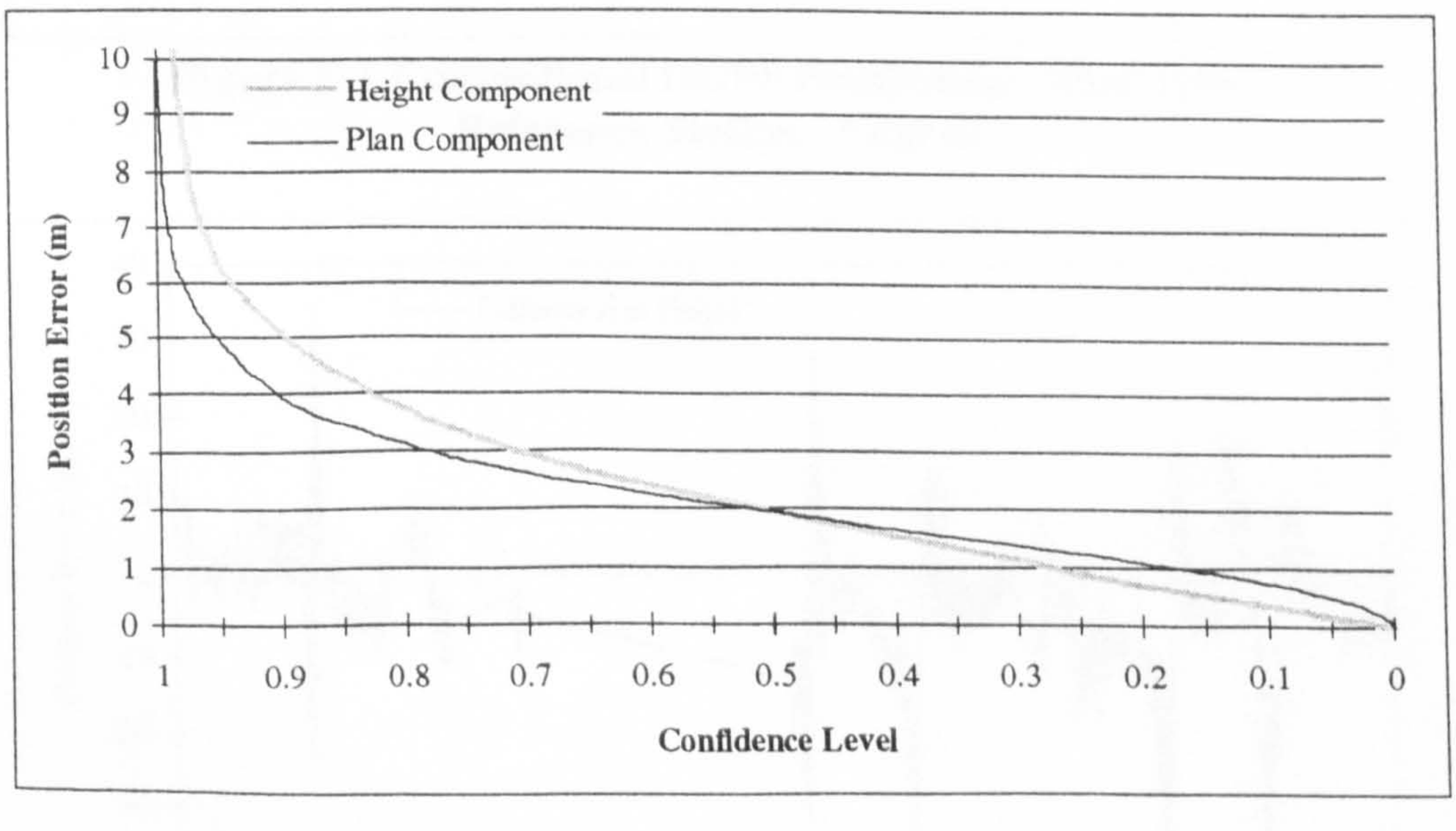

Figure D.3 Distribution of Position Error

Single Freq. Ionospheric Scale Factor Approach, Integrated Ephemeris

Appendix E

Conventional DGPS Positioning Results Using Cyprus as Reference Station

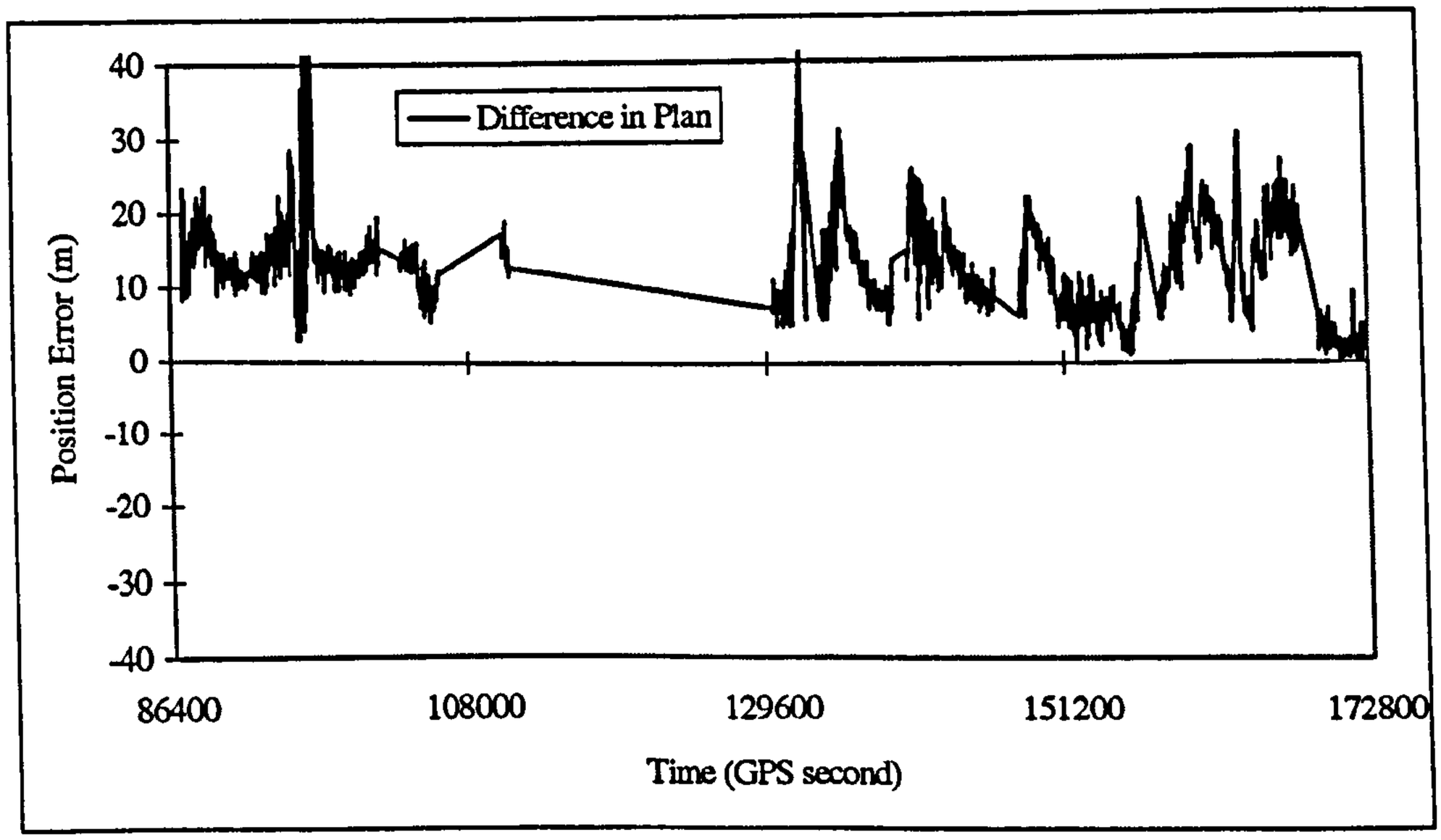

Figure E.1 Conventional DGPS Positioning - Plan Error Reference Station : Cyprus

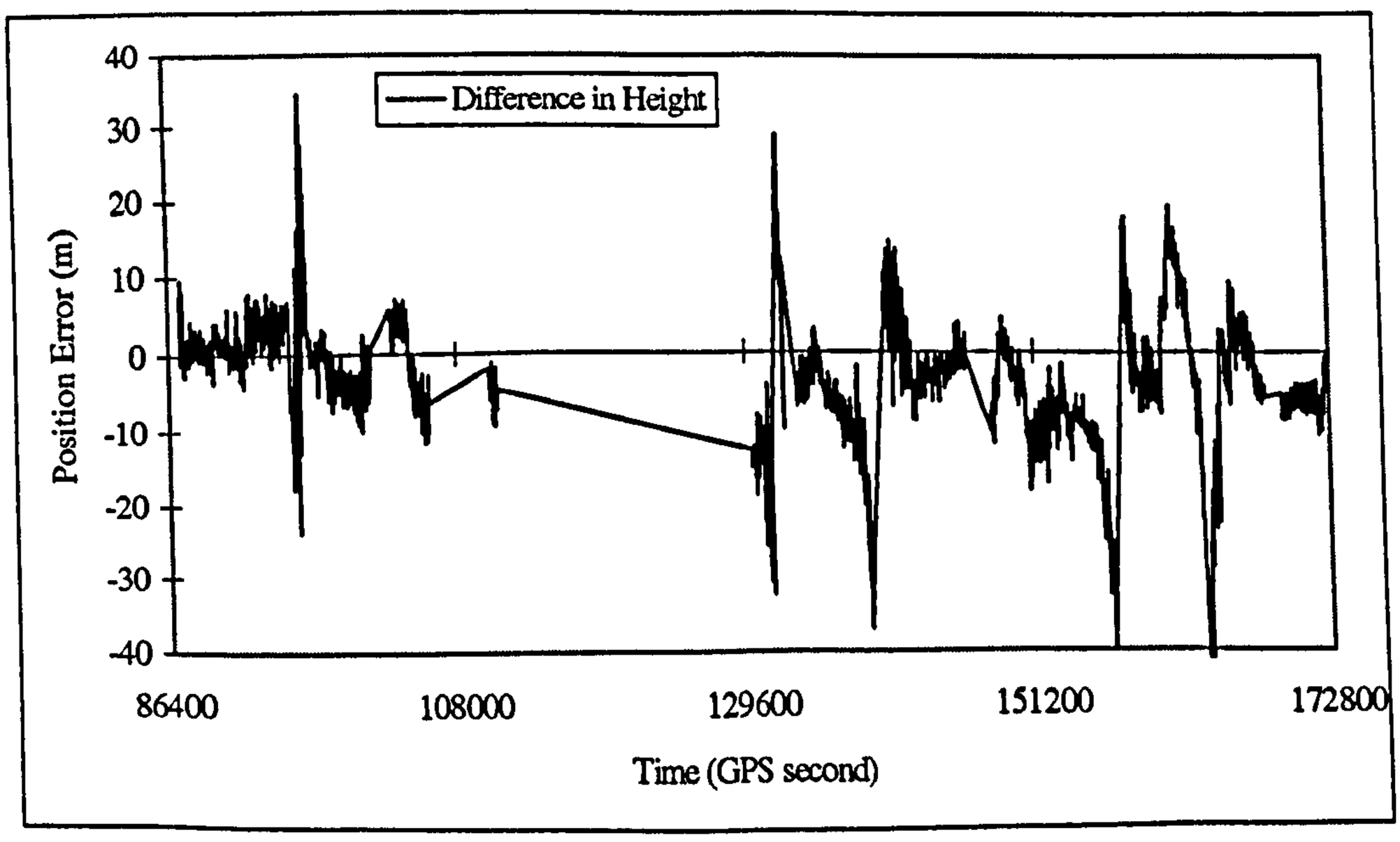

Figure E.2 Conventional DGPS Positioning - Height Error Reference Station : Cyprus